FY14-15
PGA14-1
582-14-40051
Task 1.2

Conceptual Model
Ozone Analysis of the San Antonio Region
Updates through Year 2014

Technical Report

October 23rd, 2015

Prepared by:

Alamo Area Council of Governments

Prepared Under a Grant from the
Texas Commission on Environmental Quality

The preparation of this report was financed through grants from the State of Texas through the Texas Commission on Environmental Quality.
The content, finding, opinions and conclusions are the work of the authors and do not necessarily represent findings, opinions or conclusions of the TCEQ

Title: Conceptual Model Ozone Analysis of the San Antonio Region: Updates through Year 2014	**Report Date:** October 23rd, 2015
Authors: AACOG Natural Resources/ Transportation Department	**Type of Report:** Technical Report
Performing Organization Name & Address: Alamo Area Council of Governments 8700 Tesoro Drive Suite 700 San Antonio, Texas 78217	**Period Covered:** 2005-2014

Sponsoring Agency:
Prepared In Cooperation With The Texas Commission On Environmental Quality
The preparation of this report was financed through grants from the State of Texas through the Texas Commission on Environmental Quality

Abstract: Photochemical models allow analysts to predict the impact of control strategies on ambient ozone concentrations. To predict whether control strategies will enable regions to meet federal ozone standards, photochemical models simulate the effects of control measures under meteorological and atmospheric conditions that are conducive to elevated ozone concentrations, as characterized by a region's conceptual model. Meteorological characteristics associated with high ozone in the San Antonio region include stagnant air over Texas, limited frontal movement, lack of precipitation, clear skies, morning wind directions from the northwest to northeast, back trajectories from the northeast or southeast, a large diurnal temperature change, and a low early morning mixing height followed by a rapid rise in mixing height during the afternoon. Aircraft sampling, back trajectory analysis, and upwind monitor readings indicate ozone plumes can impact cities such as San Antonio hundreds of kilometers from their origin. While ozone readings at upwind monitors have declined in recent years, indicating a decrease in background ozone, the design values at all upwind monitors still exceed 65 ppb. Since transport accounts for the majority of ozone recorded at local monitors, it will be difficult for the region to demonstrate attainment of the proposed federal ozone standards with only local emission controls. San Antonio experiences two seasonal peaks in the frequency of high ozone days. The first seasonal peak is in May and June, and the second covers a period from late August through early October. Significant differences in meteorological conditions during high ozone events exist between the seasonal peaks. A combination of greater tropospheric-stratospheric air exchange combined with higher North American upper troposphere/stratospheric ozone levels during the early months of the ozone season can be partially responsible for the higher ground level ozone observed in San Antonio during the spring ozone season peak. Closer to the surface, back trajectories out of the southeast also characterize high ozone days in the spring ozone season. Likewise, the reduction of this phenomenon and chemical loss of upper NO_X pollutants can decrease ground level ozone in July, which occurs before air mass stagnation, and northeasterly transport contributes to an increase in ground level ozone measurements during the fall ozone season peak. When high ozone events were analyzed, the August-September 2012 period demonstrated the greatest suitability for future photochemical modeling.

Related Reports:	**Distribution Statement:**	**Permanent File:**
Conceptual Model Ozone Analysis of the San Antonio Region Updates through Year 2010	Alamo Area Council of Governments, Natural Resources/Transportation Department	Alamo Area Council of Governments, Natural Resources/Transportation Department

EXECUTIVE SUMMARY

The ozone conceptual model presented in this report builds on the previous conceptual model for San Antonio in 2010 and incorporates data collected for the years 2011 thru 2014. This conceptual model documents variability of high ozone concentrations for the ozone season, weekdays, and weekends, and includes a description of the regional weather patterns and associated local meteorological conditions typically experienced during high ozone episodes in the San Antonio – New Braunfels Metropolitan Statistical Area (MSA) 8-County area, in particular, those episodes that are used to set the design values for the region. The conceptual model attempts to detect the sources of region's transported ozone entering the area, and estimates locally-formed ozone using available monitoring data. The analysis helps identify most suitable high ozone events for evaluating the effects of ozone control measures within the photochemical modeling process.

San Antonio Air Quality Status

TCEQ operates three regulatory monitors in the San Antonio area: CAMS23, CAMS58, and CAMS59. Based on the 2008 air quality standards, a region is in violation of the ozone National Ambient Air Quality Standards (NAAQS) when the design value, which is the average of 3 consecutive years' fourth highest monitored ozone data for any given monitor, exceeds 75 ppb. The following table indicates two monitors measuring ozone concentrations in violation of national standards in San Antonio region. Table ES-1 indicates in recent years, the annual fourth highest eight-hour average ozone concentrations, which are the values used in federal compliance determination, have risen from 78 ppb in 2010 to 83 ppb in 2013. However, 2014 showed a steep drop in the fourth highest eight-hour average ozone, and is the first year since 2007 to have all three regulatory monitors below 75 ppb. However, this reduction in the fourth-highest value was not enough to bring the 2014 design value into attainment. One monitor, Camp Bullis CAMS 58, remains above the 2008 NAAQS for ozone. The EPA is considering a revision to the NAAQS for ozone to a range between 65 ppb and 70 ppb. A final decision will be made on the revision no later than October 1, 2015. Only the Calaveras Lake monitor, CAMS 59, falls within the upper range of the proposed NAAQS.

Table ES- 0: 2014 Compliance with 2008 Eight-Hour Ozone Standard, San Antonio Region

CAMS	2010 4th-Highest (ppb)	2011 4th-Highest (ppb)	2012 4th-Highest (ppb)	2013 4th-Highest (ppb)	2014 4th-Highest (ppb)	2012-2014 Design Value
San Antonio Northwest C23	72	**79**	**81**	**76**	69	75
Camp Bullis C58	**78**	75	**87**	**83**	72	**80**
Calaveras Lake C59	67	71	70	69	63	67

Annual and Seasonal Frequency of High Ozone Days

Figure ES-1 depicts the total number of high ozone days recorded at regulatory monitors for assumed NAAQS standards of 60, 65, and 70 ppb and also the 2008 NAAQS of 75 ppb. According to the historical data shown in Figure ES-2, the area has experienced a more or less decreasing ozone trend from 2005 through 2014, with some fluctuation year-to-year based on meteorology.

Figure ES-1 : Total Number of High Ozone Days at San Antonio Regulatory Monitors

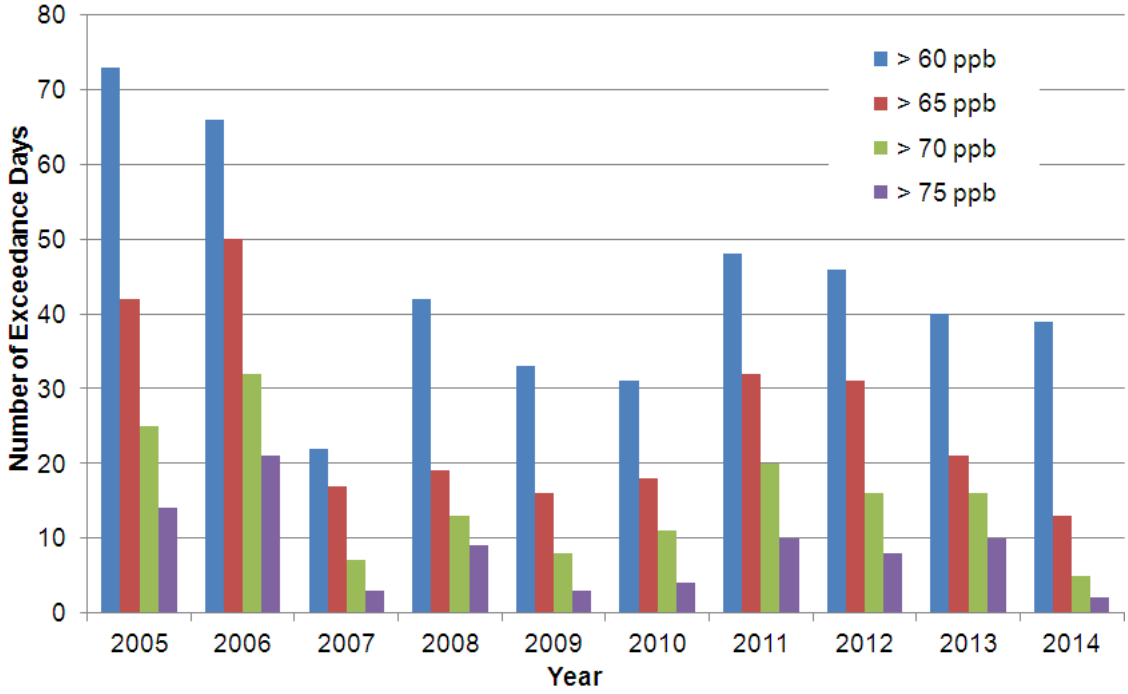

Extensive data sets were analyzed to develop an updated conceptual model for the San Antonio region including meteorology, emissions, ozone, and spatial observations. Chapter 1 defines the elements and usage of a conceptual model. This chapter describes the determining criteria desirable for modeling high ozone events as outlined in EPA's modeling guidelines.[1] Chapter 2 contains the analysis of air quality trends in San Antonio. The 2012 – 2014 design values at all regulatory-sited monitors are above this range and higher than they were in 2010, but have been declining since 2011, as have the number of exceedance days.

Estimates of Background and Locally-Formed Ozone

Chapter 3 provides typical local meteorological conditions that are conducive to ozone formation including days with stagnant air, limited frontal movements, no precipitation, low atmospheric moisture content in the afternoon, a large diurnal temperature change, and clear skies. Mixing heights are typically lower in the early morning hours and experience a rapid rise in the late morning through early afternoon on high ozone days. Timing, location, and intensity of ozone events are influenced by the interaction between local and regional wind patterns. Wind vectors on high ozone days were more stagnated and originated from the east and northeast. At C23, winds slowly change direction at the monitor from the north to the east in a clockwise fashion during the day. The directions of the wind vectors indicate that transported emissions from the north and northeast on high ozone days combine with local emissions to produce elevated ozone conditions. C58 wind vectors show there is a flow reversal of winds arriving at the monitors from the northwest in the morning before 7 am. These winds can re-circulate local ozone precursor emissions and ozone from the previous day that combine with local and transported emissions resulting in elevated ozone levels.

[1] U.S. Environmental Protection Agency Office of Air Quality Planning and Standards Emissions, Monitoring, and Analysis Division Air Quality Modeling Group, October 2005. "Guidance on the Use of Models and Other Analyses in Attainment Demonstrations for the 8-hr Ozone NAAQS", Research Triangle Park, North Carolina. EPA -454/R-05-002. Available online: http://www.epa.gov/scram001/guidance/guide/final-03-pm-rh-guidance.pdf. Accessed 04/25/15.

The impact of background ozone and ozone-precursor transport is considered in Chapter 5. There are currently six active NO_X monitors in the San Antonio region, all of which typically indicate low NO_X levels with the exception of C678 and C1069, which often record moderate NO_X concentrations due to their central location and proximity to highways. Although C1069 has the highest recorded NO_X in the region, it only began operation in January 2014. NO_X emissions at C678 have significantly decreased since 2000. Decreases in recorded NO_X are attributed to controls put on major NO_X sources including power plants and cement kilns, and significant reductions of NO_X emissions from on-road and off-road vehicles. Local NO_X emissions should continue a downward trend, in large part due to improvements in vehicle emission standards, while local VOC emissions are expected to remain steady. C59 is an upwind monitor site on most high ozone days and NO_X measurements from 2000 to 2014 were minimal at the monitor indicating there was not a significant amount of NO_X being transported into San Antonio from the southeast.

Impact of the Eagle Ford Shale

Breakthroughs in drilling technology, coupled with the high price of oil, have made possible the extraction of oil and natural gas from the Eagle Ford Shale, a geological formation which extends from the Mexico border just north of Laredo, northeast for hundreds of kilometers to the Bryan-College Station area. The bulk of the drilling activity is concentrated in the southwestern two-thirds of the formation and this activity is responsible for emissions of ozone precursors. Because prevailing winds in San Antonio are usually out of the southeast and cross the Eagle Ford Shale, it is important to assess the impact, if any, that these new emissions may have on ozone in San Antonio.

The addition of two new CAMS in Floresville and Karnes County will greatly improve the analysis of ozone precursors upwind of San Antonio. In addition to monitoring NO_X and meteorological parameters, these monitors are equipped with Auto Gas Chromatographs that measure VOCs. These are the first Auto-GCs established in the San Antonio region. The Auto-GC monitor at Floresville CAMS 1038 has been in operation since July 2013 and was the only such monitor in the San Antonio region until the end of 2014, when the Karnes County Courthouse Auto-GC station began operation. Measurements for 46 different species of VOCs are identified and reported at these Auto-GCs, with measurements taken for 40 minutes out of every hour. The Floresville monitor lies just outside and downwind of the heaviest oil and gas activity, while the Karnes County monitor lies in the middle of the oil and gas activity. The Karnes County monitor has been recording higher concentrations of VOCs than in Floresville and sometimes captures local emissions plumes with 1-hour concentrations of ethane as high as 900 ppb-V.

Large-Scale Weather Patterns and Transport Conditions during High Ozone Events

While ozone readings at upwind monitors have declined in recent years, indicating a decrease in background ozone, ozone readings at upwind monitor sites still exceed the range of the proposed revision to the standard on some days. Since the majority of ozone recorded at local monitors is the result of transport from other areas, it is difficult for the San Antonio region to demonstrate attainment with only local emission controls. Easterly to northeasterly winds bring high levels of background ozone into San Antonio from the Midwest U.S, Dallas, Austin and other regions. Sampling of industrial point sources and urban ozone plumes by aircraft increases the knowledge of regional ozone development.

Variations in both local ozone levels and transported ozone throughout the ozone season are addressed in Chapter 5, as it has become more apparent that seasonal meteorological trends have an important role in monitored ozone readings in San Antonio. In May and June, there is a seasonal peak in the frequency of high ozone days in most Texas cities. This period represents the first high ozone seasonal peak that San Antonio typically experiences, and corresponds to the yearly beginning of intermittent high pressure systems which result in the light winds, clear skies, and high solar radiation that drive high ozone production.

A significant amount of transport occurs during the spring ozone season peak. A combination of greater tropospheric-stratospheric air exchange combined with higher North American upper troposphere/stratospheric ozone levels during the early months of the ozone season are contributing factors. Likewise, the reduction of this phenomenon and chemical loss of upper NO_X pollutants could explain the decrease in ground level ozone in July, which occurs before the air mass stagnation and northeasterly transport that contribute to an increase in ground level ozone measurements during the fall ozone season peak. The second seasonal peak covers a period from August through October. Resulting wind vectors during the May – June ozone season peak tend to be from the east and southeast on high ozone days, while the late August to early October ozone season peak wind vectors are dominated by winds from the northeast.

Future Photochemical Modeling

The suitability of each high ozone event as a basis for photochemical modeling is analyzed in Chapters 7 and 8. The September 2011, June 2012, September 2012 and August 2013 high ozone events were generally suitable for future photochemical modeling, having typical ozone readings, typical wind directions on high ozone days, typical back trajectories on high ozone days, and extensive meteorological and ozone data sets available for modeling. Of these high ozone events, the June 2012 and September 2012 are under consideration for joint photochemical modeling by other cities in Texas, making them more desirable from a cost perspective. The remaining two high ozone events had poor rankings in several categories, most notably having atypical back trajectories and winds, and these episodes would not be ideal candidates for modeling. When choosing a new episode for photochemical modeling in the San Antonio region, the information provided in this conceptual model, in addition to any new information, should be considered, as well as cost and whether or not multiple regions could benefit from the development of a modeling episode.

TABLE OF CONTENTS

LIST OF TABLES

LIST OF FIGURES

1 INTRODUCTION

The U.S. Environmental Protection Agency (EPA) is charged with the maintenance of air quality across the United States through a series of standards, the National Ambient Air Quality Standards (NAAQS). When regions fail to comply with these standards, the Clean Air Act requires that the state, in consultation with local political subdivisions, develop a state implementation plan (SIP) to address the violation. "A State Implementation Plan (SIP) is an enforceable plan developed at the state level that explains how the state will comply with air quality standards according to the federal Clean Air Act. A SIP must be submitted by the state government of any state that has areas that are designated in nonattainment of federal air quality standards."[2] The current NAAQS standard of 75 ppb is proposed to be lowered to a range of 65 ppb to 70 ppb. The EPA also requested comments on a 60 ppb proposed standard.

Forecasting future air quality and modeling of air quality control strategies are among the basic elements of a SIP. Since control strategy modeling requires extensive technical analyses of control strategy impacts under a variety of typical meteorological conditions that produce high ozone, it is important that each photochemical modeling episode be based on a time period characterized by such meteorological conditions. Careful selection of photochemical episodes for use in the SIP is critical.

A conceptual model is one of the main tools used when selecting photochemical modeling episodes that are representative of high ozone events. Results from the conceptual model are used to assess and evaluate performance of a photochemical model. Air quality trends, meteorology patterns, oil and gas development in the Eagle Ford, ozone precursor emissions, and ozone transport are evaluated for the San Antonio region in the conceptual model.

1.1 Conceptual Description

Elevated ozone episodes occurring in the San Antonio area are described in chapter 7. Factors that contributed to elevated ozone concentrations in the San Antonio area were identified, and cumulatively, formed the *conceptual description* for the region. The conceptual description includes ozone formation trends, local meteorological analysis, ozone transport, and seasonal ozone variations, as described in the following chapters.

Chapter 2: Air Quality Trends in the San Antonio Area

- Surface measurements of ozone concentrations
- Changes in ozone readings from year to year
- Frequency and location of monitored ozone violations
- Correlation between 8-hour and 1-hour ozone readings

Chapter 3: Meteorological and Ozone Precursor Emissions in the San Antonio Area

- Regional meteorological patterns
- Local ground level meteorological patterns including precipitation, relative humidity, solar radiation, temperature, atmospheric pressure, wind speed, and wind direction.
- Correlation of monitored ozone readings with other pollutants including NO_X, SO_X, $PM_{2.5}$.
- Elevated meteorological patterns including mixing height
- Trends in local emissions

[2] TCEQ, October 23, 2014. "SIP: Introduction". Available online: http://www.tceq.state.tx.us/airquality/sip/sipintro.html. Accessed: 04/27/15.

Chapter 4: Eagle Ford Emissions

- Diurnal and seasonal VOC profile at the Floresville monitor
- Transport of NO_X and VOCs over the Eagle Ford Shale
- University of Texas Mobile Monitoring study
- June 2006 Photochemical model runs using 2018 Eagle Ford Moderate Emissions Scenario

Chapter 5: Background Ozone and Ozone Transport into the San Antonio Area

- Back trajectories analysis
- Upwind monitor readings
- Aircraft sampling of urban and industrial plumes
- Transport analysis in the photochemical model
- Regional point source contributions

Chapter 6: Seasonal Ozone Variations

- Seasonal and daily variation in high ozone
- Meteorological Impact on Ozone Season Variations
- Impact of Upper Troposphere Ozone

Chapter 7: Meteorological Patterns During San Antonio High Ozone Events

- Suitability of recent high ozone events for future photochemical modeling
- Descriptive meteorological summary of high ozone events

Chapter 8: Conclusion and Summary of High Ozone Events

- Summary of factors influencing ozone formation
- Desirability ranking of 2010-2014 high ozone events

EPA recommends a conceptual description of the ozone problem be developed to aid the selection of modeling episodes. "A conceptual description is useful for helping a State/Tribe identify priorities and allocate resources in performing a modeled demonstration."[3] Thus, a successful conceptual model characterizes the nature of the ozone problem and helps identify suitable time periods for photochemical model development used for control strategies evaluation.

1.2 Air Quality Trends

Ground-level ozone is one of the most common air pollutants in the country as well as one of the six "criteria" pollutants for which the EPA has established standards. A region is in violation of the Clean Air Act if the annual fourth highest 8-hour average ozone concentration, averaged over three consecutive years, exceeds 75 parts per billion (ppb).[4] This average is referred to as the ***design value***. The fourth highest 8-hour averages and design values for the three most recent complete years of data, 2012-2014, from the regulatory continuous ambient monitoring stations (CAMS) in the San Antonio region are listed in Table 1-1.

[3] U.S. Environmental Protection Agency Office of Air Quality Planning and Standards Air Quality Analysis Division Air Quality Modeling Group, April 2007. "Guidance on the Use of Models and Other Analyses for Demonstrating Attainment of Air Quality Goals for Ozone, PM2.5, and Regional Haze", Research Triangle Park, North Carolina. EPA -454/B-07-002. p. 126. Available online: http://www.epa.gov/scram001/guidance/guide/final-03-pm-rh-guidance.pdf. Accessed 05/08/15.

[4] EPA, March 2008. "Fact Sheet: Final Revisions to the National Ambient Air Quality Standards For Ozone". Available online: http://www.epa.gov/groundlevelozone/pdfs/2008_03_factsheet.pdf. Accessed 04/26/15.

Table 1-1: 4th Highest Ozone Values[5] and Design Values at San Antonio Regional Monitors, 2012-2014

CAMS	2012 (ppb)	2013 (ppb)	2014 (ppb)	**2012-2014 Design Value**
C23	**81**	**76**	69	75
C58	**87**	**83**	72	**80**
C59	74	69	63	67

The 2008 revision to the Clean Air Act modified the ozone standard to improve the law's ability to protect human health and the environment. Under the 2008 revision, a region is in violation of the ozone NAAQS when the design value exceeds 75 ppb. As shown in Table 1-1, the 2012 - 2014 design value is 80 ppb at C58, 75 ppb at C23, and 67 ppb at C59, indicating that the San Antonio region has one monitor measuring concentrations in violation of the 75 ppb eight hour ozone NAAQS. The proposed NAAQS under consideration by the EPA ranges from 60 ppb to 70 ppb. At the midpoint of the proposed range, all regulatory monitors are in violation.

1.3 Meteorological and Ozone Pre-Cursor Emissions

Preliminary analysis of the San Antonio region indicates a number of factors that are associated with elevated ozone concentrations, forming a specific conceptual description. This model includes regional as well as local factors, which in aggregate contribute to ozone elevation in the San Antonio region. Areas of stagnated air over Texas, few frontal movements, no precipitation, and clear skies characterize high ozone events. Local meteorological conditions during high ozone events include no precipitation, low atmosphere moisture content present in the afternoon, clear skies, and morning wind direction from the northwest or north. Mixing heights on high ozone days are typically lower in the early morning hours followed by a rapid rise in the late morning through early afternoon.

Significant amounts of volatile organic compound (VOC) and nitrogen oxide (NO_X) emissions are emitted in the San Antonio region from mobile sources, power plants, industrial facilities, coating operations, petroleum products, and biogenic sources. Mobile sources include cars, trucks, heavy construction equipment, land and garden equipment, locomotives, and aircraft. Results from photochemical modeling indicate that San Antonio is NO_X-limited: high ozone formation is more influenced by NO_X emissions than by VOC emissions.

1.4 Impact of the Eagle Ford Shale

Recent horizontal drilling operations in the Eagle Ford Shale may have resulted in increased emissions of VOCs that have necessitated the addition of two Automated Gas Chromatographs (Auto-GCs): one in Floresville, C1038, and the other just outside the San Antonio-New Braunfels MSA in Karnes County, C1070. These Auto-GCs measure the concentrations of 46 different VOCs. C1070 has only been in operation since the beginning of 2015, while C1038 was operational beginning in July 2013. The lack of data makes it difficult to discern any trends over time, but allows the general diurnal and seasonal behavior of VOCs to be assessed. VOCs follow a similar diurnal pattern as NO_X, with peak concentrations just before sunrise, declining through the morning and afternoon, and rising again in the late evening. Seasonally, VOCs peak in the winter, and the ozone season

[5] Texas Commission on Environmental Quality (TCEQ). "Four Highest Eight-Hour Ozone Concentrations." Austin, Texas. Available online: http://www.tceq.state.tx.us/cgi-bin/compliance/monops/8hr_4highest.pl. Accessed 05/08/15.

represents the seasonal minimum for VOC concentrations. Morning wind directions out of the south and east tend to result in higher VOC concentrations at the Floresville monitor.

VOCs are emitted through various sources, both anthropogenic and biogenic. Of the anthropogenic sources near the Eagle Ford Shale, there were found to be two potential factors that contributed to VOCs: oil and gas exploration and vehicle combustion. Additionally, some species of VOCs react more readily to produce ozone. TCEQ has identified six highly-reactive VOCs (HRVOCs) that have the greatest effect on the photochemical process in the Houston area, and those species are used to delineate HRVOCs for the San Antonio region as well. The six HRVOCs are ethylene, propylene, 1-3 butadiene, and butenes (t-2-butene, c-2-butene, and 1-butene). These HRVOCs were found to be a slightly better predictor of background ozone for the San Antonio region based on a simple linear regression. In other words, on days where 48-hour back trajectories crossed the Eagle Ford, the sum of HRVOC concentrations were more strongly correlated with peak 8-hr ozone at CAMS 59 than the sum of all VOC concentrations. Additionally, these HRVOCs tend to be more a factor of vehicle combustion, rather than oil and gas activity. The Eagle Ford Shale may enhance the concentration of ethane by an average of 6 ppb-V, with potential enhancement values as high as 40 ppb-V during the University of Texas Mobile Monitoring Study. Ethylene enhancement appears to be present as well, but smaller in scope than ethane.

1.5 Background Ozone and Ozone Transport

Back trajectories, upwind monitor readings, aircraft sampling, and photochemical models can be used to analyze transport. San Antonio is located to the southwest of Dallas/Fort Worth (DFW) and to the west of Houston, two nonattainment areas in Texas. Regional winds generally enter the city from the northeast to the southeast on high ozone days and often ozone and/or ozone precursor pollutants that originate from other regions and countries can impact local ozone monitors.

Surface back trajectories on days with low ozone are predominately from the southeast, while winds on high ozone days tend to be from the northeast, east, and southeast. The end points of 48-hour back trajectories on low ozone days tend to originate far out in the Gulf of Mexico, while the back trajectories on high ozone days tend to originate closer to San Antonio over eastern Texas. Since back trajectories on high ozone days travel fewer kilometers before arriving at local ozone monitors, high ozone days are associated with lighter transport level winds and local stagnation.

The difference between the maximum peak ozone reading at local downwind ozone monitors and the minimal peak ozone readings at local upwind ozone monitors on high ozone days > 65 ppb from 2005 to 2014 was 16.8 ppb or 22.8%, indicating that transport may be responsible for up to 77% of ozone in the San Antonio area. Aircraft sampling indicates large ozone plumes from Houston and large point sources can impact areas hundreds of kilometers downwind including San Antonio monitors. This may increase the ozone levels at downwind monitors and increase the difficulty of attaining the new proposed 8-hour ozone standard.

1.6 Seasonal Variations in Ozone Formation

From April through June, there is a seasonal increase in the number of high ozone days in most Texas cities. This period represents the first and longest high ozone seasonal peak that San Antonio typically experiences. However, by early July the number of high ozone days decline. The next seasonal increase covers a period beginning in August and ending in late October, during which the frequency of high ozone days is slightly lower than the spring period.

Ozone readings fluctuate by season depending on several factors including variations in transport, meteorology, chemical loss of ozone, and upper stratospheric ozone levels. Since transport significantly influences local ozone concentrations, seasonal variations in wind direction, distance and direction of back trajectories and chemical loss of ozone are important factors to include in the analysis. There is a significant amount of ozone transport during the spring and fall ozone season peaks. Ozone transport is lowest in July before increasing again into the late summer and fall.

It is possible that a combination of greater tropospheric-stratospheric air exchange combined with higher North American stratospheric ozone levels during the early months of the ozone season is partially responsible for the higher ground level ozone observed in San Antonio during these months. Decreases in observed tropospheric and stratospheric ozone in the Northern Hemisphere from the spring to the fall seasons can be explained by increased chemical destruction of ozone. Chemical loss of tropospheric and stratospheric ozone can occur through the catalysis by NO_X in the summer time. The secession of this phenomenon could explain the decrease in ground level ozone from late June through July, which occurs before air mass stagnation and northeasterly winds contribute to a rebound in ground level ozone measurements during the fall ozone season peak.

1.7 High Ozone Events

Conceptual models can be used for selecting high ozone events for photochemical modeling episodes that are in compliance with EPA's guidelines. The conceptual model process undertaken for identifying candidate photochemical modeling episodes, the analysis of these candidate episodes, and the determination of desirability of each candidate episode are provided in this report. The first Conceptual Model for the San Antonio region was developed in 2000 as a tool used to select the September 1999 photochemical modeling episode and later conceptual models were refined to select the June 2006 photochemical modeling episode.

High ozone events between 2010-2014 were analyzed to identify possible additional modeling episodes. Modeling episodes should be long enough to include the full synoptic cycle of ozone formation, peak and dissipation at San Antonio monitors. Candidate modeling episodes should also include days with observed concentrations that are close to site-specific design values and reflect meteorological conditions that are commonly observed on high ozone days.

The more recent the episode, the more desirable it is for photochemical modeling. As more monitors and meteorological stations are installed, more data becomes available to verify the performance of the photochemical model; this makes the development of a more recent episode desirable. Additional data, such as the 2005-2006 profiler measurements recorded at the New Braunfels Weather Station as well as aircraft sampling augment the model verification process and help determine episode desirability.

The Conceptual Model is continually updated in preparation for new modeling episodes as they become necessary. Based on EPA recommendations, "at a minimum, four criteria should be used to select time periods which are appropriate to model:

1) Simulate a variety of meteorological conditions:

"8-Hour Ozone- Choose time periods which reflect a variety of meteorological conditions which frequently correspond with observed 8-hour daily maxima" > 70 ppb at multiple monitoring sites[6].

2) "Model time periods in which observed concentrations are close to the appropriate baseline design value.
3) Model periods for which extensive air quality/meteorological databases exist.
4) Model a sufficient number of days so that the modeled attainment test applied at each monitor violating the NAAQS is based on multiple days."[7]

"Those implementing the modeling/analysis protocol may use secondary episode selection criteria on a case by case basis. For example, prior experience modeling an episode or year may result in its being chosen over an alternative. Another consideration should be to choose time periods occurring during the 5-year period which serves as the basis for the baseline design value (DVB). If observed ozone exceedances occur on weekends, weekend days should be included within some of the selected time periods. If it has been determined that there is a need to model several nonattainment areas simultaneously (e.g., with a nested regional scale model application), a fourth secondary criterion is to choose time periods containing days of common interest to different nonattainment areas".[8] One of the key reasons the June 2006 photochemical model was selected was because many areas in Texas experienced elevated ozone events during this time period. Episodes that can be modeled in conjunction with other regions, like Austin or Houston, are more cost-efficient. The sharing of data makes this approach beneficial to all regions involved by reducing the cost for each region.

Keeping EPA's guidelines in mind, the next step is to garner available data relating to meteorological measurements, transport, and ozone levels. Analysis of this data will be used to determine the desirability, based on the selection criteria, of the candidate episodes for San Antonio. The conceptual model compares these results and ranks episodes based on desirability alone. This is the first step in considering an episode for photochemical modeling selection. Other factors will ultimately direct the choice of the models; these other factors include: the need for a new episode, cost issues, compatibility with desired episodes of other regions, additional information obtained through further study, and other relevant factors.

[6] U.S. Environmental Protection Agency Office of Air Quality Planning and Standards Air Quality Analysis Division Air Quality Modeling Group, April 2007. "Guidance on the Use of Models and Other Analyses for Demonstrating Attainment of Air Quality Goals for Ozone, PM2.5, and Regional Haze", Research Triangle Park, North Carolina. EPA -454/B-07-002. p. 140. Available online: http://www.epa.gov/scram001/guidance/guide/final-03-pm-rh-guidance.pdf. Accessed 04/24/15.
[7] *Ibid*, p. 141.
[8] *Ibid*.

2 AIR QUALITY TRENDS IN THE SAN ANTONIO AREA

Analysis of air quality data between 2009 and 2014 indicates yearly variations in the design values, but a general decrease in the number of high ozone days. This suggests a gradual improvement in air quality, although meteorological variations can greatly influence daily concentrations. The region is violating the 75 ppb 8-hour average ozone standard and the proposed revision to the standard, which could lower the allowable 8-hour average ozone concentration to either 65 ppb or 70 ppb and will likely present serious challenges to the San Antonio region.

2.1 Ozone Trends

There are 21 regulatory and non-regulatory air quality monitors in the San Antonio-New Braunfels MSA that record meteorological data and air pollutant concentrations, including ozone levels. The data collected at these sites is processed for quality assurance by the Texas Commission on Environmental Quality (TCEQ) and is accessible via the Internet.[9] Figure 2-1 displays the location of the monitors within the region. Meteorological data measured at these sites includes temperature, wind speed, wind direction, precipitation, solar radiation, and relative humidity. Most stations measure one or more air pollutants including ozone (O_3), carbon monoxide (CO), nitrogen oxides (NO, NO_2), particulate matter equal to or less than 2.5 micrometers in diameter (PM2.5), particulate matter greater than 2.5 but less than 10 micrometers in diameter (PM10), and volatile organic compounds (VOCs). Table 2-1 lists each ozone-reporting monitor, along with any other parameters they record, as well as the address and start date.

Ozone is monitored at C23, C58, C59, C501, C502, C503, C504, C505, C506, C622, and C678. Other ambient air monitors include: C140 (meteorological data), C301 (PM 2.5), C676 (meteorological data and PM 2.5), C677 (meteorological data, PM 2.5, and VOC canister sampling), C1069 (meteorological data and NO_X), and C5004 (meteorological data). C623, C626, and C625 measures total suspended particulate, while C1038 in Floresville has an Automated Gas Chromatograph (Auto-GC) used to measure 46 species of volatile organic compounds (VOC) in addition to NO_X and meteorological data. The Karnes County Courthouse now has a monitor, C1070, which is also equipped with an Auto-GC. Although this monitor lies outside of the MSA boundary, it may be a valuable source of emissions transport data from the Eagle Ford Shale.

The 8-hour ozone design values at the regulatory ozone monitors in the San Antonio-New Braunfels MSA from 2005 to 2014 are provided in Figure 2-2. C58 and C23 ozone monitors have had the highest design values in the San Antonio region since 2005. Although design values have increased at these monitors since 2009 only one monitor, CAMS 58, is exceeding the 75 ppb ozone standard. At C23, the fourth-highest ozone reading dropped from 76 ppb to 69 ppb and at C58, from 83 ppb to 72 ppb from 2013 to 2014.

[9] TCEQ, “Air and Water Monitoring”. Austin, Texas. Available online: http://www.tceq.state.tx.us/assets/public/compliance/monops/graphics/clickable/region13.gif. Accessed 04/26/15.

Figure 2-1: Monitoring Sites the San Antonio-New Braunfels MSA

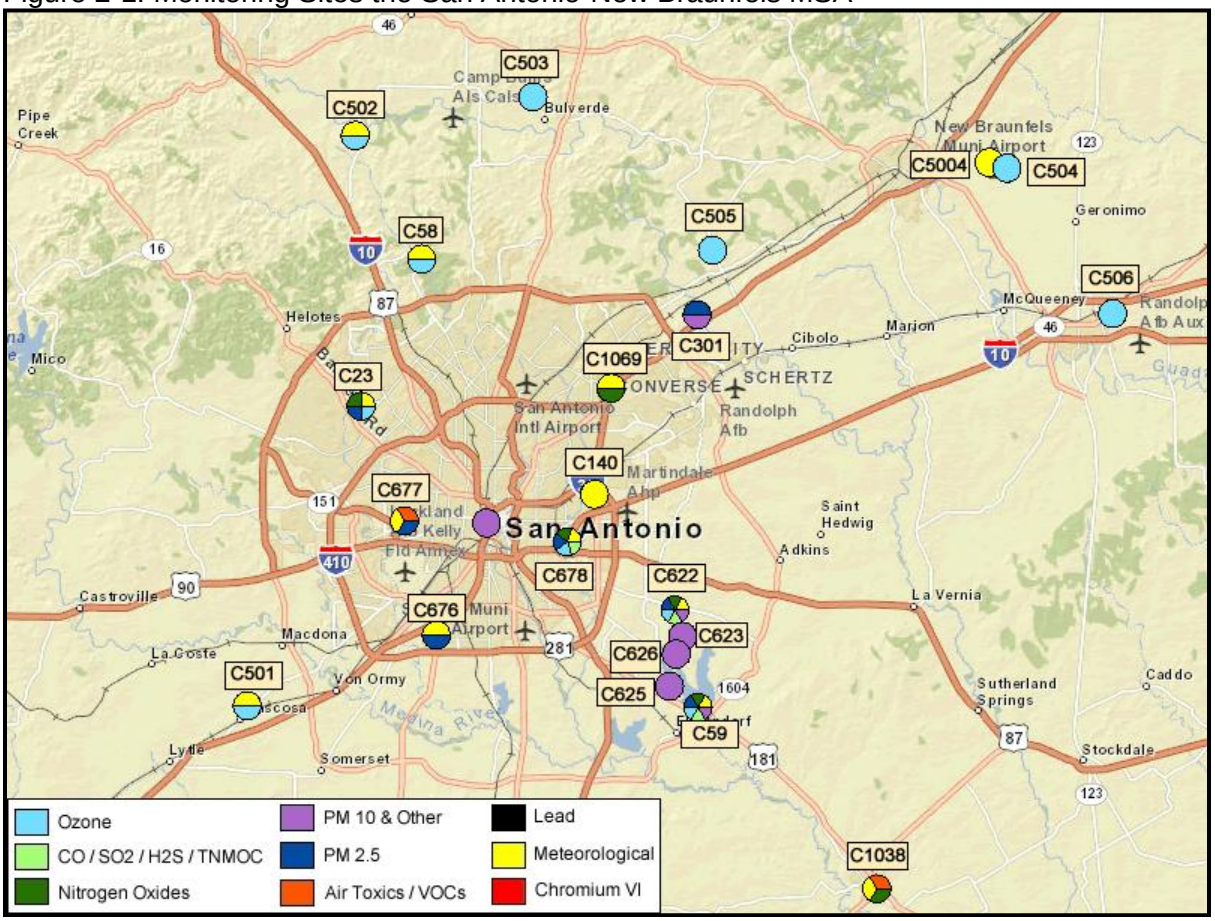

Table 2-1: Regulatory and Non-Regulatory Ozone Monitors in the San Antonio –New Braunfels MSA, Ozone Season 2014

Designation / Site Name	Regulatory Monitor	Location Description	Data Measured	First date of reporting (online), Currently maintained by
CAMS 23 Marshall High School	Yes	6655 Bluebird Lane, San Antonio	NO_X, Ozone, Meteorology, $PM_{2.5}$	September 17,1996 TCEQ
CAMS 58 Camp Bullis	Yes	Near Wilderness road, San Antonio	Ozone, Meteorology	August 12, 1998 TCEQ
CAMS 59 Calaveras Lake	Yes	14620 Laguna Road, San Antonio	CO, SO_2, NO_X, Ozone, Meteorology, $PM_{2.5}$	May 13, 1998 San Antonio Metro Health District and Dios-Dado
CAMS 501* Elm Creek Elementary	No	11535 Pearsall Rd., Bexar County	Ozone, Meteorology	June 17, 2002 Dios-Dado for AACOG
CAMS 502* Fair Oaks Ranch	No	7286 Dietz Elkhorn Rd., Fair Oaks Ranch	Ozone, Meteorology	June 28, 2002 Dios-Dado for AACOG
CAMS 503* Bulverde Elementary	No	1715 E. Ammann Rd. Bulverde, Comal County	Ozone	August 26, 2002 Dios-Dado for AACOG
CAMS 504* New Braunfels Airport	No	2090 Airport Rd. NB, Guadalupe County	Ozone	August 30, 2002 Dios-Dado for AACOG
CAMS 505* Garden Ridge	No	21340 FM 3009, City of Garden Ridge	Ozone	March 26, 2003 Dios-Dado for AACOG
CAMS 506* Seguin Outdoor Learn.	No	1865 Hwy 90 E, City of Seguin	Ozone	March 26, 2003 Dios-Dado for AACOG
CAMS 678 CPS Pecan Valley	No	802 Pecan Valley Dr. Eastern, San Antonio	CO, NO_X, Ozone, Meteorology, $PM_{2.5}$	March 4, 1999 Dios-Dado for CPS
CAMS 622 Heritage Middle School	No	7145 Gardner Road, San Antonio	CO, SO_2, NO_X, Ozone, Meteorology, $PM_{2.5}$	July 29, 2004 Dios-Dado for CPS

Figure 2-2: Monitored 8-Hour Ozone Design Values at C23, C58, and C59, 2005-2014

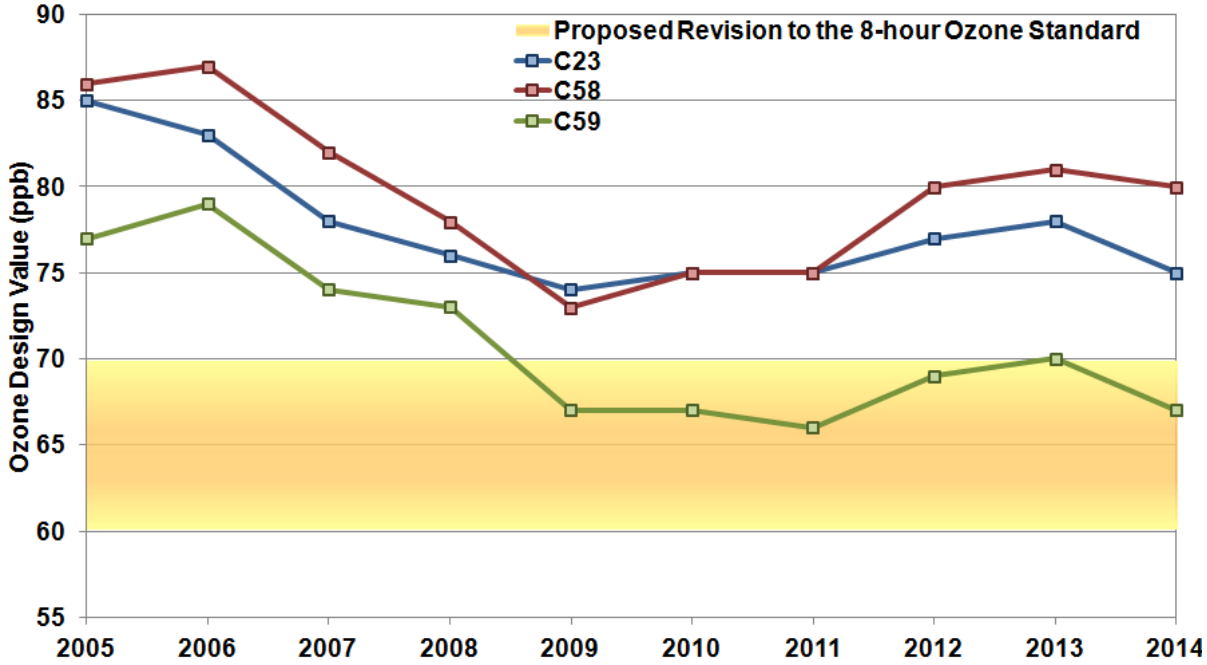

The numbers of high ozone days exceeding the 65 ppb proposed ozone standard at regulatory monitors in the San Antonio area are provided in Figure 2-3. Taking all EPA regulatory monitors into consideration together, significant reductions in the number of exceedances of days > 65 ppb occurred from 2007 through 2014, with a p-value of 0.026. Up until 2010, reductions in the numbers of exceedances of 65 ppb were particularly steep, with 2007-2010 averages dropping 53% from the 2000-2006 averages. However, since 2010, there has been an increase of number of ozone exceedances. Comparing 2007-2010 averages with 2011-2014 averages the number of exceedances increased by 39%. This clearly demonstrates that while the design values, as moving averages, can be slower to change, the number of high ozone days occurring per year can fluctuate dramatically. All exceedances of the proposed ozone standard occurred during the ozone season, which extends from April through October in San Antonio.

Figure 2-3: Number of 8-Hour Ozone Exceedances of 65 ppb at EPA Regulatory CAMS in the San Antonio-New Braunfels MSA, 2005-2014

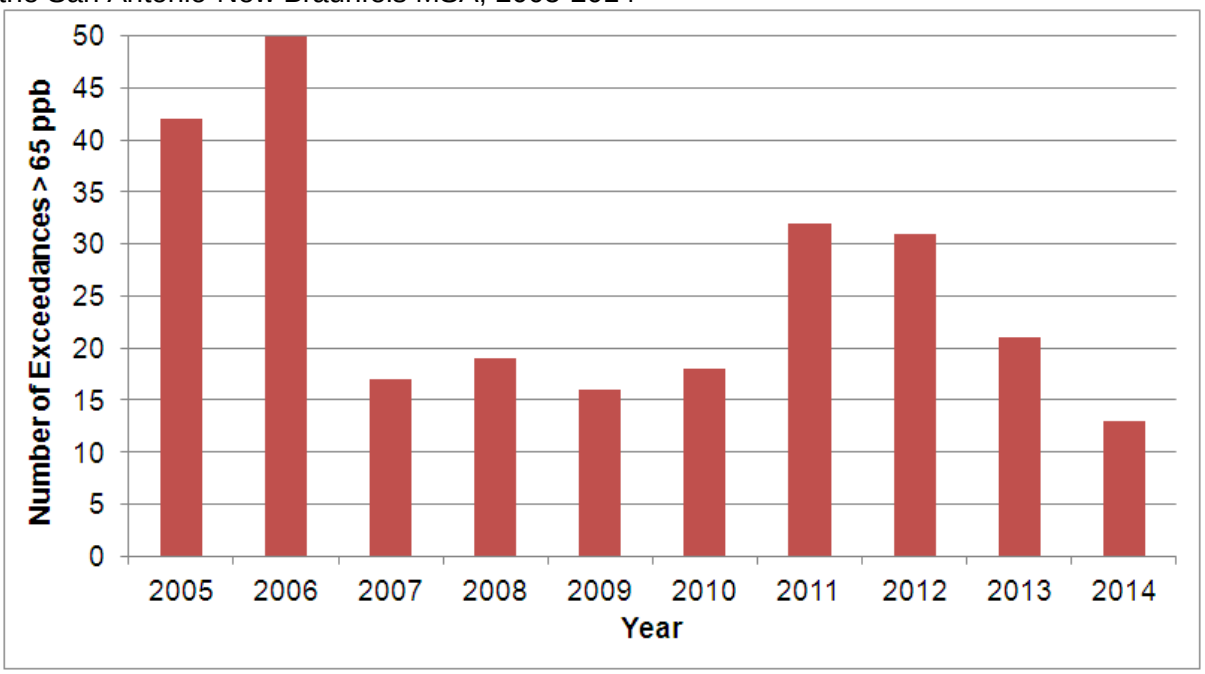

2.2 Variation between San Antonio Monitors

Table 2-2 shows the relationships between selected monitor pairs in the region on all days as well as days with >65 ppb ozone. The monitor pairs selected were in close physical proximity to each other. The monitor pairs with strong correlations are influenced by similar meteorological and photochemical conditions.

The strongest correlations for all days are between the C504/C506 and C59/C622 monitor pairs, on the northeast and southeast parts of the region. Both monitor pairs are usually upwind monitors and typically have lower ozone concentrations than downwind monitors. The R^2 value provides a "goodness of fit" test between 0.0 and 1.0. A higher R^2 value indicates two variables may have a closer correlation. The high R^2 values for these monitor pairs that are located in close proximity to each other indicate, on most days, the monitors cover areas of similar meteorology and ozone-forming chemistry, and thus introduce some redundancy in the monitoring network.

However, the correlation of ozone measurements between monitors becomes weaker at higher proposed ozone standards, as shown in Table 2-2. On days when locally produced ozone is not accumulated, all monitors are closer to background levels and therefore similar in ozone readings. This is especially true for the pair of C23 and C58, which shows high correlation on all days, $R^2 = 0.92$, but weaker correlation on days above 65 ppb, $R^2 = 0.52$. As will be discussed in following sections, both are located in a region that experiences high ozone, relative to the rest of the San Antonio area. Prevailing winds can produce narrow, concentrated ozone urban plumes that may not impact both C23 and C58 during the same high ozone event. The moderate correlation on high ozone days > 65 ppb between C23 and C58 is in contrast to the relatively high correlation on high ozone days between C59 and C622 ($R^2 = 0.87$); two monitors that are further away from the urban core and are usually located upwind from San Antonio. This can also been seen with the C504/C506 ($R^2 = 0.75$) and C504/C675 ($R^2 = 0.79$) monitor pairs. Both of these pairs are located northeast of the urban core.

Table 2-2: Variation in Daily Peak 8-hr Ozone between CAMS in San Antonio Region, 2005-2014

Proposed 8-hour Standard	Parameter	CAMS Comparison									
		58-23	58-502	502-503	58-503	504-506	504-505	505-506	504-675	59-622	622-678
All Days	R^2	0.92	0.91	0.91	0.90	0.96	0.87	0.85	0.93	0.95	0.91
	SD (σ)	3.93	4.04	3.70	4.21	2.56	5.00	5.36	3.48	3.48	4.22
	Avg. Diff.	1.92	3.24	0.28	3.55	0.16	-0.50	0.61	-1.51	-0.57	-0.47
> 65 ppb	R^2	0.52	0.55	0.66	0.50	0.75	0.63	0.52	0.79	0.87	0.68
	SD (σ)	5.66	5.67	5.43	6.20	4.28	7.19	7.32	3.81	3.12	6.43
	Avg. Diff.	0.97	6.93	-0.67	6.06	0.97	-5.79	6.87	-3.94	-4.97	1.65

2.3 Spatial Variation in Ozone

Ozone concentrations can vary by location in the San Antonio area. A spatial interpolation method was employed to identify typical ozone distributions on high ozone days. These patterns provide a more detailed description of the spatial variability in the factors contributing to high ozone levels. The 8-hour ozone design values at the 11 ozone monitors in the San Antonio area were used to create the contoured areas of equal ozone concentration presented in Figure 2-4: Contour Plots of 8-Hr Ozone Design Values, 2009 -- 2014. Also included are 8 ozone monitors outside the San Antonio region: Big Bend (CAMS 67) to the west, Laredo (CAMS 44) to the southwest, Mission (CAMS 43) to the south, Odem (CAMS 686) to the southeast, Fayette County (CAMS 601) to the east, and Dripping Springs (CAMS 614) and San Marcos (CAMS 675/1675) to the northeast. The design values for the latest six years, 2009 - 2014, were selected for analysis. This analysis shows year-to-year fluctuations in ozone design values and makes it difficult to discern a trend over the period. The analysis begins at 2009 as several stations presented did not begin operation until that year.

The highest 8-hour ozone design values in 2009, based on monitored ozone concentrations, exceeded 72 ppb and occurred in the northwestern portion of Bexar County: just northwest of the San Antonio city limit at Camp Bullis (CAMS 58), northwest of downtown at San Antonio Northwest (CAMS 23), and along the north-northwest border of Bexar County (CAMS 502 and 503). The lowest 8-hour ozone design values in 2009 occurred in the southeastern part of San Antonio (CAMS 622), and along a southwest-to-northeast aligned swath running from CAMS 59 at Calaveras Lake to CAMS 506 in Seguin. However, even the minimum 8-hour ozone design values at any monitor in 2009 were above 65 ppb.

Through 2011, 8-hour ozone design values generally decreased across the San Antonio MSA. Only three monitors saw an increase in ozone (CAMS 23, CAMS 58, CAMS 622), with an average increase of 2 ppb. Of the remaining eight monitors within the San Antonio MSA, all but one (CAMS 678) saw a decrease in ozone design values from 2009 to 2011, with an average decrease of 3.3 ppb. While the highest concentrations still occurred at Camp Bullis (CAMS 58), and San Antonio Northwest (CAMS 23), the gradient between the lowest and highest values within the MSA was smaller in 2011. The prevailing wind direction on high ozone days allows transported ozone to combine with local precursor contributions to form high ozone at C23 and C58. Every monitor outside of the MSA that was analyzed saw an increase in ozone design values between 2009 and 2011. Since 2011, every monitor in the San Antonio MSA has seen an increase in ozone design values and the gradient between design values in the MSA and those in outlying areas has been steepening. Comparing 2011 and 2014, no monitor within the MSA saw a decrease in design values, and all monitors recorded a peak design value in 2013.

Figure 2-4: Contour Plots of 8-Hr Ozone Design Values, 2009 -- 2014

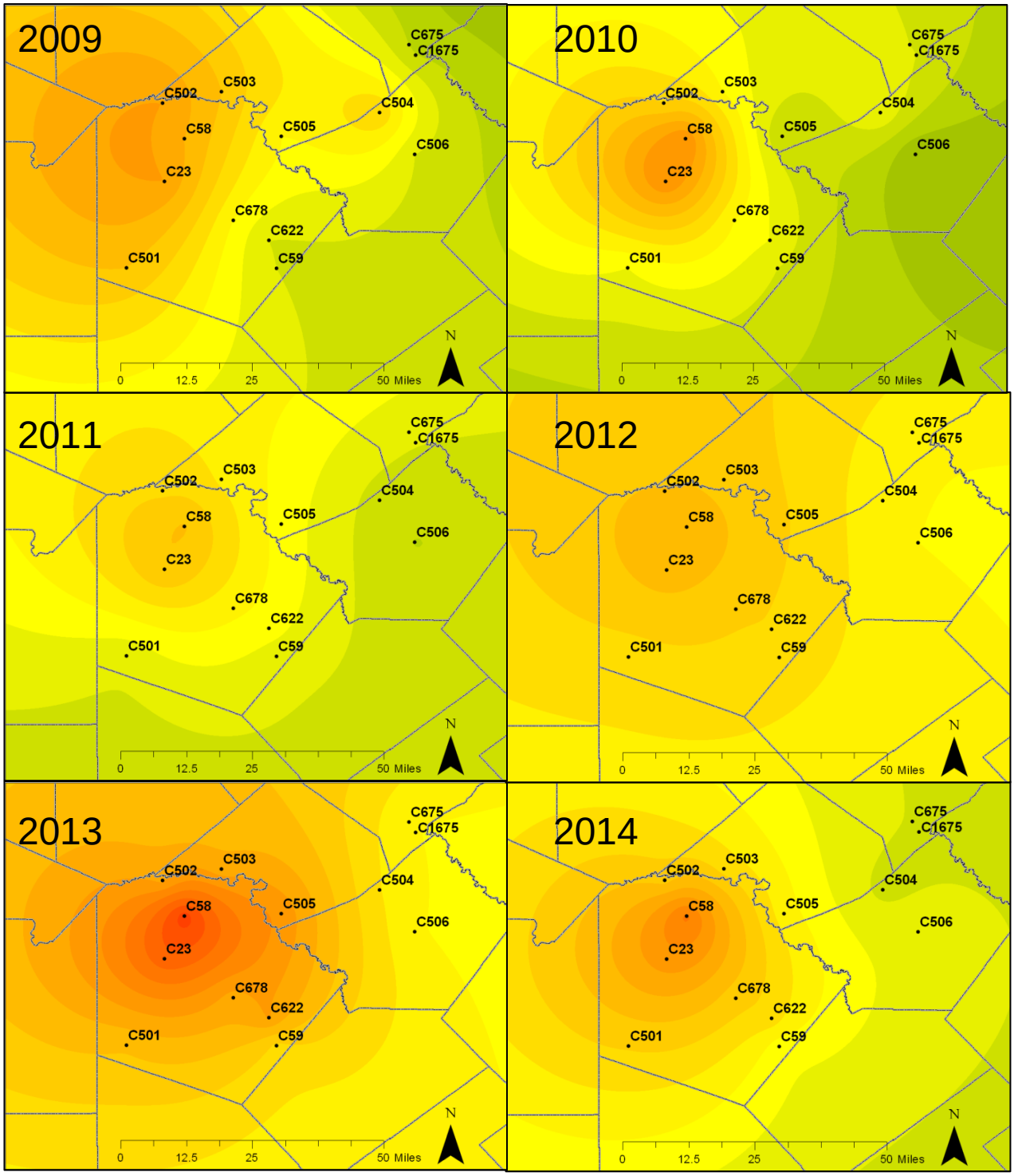

An analysis of high ozone days from 2005 – 2014 shows that 24% of the time, only one monitor exceeded 65 ppb. More typically, multiple monitors in the San Antonio MSA recorded ozone concentrations exceeding 65 ppb on high ozone days. Concentrations of high ozone were observed on multiple monitors during the same ozone event. For example, on 36% of the high ozone days, more than half of the monitors measured exceedances of 65 ppb. On days when there were eight or more monitors exceeding 65 ppb, upwind monitors indicated there were significant amounts of ozone transport above 65 ppb before local ozone contributions were added.

The number of high ozone days above 65 ppb at each monitor, as well as all the monitors, is displayed in Table 2-3. The percentages of ozone season days where ozone was > 65 ppb is given for each monitor and for all monitors in Table 2-4. The total number of 8-hour average ozone measurements above 65 ppb fell from a high of 317 in 2005 to 50 in 2014, a reduction of 84%. This represents a significant decrease in the frequency of high ozone days.

C58 (209 days) and C23 (173 days) recorded the most 8-hour ozone averages above 65 ppb between 2005 and 2014 among regulatory monitors. C502 (153 days) and C503 (162 days) also had a high frequency of ozone days above 65 ppb over the same time period. All four monitors are located on the northwest side of San Antonio that is usually downwind of San Antonio‘s urban core, power plants, cement kilns, and industrial sites on high ozone days.

Table 2-3: Variation in Occurrences of Peak 8-hr Ozone (>65 ppb) at CAMS in the San Antonio Area, 2005 – 2014

Monitor	2005	2006	2007	2008	2009	2010	2011	2012	2013	2014	Total	Average
Camp Bullis C58	33	42	14	14	13	14	20	29	21	9	209	21
San Antonio Northwest C23	32	23	13	16	14	7	24	21	17	6	173	17
CPS Pecan Valley C678	10	25	2	13	7	3	23	6	12	4	105	11
Calaveras Lake C59	25	30	5	9	0	6	14	7	7	2	105	11
Elm Creek Elementary C501	18	7	4	10	3	1	13	11	6	6	79	8
Fair Oaks Ranch C502	39	32	16	14	4	4	15	13	13	3	153	15
Heritage Middle School C622	31	20	4	9	2	5	27	9	11	12	130	13
Bulverde Elementary C503	37	31	16	15	8	3	19	15	16	2	162	16
City of Garden Ridge C505	39	20	14	11	3	2	18	14	14	3	138	14
New Braunfels Airport C504	36	26	13	9	0	3	14	5	6	2	114	11
Seguin Outdoor Learning Center C506	17	22	8	4	1	1	9	5	6	1	74	7
Total Monitors > 65 ppb	317	278	109	124	55	49	196	135	129	50	1,442	144
No. of Days > 65 ppb	63	51	22	29	17	18	35	37	25	22	319	32

The two regulatory-sited monitors that had the lowest number of high ozone days compared to other regulatory sited monitors are C622 and C678. These monitors are located on the southeast side of San Antonio upwind of the city on most high ozone days. Similarly, the three non-regulatory CAMS with the lowest frequently of high ozone days, C501, C505, and C506, are located either northeast or southwest of the urban area, and therefore either upwind or out of the path of prevailing winds traveling over local urban areas, power plants, or large industrial facilities. Further research should include analyzing the changes in the spatial pattern of ozone for each hour of the day to determine how high ozone progresses through the region.

Overall from 2005-2014, an exceedance of 65 ppb was observed at one or more monitors on 14.9% of all ozone season days. However, the frequency of high ozone days varied among monitors from an average of 7 per year (3.3% of the season) at C506 on the northeast side of San Antonio to 21 per year (10.2% of the season) at C58 on the northwest side.

The progress achieved in recent years in reducing the number of high ozone days in the San Antonio area is evident when comparing the year-to-year differences in high ozone days at each monitor and the yearly totals of high ozone days. Throughout the period from 2005-2014, every monitor in the San Antonio region experienced a marked decrease in the frequency of high ozone days. The number of high ozone days > 65 ppb occurring in the San Antonio area decreased 62% from 2005 to 2014, from 63 days in 2005 to 22 days in 2014. This trend has not been continuous, however, with 2011 showing substantial increases for C23 and C58 and 2012 showing substantial increases for all of the other monitors. Overall, the percentage of days over 65 ppb more than doubled from 2010 to 2012. Since 2012, all but one monitor (C622) has seen a decrease in percentage of high ozone days, with most reporting a decrease of over 50%. For five monitors, including two EPA-regulatory monitors, the percentage of high ozone days in 2014 is the lowest in the period from 2005-2014.

Table 2-4: Percent of Days With Peak 8-hr Ozone Values > 65 ppb at CAMS in the San Antonio MSA, 2005-2014

Monitor	2005	2006	2007	2008	2009	2010	2011	2012	2013	2014	Average
Camp Bullis C58	15.9%	20.0%	6.7%	6.8%	6.1%	6.6%	10.4%	14.8%	10.1%	4.4%	10.2%
San Antonio Northwest C23	15.1%	11.0%	6.3%	7.8%	6.6%	3.3%	11.8%	10.0%	8.0%	2.8%	8.2%
CPS Pecan Valley C678	4.8%	11.7%	1.0%	6.1%	3.3%	1.5%	1.4%	2.8%	5.8%	1.9%	4.0%
Calaveras Lake C59	12.0%	14.1%	2.4%	4.4%	0.0%	2.9%	2.8%	3.5%	3.3%	0.9%	4.6%
Elm Creek Elementary C501	9.0%	4.6%	2.8%	4.9%	1.5%	0.7%	0.5%	5.4%	2.9%	2.8%	3.5%
Fair Oaks Ranch C502	19.2%	16.8%	7.6%	6.7%	1.9%	2.7%	1.9%	6.1%	6.1%	1.4%	7.0%
Heritage Middle School C622	15.3%	9.5%	1.9%	4.2%	1.0%	2.3%	2.4%	4.5%	5.2%	5.8%	5.2%
Bulverde Elementary C503	17.7%	16.5%	7.6%	7.0%	4.5%	2.8%	1.4%	7.9%	7.7%	0.9%	7.4%
City of Garden Ridge C505	19.5%	13.2%	6.9%	5.2%	1.4%	1.4%	0.9%	8.5%	7.3%	1.4%	6.6%
New Braunfels Airport C504	17.4%	14.0%	6.3%	4.2%	0.0%	2.0%	1.4%	2.4%	2.8%	0.9%	5.1%
Seguin Outdoor Learning Center C506	9.1%	13.7%	3.8%	1.9%	0.5%	0.7%	0.5%	2.5%	0.3%	0.5%	3.3%
Percentage of All Days Exceeding 65 ppb	29.4%	23.8%	9.8%	13.6%	7.9%	8.4%	16.4%	17.3%	11.7%	10.3%	14.9%

Eight-hour daily maxima in excess of 65 ppb are associated with characteristic spatial patterns on many high ozone days. High ozone occurs at clusters of monitors located in proximity to each other on these days. Clusters of monitors that recorded elevated ozone levels were grouped based on readings above 65 ppb from 2005-2014. By selecting monitors that recorded ozone within one standard deviation of peak 8-hour values within the San Antonio area on high ozone days, spatial clusters of monitors were determined. The most common patterns of elevated ozone that were found and the percentages of all high ozone days that each pattern accounted for are as follows:

- CAMS 23, 58, 502, 503, and 505: 27.6 % Northwest
- CAMS 59, 622, and 678: 1.3 % Southeast
- CAMS 504, 506, and 675: 2.0 % Northeast
- CAMS 501 0.7% Southwest
- On more than 5 monitors 26.6% Region Wide Event
- All other combinations of monitors: 41.9%

A cluster of monitors located in the northwest San Antonio area (CAMS 23, 58, 502, 503, and 505) recorded elevated ozone values with high frequency. Combinations involving at least one of these monitors but no others in the San Antonio area accounted for 28 percent of all high ozone days. This dominant pattern suggests that winds out of the south, southeast, and east, which are frequently observed on high ozone days, arrive at the monitors after accumulating additional local ozone and ozone precursors from the urban core, power plants, cement kilns, and other industrial sources.

Another two clusters were observed in the southeastern (consisting of CAMS 59, 622, and 678) and far northeastern (CAMS 504, 506, and 675) vicinities of the San Antonio area, but these clusters accounted for far fewer days. Transported ozone precursor emissions and ozone from the north could be impacting these monitor clusters. The ozone plumes could continue farther southeast, south, and southwest while not impacting other monitors in the region. Only 0.7% of the high ozone days had only exceedances at CAMS 501 on the southwest side of San Antonio.

2.4 Day of the Week Variation

Different mixtures of emission sources, meteorological patterns, and transport can cause temporal variations in ozone formation and accumulation. It is important to determine if there is a correlation between the day of the week and ozone readings. Differences in the frequency of weekday and weekend ozone give a preliminary indication as to the most effective ozone control strategy. For example, if high ozone measurements occur on a weekday, a different mixture of emission sources could be impacting ozone formation and different control strategies may be needed to reduce peak ozone concentrations during the week versus the weekend. High ozone on the weekend may be caused by a decrease in the occurrence of a NO_X disbenefit on the weekend when NO_X emissions are reduced.

Figure 2-5 shows the number of days > 65 ppb recorded on each day of the week from 2005-2014. The red dashed lines on the chart represent the average number of high ozone days: 37 days. The days with the most high ozone days were Thursday and Friday. There were both weekday and weekend high ozone days. Between 2005 and 2014, 24% of ozone days > 65 ppb occurred on the weekends (62 days out of 259 high ozone days recorded at regulatory monitors).

Figure 2-5: Number of High Ozone Days by Day of the Week, Regulatory Monitors, 2005-2014

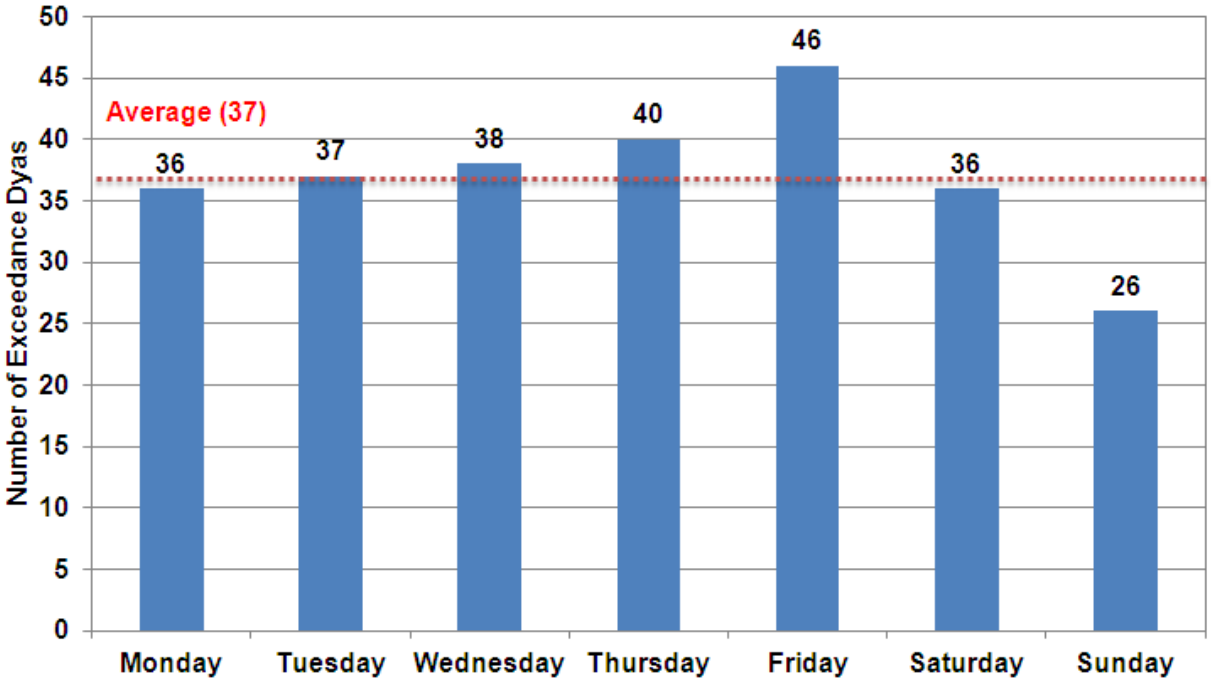

The chi-square (X^2) goodness-of-fit test[10] was performed on the day-of-the-week distribution of high ozone days for each proposed standard to determine whether the distributions are random or significant in the San Antonio region. Following is the calculation used to determine if the distribution is significant.

Equation 2-1: Chi-Square goodness-of-fit test

$$X^2 = \sum (f_o - f_e)^2 / f_e$$

Where,

X^2 = Chi-square (X^2) goodness-of-fit

f_o = Frequency of "Observed" value (from Figure 2-5)

f_e = Frequency of "Expected" value or total in sample divided by number of categories (259 high ozone days / 7 time periods = 37.0)

Chi-Square goodness-of-fit test for high ozone days' day-of-the-week frequency in San Antonio:

X^2 = 5.784

The Phi or Cramer's V test is used to determine the degree of significance of the chi-square results by eliminating sample size impact.[11] The chi-square value has a range of [0 – ∞]; when augmenting with the phi test, the results are reduced to a more manageable range of [0 – 1.0]. For a chi-square representing a uniform distribution, the phi results would be closer to 0.0.

[10] Jones, James, Professor of Mathematics, Richland Community College. "Math 170: Intro to Statistics Chapter 12 Lecture Notes". Available online: http://www.richland.edu/james/lecture/m170/ch12-fit.html. Accessed 04/27/15.

[11] Dattalo, Pat. Virginia Commonwealth University. "Nominal Association: Phi and Cramer's V." Available online: http://www.people.vcu.edu/~pdattalo/702SuppRead/MeasAssoc/NominalAssoc.html. Accessed 04/29/2015.

Equation 2-2: Cramer's V test

$$\varphi = \sqrt{X^2 / f_o}$$

Where,

φ = Phi value
X^2 = Chi-square (from Equation 2-1)
f_o = Frequency of "Observed" value (259)

The phi results for the high ozone days > 65 ppb based on daily periods:

$$\varphi = \sqrt{(5.784 / 259)}$$
$$= 0.15$$

The chi-square (X^2) goodness-of-fit test and Phi (φ) were performed on the daily distribution for high ozone days to determine if there was a significant difference in the distribution of high ozone by the day of the week. The results are not significant at 90% (5.784 chi square result < 10.645 from the probability chart for 6 degrees of freedom and 0.1 probability values).

The chi-square test confirms that, except for random variation, high ozone days ***occur with equal frequency*** in the San Antonio region for any day of the week. It is just as likely to have high ozone concentrations on one given day of the week as on another day of the week. Although the results were not significant for the 65 ppb proposed standard, the analysis did indicate a moderate Phi value. It should be kept in mind that EPA guidance recommends selecting modeling episodes that contain weekend days, if it is common for a region to have high ozone days on weekends.[12]

2.5 Ozone Diurnal Variations

Since ozone forms in the presence of ultraviolet energy from sunlight, there are variations in the ground level ozone diurnal cycle, starting from low (regional background) levels before sunrise and increasing during the morning and into the afternoon, before decreasing in the evening as energy flux from the sun ceases to drive ozone production. Another driver of ozone formation is precursor concentrations, which experience diurnal variations partly caused by mixing height levels responding to warming of the atmosphere. Ozone concentrations rise rapidly in the morning sunlight because local NO_X and VOC emissions react with precursor emissions remaining from the previous day as well as with transported emissions. Figure 2-6 provides the average high ozone day's diurnal profile based on ozone measurements recorded at C23, C58, and C678, between 2005 and 2014, for the proposed standard of 65 ppb. On average, the lowest 1-hour ozone readings at all monitors are recorded just before sunrise from 5-6 a.m.

Although the four monitors are in different parts of the city, they all show similar patterns in the morning when ozone values increase between the 6 a.m. morning minimum and the 2 p.m. afternoon peak. Comparison of the peak ozone levels at these four monitors reflects the higher average 8-hour ozone values recorded at C23 and C58, which are typically downwind monitors, compared to the other two monitors. C678 recorded the lowest ozone

[12] U.S. Environmental Protection Agency Office of Air Quality Planning and Standards Air Quality Analysis Division Air Quality Modeling Group, April 2007. "Guidance on the Use of Models and Other Analyses for Demonstrating Attainment of Air Quality Goals for Ozone, PM2.5, and Regional Haze", Research Triangle Park, North Carolina. EPA -454/B-07-002. p. 141. Available online: http://www.epa.gov/scram001/guidance/guide/final-03-pm-rh-guidance.pdf. Accessed 04/27/15.

profile during the nighttime. Since C678 is located near downtown San Antonio, this may be the result of NO_X scavenging of ozone during the nighttime. It is possible that the monitor's proximity to the urban core produces measurements that are affected by elevated NO_X emissions occurring overnight from urbanized sources and accumulating at the monitor due to light winds and limited nocturnal mixing as the mixing height retreats back toward the surface.

Figure 2-6: Average Diurnal Profiles on 65 ppb 8-Hour High Ozone Days, 2005-2014

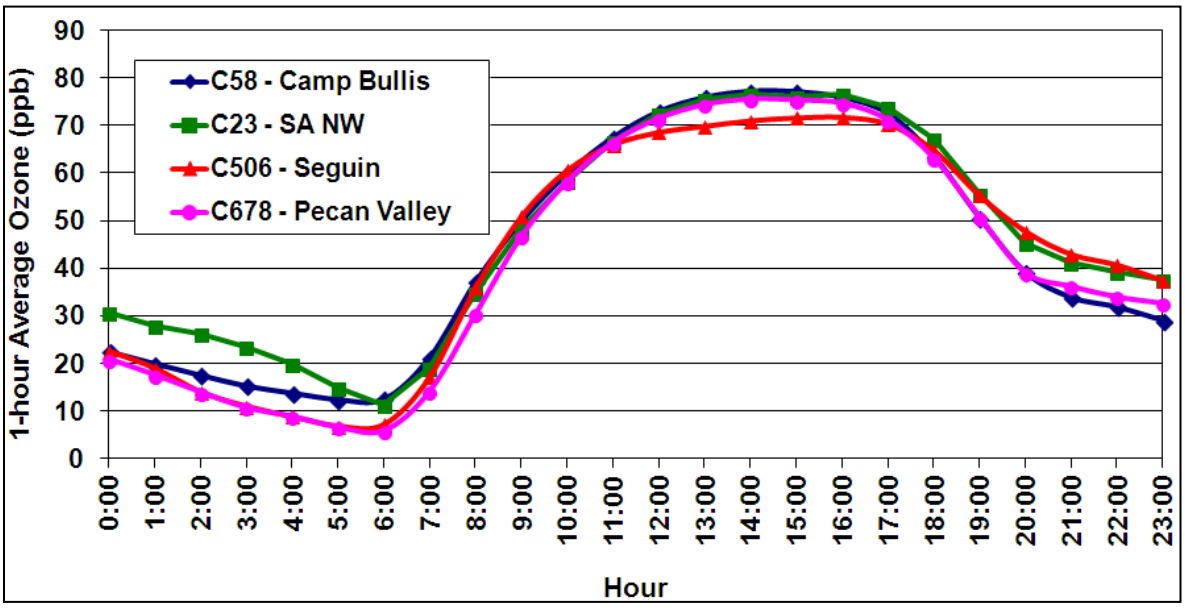

2.6 Summary of Air Quality Trends in the San Antonio Area

Analysis of local trends shows monitored ozone readings are decreasing over time and San Antonio's air quality is improving. As the ozone standard is lowered, San Antonio will have a challenge to meet the new proposed standard. Air quality trends in the San Antonio area include:

- Between 2005 and 2014, the local design value has decreased by 11.8% at C23 and 7.0% at C58.
- The 8-hour design values decreased at an average rate of 1.1 ppb per year at C23 and 0.7 ppb per year at C58 between 2005 and 2014.
- Significant reductions in the number of high ozone days of each proposed standard occurred between 2005 and 2014.
- The number of high ozone days > 65 ppb occurring in the San Antonio area decreased from 2005 to 2014, from 42 days in 2005 to 13 days in 2014, a decrease of 69%. However, 2011 experienced an increase in high ozone occurrences.
- There is a strong correlation between C23 and C58 ozone monitors for all days, indicating they are usually influenced by similar conditions. However, the two monitors have a weaker correlation on high ozone days, perhaps because weaker prevailing winds can produce narrow, concentrated ozone urban plumes that may not impact both C23 and C58 during the same high ozone event.
- Ozone readings between C502/C503 and C504/C506 monitors located northeast of San Antonio had a relatively high correlation for all days and high ozone days, likely because the pairs are either upwind or downwind of San Antonio on many days.
- Ozone readings at monitors located in southeast Bexar County, C59 and C622, had a high correlation due to their proximity to each other and positioning upwind of San Antonio or out of the path of San Antonio's urban plume on most days.
- The high R^2 values for ozone date from these monitor pairs that are located in close proximity to each other indicate, on most days, the monitors cover areas of similar meteorology and ozone-forming chemistry, and thus introduce some redundancy in the monitoring network.
- Ozone measurements at C505 were not as strongly correlated with those of C504 and C506. This might result from nearby point source plumes influencing C505.
- The 8-hour ozone design values at all monitors were above 75 ppb in 2006. By 2014, only one monitor, C58, was above 75 ppb.
- No regulatory monitor in the San Antonio region meets the 65 ppb proposed revision to the ozone NAAQS, and C23 and C58 fail to meet the 70 ppb proposed revision.
- On days when there were more than 8 monitors exceeding 65 ppb, there was a significant amount of ozone transport arriving into the region before local ozone contributions were added.
- The three non-regulatory CAMS which least frequently recorded high ozone days, C501, C504, and C506, are located either northeast or southwest of the urban area, and therefore either upwind of the city or not in the path of prevailing winds traveling over local urban areas, power plants, or large industrial facilities.
- When 8-hour daily maxima in excess of 65 ppb do occur, there is a characteristic (typical) spatial pattern where the high values were measured. A cluster of monitors located in the northwest of the San Antonio area (CAMS 23, 58, 502, 503, and 505) recorded high ozone values with high frequency. Combinations involving at least one of these monitors but no other monitors in the San Antonio area accounted for 28 percent of all high ozone days. This frequent pattern suggests that winds out of the southeast and east, which are often observed on high ozone days, allows local emissions from the urban core combine with transported emissions to produce ozone

at downwind monitors. Also, these monitors may be impacted from transported emissions northeast of San Antonio,

- Another two clusters were observed in the southeast (consisting of CAMS 59, 622, and 678) and far northeast (CAMS 504, 506, and 675) vicinities of the San Antonio area, but these clusters only accounted for few days Transported ozone precursor emissions and ozone from the north could be impacting these monitor clusters. The ozone plumes could continue farther southeast, south, and southwest while not impacting other monitors in the region.
- For all proposed standards, high ozone days occur on both weekdays and on weekends. Between 2005 and 2014, 23.9% percent of high ozone days > 65 ppb occurred on the weekends. A different mixture of emission sources could be impacting ozone formation on the weekend and different control strategies may be needed to reduce peak ozone concentrations on those days. High ozone on the weekend can be caused by a decrease in the occurrence of a NO_X disbenefit on the weekend because NO_X emissions are lower.
- Since ozone forms in the presence of ultraviolet energy from sunlight, ground level ozone concentrations vary during the diurnal cycle, starting from low ozone before sunrise and increasing during the morning and into the afternoon, and then decreasing in the evening as energy flux from the sun ceases to drive ozone production. Ozone readings rise rapidly in the morning because local NO_X and VOC emissions react with precursor emissions remaining from the previous day and transported emissions.
- Urban core monitors tended to have lower nighttime diurnal ozone readings. These readings may be due to NO_X scavenging in the urban core from vehicle and point source NO_X emissions.

3 Meteorological Conditions and Ozone Precursor Emissions in the San Antonio Area

Meteorological processes have a significant impact on ozone formation because meteorology influences the concentration, location, and transport of ozone pre-cursor emissions. Other key processes impacting ozone levels, including chemical reaction rates and some human behavior, are also influenced by meteorological factors.

Certain identifiable regional-scale meteorological pressure systems are associated with high ozone events. Prevailing wind directions, wind speeds, mixing heights, and dispersion conditions are influenced by high-pressure systems. High-pressure systems suppress vertical mixing of pollutants and influence wind direction, and are characterized by clear skies, relatively low wind speeds, and low humidity in San Antonio. These meteorological conditions typically cause ozone formation and transport of pollutants into the San Antonio area.

The study of daily weather maps,[13] courtesy of the National Oceanic and Atmospheric Administration (NOAA) Central Library Data Imaging Project, provides a means of characterizing weather patterns. As discussed, weather patterns can produce conditions suitable for the formation of ozone; therefore, weather maps were reviewed to determine meteorological patterns on high ozone days. Areas of high pressure lead to stagnant air over Texas, limited frontal movement, and clear skies typical of high ozone days. Figure 3-1 displays the NOAA weather maps for June 28, 2006 when peak 8-hour ozone in San Antonio reached 88 ppb. This is one of the days in the June 2006 photochemical modeling episode. As indicated in the figure, there was a high-pressure system over San Antonio, stagnant air, clear skies, and no precipitation during this period of high ozone. A high-pressure system occurred at both the surface level and 500-millibar height over the south central U.S. This pattern is typical of conditions on high ozone days in the San Antonio-New Braunfels MSA.

Movement of frontal and high-pressure systems can impact ozone formation in the San Antonio region. Figure 3-2 shows the movement of a front through the San Antonio region on May 14th and 15th, 2006. On both of these days, wind vectors changed and the area recorded moderate peak ozone measurements (65 ppb on May 14th and 63 ppb on May 15th). Once the frontal zone moved through the region, a high-pressure system arrived over San Antonio resulting in elevated 8-hour ozone from May 17th – 19th, 2006 at local monitors (78, 79, and 76 ppb). For the Houston area TCEQ states, “the low ozone wind pattern seems to occur when the synoptic scale pressure gradient is strong enough to result in persistent easterly and southeasterly winds.”[14] These regional meteorological patterns also increase ozone formation in the San Antonio area.

[13] NOAA National Centers for Environmental Prediction, Hydrometeorological Prediction Center. “Daily Weather Maps”. Available online: http://www.hpc.ncep.noaa.gov/dailywxmap/index.html. Accessed 04/09/15.

[14] TCEQ Technical Analysis Division, December, 2002. “Conceptual Model for Ozone Formation in the Houston-Galveston Area”. Austin, Texas. p. 1-40. Available online: http://www.tceq.state.tx.us/assets/public/implementation/air/am/docs/hgb/protocol/HGMCR_Protocol_Appendix_A.pdf. Accessed 04/13/15. Originally published in Banta, R.M., C.J. Senff, J. Nielson-Gammon, L.S. Darby, T.B. Ryerson, R.J. Alvarez, S.P. Sandberg, E.J. Williams, and M. Trainer. 2005. “A Bad Air Day in Houston”. Bulletin of the American Meteorological Society. 86(5): 657-669.

Figure 3-1: Daily Weather Maps for June 28, 2006

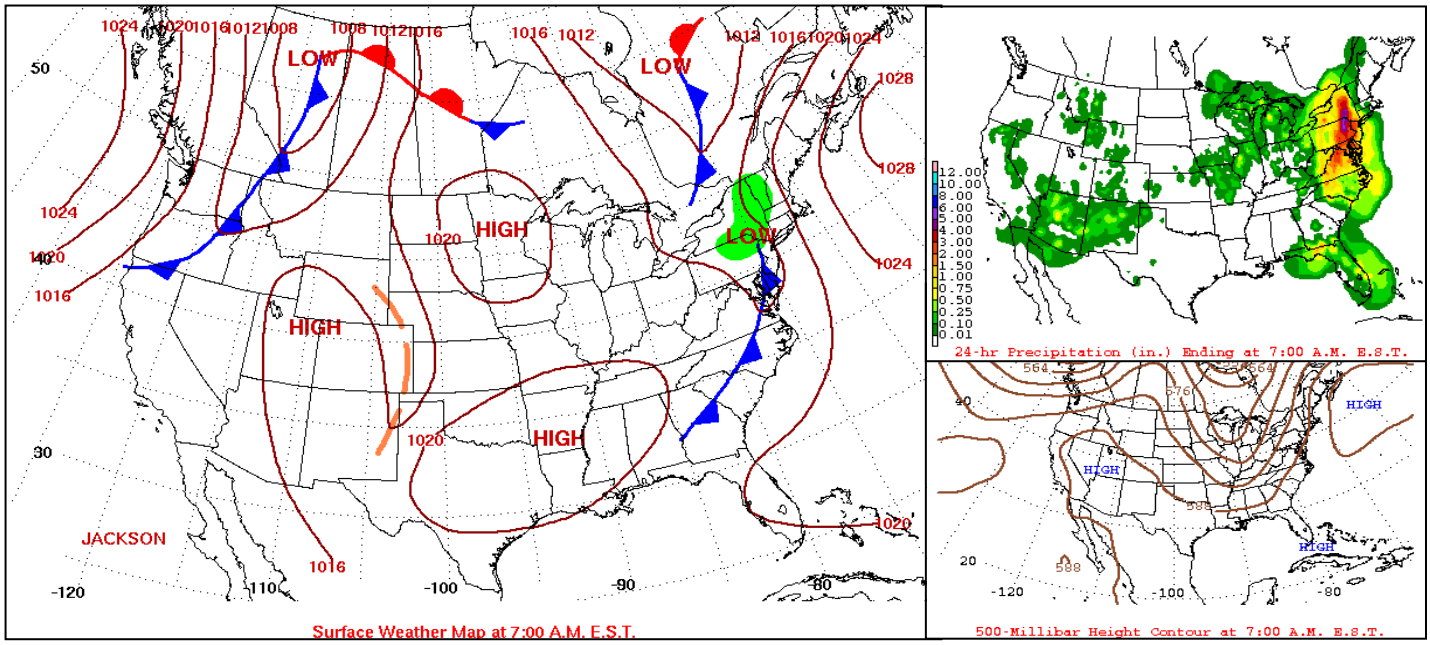

Figure 3-2: Weather Maps Indicating Cold Front: May 14, 2006 (Left) and May 15, 2006 (Right)

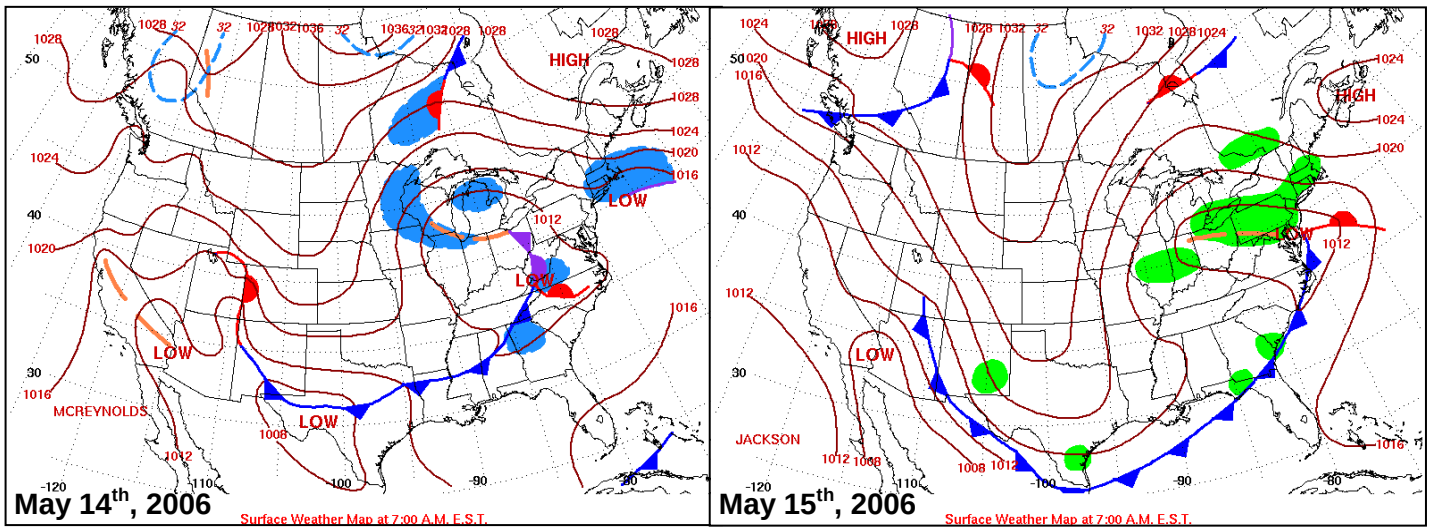

Historical meteorological data can play a significant role in identifying factors that lead to elevated ozone. Meteorological variables analyzed included precipitation, relative humidity, temperature, solar radiation, atmospheric stability, and wind speed and direction. Three criteria pollutants (NO_X, SO_2, and $PM_{2.5}$), were also analyzed. Days that had insufficient data capture rates (less than 70%) or were missing critical time periods were removed from the analysis.

The meteorological variables were determined by taking the maximum daily average among the regulatory monitors for each parameter. These were compared to the maximum 8-hour ozone concentrations for each day from 2005-2014 using ordinary least squares regression to show which parameters have the most influence on ozone formation. Additionally, these variables are correlated with each other to show the degree of collinearity among meteorological predictors of ozone. Table 3-1 and Table 3-2 show the Pearson product-moment correlation coefficients and associated R^2 values among all paired variables. The best predictors of ozone (those with the highest R^2 values) are diurnal temperature change, humidity, peak solar radiation, and 48-hr 100-m back trajectory distance. The Pearson table shows that of these four meteorological predictors, diurnal temperature change and peak solar radiation are positively correlated with ozone, while humidity and back trajectory distance are negatively correlated. This is to be expected as lower humidity enables quicker heating of the atmosphere, and is supported by the higher R^2 value for humidity-diurnal temperature change. Back trajectory distance shows a moderate inverse relationship with ozone. Shorter back trajectory distances suggest stagnant air flow, which is conducive to ozone formation due to limited mixing and venting of precursor pollutants. Larger back trajectory distances typically lead to lower ozone levels as there is sufficient mixing and venting of precursors, serving to slow the photochemical process.

Table 3-1: R^2 Table for Ozone, Meterological Parameters, and other Pollutants (All Monitors)

	Peak 8-hour Ozone	Peak NO_X	Peak SO_2	Peak $PM_{2.5}$	Diurnal Temp. Change	Morning Wind Speed[1] m/s	Afternoon Wind Speed[1] m/s	Peak Solar Radiation langleys	Peak Temp.	Back Trajectory Distance[2]	Atmos. Pressure Sea level	2 pm Humidity
Peak 8-hour Ozone	1.000											
Peak NO_X	0.134	1.000										
Peak SO_2	0.042	0.032	1.000									
Peak $PM_{2.5}$	0.031	0.005	0.012	1.000								
Diurnal Temp. Change	0.319	0.246	0.108	0.020	1.000							
Morning Wind Speed[1]	0.073	0.061	0.085	0.006	0.098	1.000						
Afternoon Wind Speed[1]	0.079	0.033	0.068	0.004	0.037	0.355	1.000					
Peak Solar Radiation	0.145	0.011	0.092	0.017	0.295	0.043	0.011	1.000				
Peak Temp.	0.004	0.009	0.091	0.065	0.053	0.066	0.038	0.261	1.000			
Back Trajectory Distance[2]	0.109	0.038	0.026	0.000	0.037	0.253	0.139	0.007	0.033	1.000		
Atmospheric Pressure	0.004	0.023	0.001	0.040	0.003	0.002	0.008	0.004	0.127	0.002	1.000	
2 pm Humidity	0.274	0.086	0.110	0.025	0.488	0.0133	0.007	0.393	0.123	0.000	0.007	1.000

[1] Wind speed is based on the monitor with the peak 8-hour ozone value
[2] Back Trajectory Distance and Direction are based on 48-hour 100-meter back trajectories ending at C58 at the peak1-hour ozone

Table 3-2: Pearson Table for Ozone, Meterological Parameters, and other Pollutants (All Monitors)

	Peak 8-hour Ozone	Peak NO_X	Peak SO_2	Peak $PM_{2.5}$	Diurnal Temp. Change	Morning Wind Speed m/s[1]	Afternoon Wind Speed m/s[1]	Peak Solar Radiation langleys	Peak Temp.	Back Trajectory Distance[2]	Atmos. Pressure Sea level	Humidity
Peak 8-hour Ozone	1.000											
Peak NO_X	0.366	1.000										
Peak SO_2	0.204	0.180	1.000									
Peak $PM_{2.5}$	0.176	0.067	0.107	1.000								
Diurnal Temp. Change	0.565	0.496	0.329	0.143	1.000							
Morning Wind Speed	-0.271	-0.247	-0.291	-0.079	-0.313	1.000						
Afternoon Wind Speed	-0.281	-0.181	-0.260	-0.060	-0.191	0.596	1.000					
Peak Solar Radiation	0.381	0.105	0.304	0.131	0.544	-0.207	-0.105	1.000				
Peak Temp.	0.066	-0.095	0.301	0.255	0.230	-0.256	-0.194	0.511	1.000			
Back Trajectory Distance[2]	-0.330	-0.196	-0.161	-0.004	-0.192	0.503	0.372	-0.083	-0.182	1.000		
Atmosphere Pressure	0.063	0.152	0.024	-0.199	0.056	-0.047	-0.089	-0.059	-0.356	-0.040	1.000	
Humidity	-0.523	-0.293	-0.332	-0.158	-0.698	0.115	0.085	-0.627	-0.351	0.001	-0.086	1.000

[1] Wind speed is based on the monitor with the peak 8-hour ozone values
[2] Back Trajectory Distance and Direction are based on 48-hour 100-meter back trajectories ending at C58 at the peak1-hour ozone

3.1 Wind Direction

C58 and C23 wind roses that compare the frequency of wind directions on high ozone days (above 65 ppb) and low ozone days (below 50 ppb) are presented in Figure 3-3 through Figure 3-10. The wind rose charts were created using WRPLOT View software developed by Lakes Environmental Software.[15] The length of the bar within each sector indicates the frequency of occurrence of a particular wind direction, while the color chart indicates the distribution of wind speeds. Surface winds were summarized by morning time period: 0600–0900 CST and afternoon time period: 1200–1500 CST. The red line represents the resulting wind direction for each wind rose. Distinguishing features in the wind roses for high ozone days, when contrasted to those of low ozone days, may help to define the wind and/or transport patterns leading to high ozone.

The distribution of observed surface winds at C58 indicates prevailing morning winds from the northwest on high ozone days. A comparison of the charts for days with 8-hour ozone averages above 65 ppb suggests air flow reversal is associated with high ozone, with winds arriving at the monitors from the northwest in the morning and shifting so that winds arrive from the southeast in the afternoon. This may result in recirculation of local and transported ozone precursor emissions. In contrast, low ozone days exhibit persistent morning and afternoon wind directions from the south to southeast. Morning winds were more likely to be calm (< 1 m/s) on days when 8-hour ozone averages exceeded 65 ppb (33.7%) than on low ozone days (13.3%).

A slightly different pattern exists at C23, with a strong tendency for winds to be from the north-northeast to northwest during the mornings on high ozone days and to shift to the east and southeast in the afternoon. Similar to C58, low ozone days at C23 exhibit a different morning wind direction from the south to southeast. High ozone days had more calm morning winds (49.4% for days when the 8-hour average exceeded 65 ppb) than days of low ozone (9.8%). Overall, morning wind speeds on high ozone days were lower than days of low ozone at C58 and C23. The mean morning wind speeds for C58 and C23 on high ozone days were 1.4 m/s and 1.1 m/s, respectively, while the mean morning wind speeds on low ozone days were 2.3 m/s at both monitors.

During the afternoon, winds tended to have a south to southeast component on all days for both high and low ozone days. For both monitors, afternoon winds were slightly more easterly on days of high ozone than on days of low ozone. Mean afternoon wind speeds at C58 on high ozone days were 2.2 m/s and 3.1 m/s on low ozone days. Mean afternoon wind speeds at C23 on high ozone days were 1.9 m/s and 2.9 m/s on low ozone days. Transport of ozone and ozone pre-cursor emissions in the morning have a greater impact on ozone formation later in the day at local monitoring sites. Although afternoon wind speeds are not as great of a determining factor for ozone production as morning wind speeds, the difference in afternoon wind speeds on high ozone days versus low ozone days at both monitors is significant at $\alpha = 0.05$.

[15] Lakes Environmental Software. May 19, 2010. "WRPLOT View: Wind Rose Plots for Meteorological Data". Version 6.5.1. Available online: http://www.lakes-environmental.com/lakewrpl.html. Accessed 04/27/15.

Figure 3-3: Morning Wind Rose on High Ozone Days (>65 ppb) at C58, 0600-0900 CST, 2005-2014

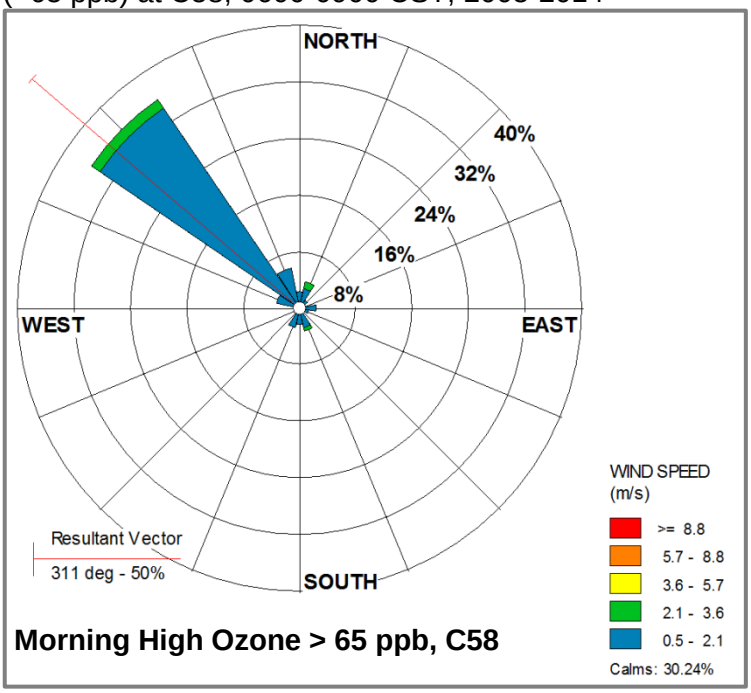

Figure 3-4: Morning Wind Rose on Low Ozone Days (<50 ppb) at C58, 0600-0900 CST, 2005-2014

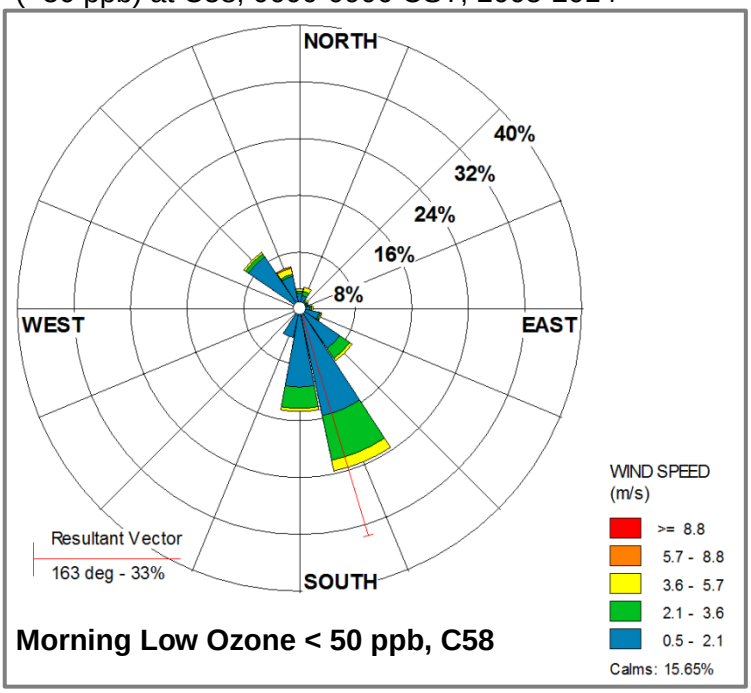

Figure 3-5: Afternoon Wind Rose on High Ozone Days (>65 ppb) at C58, 1200-1500 CST, 2005-2014

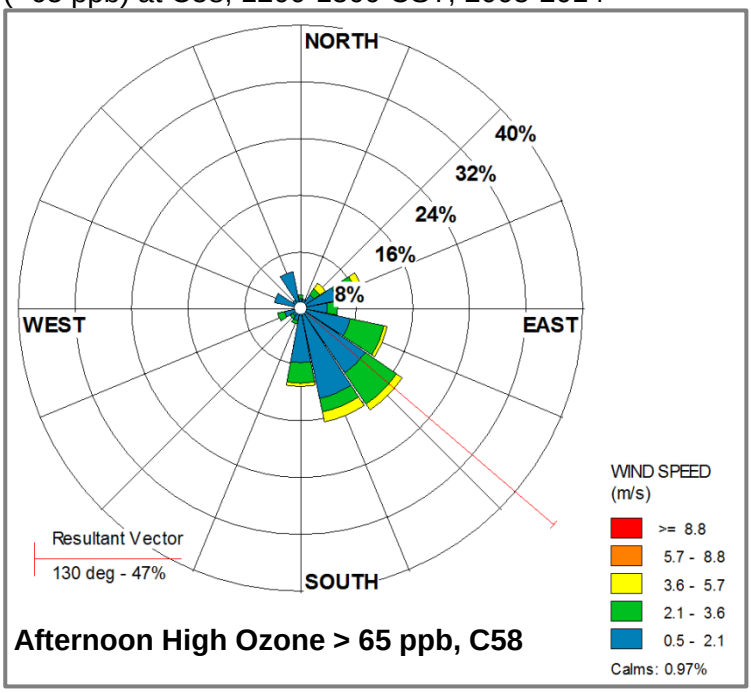

Figure 3-6: Afternoon Wind Rose on Low Ozone Days (<50 ppb) at C58, 1200-1500 CST, 2005-2014

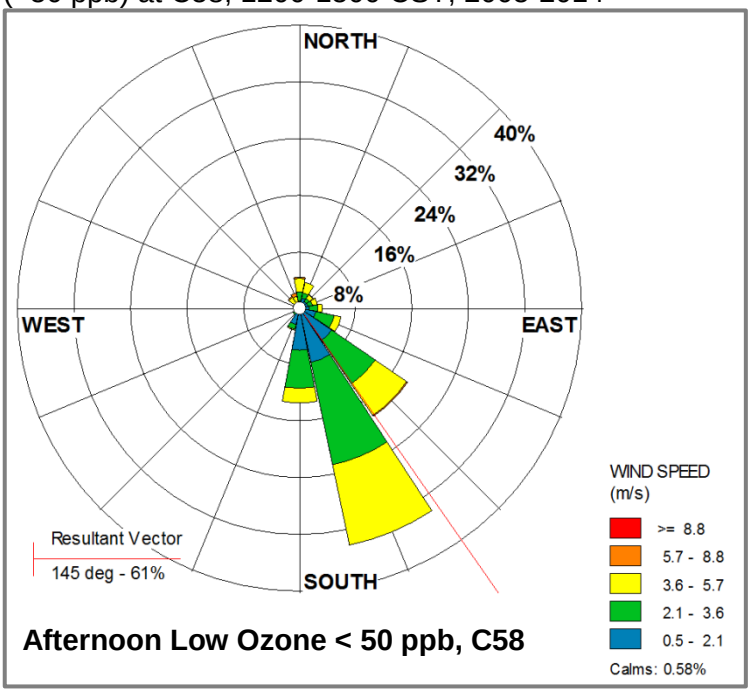

Figure 3-7: Morning Wind Rose on High Ozone Days (>65 ppb) at C23, 0600-0900 CST, 2005-2014

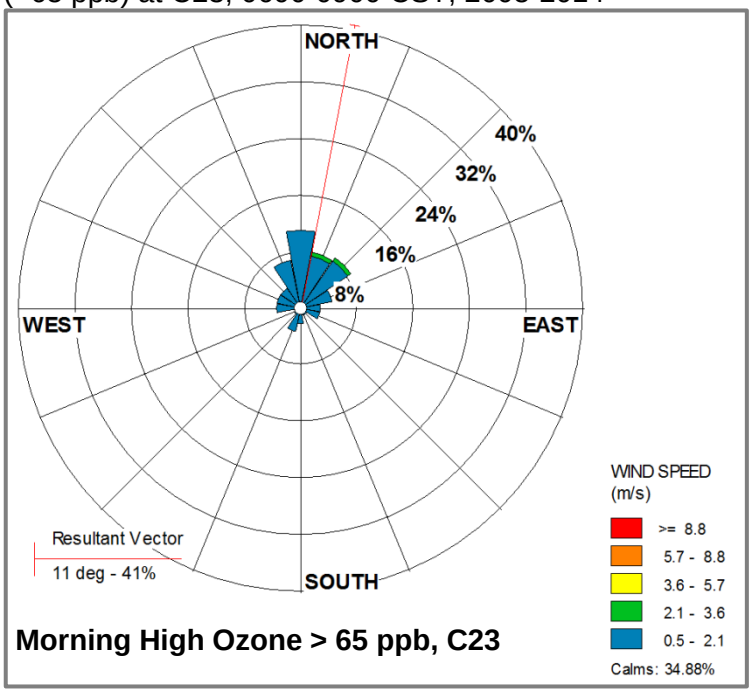

Figure 3-8: Morning Wind Rose on Low Ozone Days (<50 ppb) at C23, 0600-0900 CST, 2005-2014

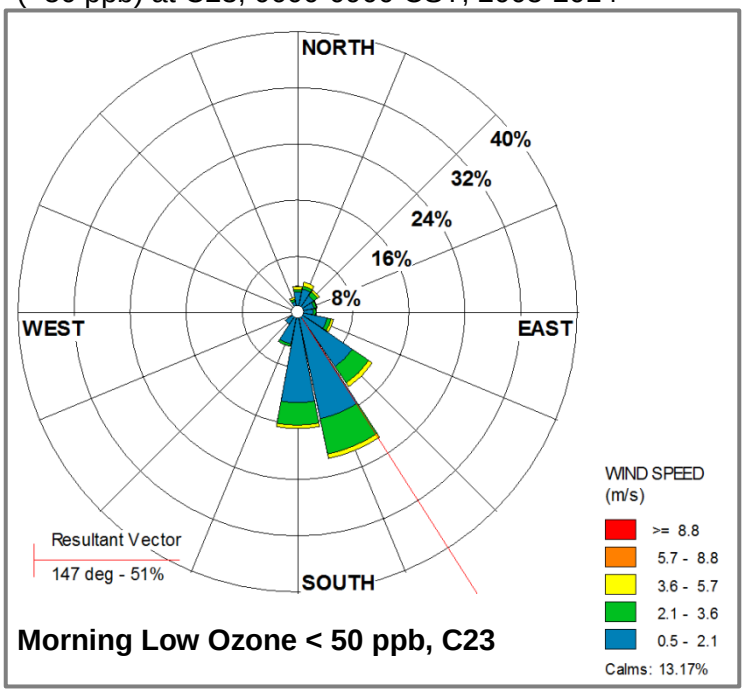

Figure 3-9: Afternoon Wind Rose on High Ozone Days (>65 ppb) at C23, 1200-1500 CST, 2005-2014

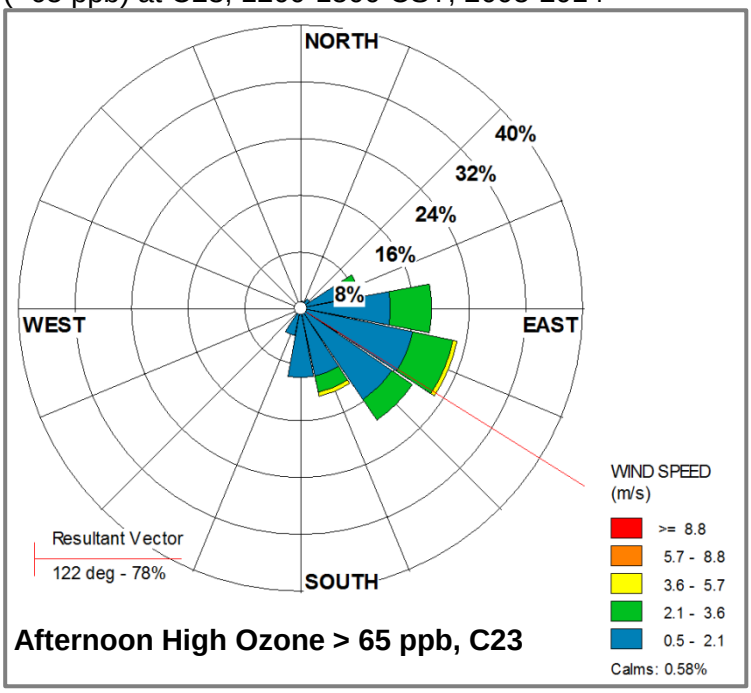

Figure 3-10: Afternoon Wind Rose on Low Ozone Days (<50 ppb) at C23, 1200-1500 CST, 2005-2014

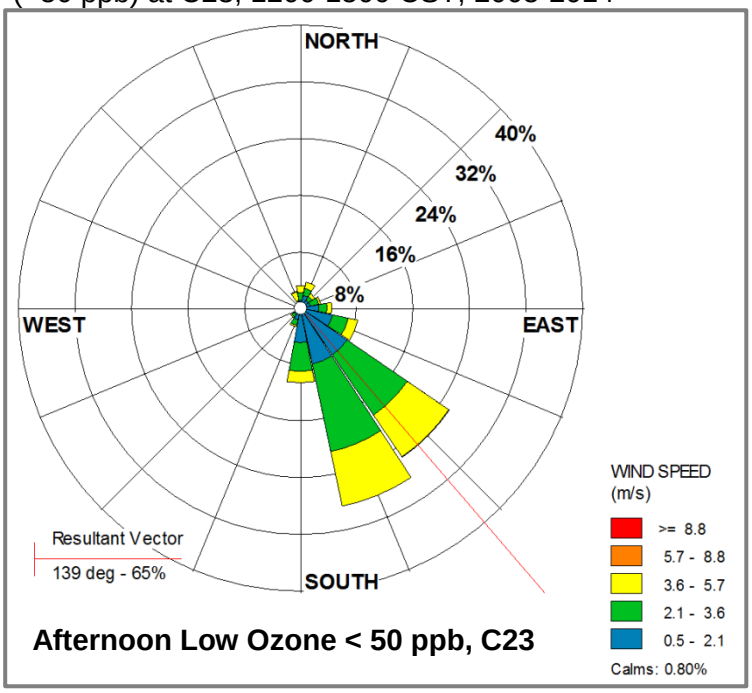

Loops of resultant wind vectors for C23 and C58 are presented in Figure 3-11 for both low ozone days and high ozone days of 8-hour ozone values above 65 ppb.[16] The average wind vectors were plotted for every hour of the day and wind speeds were represented by distance from the origin. Average ozone values during the ozone season were calculated for each hour and are represented by the color code for each data point. The daily average wind bar distance and direction were plotted as a blue arrow on the chart. The average wind vector at both CAMS tended to be from the southeast on low ozone days. The wind directions were from areas over the Gulf of Mexico that contained lower precursor emissions. The higher wind speeds associated with these days prevent accumulations of emissions and higher ozone levels in the area.

There are several different and distinct meteorological conditions that result in high ozone events in the San Antonio area. The wind vectors on high ozone days were slower and originated from the east and northeast. At C23, the wind slowly changes direction at the monitor from the north to the east in a clockwise fashion. The directions of the wind vectors indicate that there is some short distance transport of emissions from the north and northeast on high ozone days that accumulates with local and transported emissions from San Antonio to the east of the monitor later in the day to form ozone.

Analysis of C58 wind vectors shows there is often a flow reversal of winds arriving at the monitor from the northwest in the morning before 7 am on days when the 8-hour ozone average exceeds 65 ppb. In the Houston area according to the TCEQ, "under this pattern, the early morning emission plumes are pushed back over the high-emission industrial and urban areas, where they can receive a second dose of fresh emissions. The winds that cause a flow reversal can be a rapid veering pattern, a rapid backing pattern (i.e., counterclockwise wind shift), or simply an abrupt ~180° wind shift."[17] These winds can bring in recirculation of local and transported ozone precursor emissions and ozone from the previous day that combines with emissions from the east to form ozone. Local precursor, transported, and previous day emissions are accumulated in the morning from the rotating wind vectors to form high ozone readings in the afternoon under sunny conditions.

[16] Average standard deviation for all wind directions was 79 degrees at C23 and 83 degrees at C58. The average standard deviation for wind speed was 1.1 m/s at C23 and 1.4 m/s at C58.

[17] Ellis B. Cowling, Cari Furiness, Basil Dimitriades, Southern Oxidants Study Office of the Director at North Carolina State University, and David Parrish, Earth System Research Laboratory, National Oceanic and Atmospheric Administration, 31 October 2006 [8 November revision]. "Preliminary Findings from the Second Texas Air Quality Study (TexAQS II)". A Report to the Texas Commission on Environmental Quality by the TexAQS II Rapid Science Synthesis Team TCEQ Contract Number 582-4-65614. p. 21. Available online: http://www.tceq.state.tx.us/assets/public/implementation/air/am/workshop/20061012-13/RSST_Preliminary_Findings_Report_20061031.pdf. Accessed 04/29/15.

Figure 3-11: Ozone Correlation with Hourly Average Resultant Wind Bar at C23 and C58, 2005-2014

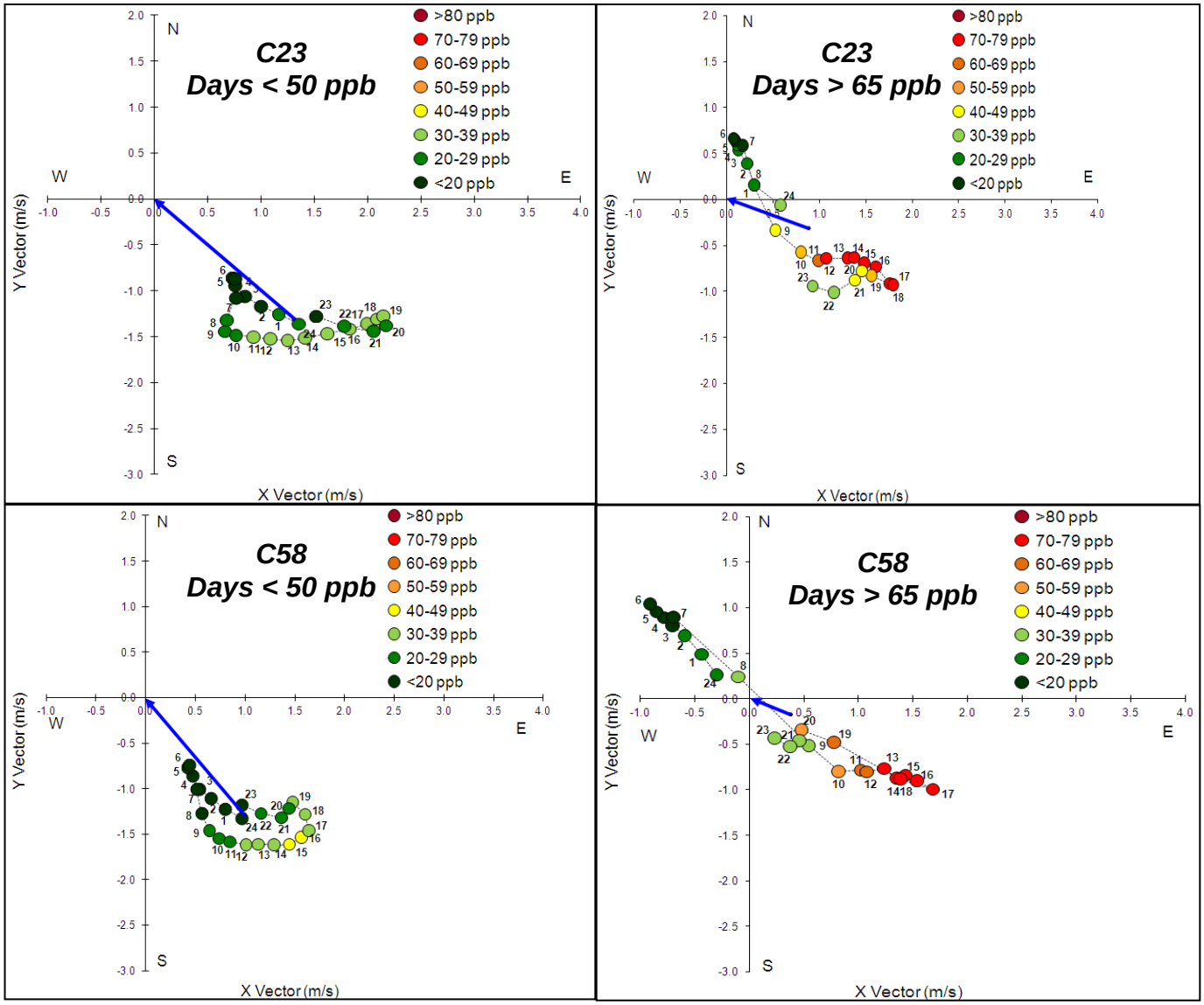

3.2 Criteria and Other Pollutants

The EPA Office of Air Quality Planning and Standards (OAQPS) sets the NAAQS for six criteria pollutants: carbon monoxide (CO), lead (Pb), nitrogen dioxide (NO_2), particulate matter (PM_{10} and $PM_{2.5}$), ozone, and sulfur dioxide (SO_2). Except for Pb, all the criteria pollutants are monitored in the San Antonio region. NO_X, SO_2, and $PM_{2.5}$ were analyzed to determine whether correlations exist between these criteria pollutants and ozone.

3.2.1 NO_X

A majority of NO_X emissions are created from the combustion of fossil fuel in on-road vehicles, power plants, cement kilns, off-road equipment, and boilers. Higher NO_X concentrations can scavenge ozone under certain conditions, so a positive correlation with ozone becomes untenable. NO_X readings at downwind monitors can be diluted before arriving while continuously forming ozone en-route, leading to a situation of elevated ozone with low NO_X concentrations.

Average ozone season NO_X concentrations reached 7.3 ppb in 2014 at C678, located east of downtown San Antonio. C58, C59, and C622 are sited in rural areas removed from major NO_X sources. Consequently, average NO_X concentrations are low at these three monitors and there is no significant difference between NO_X averages measured from 2005 to 2014. These rural sites lack major sources of ground level NO_X emissions that directly impact monitoring sites. C59 is recording low background NO_X emissions coming into the San Antonio region and there has not been a significant change ($p = 0.485$) in transported NO_X emissions from this direction in the last 10 years. This monitor site is located at ground level and below the Calaveras dam, thus it is not often impacted by the elevate stakes of CPS Energy power plants located nearby.

Since 2012, the NO_X monitoring system has been greatly expanded for the San Antonio area with C23 in the northwest reporting NO_X since October 2012, C1069 being implemented in January 2014 near one of the most heavily congested stretches of highway in the city, C1038 in Floresville in operation since 2013 and most recently, C1070 in Karnes County. The latter two monitors were implemented to investigate background emissions coming into the region from the newly-developed Eagle Ford Shale. The former two monitors are in more urban areas. Average ozone season NO_X for C1069 in 2014 was 12.5 ppb, more than 5 ppb above the average NO_X at C678 for that same year. C1038 is recording low levels of NOx, with an average NO_X concentration of 2.1 ppb for 2014. There is not enough data at any of these new monitors to determine a trend at this time.

As shown in Table 3-3 and Figure 3-12, C678 recorded significant decreases in average daily NO_X emissions from 2005 to 2014 ($p < 0.001$). Since this monitor is located within the urban core, the decrease in NO_X may be attributed to controls put on major NO_X sources including power plants and cement kilns, and additional reductions of NO_X emissions from on-road and off-road vehicles.

Table 3-3: Annual Maximum and Average NO_X Values in the San Antonio Area by Monitor

	Ozone Season Maximum Hourly NO_X (ppb)						Ozone Season Average NO_X (ppb)					
Year	C58	C59	C678	C622	C27	C23	C58	C59	C678	C622	C27	C23
2000	33.9	105.5	246.6	-	223.9	-	4.7	3.8	11.9	-	23.2	-
2001	35.7	80.2	238.8	-	305.3	-	4.3	2.3	12.6	-	23.1	-
2002	-	138.8	274.6	-	222.7	-	-	3.3	12.8	-	21.4	-
2003	72.6	101.0	262.3	-	251.2	-	2.8	4.3	12.9	-	20.8	-
2004	28.9	106.8	249.4	99.3	275.6	-	3.5	3.3	11.4	6.7	20.9	-
2005	30.1	124.0	223.3	143.6	193.1	-	4.2	3.7	10.4	6.0	19.3	-
2006	32.4	64.6	208.3	83.9	160.1	-	4.3	4.3	8.7	5.2	15.8	-
2007	42.3	95.0	187.5	148.5	230.0	-	4.3	3.6	10.1	4.0	17.7	-
2008	75.2	90.7	210.5	121.8	238.0	-	4.1	4.5	10.5	4.2	15.7	-
2009	41.5	84.0	174.0	75.9	322.0	-	3.6	3.7	8.2	5.3	13.3	-
2010	42.1	90.5	167.8	96.7	322.0	-	3.7	3.7	8.7	5.2	15.2	-
2011	39.6	47.3	174.8	73.5	-	-	4.6	3.6	6.9	4.1	-	-
2012	42.7	76.4	130.0	88.7	-	-	2.8	3.6	8.0	3.9	-	-
2013	-	85.3	163.8	108.9	-	92.4		3.7	7.8	4.5	-	3.4
2014	-	96.3	149.6	104.8	-	103.4		4.0	7.3	4.8	-	6.1

Figure 3-12: Annual Average NO_X Trends in the San Antonio Area by Monitor, 2005 – 2014[18]

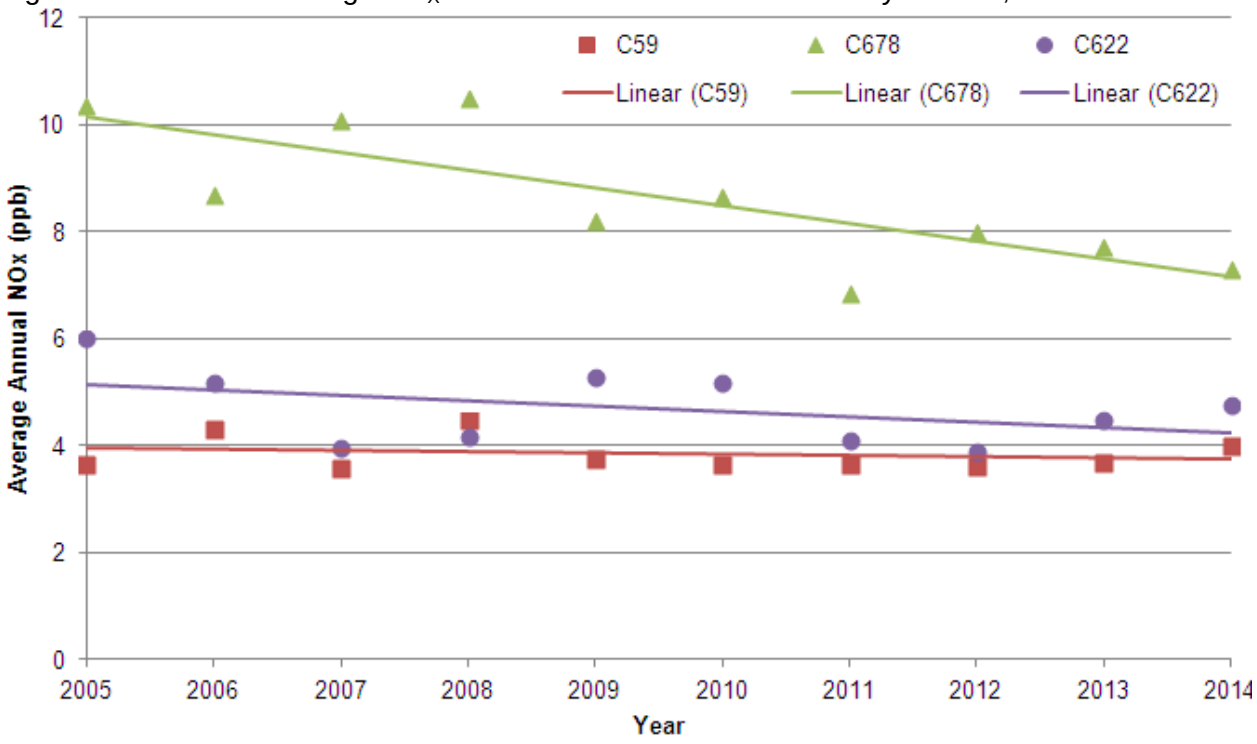

[18] Standard Deviation (σ) of NO_x emissions from 2005-2014 for each CAMS is: C678 = 1.28, C59 = 0.32, and C622 = 0.69

Hourly NO_X concentrations at each monitoring site were plotted for all days, for days with peak 8-hr ozone above 65 ppb, and for days with peak 8-hr ozone under 40 ppb. These plots are shown in Figure 3-13. The diurnal NO_X pattern is similar for each monitor, with a maximum peak between 5 am and 8 am and rapidly declining concentrations thereafter. This diurnal pattern can be attributed to both photochemical and meteorological forces. Before sunrise, there is a higher concentration of NO_X emissions at C678 relative to other area monitors due to its proximity to highways and urbanized areas. In the absence of strong synoptic scale weather systems, NO_X levels increase in the early morning hours, prior to daytime heating while the inversion layer is closer to the surface. After sunrise, NO_X emissions react with VOCs to form ozone in the presence of sunlight (Figure 3-15), which has the effect of lowering NO_X concentrations. Additionally, NO_X is diluted by the diurnal rising of the inversion layer, further lowering concentrations. After sunset, the photochemical process stops and residual ozone is destroyed by fresh NO_X emissions, which again can become trapped at or near the surface as the inversion layer retreats with the loss of daytime heating.

Figure 3-14 shows the yearly average of 8-hr ozone values and NO_X values for CAMS 59, CAMS 622, and CAMS 678. These stations are the only ones in the region that measured NO_X the entire period from 2005-2014. The yearly 8-hr ozone averages for each station roughly parallel the regional ozone design values trend from 2005-2014, with a steady decline through 2010 and a peak in 2011, followed by another decline through 2014. The R^2 and associated p-values for the relationship between average ozone and average NO_X by year from 2005-2014 are shown in Table 3-6. No monitor shows a significant correlation between yearly average ozone and yearly average NO_X, and variations in correlation strength at each monitor may be caused by other meteorological and/or photochemical factors.

Figure 3-13: NO_X Diurnal Pattern by Monitor for San Antonio, 2005-2014

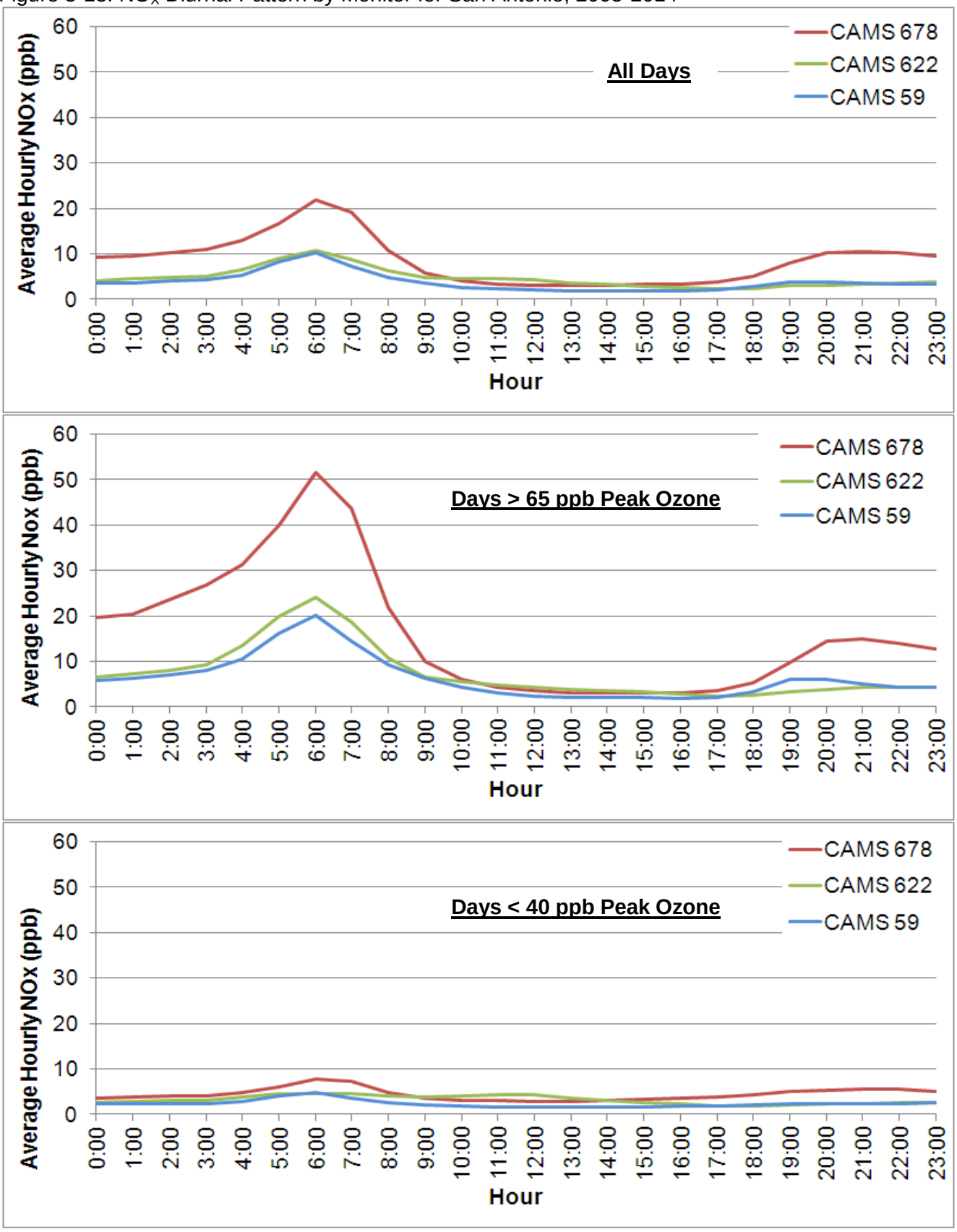

Figure 3-14: Yearly averages of 8-hr ozone and NOx for CAMS 59, 622, and 678 (2005-2014)

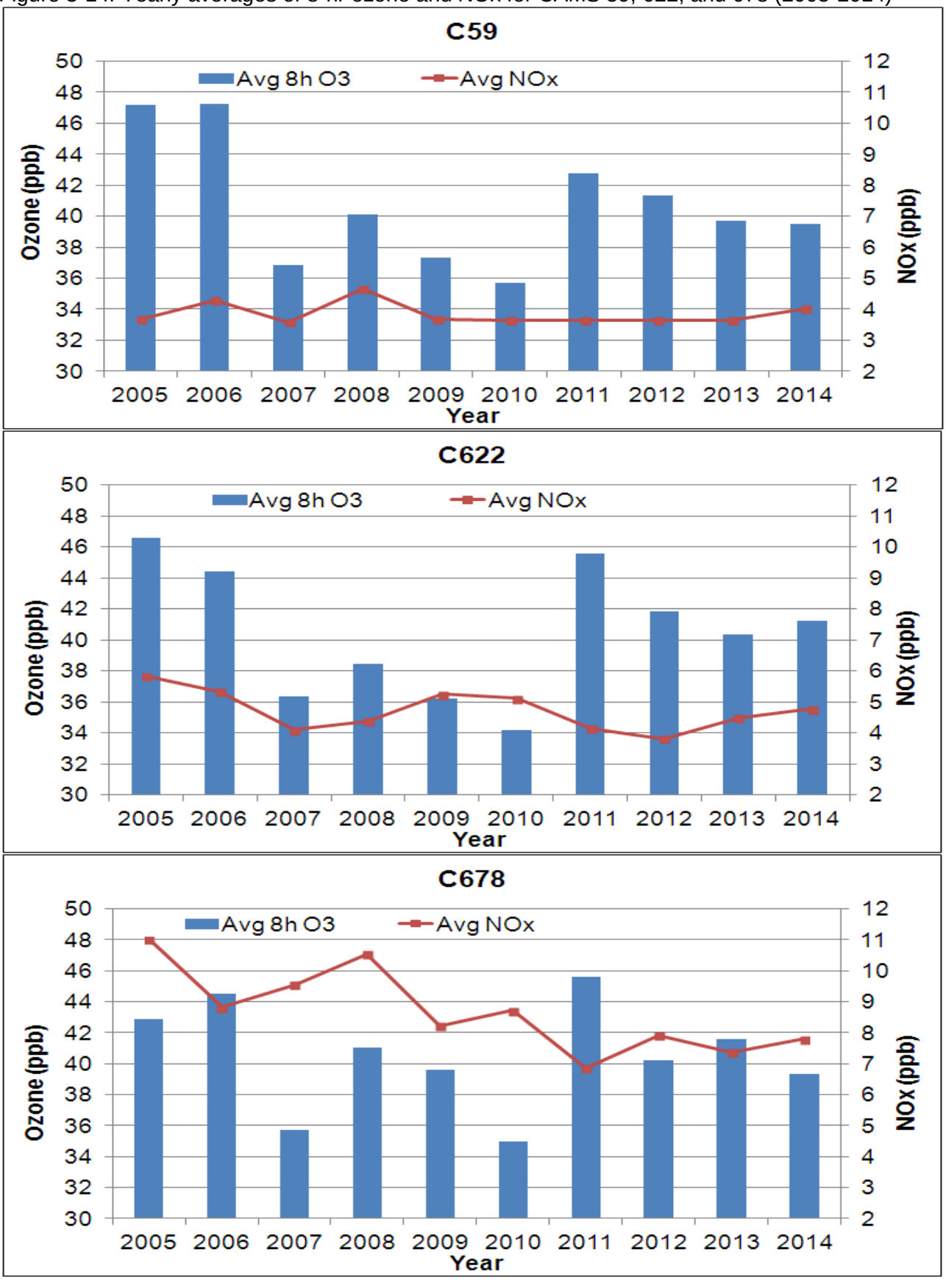

Table 3-4 shows that average NO_X values at C59 and C622 did not change significantly from 2005-2014 with p-values of 0.485 and 0.152, respectively. However, C678 did see a significant reduction in average NO_X from 2005-2014 (p = 0.007). C678 lies in the urban core of San Antonio and the reduced NO_X values at that station may be attributed to more stringent emissions standards for automobiles.

Table 3-4: Yearly average ozone and NO_X concentrations for C59, C622, and C678

	CAMS 59		CAMS 622		CAMS 678	
Year	**Avg 8-hr ozone (ppb)**	**Avg NOx (ppb)**	**Avg 8-hr ozone (ppb)**	**Avg NOx (ppb)**	**Avg 8-hr ozone (ppb)**	**Avg NOx (ppb)**
2005	47.2	3.7	46.6	5.8	42.9	11.0
2006	47.3	4.3	44.4	5.3	44.5	8.8
2007	36.8	3.6	36.4	4.1	35.7	9.6
2008	40.1	4.6	38.5	4.4	41.0	10.5
2009	37.3	3.7	36.2	5.3	39.6	8.2
2010	35.7	3.7	34.2	5.1	35.0	8.7
2011	42.8	3.6	45.6	4.1	45.6	6.9
2012	41.3	3.7	41.9	3.8	40.2	7.9
2013	39.7	3.6	40.4	4.5	41.5	7.4
2014	39.5	4.0	41.2	4.8	39.3	7.8

Figure 3-15: Percentage of Peak NO_X – Percentage of Peak Ozone by Monitor for San Antonio Area, 2005-2014 demonstrates the general relationship between NO_X and ozone concentrations which occur as diurnal cycles. Early morning hours at each of the three monitors are dominated by NO_X, as ozone has been sufficiently scavenged by the reaction of NO and ozone to form NO_2 and oxygen. NO_X concentrations are also dominant in these hours due to the surge in NO_X production in the early morning due to increased traffic and industrial activity. Beginning shortly after sunrise, ozone is produced by the reaction of NO_X and VOCs in sunlight, causing ozone concentrations to become dominant during the remaining daylight hours. After sunset, surface ozone depletion begins once again, and the process repeats itself.

Average daily NO_X concentrations were further investigated on a day of the week basis to determine if a weekday or weekend effect exists. Table 3-5 shows average daily NO_X and average daily peak 8-hr ozone at the only three monitors in the region that have continuously reported NO_X since 2005. A chi-square goodness-of-fit test for significance suggests that there is no difference between NO_X concentrations by day of the week at any monitor.[19]

[19] C59 p-value = 0.999; C622 p-value = 0.995; C678 p-value = 0.964

Figure 3-15: Percentage of Peak NO_X – Percentage of Peak Ozone by Monitor for San Antonio Area, 2005-2014

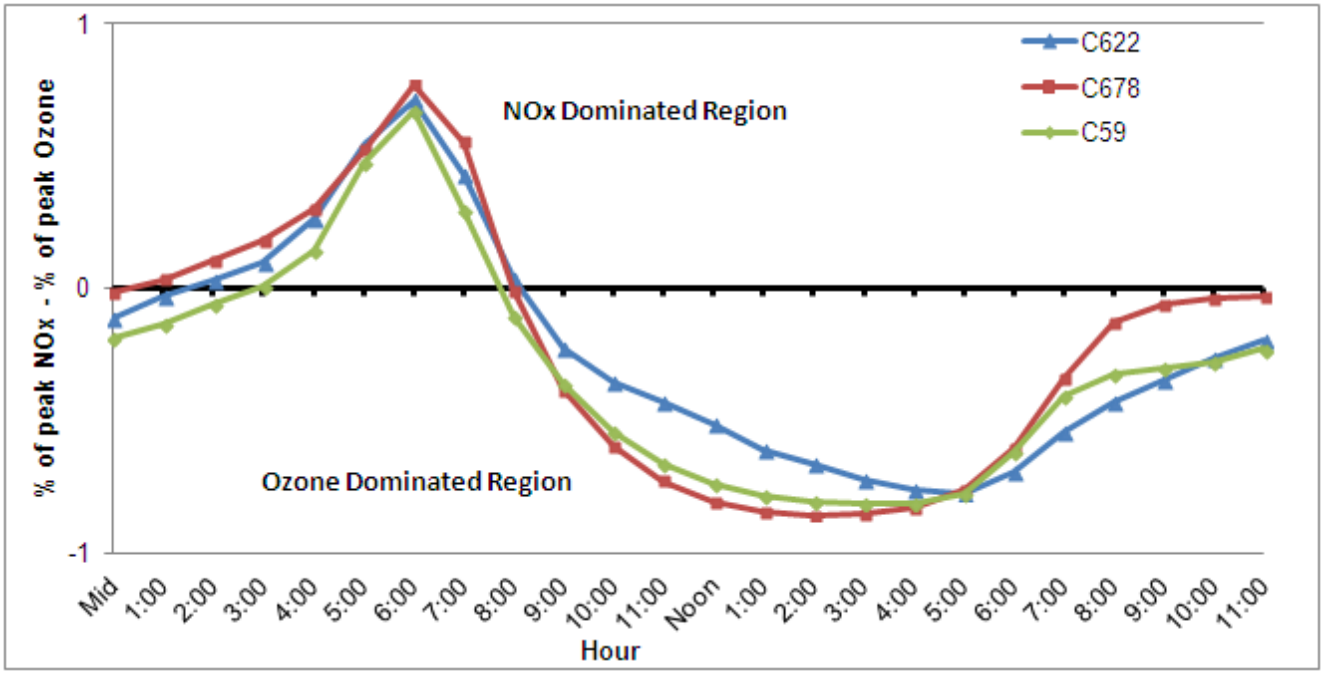

Table 3-5: Average Peak 8-Hr Ozone and Average Daily NO_X by Day of the Week, 2005 – 2014

Day of the Week	C59		C622		C678	
	Ozone (ppb)	NO_X (ppb)	Ozone (ppb)	NO_X (ppb)	Ozone (ppb)	NO_X (ppb)
Monday	40.64	3.85	40.07	4.79	39.72	8.29
Tuesday	40.83	4.39	40.33	5.30	40.60	9.84
Wednesday	41.08	4.19	40.72	5.44	40.95	9.60
Thursday	40.49	3.72	40.36	4.71	40.36	8.82
Friday	41.54	4.11	41.38	4.93	41.57	9.90
Saturday	41.03	3.50	40.94	3.92	41.02	7.56
Sunday	39.94	2.86	39.52	3.45	39.86	5.99
Weekday	40.92	4.05	40.57	5.03	40.64	9.29
Weekend	40.48	3.18	40.23	3.68	40.44	6.77

Figure 3-16 differentiates between the two most abundant species of NO_X: nitric oxide (NO) and nitrogen dioxide (NO_2) and shows that NO_2 concentrations are higher than NO in the early morning. This is due to the ozone scavenging process explained previously whereby NO becomes NO_2 and O_2 after reacting with residual ozone from the day before. NO concentrations increase faster than NO_2 during morning rush hour because NO is primarily associated with combustion from vehicles. The steep decline in NO after sunrise can be attributed to the presence of ozone which it rapidly reacts with to form NO_2. This rapid conversion process explains why there is much less NO at the surface in the daylight hours than NO_2. [20]

[20] Clean Air Technology Center (MD-12), Information Transfer and Program Integration Division, Office of Air Quality Planning and Standards, U.S. Environmental Protection Agency, November 1999. "Nitrogen Oxides (NO_X), Why and How They Are Controlled." Research Triangle Park, NC. p. 3. Available online: http://www.epa.gov/ttncatc1/dir1/fnoxdoc.pdf. Accessed 04/20/2015.

Figure 3-16: Diurnal Profile of Ozone, NO_X, Nitric Oxide (NO) and Nitrogen Dioxide (NO_2) at CAMS 678

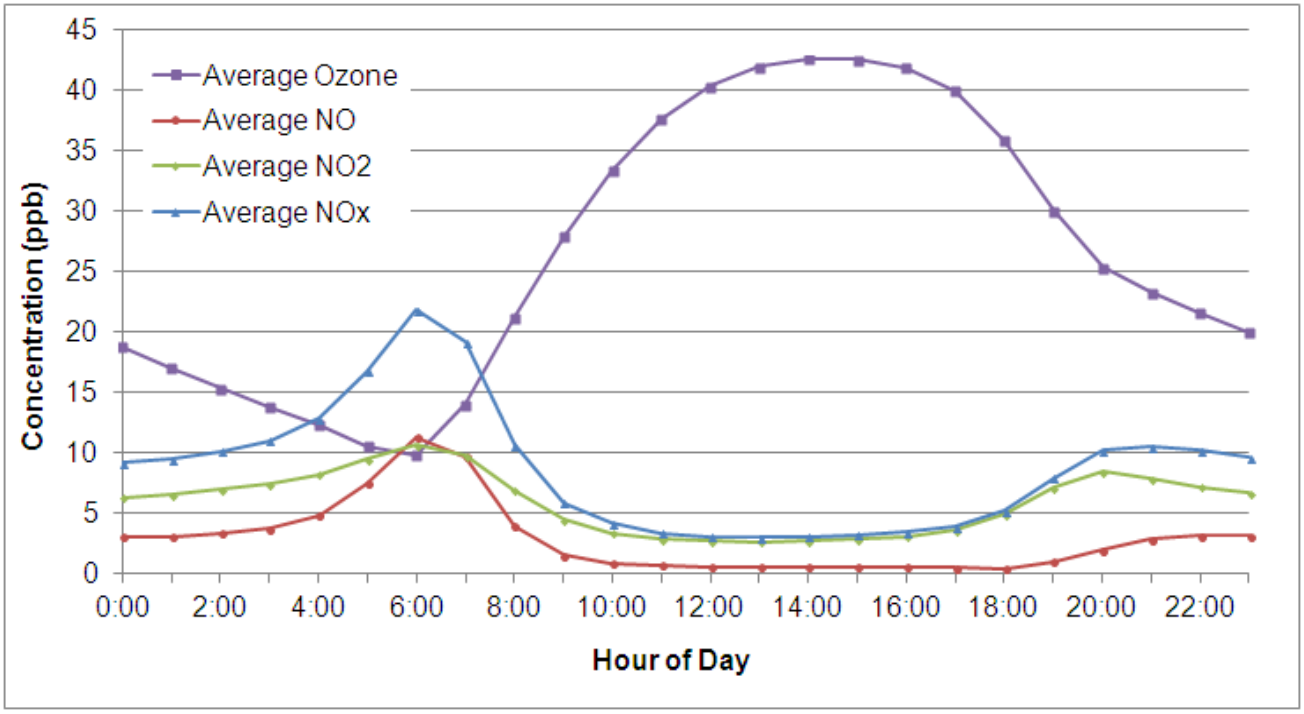

3.2.2 <u>*SO2*</u>

Figure 3-17: Daily Ozone 8-Hour Maximums and SO_2 Maximums (6 am – 2 pm) C678, 2005-2014

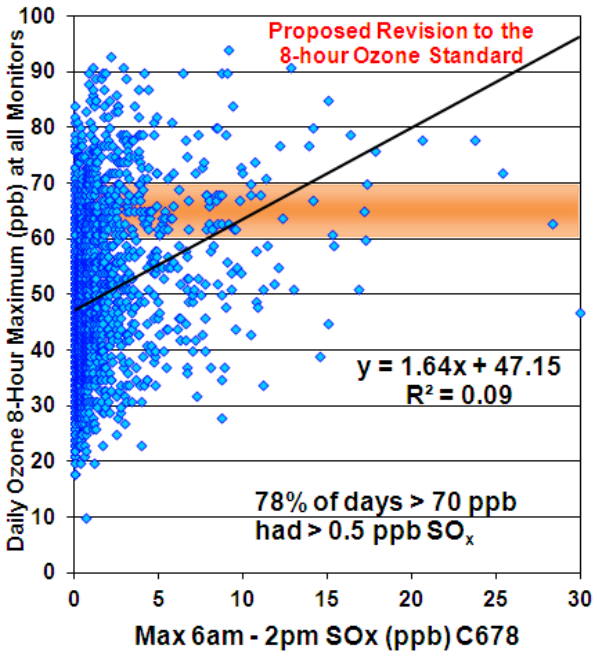

SO_2 concentrations are measured at C622 and C678. Although C59 currently reports SO_2 concentrations, there are only two years of data available. When 2005 – 2014 data collected at these monitors was compared with ozone measurements, the results indicated a very weak relationship between maximum morning SO_2 readings and maximum 8-hour ozone values (Figure 3-17). Maximum morning SO_2 was above the median of 0.5 ppb on 75 percent of the days when eight-hour ozone averages were above 65 ppb. On low ozone (<40 ppb) days, maximum morning SO_2 values were above 0.5 ppb only 25 percent of the time.

When the diurnal cycle of SO_2 emissions are plotted by hour in Figure 3-18, C622 records higher levels of SO_2 during the daytime than C678. Being located downwind of nearby power plants, C622 could be impacted by local SO_2 point source emissions. During the midday, diurnal winds typically shift to the southeast to transport SO_2 from local point sources to C622. Although SO_2 emissions are present at C678, SO_2 emissions are low and measurements decreased about 53 percent at C678 between 2005 and 2014. SO_2 emissions appear to have abruptly increased at C622 in 2013 by over 300% compared to the previous year, with a continuation of

elevated SO_2 in 2014. Additional years of data will be needed to determine if a trend of increased SO_2 concentrations is occurring or of this is due to differing meteorological conditions from year to year.

Figure 3-18: SO_2 Diurnal Pattern by Monitor for San Antonio, 2005-2014

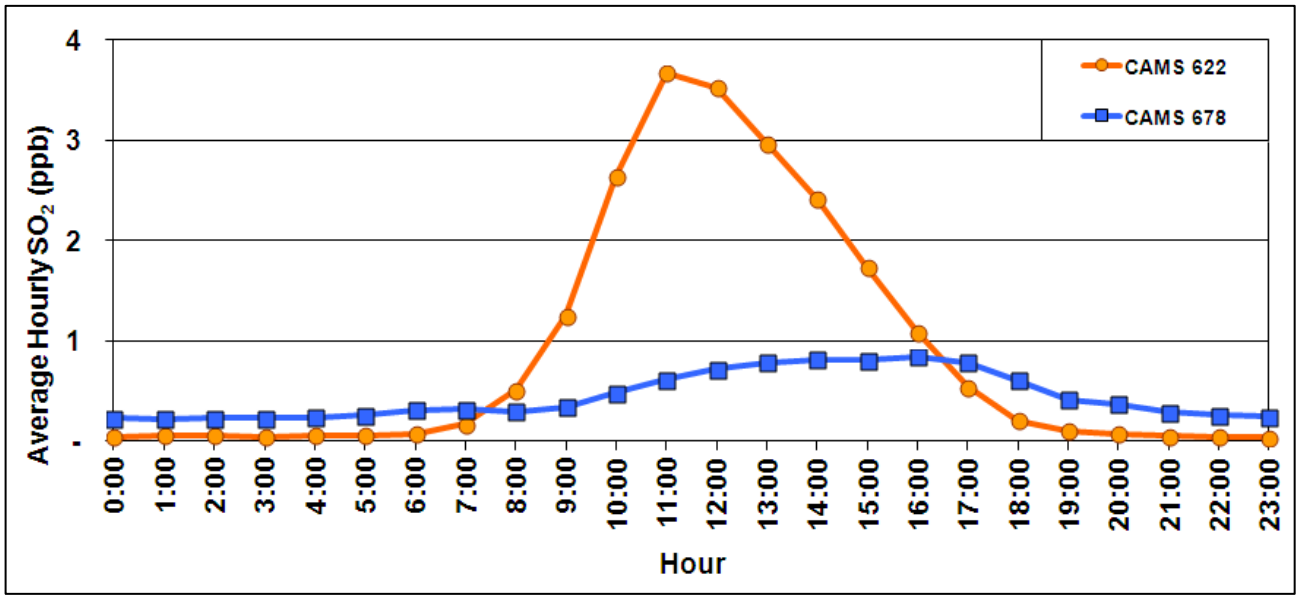

Yearly average SO_2 concentrations were graphed against the yearly average 8-hr ozone at CAMS 622 and 678 in
Figure 3-19. A simple regression between the two variables did not indicate a significant relationship between average SO_2 and ozone on a year-to-year basis. Correlation strength and p-values for each monitor are provided in
Table 3-6.

Figure 3-19: Yearly Averages of 8-Hour Ozone and SO2 for CAMS 622 and 678 (2005-2014)

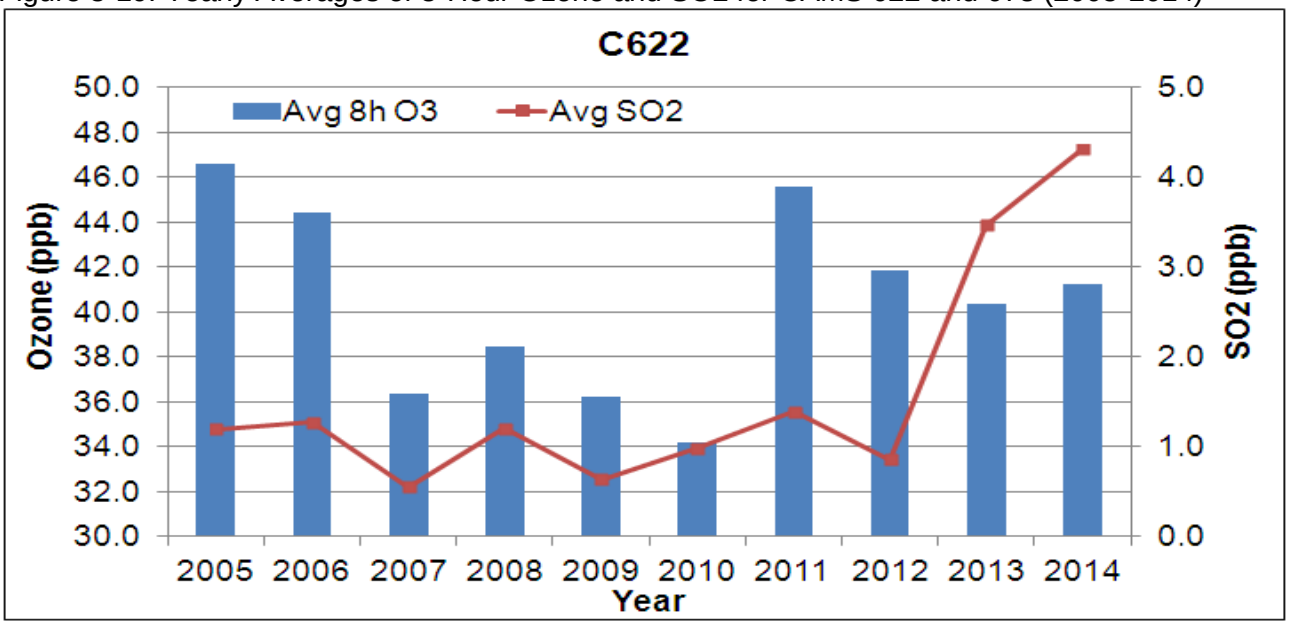

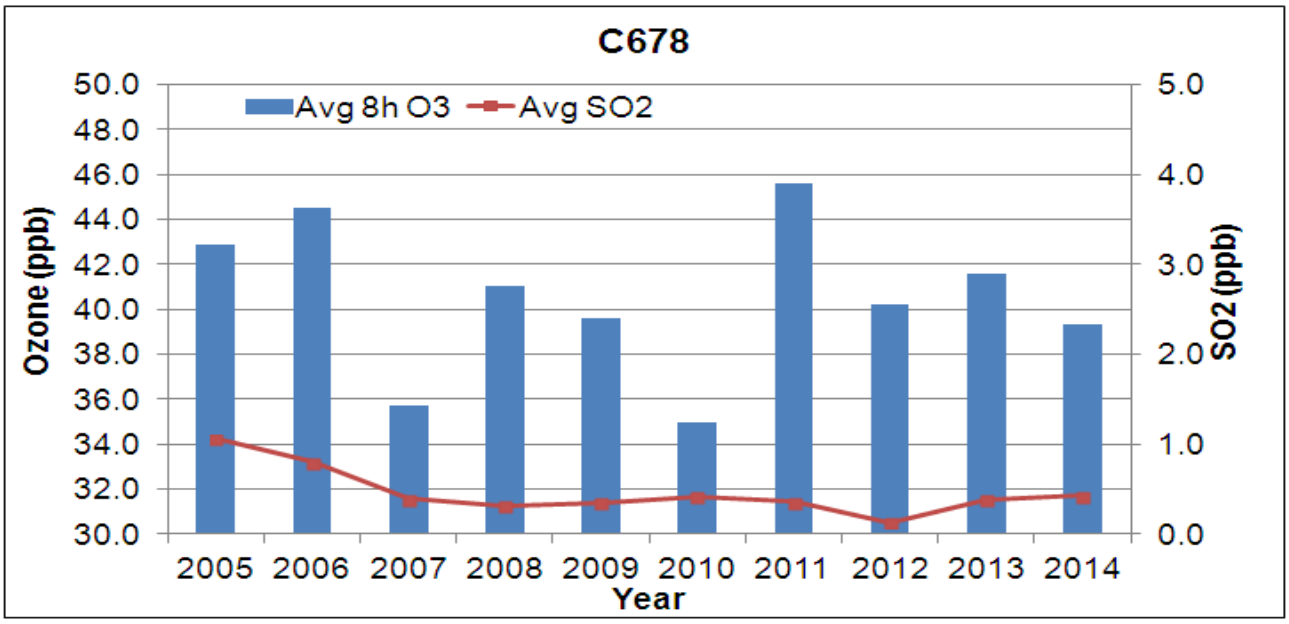

3.2.3 PM2.5

Particulate matter (PM) in the atmosphere is comprised of a variety of solids and liquids including sulfates, dust, and smoke. For the purposes of this analysis, PM particles with diameters of 2.5 micrometers or less ($PM_{2.5}$) were used because $PM_{2.5}$ can stay suspended in the atmosphere over long periods of time and be transported over great distances.

The 24-hour average $PM_{2.5}$ for the 2005-2014 ozone seasons was analyzed; although, this is not the same as the measure used for a $PM_{2.5}$ violation under the NAAQS. According to the NAAQS, "the 3-year average of the 98th percentile of 24-hour concentrations at each population-oriented monitor within an area must not exceed 35 µg/m^{3}". Also, "the 3-year average of the weighted annual mean $PM_{2.5}$ concentrations from single or multiple community-oriented monitors must not exceed 15.0 µg/m^{3}".[21] The San Antonio region is not currently in danger of violating the $PM_{2.5}$ NAAQS and all the local $PM_{2.5}$ monitors are non-regulatory. The 2012-2014 three-year average of the 24-hour 98th percentile concentration is 21.78 µg/m^3 and the 2012-2014 three-year annual mean is 8.90 µg/m^3

Figure 3-20: 8-Hour Ozone and PM2.5 Daily Averages at C301, 2005-2014

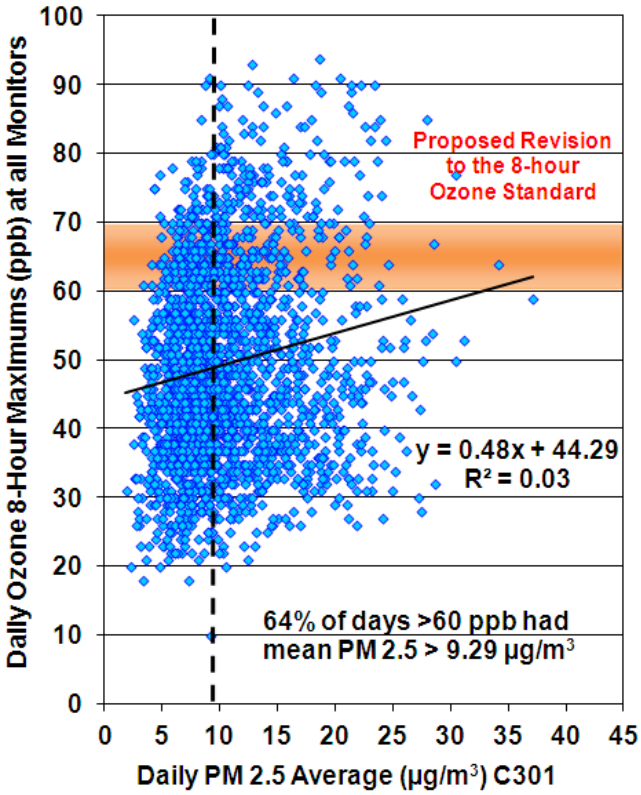

Figure 3-20 displays ozone season $PM_{2.5}$ readings at CAMS 301 plotted against daily ozone 8-hour maximums. As shown in the

[21] EPA, October 20th, 2008. "National Ambient Air Quality Standards". Available online: http://www.epa.gov/air/criteria.html. Accessed 04/22/15.

scatter plot, the relationship between $PM_{2.5}$ and 8-hour ozone peaks is very weak with an R^2 value of only 0.03. 64 percent of days when eight-hour ozone averages exceeded 60 ppb the average $PM_{2.5}$ was above the median of 9.29 µg/m^3, whereas only 44 percent of days below 40 ppb ozone had a $PM_{2.5}$ average above 9.29 µg/m^3.

It is uncertain to what extent, and under what conditions, $PM_{2.5}$ has a direct or indirect effect on ozone levels or the duration of high ozone levels. Dave Sullivan, formerly with TCEQ, offered three main points to consider when studying ozone levels in comparison to monitored PM. The main points are:

1. Air stagnation leads to air pollution accumulation; thus, many pollutants will have elevated readings when wind speeds are low. This may cause a positive correlation without a causal relationship.
2. Unlike ozone, PM is both a primary and a secondary pollutant. It is difficult to determine what portion is emitted directly and what portion is formed in the air. It can be assumed, however, that if "there is significant photochemistry forming ozone, we can expect PM to be formed also."
3. At times, the source of primary PM can also be a source of secondary ozone. This could be true in the case of a fire, which produces smoke, NO_X, and VOC.[22]

In essence, the relationship between ozone and PM cannot be simply determined. Even though the relationship may seem to have a positive correlation at times, this cannot be proved as of yet.[23] Figure 3-21 shows the lack of a clear regional relationship between PM and ozone. CAMS 59 has a significant correlation between yearly averages of 8-hr ozone and $PM_{2.5}$, although this is not necessarily a causal relationship since PM and ozone are affected by similar meteorological processes. CAMS 678 has a much weaker correlation and is not significant at $\alpha = 0.05$ (
Table 3-6).

Figure 3-21: Yearly Averages of 8-Hr Ozone and PM2.5 for CAMS 59, 622, and 678 (2005-2014)

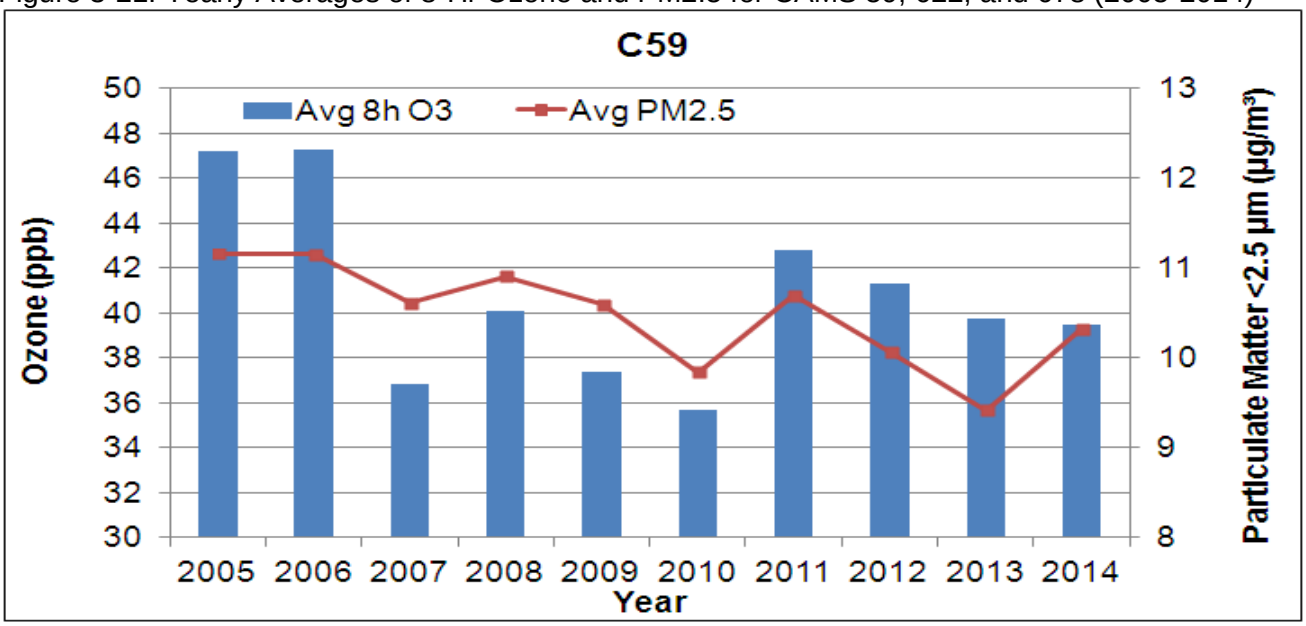

[22] TCEQ, E-mail correspondence from Dave Sullivan, Manager, Monitoring Data Management & Analysis Section, Monitoring Operations Division. Subject: Re: Ozone 2002 spreadsheet and Excuse Petition. Received 3/4/03.
[23] *Ibid*.

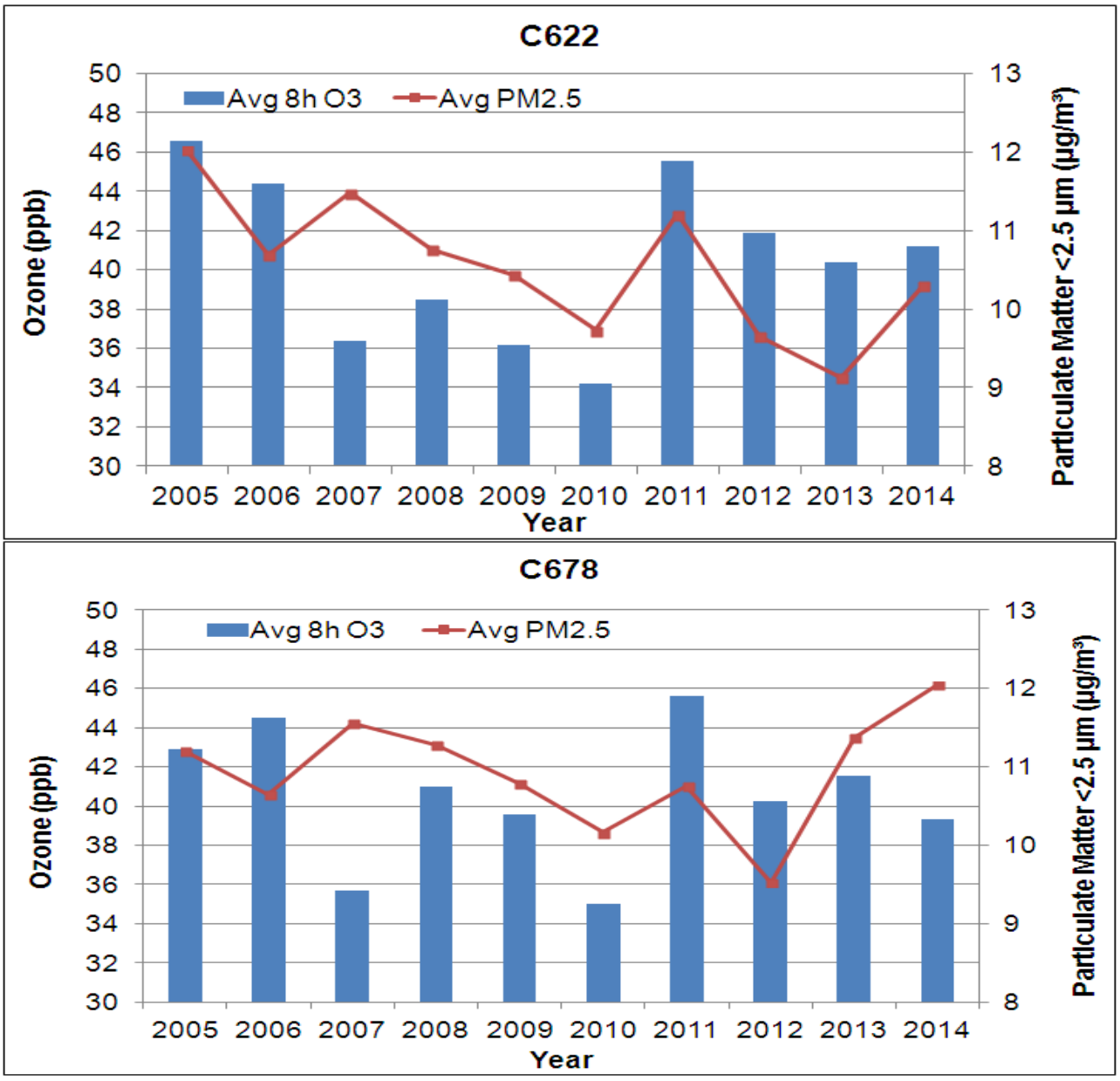

Table 3-6: R^2 and P-Values for Correlations Between Yearly Averages of Criteria Pollutants and Ozone at Selected Monitors, 2005 -- 2014

Pollutant	Monitor	R^2	p-value
NO_X	**C59**	0.068	0.267
	C622	0.020	0.549
	C678	0.024	0.513
SO_2	**C622**	0.036	0.425
	C678	0.124	0.127
$PM_{2.5}$	**C59**	0.362	0.005
	C622	0.151	0.090
	C678	0.000	0.999

A summary of the relationships between criteria pollutants and ozone is given in Table 3-6. None of the relationships showed a significant correlation, except for $PM_{2.5}$ and ozone at CAMS 59. It is unknown at this time why the correlation is so strong with that pairing, but not for the others. There is potential for further research by only including high ozone days in the analysis, or by using percentile concentration rather than average concentration.

3.3 Analysis of Upper Air Measurements

In 2005, a 915-MHz radar wind profiler (RWP), radio acoustic sounding system (RASS), and surface meteorological station were installed in Guadalupe County, east of I-35. The profiler recorded upper air measurements from June 30th to October 15th in 2005 and 2006. The data included measurements on 46 high ozone days > 60 ppb eight hour average, 22 of which were during the existing June 2006 episode.

The mixing height was calculated based on the RWP reflectivity data (or signal-to-noise ratio [SNR] data). As calculated by STI, the "RWP reflectivity data are strongly influenced by the refractive index of the atmosphere. Turbulence produces variations in atmospheric temperature, humidity, and pressure, which in turn cause variations in the radar refractive index. In the planetary boundary layer (PBL) or mixing height, humidity fluctuations contribute most to the variations in the radar refractive index."[24] Temperature data collected by RASS, coupled with surface temperature measurements, were used to provide estimates of the shallow boundary layers depths.[25]

"Viewing time-height cross-sectional plots of the SNR data can be an effective method of estimating mixing height in real time or for post-analysis. Figure 3-22 shows time-height SNR data at New Braunfels. Blue and green in the cross-section show weak signal returns, and orange and red show strong returns. The black line during daylight hours indicates the mixing height analyzed from the SNR."[26] It is important to "view SNR plots in conjunction with vertical velocity, spectral width, and RASS temperature to ensure that peak SNR properly characterizes the surface-based mixing height."[27] Since several variables are used to estimate the mixing layer, the accuracy of the calculated mixing-height may vary and should be noted when comparing the profiler data to predicted mixing height in meteorological models.

The impact of mixing height on ozone formation can be significant. On days when the peak 8-hr ozone average was less than 40 ppb, mixing heights were higher in the early morning (before 9 am) compared to high ozone days. Through the hours of 9 am to 2 pm there was a gradual rise in the mixing height level on low ozone days before leveling off in the late afternoon hours (Figure 3-23). In contrast, mixing heights on high ozone days were lower in the early morning hours. This was followed by a rapid rise in mixing height, occurring between 8 am – 2 pm, and then a leveling out through the late afternoon hours. Late afternoon mixing height was greater on high ozone days compared to the mixing heights on low ozone days.

[24] Clinton P. MacDonald and Charley A. Knoderer, December 28, 2006. "Summary Of The New Braunfels 2005 And 2006 Radar Profiler Operations and Data Availability Final Report STI-905027.12-3092A-FR". Sonoma Technology, Inc. Petaluma, CA, p. 6-1.
[25] *Ibid*.
[26] *Ibid*.
[27] *Ibid*.

Figure 3-22: Time-height Cross-Section of RWP SNR Data at New Braunfels on August 12, 2005 (Top of CBL Shown as Black Solid Line)[28]

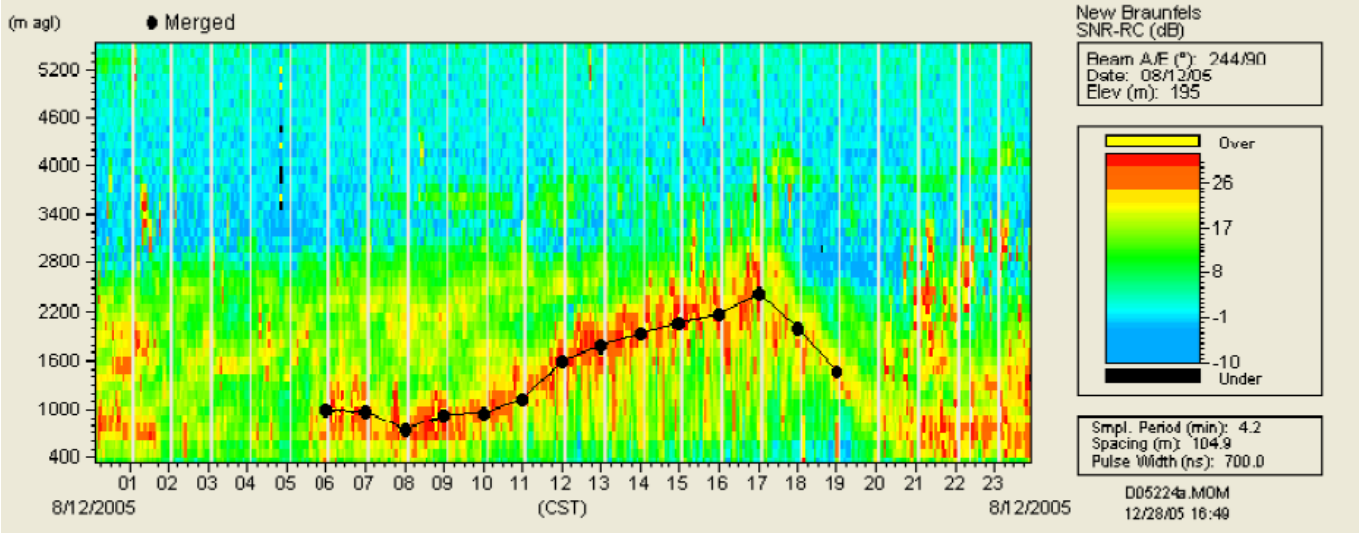

Figure 3-23: Hourly Mixing Height Measured by New Braunfels Profiler, < 40 ppb and > 75 ppb 8-Hour Average Ozone, 2005-2006[29]

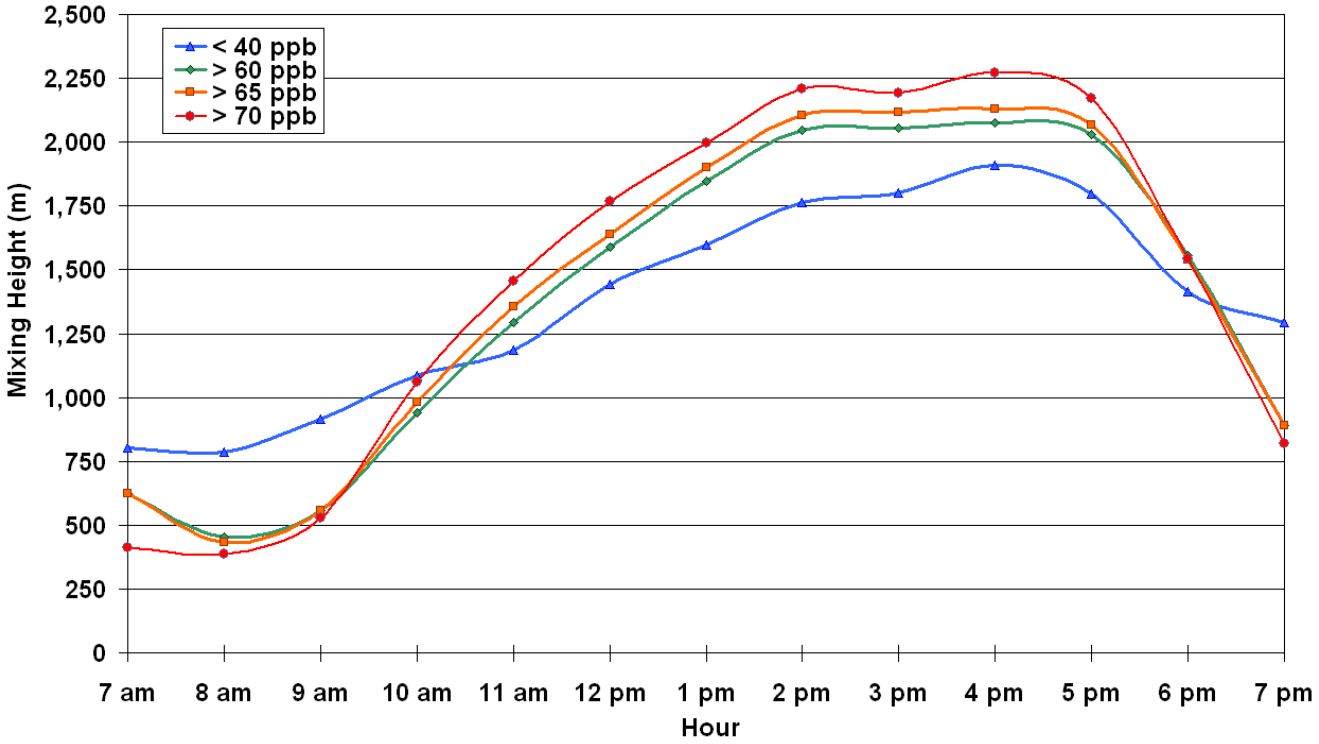

Low nighttime mixing heights can trap nocturnal pollutants from the local area as well as emissions from the previous day; when combined with a rapid rise in mixing height that allows downward mixing

[28] *Ibid.*, p. 6-2.
[29] For days > 65 ppb, the results was significant at α = 0.01 for the morning, 7 a.m. – 9 a.m. (Chi-square = 9.6) and the afternoon, noon – 5 p.m. (Chi-square = 13.3)

of transported pollutants from higher inversion layers, ozone can become significantly elevated.[30] With low wind speeds on mornings of high ozone, the "trapped" ozone concentrations from the previous day remain in the region.[31] Thus, a major factor in high ozone formation is convective activities that lead to mixing height rise. According to a study performed by the New York State Department of Environmental Conservation,

> "Occurrence and timing of convective development is crucial in terms of peak ozone since cloudiness … will act to limit insolation and halt the chemical production of surface-based ozone. The stable layer also acts to limit the vertical extent of the mixed layer, reducing "venting" of pollutants. At the same time, sufficient vertical mixing is maintained to allow transport of ozone from the layers just above the surface that can exist from the previous day's activity."[32]

Mixing height is an important consideration in evaluating the formation of ground-level ozone. Lower nighttime mixing height with low wind speed and a rapid mixing height rise in the early afternoon hours appear to be key factors in the photochemical process leading to high ozone concentrations in the San Antonio region. In the future, collection of additional upper air data could aid greatly in the analysis of ozone formation and meteorological trends that can influence ground level ozone measurements. In light of seasonal ozone patterns and changes in seasonal transport, it is particularly important to understand the effect of mixing height evolution on ozone formation. Downward mixing of ozone and ozone precursors from upper layers of the atmosphere may play an important, not fully recognized role in ground level ozone formation.

3.4 Local VOC and NO_X Emission Trends

A trend analysis of local ozone season daily VOC and NO_X emissions was developed to provide insight into historical and future emissions, while accounting for the impacts of population and economic changes. The following figure (Figure 3-24), which was generated from available historical estimates and forecasted emission factors and growth, depicts a downward trend in emissions.[33] Since population continues to rise in the region, the future reductions in emissions are significant. It is projected that NO_X emissions shall continue a downward trend, in large part due to improvements in vehicle emission standards, while VOC emissions have remained steady since 2005 and are expected to remain steady through 2023.

[30] Richard S. Artz, 2006. NOAA ARL Monthly Activity Report March 2006: "*14. Coupling of CMAQ and HYSPLIT Models,*" pp. 4-5. Available online: http://www.arl.noaa.gov/documents/activity/monthly/mar2006.pdf. Accessed on 05/10/2015.
[31] *Ibid*.
[32] Gaza, Robert S, 1997. Journal of Applied Meteorology, Article: pp. 961–977: *Mesoscale Meteorology and High Ozone in the Northeast United States*, p. 4 of 13. Available online: http://ams.allenpress.com/perlserv/?request=get-document&doi=10.1175%2F1520-0450(1998)037%3C0961%3AMMAHOI%3E2.0.CO%3B2. Accessed on 04/29/2015.
[33] AACOG, October 2013. "Emissions Trend Analysis for the San Antonio MSA: 1999, 2002, 2006, 2012, 2018, & 2023". San Antonio-Bexar County Metropolitan Planning Organization, San Antonio, Texas, p. 8-2.

Figure 3-24: Trend Lines for VOC and NOx Emissions in the San Antonio MSA 1996 to 2023

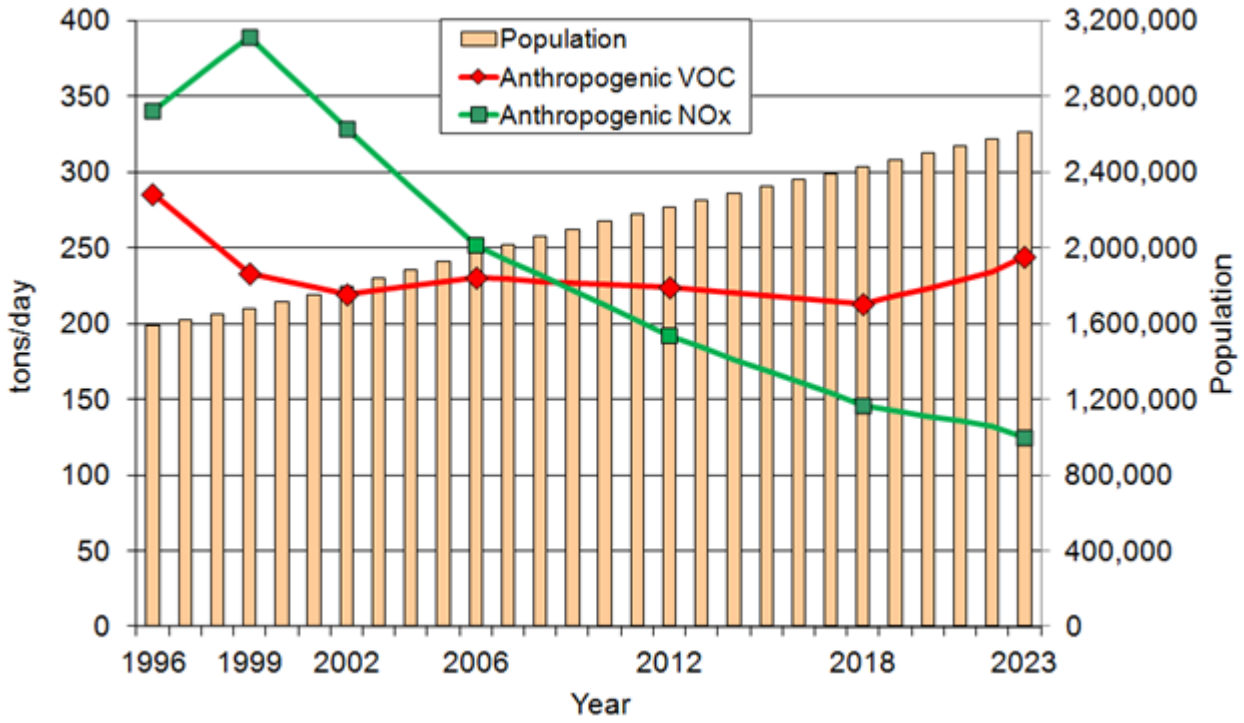

Due to federal, state, and local emission control policies, the downward trend of NO_X emissions should be sustained through 2023, despite predicted growth in population and economic activities, and the addition of several new or proposed point sources including the Spruce 2 power plant, Toyota manufacturing facility, and several new cement kilns. The MOVES model shows a downward trend in on-road emissions even with the increase in vehicle population. Texas Water Development Board provided the population projections for the San Antonio MSA.[34]

A comparison between ozone trends and local annual ozone precursor emission rates is provided in Figure 3-25 and Figure 3-26. While VOC emissions have remained steady since 2005, NO_X emission reductions are occurring. In the future, NO_X emissions are predicted to decrease further through the next decade from improvements in on-road emission controls, and this trend may result in further reductions in the design value and the frequency of high ozone days. When a multiple regression analysis was conducted for each figure above, it was found that neither design value nor number of exceedance days were adequately predicted by NOx and VOCs for a given year. The p-values for predictor variables were around 0.30 for design value and 0.50 for number of exceedance days.

[34] Texas Water Development Board. "2016 Regional and 2017 State Water Plan Projections Data". Texas. Available online: http://www.twdb.state.tx.us/waterplanning/data/projections/2017/demandproj.asp. Accessed 04/29/2015.

Figure 3-25: Ozone Design Values and Trend Lines for VOC and NOx Emissions in the San Antonio MSA, 2005 to 2014

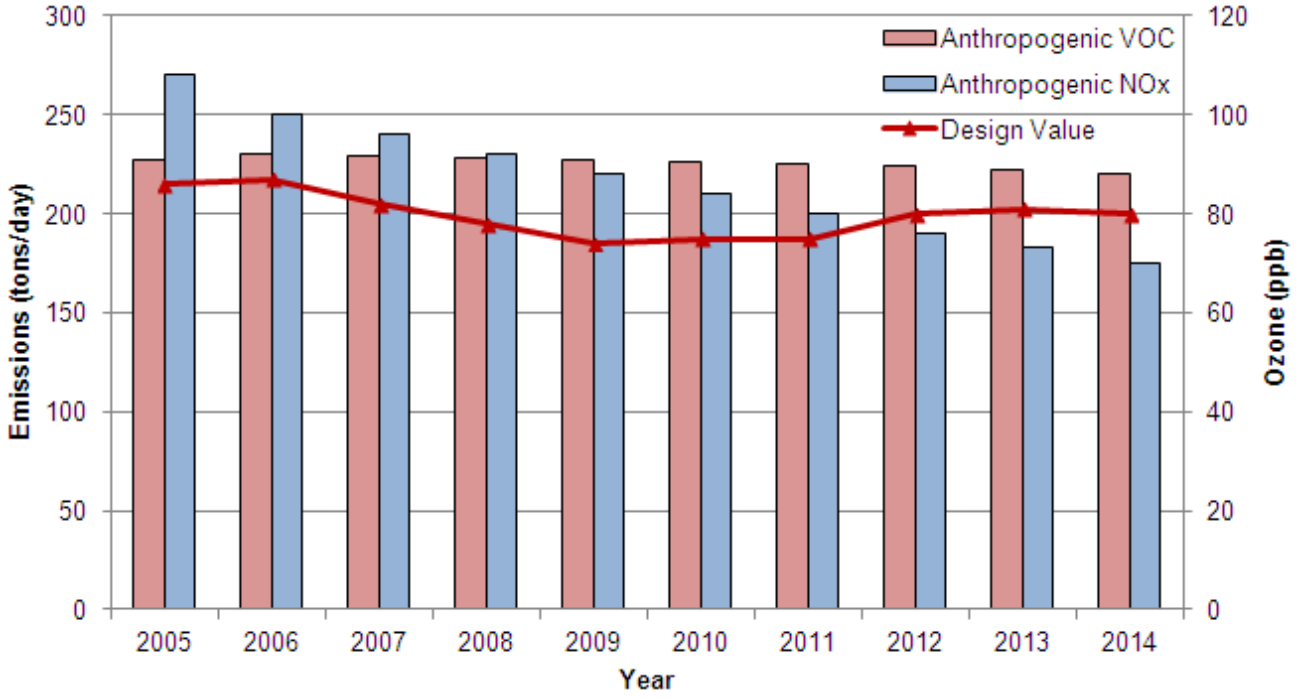

Figure 3-26: Number of High Ozone Days > 65 ppb and Trend Lines for VOC and NOx Emissions in the San Antonio MSA, 2005 to 2014

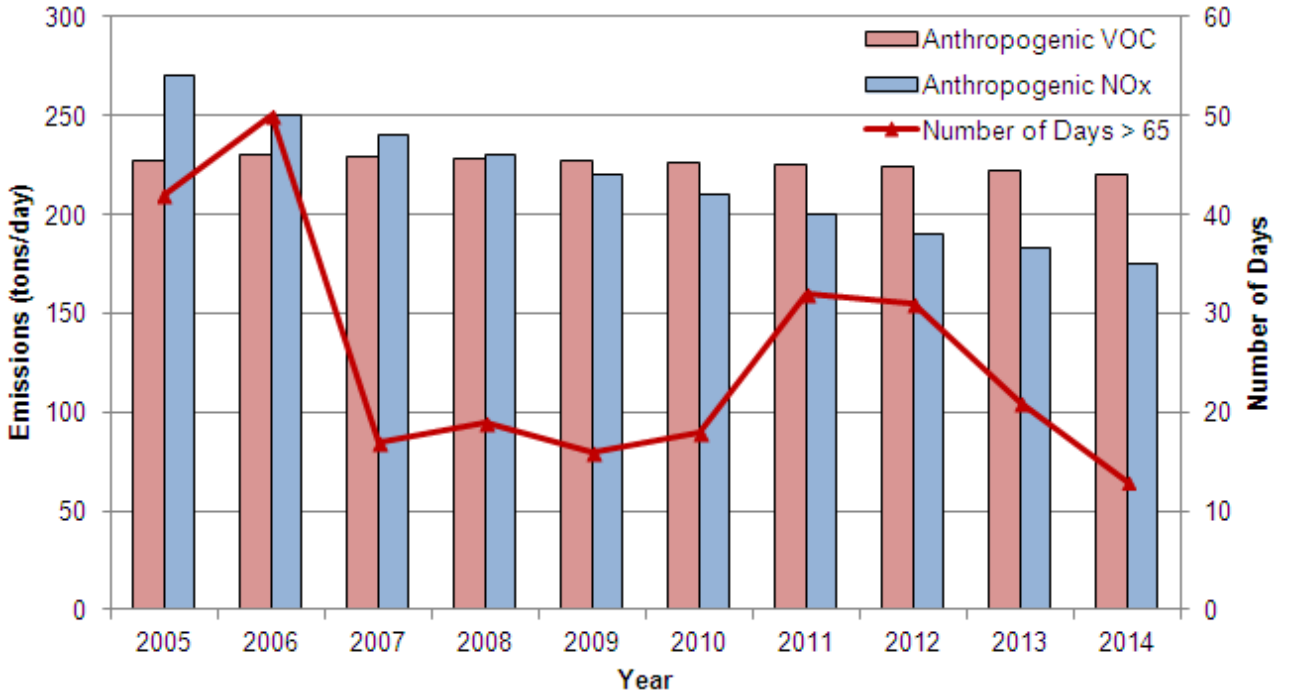

3.5 Summary of Meteorological Data and Ozone Precursor Emissions in the San Antonio Area

Preliminary analysis indicates a number of local meteorological and emission factors that contribute to elevated ozone concentrations in the San Antonio region. The following summarize the relationship between local meteorology and ozone photochemistry:

- Days with elevated ozone readings typically include stagnated winds over Texas, limited frontal movement, no precipitation, reduced mixing, and clear skies, and no strong synoptic weather systems.
- Local meteorological conditions during high ozone days include no precipitation, low atmospheric moisture content present in the afternoon, and clear skies.
- There was no significant correlation between peak ozone season temperature and ozone readings.
- Wind vectors on high ozone days were more stagnated and often originated from the east and northeast.
- At C23 on high ozone days, the wind slowly changed direction at the monitor from the north-northeast to the east-southeast in a clockwise fashion during the day.
- C58 wind vectors on high ozone days show there is a flow reversal of winds arriving at the monitors from the northwest in the morning before 7 am to arrive from the southeast in the afternoon. These winds can bring in recirculation of local ozone precursor emissions and ozone from the previous day that combines with emissions from the east to form ozone. This wind reversal with recirculation of pollutants is similar to diurnal sea-breeze patterns observed in the Houston area.
- The meteorological variables that have the strongest correlation with peak 8-hour ozone are diurnal temperature change, humidity, peak solar radiation, and back trajectory distance. Other strongly correlated pairs of meteorological variables include diurnal temperature change and humidity, peak solar radiation and humidity, and peak solar radiation and diurnal temperature change.
- There was a significant decrease in NO_X emissions from 2005 to 2014 at C678. The decrease can be attributed to controls put on major NO_X sources including power plants and cement kilns, and significant reductions of NO_X emissions from on-road vehicles.
- C59 is recording low background NO_X emissions coming into the San Antonio region from the southeast, owing to the lack of large scale low llevel NO_X sources near the monitor.
- Before sunrise, there can be significant concentrations of NO_X emissions at the C678 urban monitor. After sunrise, NO_X emissions react with VOCs to form ozone in the presence of ultraviolet energy from sunshine, which has the effect of lowering NO_X concentrations.
- There is no correlation between yearly average 8-hr ozone and yearly average NO_X or between yearly average 8-hour ozone and yearly average SO_2 for any monitor.
- There was no correlation between maximum morning SO_2 readings and ozone.
- There is a strong correlation between yearly average 8-hr ozone and yearly average PM2.5 at CAMS 59, although this is likely not a causal relationship. The meteorological conditions that cause transported $PM_{2.5}$ may contribute to a *regional* impact on ozone readings. The relationship between ozone and PM cannot be simply determined. Even though the relationship may seem to have a positive correlation at times, this cannot be proved as of yet.
- Mixing heights are typically lower in the early morning hours and experience a rapid rise in the late morning through early afternoon on high ozone days. Low nighttime mixing heights can trap nocturnal pollutants from the local area as well as emissions from the previous day. When combined with a rapid rise in mixing height that allows downward mixing of transported pollutants from higher inversion layers, ozone can become significantly elevated.
- Trend line analysis indicates local NO_X emissions should continue a downward trend, in large part due to improvements in vehicle emission standards, while local VOC emissions are expected to

remain steady. It is unclear whether this will lead to a decrease in ozone design values as there is no significant correlation between yearly ozone design values and yearly NO_X emissions.

4 Impact of the Eagle Ford Shale

"The Eagle Ford Shale is a hydrocarbon producing formation of significant importance due to its capability of producing both gas and more oil than other traditional shale plays. It contains a much higher carbonate shale percentage, upwards to 70% in south Texas, and becomes shallower and the shale content increases as it moves to the northwest. The high percentage of carbonate makes it more brittle and 'fracable'."[35] Hydraulic fracturing is a technological advancement which allows producers to recover natural gas and oil resources from these shale formations. "Experts have known for years that natural gas and oil deposits existed in deep shale formations, but until recently the vast quantities of natural gas and oil in these formations were not able to be technically or economically recoverable."[36] Today, significant amounts of natural gas and oil from deep shale formations across the United States are being produced through the use of horizontal drilling and hydraulic fracturing.[37]

Hydraulic fracturing is the process of creating fissures, or fractures, in underground formations to allow natural gas and oil to flow up the wellbore to a pipeline or tank battery. In the Eagle Ford Shale, product is extracted by pumping "water, sand and other additives under high pressure into the formation to create fractures. The fluid is approximately 98% water and sand, along with a small amount of special-purpose additives. The newly created fractures are "propped" open by the sand, which allows the natural gas and oil to flow into the wellbore and be collected at the surface. Variables such as surrounding rock formations and thickness of the targeted shale formation are studied by scientists before fracking is conducted."[38] Unlike the Haynesville and Barnett Shale formations in northern Texas that primarily produce gas, the Eagle Ford Shale features high oil yields and wet gas/condensate across much of the play. Consequently, equipment types, processes, and activities in the Eagle Ford may differ from those employed in more traditional shale formations. Emission processes addressed in the inventory include exploration and pad construction, drilling, hydraulic fracturing and completion operations, production, and midstream facilities. Emissions sources can include drill rigs, compressors, pumps, heaters, other non-road equipment, process emissions, flares, storage tanks, and fugitive emissions. Figure 4-1 shows the rapid increase in the Eagle Ford production since 2008.

[35] Railroad Commission of Texas, April 27, 2015. "Eagle Ford Shale Information". Austin, Texas. Available online: http://www.rrc.state.tx.us/oil-gas/major-oil-gas-formations/eagle-ford-shale/. Accessed 04/29/2015.
[36] Chesapeake Energy, May 2012. "Eagle Ford Shale Hydraulic Fracturing". Available online: http://sustainabilityproblems.wikispaces.com/file/view/Eagle+Ford+Shale+Hydraulic+Fracturing+Fact+Sheet.pdf. Accessed: 04/29/2015.
[37] *Ibid*.
[38] *Ibid*.

Figure 4-1: Oil, Natural Gas, and Condensate Liquid Production in the Eagle Ford Shale Formation, 2008-2014[39]

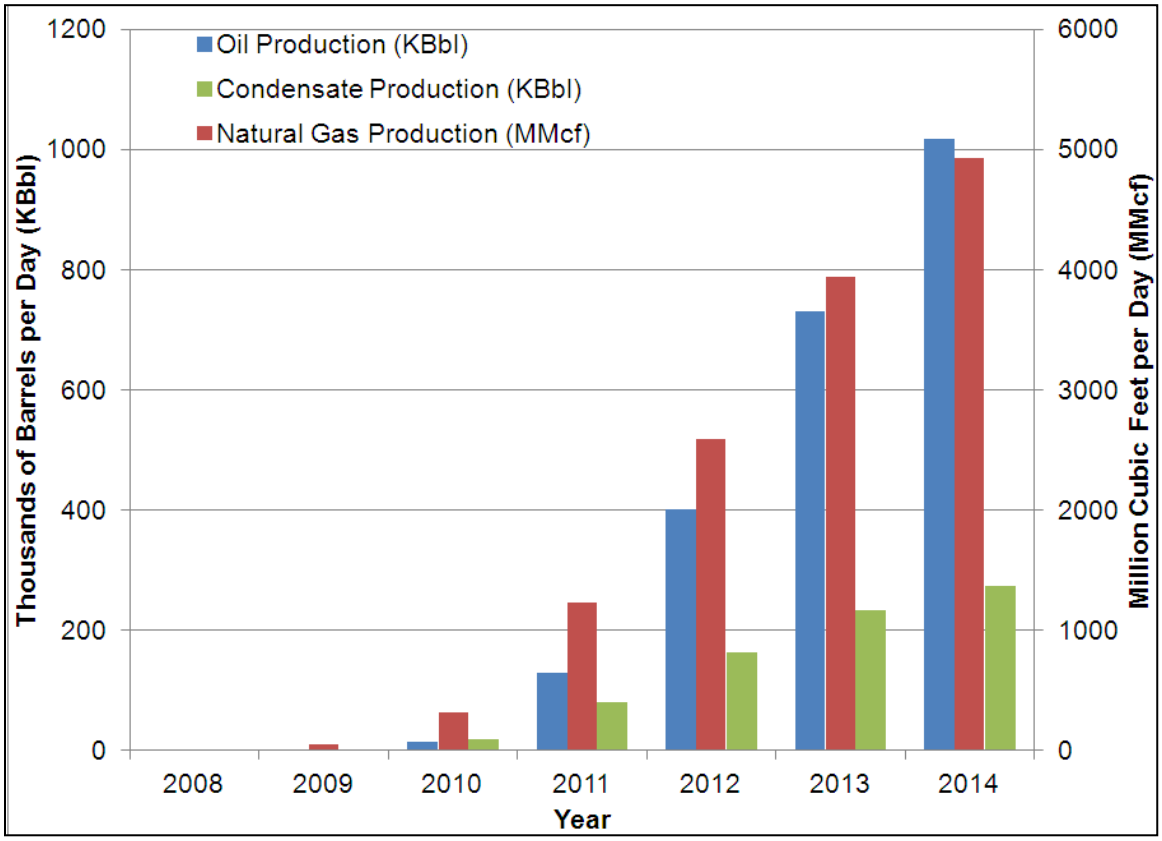

4.1 Eagle Ford Emission Inventory

Production in the Eagle Ford emitted 193 tons of NO_X and 310 tons of VOC per ozone season day in 2012 (Table 4-1). NO_X emissions increase slightly for the low development scenario in 2018 (219 tons per day). NO_X emissions also increase under the 2018 moderate scenario (302 tons per day) and the high scenario (423 tons per day). By 2018, VOC emissions are expected to increase significantly to 689 tons per ozone season day under the low development scenario and to 1,248 tons per ozone season day under the high development scenario

Table 4-1: Emissions Summary for the Eagle Ford, 2012 and 2018.

Year	Scenario	VOC	NO_X	CO
2012	All Scenarios	223	121	139
2018	Low Development	689	219	481
	Moderate Development	929	302	674
	High Development	1,248	423	927

A significant portion of NO_X emissions from oil and gas operations in the Eagle Ford in 2012 were emitted by drill rigs and well hydraulic pump engines (33% from Figure 4-2). By 2018, these sources are expected to account for only 2% of the NO_X emissions from the Eagle

[39] Railroad Commission of Texas. "Eagle Ford Shale Information." Texas. Available online: http://www.rrc.state.tx.us/oil-gas/major-oil-gas-formations/eagle-ford-shale/. Accessed: 04/15/2015

Ford as equipment turnover replaces older engines with those that meet TIER4 standards. In contrast, compressors and mid-stream sources accounted for 35% of the NO_X emissions in 2012, but are projected to increase to 85% of total NO_X emissions under the 2018 moderate development scenario because of the significant increase in oil and gas production that's expected in the region. Other sources of NO_X emissions in 2018 include production flares (7%).

The majority of VOC emissions in the 2018 moderate scenario are from storage tanks (29%), mid-stream sources (29%), and loading loss (27%). Other significant sources of VOC emissions are pneumatic devices (7%), production flares (5%), and fugitives (2%). Table 4-1 provides a detailed breakdown of NO_X and VOC emissions for each projection year scenario.

Figure 4-2: NO_X and VOC Emissions by Source Category, Eagle Ford Moderate Scenario

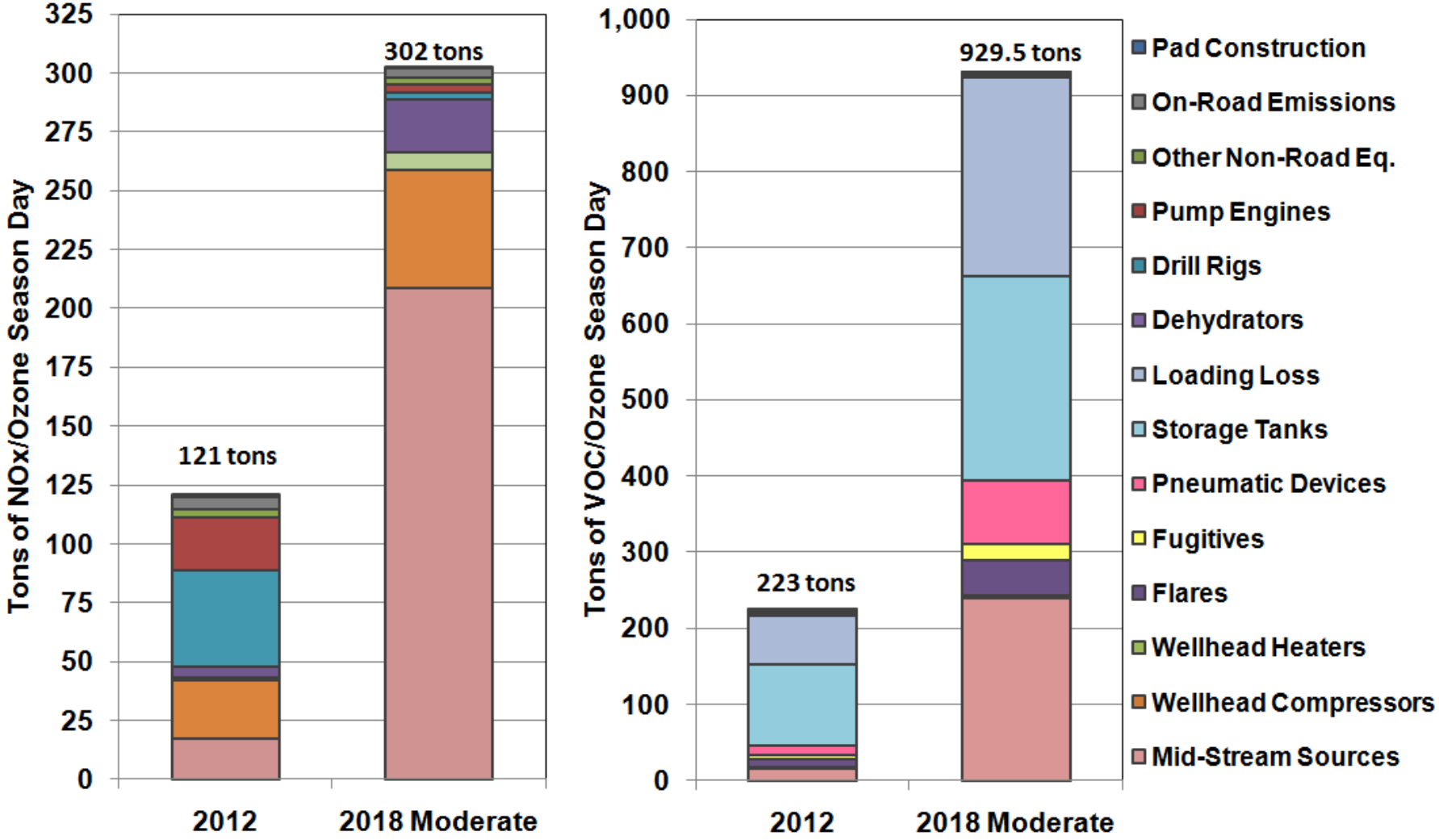

Table 4-2: Emissions by Source in the Eagle Ford, 2012 and 2018.

Source	2012		2018 Low		2018 Moderate		2018 High	
	VOC	NO_X	VOC	NO_X	VOC	NO_X	VOC	NO_X
Seismic Trucks	0.00	0.03	0.00	0.01	0.00	0.01	0.00	0.01
Pad Construction Non-Road	0.07	0.89	0.05	0.40	0.07	0.55	0.09	0.69
Pad Construction On-Road	0.05	0.30	0.02	0.10	0.03	0.14	0.04	0.18
Drill Rigs	2.98	40.98	0.82	2.88	0.84	2.95	0.88	3.10
Drilling Non-Road	0.05	0.62	0.03	0.25	0.03	0.26	0.03	0.27
Drilling On-Road	0.12	0.82	0.05	0.28	0.07	0.39	0.08	0.49
Pump Engines	1.34	22.22	0.65	2.42	0.89	3.35	1.13	4.23
Hydraulic Fract. Non-Road	0.35	2.68	0.25	1.82	0.34	2.52	0.43	3.18
Hydraulic Fract. On-Road	0.44	3.68	0.18	1.26	0.24	1.75	0.31	2.20
Completion Flares	0.97	0.47	0.98	0.48	1.36	0.66	1.71	0.83
Wellhead Compressors	1.65	24.34	3.23	47.53	3.39	49.83	3.58	52.59
Wellhead Heaters	0.12	1.23	0.64	6.82	0.70	7.43	0.76	8.07
Production Flares	9.06	4.41	32.64	16.16	44.43	22.01	58.06	28.76
Dehydrators	2.11	0.00	2.82	0.00	3.70	0.00	4.81	0.00
Storage Tanks	106.33	0.00	199.54	0.00	269.38	0.00	357.98	0.00
Fugitives	4.63	0.00	18.77	0.00	20.29	0.00	21.91	0.00
Loading Loss	63.30	0.00	193.37	0.00	260.00	0.00	341.76	0.00
Well Blowdowns	0.70	0.00	1.37	0.00	1.43	0.00	1.51	0.00
Pneumatic Devices	13.03	0.00	76.16	0.00	83.05	0.00	90.25	0.00
Production On-Road	0.13	0.65	0.32	1.48	0.35	1.61	0.38	1.75
Mid-Stream Sources	15.91	17.54	157.01	137.17	238.91	208.71	362.28	316.48
Total	223	120.86	688.88	219.07	929.50	302.17	1247.97	422.83

As show in Figure 4-3, over 53% of NO_X emissions from oil and gas operations in the Eagle Ford were produced in only 4 counties: La Salle, Karnes, Dimmit, and Webb. Eagle Ford operations in La Salle County emitted 15.6 tons of NO_X per ozone season day, while operations in Karnes emitted 16.7 tons, operations in Dimmit emitted 15.3 tons, and operations in Webb emitted 16.5 tons in 2012. Other counties that produce significant emissions from Eagle Ford oil and gas production included McMullen, DeWitt, Gonzales, Live Oak, Atascosa, and Frio counties.

Figure 4-3: NO_X Emissions by County from Eagle Ford, 2012

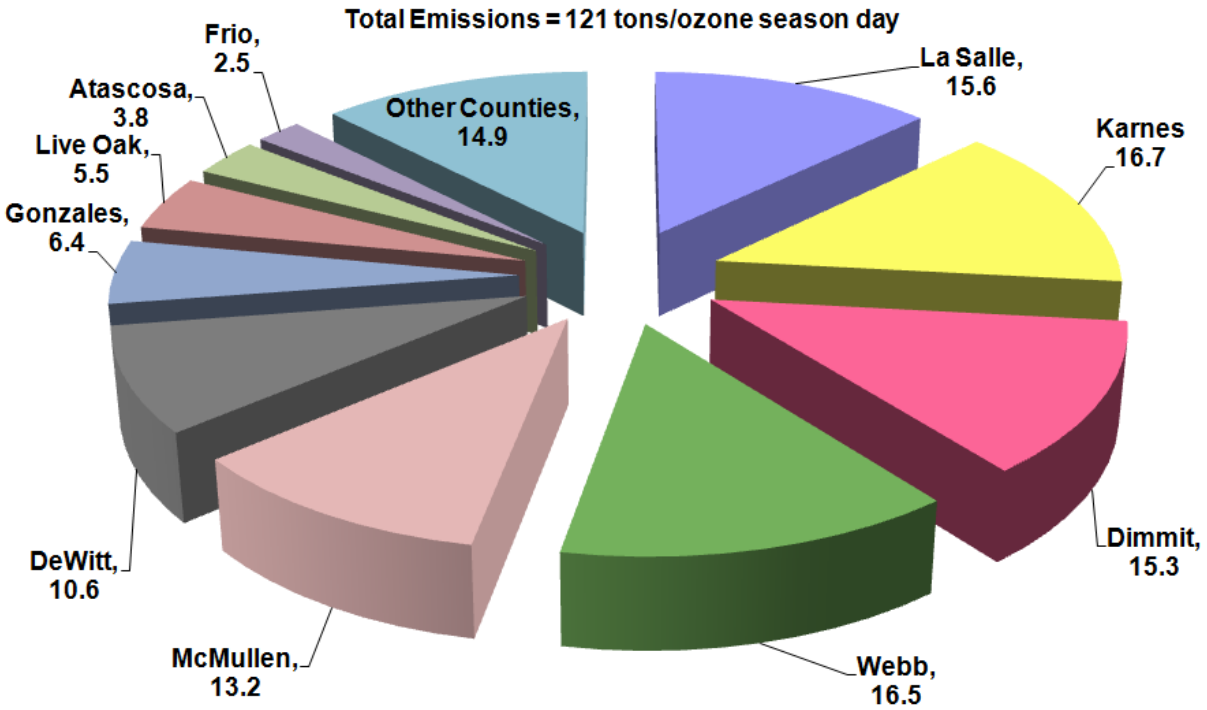

Under the 2018 moderate development scenario, oil and natural gas operations are projected to emit, on an ozone season day, 52.6 tons of NO_X in La Salle County , 32.9 tons of NO_X in Karnes , 368.5 tons of NO_X in Dimmit, , and 35.0 tons of NO_X in Webb. A similar pattern occurs with VOC emissions under the 2018 moderate scenario in which ozone season daily emissions are expected to be: 147.3 tons of VOC in La Salle County , 113.8 tons of VOC in Karnes , 131.0 tons of VOC in Dimmit, , and 84.1 tons of VOC in Webb (Table 4-3).

Table 4-3: Emissions by County in the Eagle Ford, 2012 and 2018.

County	2012		2018 Low		2018 Moderate		2018 High	
	VOC	NO_X	VOC	NO_X	VOC	NO_X	VOC	NO_X
Atascosa	5.86	3.75	22.44	6.64	33.37	9.62	44.53	13.52
Bee	1.39	1.00	2.39	2.40	3.51	3.51	5.01	5.12
Brazos	2.86	0.98	12.60	1.33	11.08	1.54	14.28	1.96
Burleson	1.46	0.38	7.86	0.60	5.93	0.66	7.61	0.84
DeWitt	20.43	10.56	46.37	21.30	67.06	29.15	92.57	40.68
Dimmit	27.45	15.26	97.48	27.68	131.00	38.52	174.67	54.81
Duval	0.00	0.00	0.01	0.00	0.01	0.00	0.01	0.00
Fayette	1.53	1.27	6.72	2.53	8.65	3.71	11.33	5.47
Frio	5.14	2.55	23.54	6.54	26.56	8.61	35.59	12.19
Gonzales	10.08	6.41	55.23	8.40	74.22	11.80	97.68	16.60
Grimes	1.87	1.29	4.45	1.89	5.22	2.58	6.83	3.65
Karnes	26.36	16.71	91.25	23.66	113.77	32.93	151.24	46.37
La Salle	28.79	15.58	99.55	36.80	147.28	52.59	199.27	74.59
Lavaca	1.76	1.81	5.53	3.50	8.46	5.23	11.55	7.76
Lee	1.16	0.38	5.28	0.44	5.70	0.47	7.32	0.52
Leon	4.23	2.17	9.39	4.21	12.72	5.80	17.46	8.18
Live Oak	11.46	5.49	26.48	11.23	37.18	15.63	52.29	21.91
Madison	1.81	1.01	10.27	2.28	13.66	3.10	18.22	4.42
McMullen	23.01	13.19	59.00	21.13	84.73	29.50	114.77	41.19
Maverick	1.87	0.80	12.68	3.31	21.51	4.56	28.74	6.27
Milam	0.22	0.32	0.68	0.09	1.05	0.10	1.35	0.11
Robertson	0.00	0.00	1.88	1.18	2.91	1.79	4.38	2.71
Washington	0.92	0.63	1.57	0.82	1.79	1.11	2.40	1.53
Webb	38.08	16.49	62.28	27.23	84.06	35.01	112.49	46.40
Wilson	2.37	1.24	11.53	2.12	13.06	2.54	16.97	3.39
Zavala	3.25	1.59	12.42	1.77	15.03	2.10	19.39	2.63
Total	223.35	120.86	688.88	219.07	929.50	302.17	1247.97	422.83

4.2 Floresville Auto-Gas Chromatograph Monitor

There are 33 monitors in Texas that are equipped with an Automated Gas Chromatograph (AutoGC), which identifies and measures the concentration of VOCs in a sample of air. The AutoGC monitor at Floresville CAMS 1038 has been in operation since July 2013 and was the only such monitor in the San Antonio region until the end of 2014, when the Karnes County Courthouse AutoGC station began operation. Measurements for 46 different species of VOC are identified and reported at the Floresville monitor, with measurements taken for 40 minutes out of every hour. The average concentrations for each compound reported in 2014 are given in Table 4-4. Some of these compounds are more reactive than others and are more effective in ozone production. TCEQ has identified these Highly Reactive Volatile Organic Compounds (HRVOCs) for the Houston-Galveston-Brazoria area and are provided in boldface type in the following table.[40]

[40] Texas Commission on Environmental Quality. 2006. Subchapter A: Definitions, 30 TAC § 115.10, adopted December 7, 2006. http://texreg.sos.state.tx.us/public/readtac$ext.TacPage?sl=R&app=9&p_dir=&p_rloc=&p_tloc=&p_ploc=&pg=1&p_tac=&ti=30&pt=1&ch=115&rl=10. Accessed 05/15/15.

Table 4-4: VOC Species at Floresville and their 2014 Average Concentrations

VOC Species (HRVOCs in Bold)	**# of Carbon Atoms**	**2014 Average (ppb-V)**	**2014 Average (ppb-C)**
Propane	3	8.948	26.843
Ethane	2	12.071	24.142
n-Butane	4	4.296	17.186
Isobutane	4	2.033	8.133
Isopentane	5	1.510	7.549
n-Pentane	5	1.381	6.907
n-Hexane	6	0.439	2.633
n-Heptane	7	0.111	0.779
Toluene	7	0.101	0.710
Methylcyclohexane	7	0.090	0.631
Methylcyclopentane	6	0.097	0.584
Ethylene	**2**	**0.255**	**0.510**
Cyclohexane	6	0.085	0.507
Benzene	6	0.083	0.496
3-Methylhexane	7	0.063	0.440
Isoprene	5	0.080	0.402
Propylene	**3**	**0.124**	**0.373**
Cyclopentane	5	0.069	0.344
2-Methylhexane	7	0.048	0.334
p-Xylene + m-Xylene	8	0.041	0.329
Acetylene	2	0.143	0.286
2,2,4-Trimethylpentane	8	0.033	0.268
n-Octane	8	0.028	0.225
n-Decane	10	0.016	0.163
1-Butene	**4**	**0.040**	**0.162**
n-Nonane	9	0.018	0.161
1,2,4-Trimethylbenzene	9	0.015	0.134
1,2,3-Trimethylbenzene	9	0.014	0.124
2-Methylheptane	8	0.011	0.091
o-Xylene	8	0.011	0.087
3-Methylheptane	8	0.011	0.085
2,2-Dimethylbutane	6	0.010	0.059
t-2-Butene	**4**	**0.015**	**0.059**
2,3-Dimethylpentane	7	0.007	0.050
1,3,5-Trimethylbenzene	9	0.006	0.050
Ethyl Benzene	8	0.006	0.044
2,4-Dimethylpentane	7	0.005	0.036
c-2-Butene	**4**	**0.008**	**0.032**
1,3-Butadiene	**4**	**0.005**	**0.022**
Styrene	8	0.002	0.019
n-Propylbenzene	9	0.002	0.017
2,3,4-Trimethylpentane	8	0.002	0.014
t-2-Pentene	5	0.003	0.013
1-Pentene	5	0.001	0.004
Isopropyl Benzene (Cumene)	9	0.000	0.003
c-2-Pentene	5	0.001	0.003

Measurements of concentration are given in parts per billion – volume (ppb-V), although sometimes these values are expressed in ppb-C, or parts per billion – carbon, which is simply the ppb-V concentration multiplied by the number of carbon atoms in the compound of interest. The four most prevalent compounds at C1038 are ethane, propane, n-butane, and isobutane, which together account for 85% of the total concentration by volume and 75% of the total concentration of carbon. However, the six HRVOCs measured at the monitor account for 0.7% of the average total concentration by volume and 1.4% of the average total concentration of carbon.

Dr. Gunnar W. Schade is an Associate Professor at Texas A&M University in the Department of Atmospheric Sciences. With a Ph.D. in Chemistry, Dr. Schade specializes in the exchange of trace gases between the biosphere and atmosphere, including biogenic VOCs.[41] Dr. Schade made a presentation to the AACOG Air Improvement Resources Technical Committee on December 8, 2014 discussing Eagle Ford Shale emissions, specifically VOCs, and the potential impact on ozone in the San Antonio region.

Because of the multicollinearity among VOC species, Dr. Schade conducted a factor analysis of VOC emissions at the Floresville monitor.[42] By correlating VOC species with one another, broader variables, or factors, can be derived that help explain variations among VOC species. The analysis concluded that the two dominant factors in explaining VOC concentrations at CAMS 1038 are oil and gas production, listed as "Factor 1" in Table 4-5, and vehicular combustion, listed as "Factor 2". Most VOC species are formed at least in part by both factors, but one factor usually dominates over the other. Values closer to one indicate a stronger influence of either factor on a particular VOC species. For example, NO_X is primarily formed through vehicle combustion (Factor 2) while n-Butane is primarily formed through oil and gas activity (Factor 1). Although a third factor is listed in the analysis, it was later found not to contribute significantly to VOC concentrations. Factor loadings under 0.2 were not included in the chart, except to show the difference between the two factors, as with NO_X.

[41] Texas A&M University, "Curriculum Vitae: Gunnar W. Schade." Available online: https://howdy.tamu.edu/Inside/HR2504/PDFs/CV_671237.pdf. Accessed 06/09/2015.

[42] Schade, Dr. Gunnar W. "Eagle Ford Shale Air Quality." Alamo Area Council of Governments Air Improvement Resources Technical Committee Meeting. San Antonio, TX. 12/08/2014. Presentation. Available online: https://www.youtube.com/watch?v=gSfJELQVKmI&feature=youtu.be. Accessed 06/09/2015.

Table 4-5: Factor Analysis of VOCs, conducted by Gunnar W. Schade of Texas A&M

Component	Factor1	Factor2	Factor3	Component	Factor1	Factor2	Factor3
NOx	0.16	0.68		Isoprene	-0.15		
Ethane	0.90	0.31	-0.24	2,2-Dimethylbutane	0.83	0.36	
Ethylene	0.38	0.81		Cyclohexane	0.94	0.25	
Propane	0.92	0.29	-0.21	3-Methylhexane	0.72	0.38	0.24
Propylene	0.62	0.66	-0.22	2,2,4-Trimethylpentane	0.39	0.72	
Acetylene	0.30	0.73		3-Methylheptane	0.80	0.44	0.23
n-Butane	0.94	0.27		Methylcyclohexane	0.93	0.28	
Isobutane	0.93	0.25	-0.19	Methylcyclopentane	0.90	0.35	
t-2-Butene		0.51		2-Methylhexane	0.78	0.40	0.19
c-2-Butene	0.20	0.50		1-Butene		0.69	
1,3-Butadiene		0.84		2-Methylheptane	0.83	0.36	0.25
n-Pentane	0.96	0.25		p&m-Xylene	0.51	0.79	0.24
Isopentane	0.93	0.32		Benzene	0.70	0.55	
n-Hexane	0.95	0.25		Toluene	0.53	0.74	
n-Heptane	0.89	0.29	0.21	Ethyl-Benzene	0.42	0.80	0.28
n-Octane	0.89	0.31	0.24	o-Xylene	0.41	0.86	0.22
n-Nonane	0.81	0.41	0.21	1,3,5-Trimethylbenzene	0.54	0.75	
n-Decane	0.71	0.44		1,2,4-Trimethylbenzene	0.39	0.85	
Cyclopentane	0.91	0.32		1,2,3-Trimethylbenzene	0.35	0.58	0.25

The HRVOCs listed in Table 4-4 are all factors of vehicle combustion. For t-2-butene, 1,3-butadiene, and 1-butene, oil and gas exploration has a negligible effect, while propylene has almost equal association with the two factors.

4.3 Variations in VOCs

Certain VOCs were analyzed to assess their daily, weekly, and monthly patterns, and to detect any differences in those patterns among each species. Ethane and propane were selected for analysis because they are the most abundant VOCs present at Floresville. Ethylene and propylene were selected as they are the most abundant HRVOCs. Additionally, the former two compounds are factors of oil and gas exploration, while the latter two are factors of vehicle combustion. The plot of average hourly concentrations as a percentage of average daily concentrations of ethane, propane, ethylene, and propylene shows a distinct diurnal pattern (Figure 4-4). VOC concentrations tend to peak between 5 a.m. and 7 a.m., when the mixing height is usually at its lowest and before the photochemical process begins to form ozone. This acts to contain local VOCs in a smaller volume close to the earth's surface. With daytime heating, the mixing height rises, providing a greater space for VOCs to occupy, thus reducing the concentration. The process reverses after around 6 p.m. as daytime heating ceases and the mixing height retreats back toward the earth's surface.

Ethylene and propylene appear to behave slightly differently than the less reactive VOCs. Leading up to sunrise, ethylene and propylene increase quicker than ethane and propane. Additionally, ethylene and propylene concentrations increase ahead of ethane and propane

around 5 p.m. These characteristics may be attributed to ethylene and propylene being factors of vehicle combustion. The Floresville monitor lies on the southeastern edge of the small urban core between two major highways: State Highway 95 and U.S. Highway 181. Vehicular emissions from these highways, in addition to those emissions occurring elsewhere in the Eagle Ford Shale, are likely responsible for the different diurnal characteristics of ethylene and propylene.

Figure 4-4: Diurnal Profile of Selected VOCs at CAMS 1038 During Ozone Season (2014)

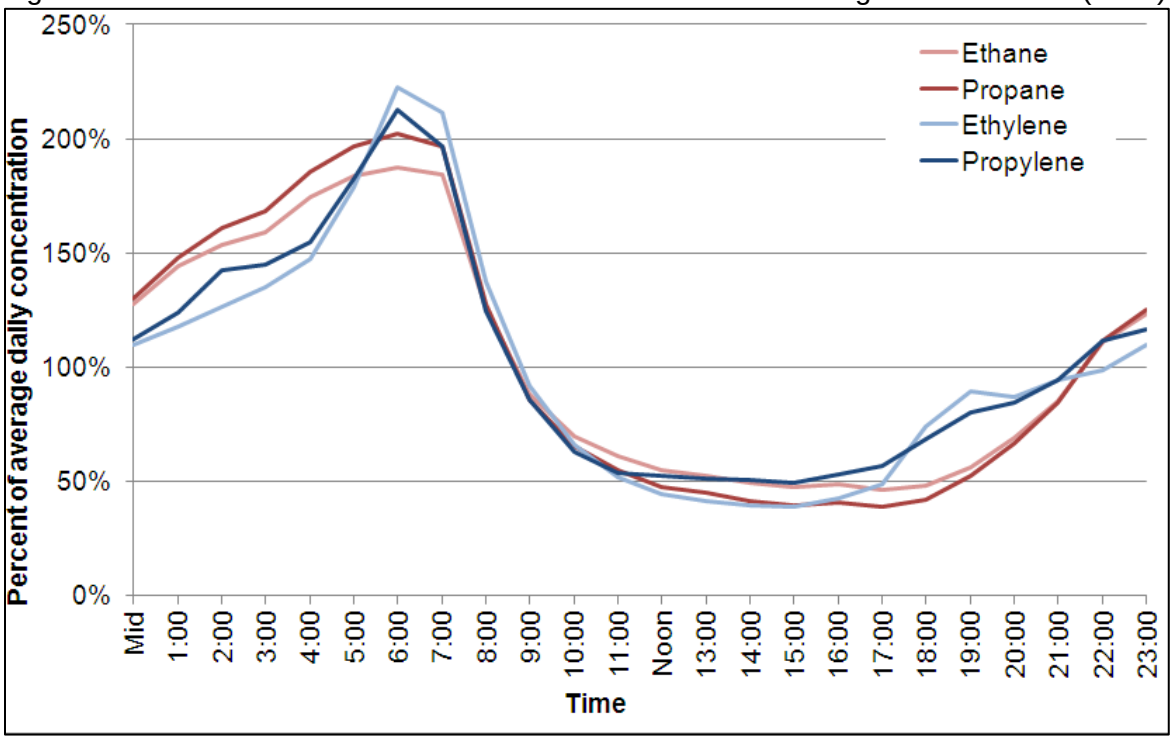

The monthly variation of VOCs can be seen in Figure 4-5, with a distinct peak in December, and a minimum in June. Elevated winter concentrations are caused by less direct solar radiation keeping the mixing height generally lower and reducing the potential for photochemical reactions of VOCs to form ozone. Mixing heights and photochemical processes are major determinants of the seasonal difference in VOC concentrations. Note that with only one complete year of data available at CAMS1038, the annual variation of VOCs is subject to change as more data becomes available. Month-to-month fluctuations in average concentrations at this point may be due to chance, but the general pattern is evident.

Figure 4-5: Monthly Profile of VOCs at CAMS 1038

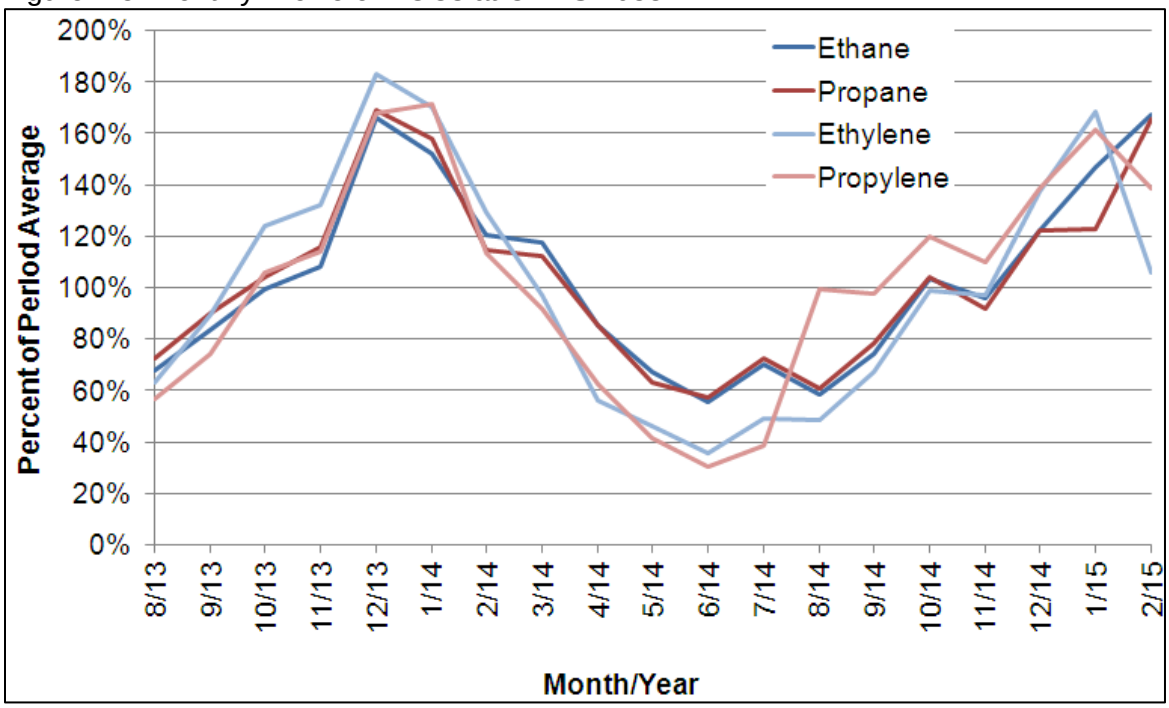

VOC concentrations at Floresville were also analyzed to determine if a weekday/weekend effect exists, and to determine if HRVOCs behave any differently from other VOCs in that respect. Figure 4-6 demonstrates that there do appear to be variations day to day in the total VOC concentration, with Monday having the lowest values and Wednesday having the highest values. However, a chi-square goodness-of-fit test for significance using median values yields a p-value of only 0.782. The same analysis was done for the total of all HRVOCs. Figure 4-7 shows more evenly distributed concentrations throughout the week. No single day stands out as having the highest or lowest HRVOC concentrations and the chi-square test confirms this, with a p-value of almost 0.999. With values so small for HRVOC concentrations, another chi-square test using concentrations converted to parts per trillion was conducted, which did yield a significant result at $\alpha = 0.05$.

Another statistical test was chosen that only considers the rankings of the data points. The Kruskal-Wallis test is ideal for skewed and heteroscedastic distributions such as these. Each day's average HRVOC concentration was assigned a rank (from 1 as the smallest to 190 as the largest) and then each rank was grouped by day of the week.[43] Performing the analysis yielded a test statistic of $H = 4.75$, which was less than the value required to be significant at $\alpha = 0.05$ with 6 degrees of freedom. The Kruskal-Wallis statistical test confirms that, aside from random variation, there is no difference in average HRVOC concentrations by day of the week at the Floresville monitor.

[43] National Institute of Standards and Technology, Statistical Engineering Division. "Kruskal Wallis." 2011. Available online: http://www.itl.nist.gov/div898/software/dataplot/refman1/auxillar/kruskwal.htm. Accessed 05/19/2015.

Figure 4-6: IQR Plot of Total VOCs by Day of the Week (2014)

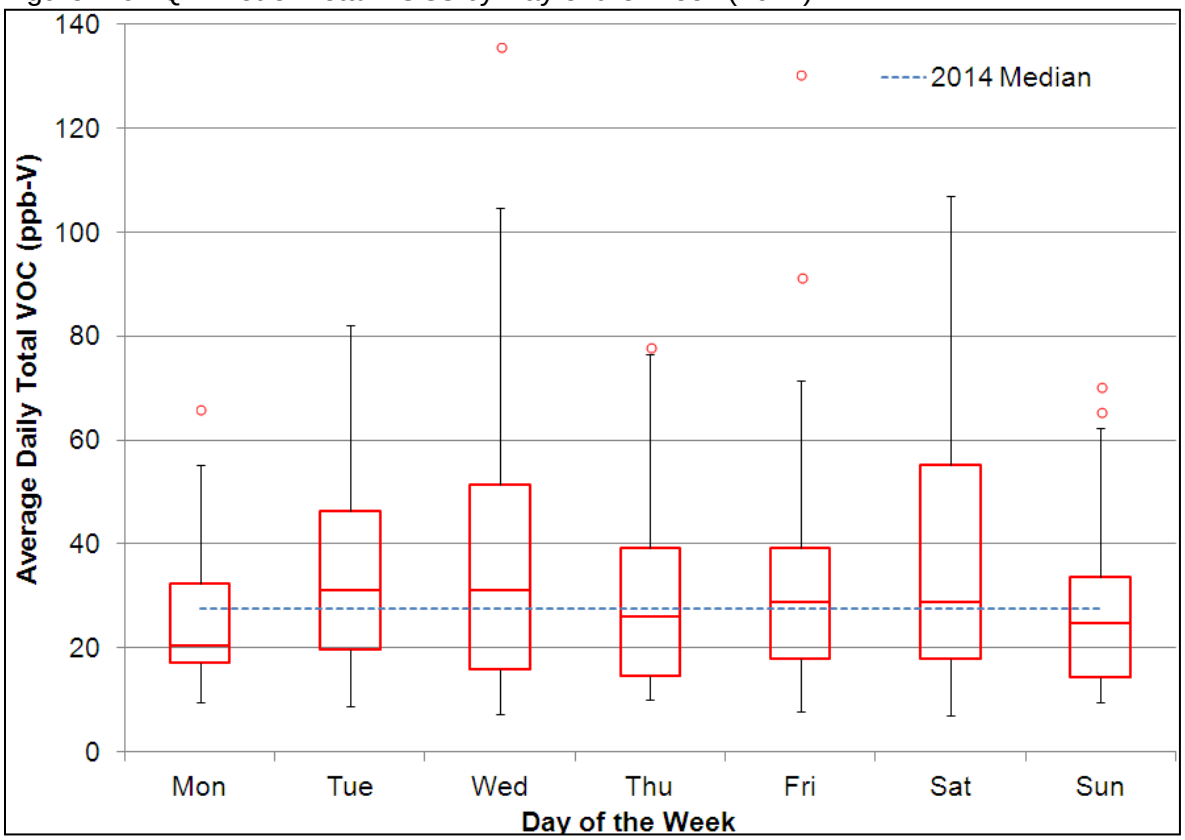

Figure 4-7: IQR Plot of Total HRVOCs by Day of the Week (2014)

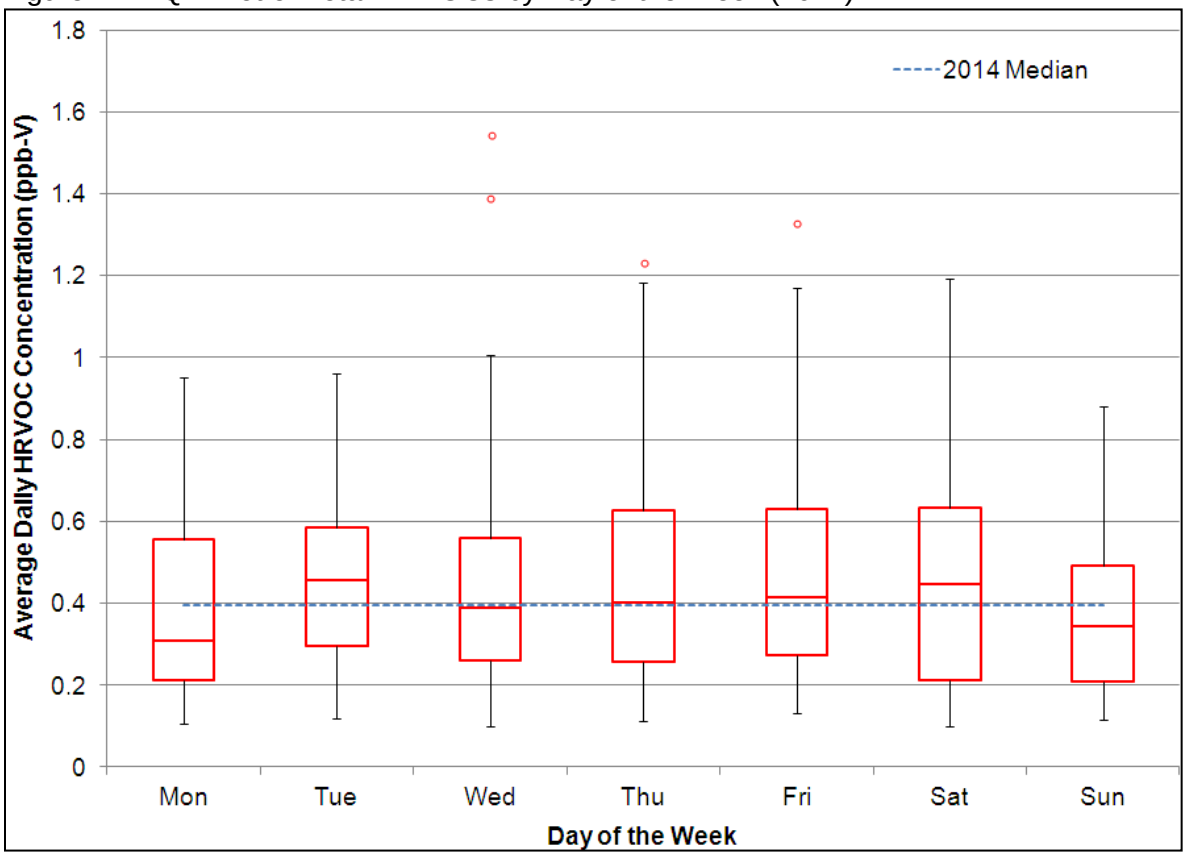

It is difficult to meaningfully analyze trends over time at CAMS 1038 due to the lack of observations. The data that is available suggests that there may be a reduction in the 90th percentile VOC and NO_X concentrations over the last year. More years of data are needed to determine if these trends are statistically significant. The reductions of the four most common VOCs as well as NO_X from 2013 to 2014 are shown in Table 4-6 and represent 2013 values after July 19th, when the AutoGC monitor first started reporting. The July 19th cutoff was used for 2014 data as well to control for seasonal variations described above. CAMS 1038 did not start reporting NO_X until August 10th, so that date is used to calculate the change in NO_X from 2013-2014. It bears repeating that these results do not imply any statistical significance at this time.

Table 4-6: 2013 and 2014 90th Percentile VOC and NO_X Concentrations at CAMS 1038

	Ethane	**Propane**	**n-Butane**	**Isobutane**	**NO_X[1]**
90th percentile July 19 – Dec. 31, 2013	29.35 ppb-V	24.01 ppb-V	11.55 ppb-V	5.54 ppb-V	10.3 ppb
90th percentile July 19 – Dec. 31, 2014	28.61 ppb-V	22.81 ppb-V	11.47 ppb-V	5.29 ppb-V	7.5 ppb
Percent change 2013-2014	-2.52%	-5.00%	-0.68%	-4.48%	-27.18%

[1] NOx values represent Aug. 10 – Dec. 31 data

Average daily VOC concentrations were plotted against daily 8-hr ozone at CAMS 59 to determine if VOC levels from the Eagle Ford Shale, as represented by the Auto-GC at CAMS 1038, affect background ozone entering the San Antonio region. Figure 4-8 shows the relationship between ozone at CAMS 59 and the total concentration of VOCs at CAMS 1038, with all 46 species of VOCs included in the analysis. The correlation is significant at $\alpha = 0.05$ with an R^2 value of 0.125. Figure 4-9 shows how the relationship changes when only the HRVOCs specified in Table 4-4 are compared to ozone at CAMS 59. The correlation is even stronger with an R^2 value of 0.236. Given the limited data available, HRVOCs at the Floresville Auto-GC monitor appear to be a better predictor of background ozone in the San Antonio region than the total of all VOCs measured.

Figure 4-8: Correlation Between 8-Hr Ozone at CAMS 59 and Average Daily Total VOC at CAMS 1038, 2014 Ozone Season

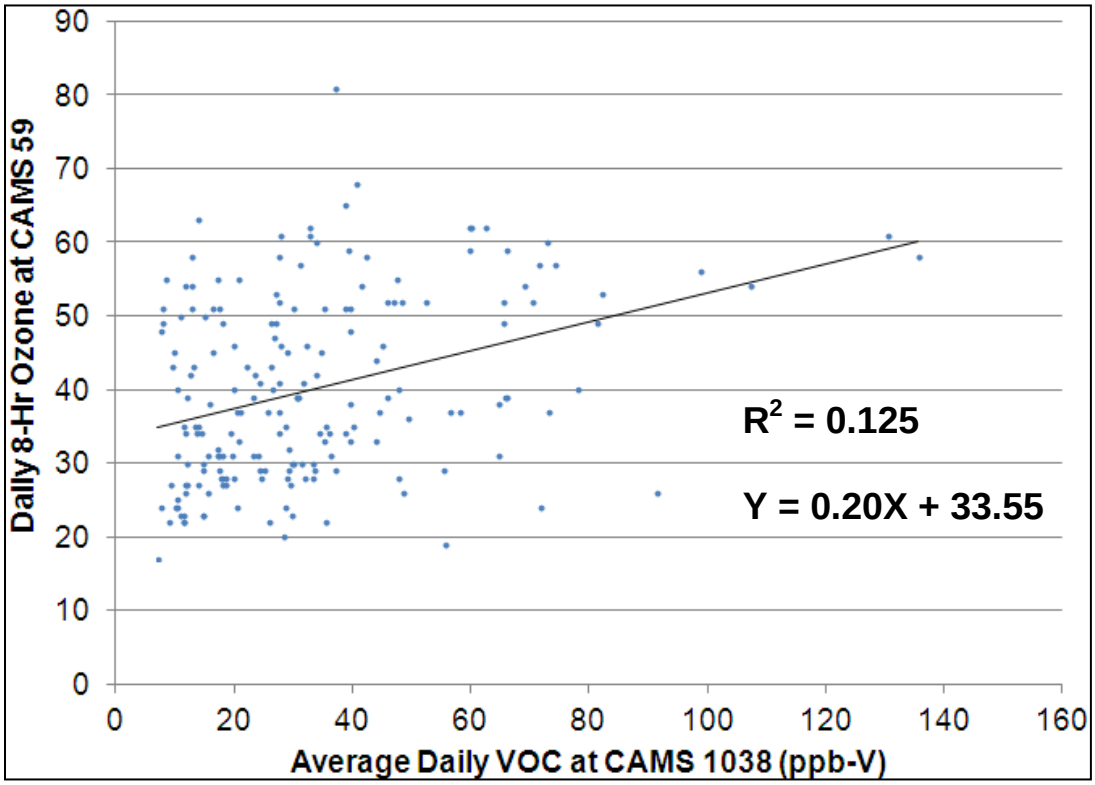

Figure 4-9: Correlation Between 8-Hr Ozone at CAMS59 and Average Daily HRVOC at CAMS1038, 2014 Ozone Season

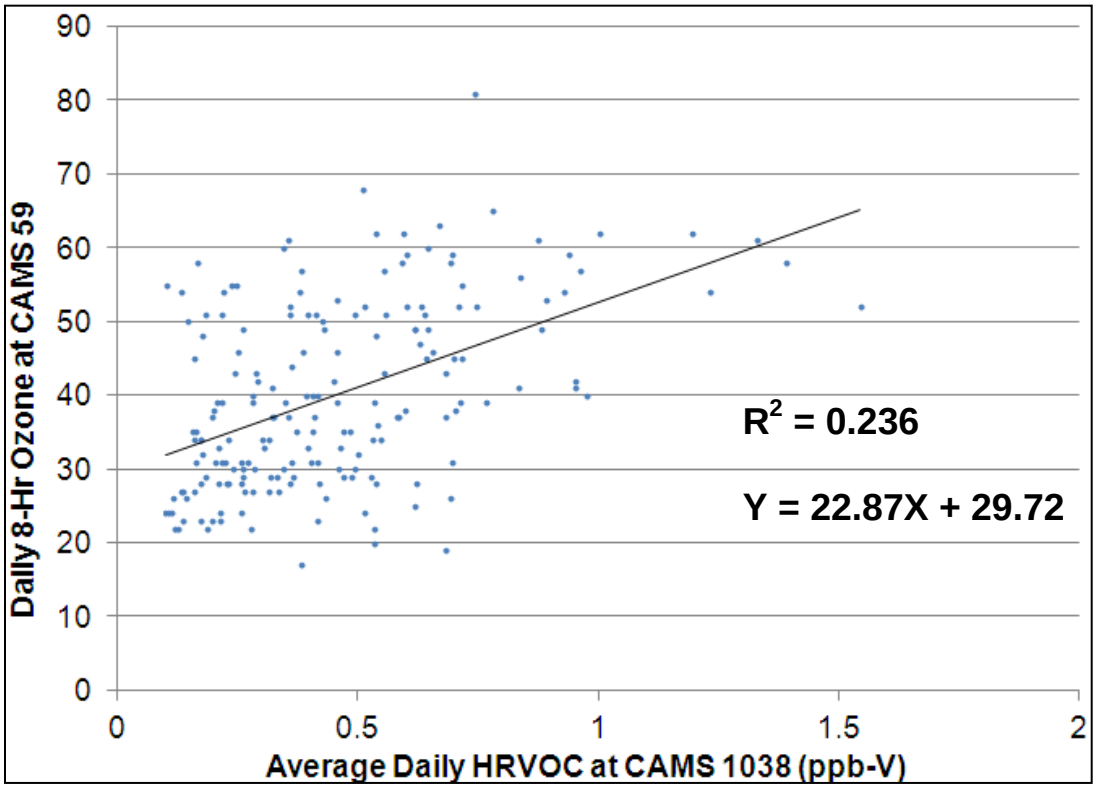

4.4 Transport of VOCs

Resultant wind directions at CAMS 1038 were analyzed in conjunction with VOC concentrations to determine any other meteorological factors that might influence VOC levels in the area. For each day during ozone season, the average ethane concentration and resultant wind direction between 5 a.m. and 7 a.m. was calculated. The average ethane concentrations were then grouped by resultant wind direction and the median ethane for each direction was calculated and compared against the median of all ethane concentrations, regardless of wind direction. Table 4-7 lists the median maximum ethane concentration according to the morning (5 a.m. to 7 a.m.) resultant wind direction.

A chi-square goodness of fit test of significance at $\alpha = 0.05$ shows that the maximum ethane concentration on any given day in Floresville is significantly influenced by wind direction. Easterly and southeasterly winds contribute the most to these high ethane levels, which may be impacted by Eagle Ford Shale oil and gas development. Westerly winds, although comparatively less common during ozone season mornings, appear to be linked to high ethane concentrations, although three of the six days that had morning ethane concentrations above the yearly median were preceded by calm conditions (wind speed <1 m/s), allowing emissions to aggregate. It is unclear at this time why ethane concentrations are lower on mornings with southerly winds. Figure 4-13 shows that the distribution of oil and gas wells in the Eagle Ford Shale is slightly less dense south and southwest of San Antonio compared to southeast and east of San Antonio. More research is needed to determine if this is the cause of lower concentrations of ethane on mornings with southerly winds. A similar analysis conducted for propane, n-butane, and isobutane in showed a similar distribution of median concentrations based on morning wind directions, but due to the small magnitude of values, each failed the chi-squared significance test.

Table 4-7: Median Ethane Concentrations (Averaged Between 5 a.m. to 7 a.m.) Grouped by Resultant Morning Wind Direction (2014)

	N wind	NE wind	E wind	SE wind	S wind	SW wind	W wind	NW wind
Median Ethane 5-7 a.m. (ppb-V)	12.36	13.23	25.51	24.31	9.53	11.82	21.90	8.82
Number of days	8	34	42	44	52	10	5	6
# of days above total median	3	11	30	36	13	3	3	1
% of days over total median	38%	32%	71%	82%	25%	30%	60%	17%

Figure 4-10: Scatterplot of Average AM (5 a.m. to 7 a.m.) Ethane Concentration and Average AM Wind Direction at CAMS 1038 (2014)

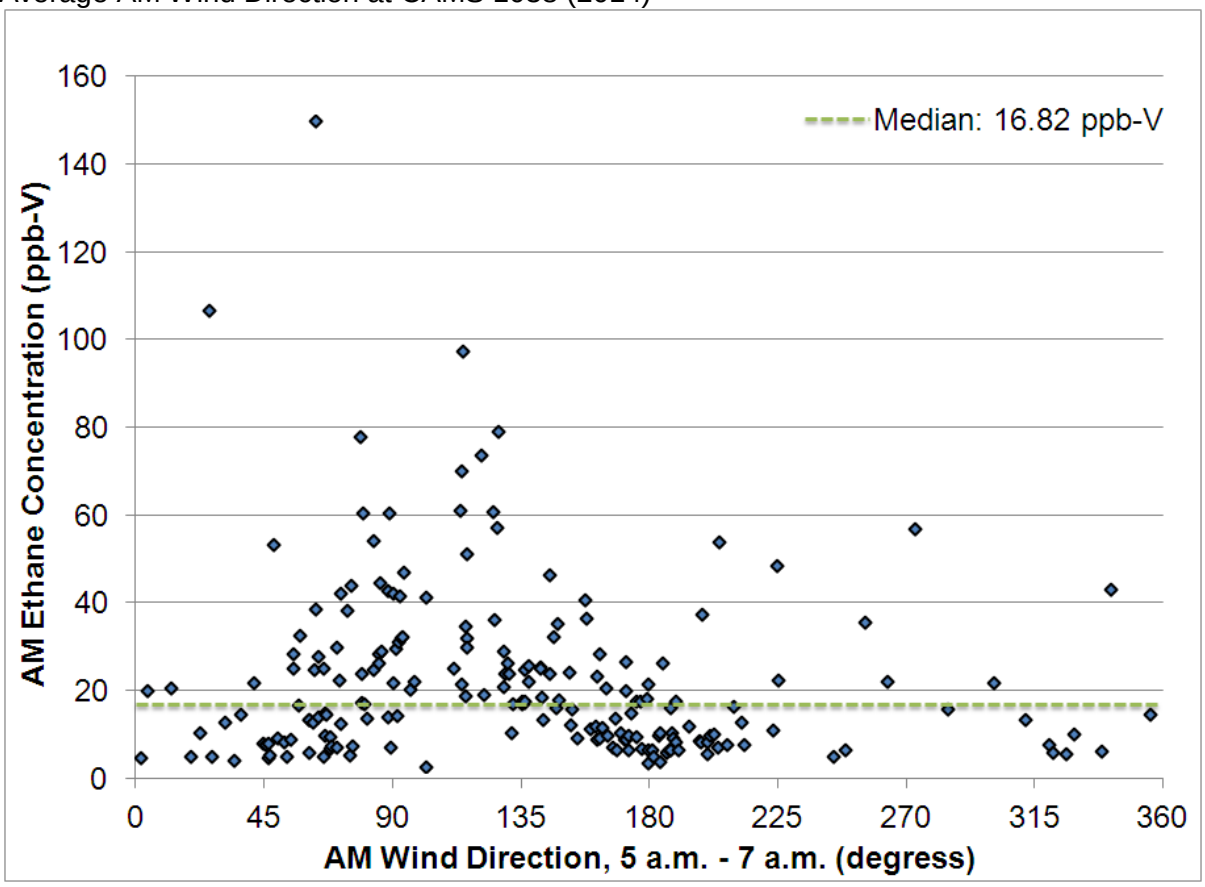

Figure 4-10 provides a visual representation of the distribution of morning ethane concentrations under different morning wind regimes. North, northeasterly, northwesterly, and southerly wind directions tend to transport less ethane while easterly and southeasterly winds transport more.

The same analysis was done for the total of all HRVOCs for each day in Table 4-8: Median HRVOC Concentrations (Averaged Between 5 a.m. to 7 a.m.) Grouped by Resultant Morning Wind Direction (2014). The chi-square goodness-of-fit test does not indicate a significant difference in HRVOC concentrations by wind direction due to the small magnitude of values. Again, the Kruskal-Wallis test for significance was used instead and yielded a test statistic of H = 68.13, which is well over the critical value of 14.07 needed for seven degrees of freedom. The Kruskal-Wallis test does not indicate between which groups the significant difference occurs, but looking at the chart makes it clear that southerly winds are not as conducive to elevated HRVOC levels. This is also evident in Figure 4-11, which shows that the southerly direction has several values associated with it, but none are over 1.0 ppb-V.

Table 4-8: Median HRVOC Concentrations (Averaged Between 5 a.m. to 7 a.m.) Grouped by Resultant Morning Wind Direction (2014)

	N wind	NE wind	E wind	SE wind	S wind	SW wind	W wind	NW wind
Median HRVOC 5-7 a.m. (ppb-V)	0.803	0.500	0.597	0.493	0.227	0.322	0.913	1.038
Number of days	8	34	42	44	52	10	5	6
# of days above total median	6	19	32	25	5	4	4	6
% of days over total median	75%	56%	76%	56%	10%	40%	80%	100%

Figure 4-11: Scatterplot of Average AM (5 a.m. to 7 a.m.) HRVOC Concentration and Average AM Wind Direction at CAMS 1038 (2014)

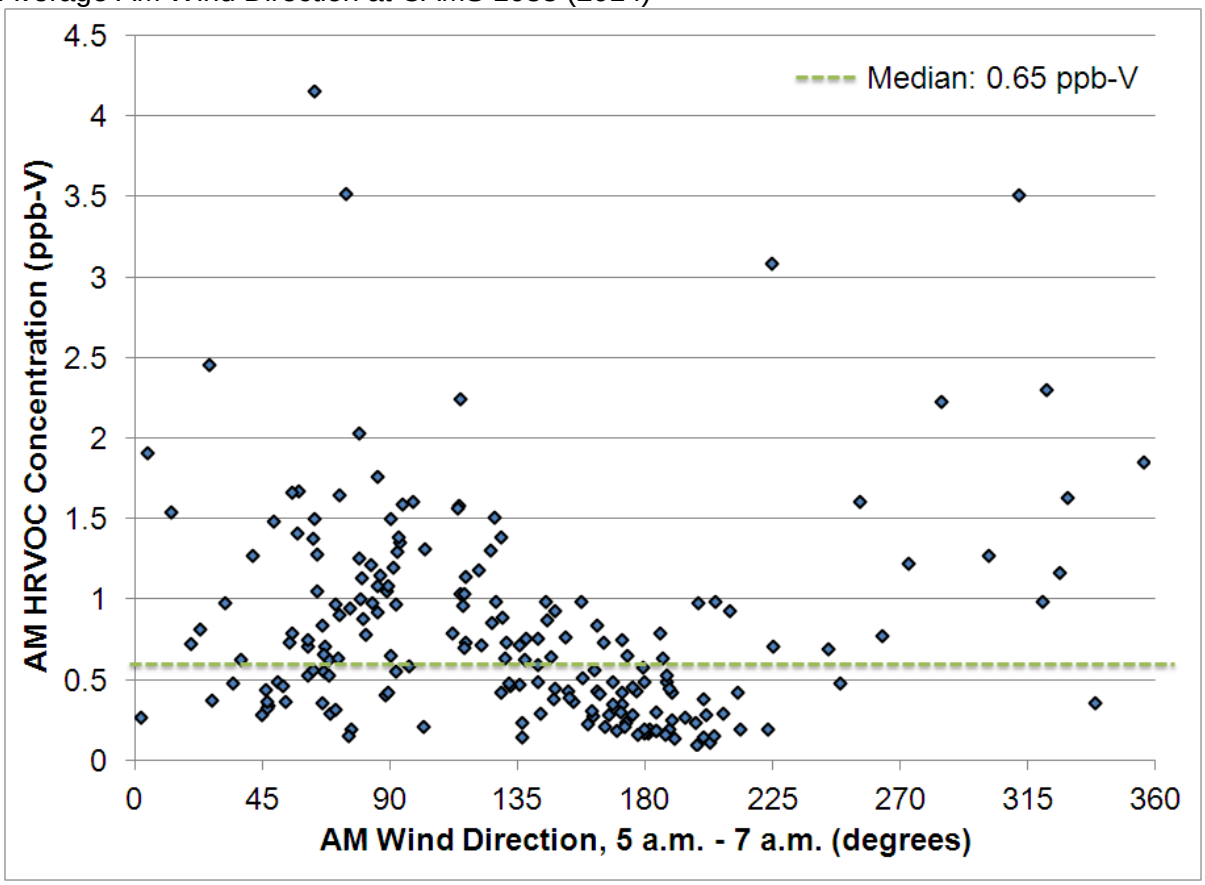

The influences of the two factors (Table 4-5) on VOC concentrations can be seen in Figure 4-12, showing how ethane and ethylene (ethene) concentrations can vary based on different wind directions. These two compounds were chosen because they are the most abundant within each of the factors. Ethane is more influenced by oil and gas activity and exhibits higher concentrations when winds come from the Eagle Ford Shale. Ethylene, being more influenced by vehicle combustion, experiences higher concentrations when winds originate from the northwest (downtown Floresville) due to vehicular traffic. Both compounds exhibit

some similar characteristics, such as a comparative lack of outliers in the data when winds come from the north, where there is no shale activity.

Figure 4-12: IQR Plot of Wind Direction Versus Ethane and Ethylene (Ethene) Concentration[44]

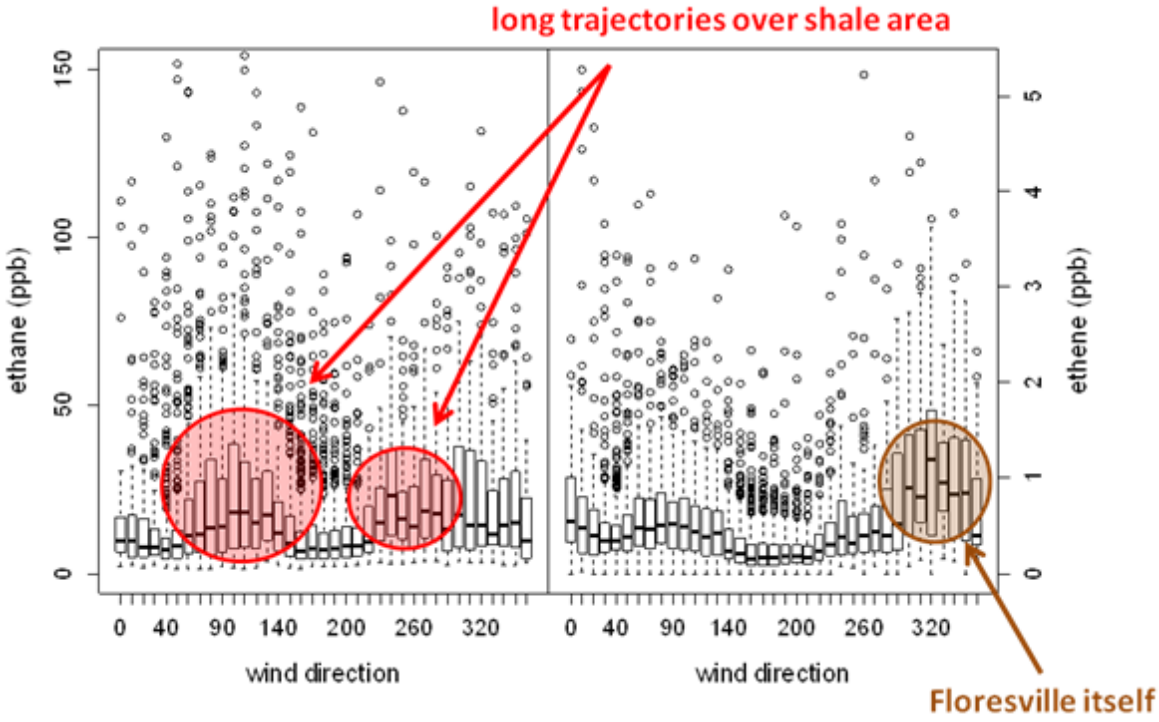

Dr. Schade's presentation to AACOG further analyzed a time series of ethane concentrations at two coastal areas and at Old Highway 90 in San Antonio on days with back trajectories from the southeast.[45] Figure 4-13 shows the region the back trajectories must have originated from and crossed over to be considered for the study. Ethane increased at the San Antonio location relative to the coastal locations starting in 2010 with a sharp increase in 2012. Starting in 2013, the Floresville monitor was included in analysis and showed higher concentrations than all three locations. The increase in ethane concentration coincides with the increase in oil and gas production around 2010, as shown in Figure 4-14: a) Rate of oil and gas production and 4th highest 8-hr ozone (2007-2013) and (b): Interquartile plot of average ethane concentration for selected regions. The peak 8-hr ozone concentration is also plotted and exhibits roughly the same characteristics over time as oil and gas production, increasing in 2010, but with fluctuations year to year based on the dominant meteorological pattern.[46]

[44] *Ibid.*
[45] *Ibid.*
[46] *Ibid.*

Figure 4-13: Map of Oil and Gas Wells in the Eagle Ford Shale, Direction of Transport and the Area to be Considered for Analysis[47]

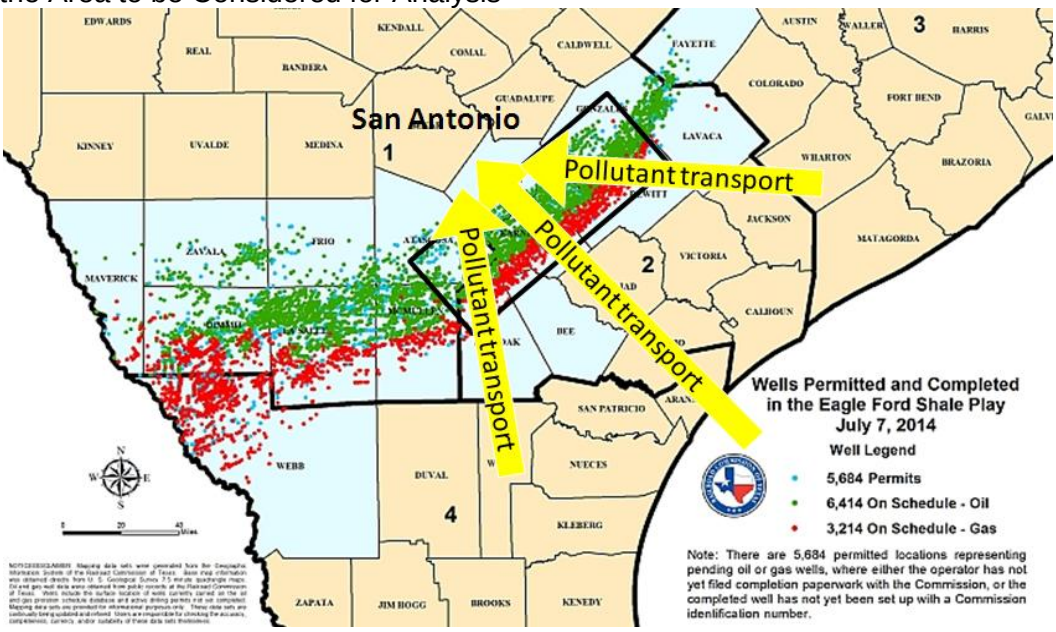

Figure 4-14: a) Rate of oil and gas production and 4th highest 8-hr ozone (2007-2013) and (b): Interquartile plot of average ethane concentration for selected regions[48,1]

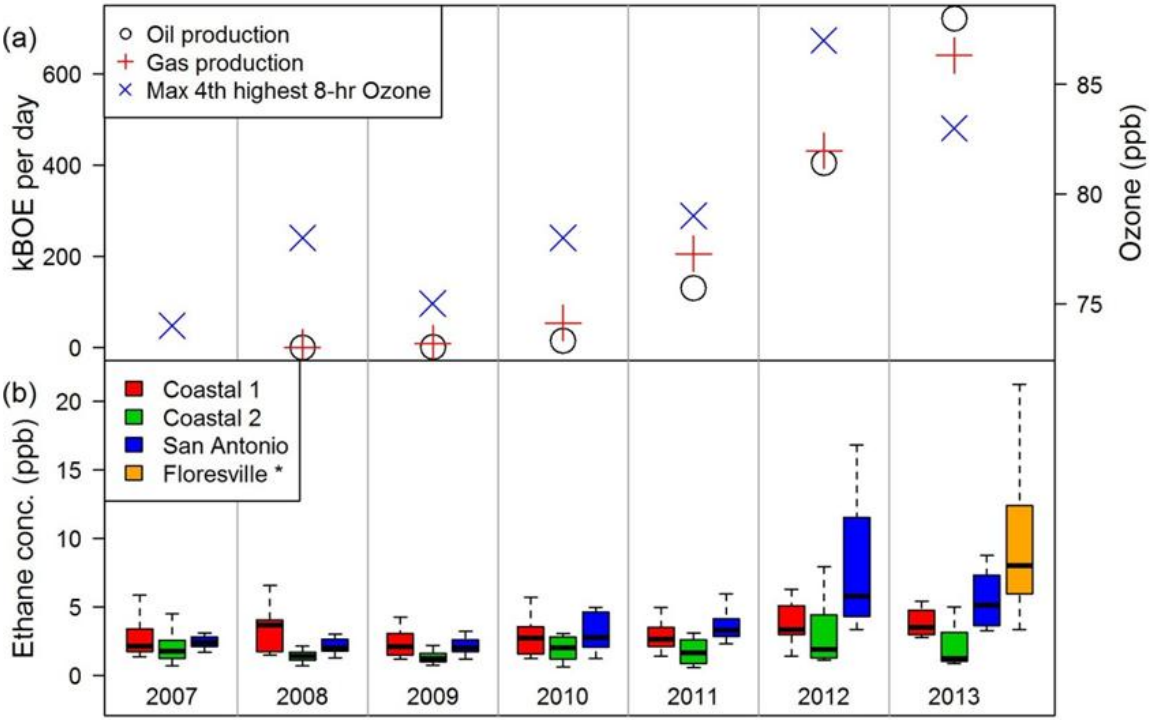

[1] San Antonio and Coastal data based on 24-hour canister samples every six days; Floresville data based on hourly Auto-GC

[47] *Ibid.*
[48] *Ibid.*

To quantify the local enhancement of VOCs from the Eagle Ford Shale over background levels, the same methodology shown in Figure 4-13 was used. Figure 4-15 shows ethane concentrations at the Solar Estates Auto-GC monitor in Corpus Christi, upwind of the Eagle Ford Shale, and the Floresville monitor located downwind of the shale. The daily average VOC concentration was analyzed for both locations to control for diurnal effects. The median daily average of ethane on days where back trajectories from San Antonio originated out of the southeast is 3.46 ppb-V for Solar Estates and 10.20 ppb-V for Floresville, indicating an average ethane enhancement of 6.74 ppb-V across the Eagle Ford Shale. The same analysis was conducted for ethylene in Figure 4-16. Although there still appears to be some ethylene enhancement across the Eagle Ford Shale (47%), it is much less than that seen for ethane (195%). In contrast to ethane, ethylene is much more reactive in forming ozone (Table 4-4). Additionally, ethylene is more a factor of vehicle combustion than oil and gas activity (Table 4-5). These facts might explain why ethylene enhancement appears to be so much lower than ethane.

Figure 4-15: Difference in Ethane Concentration between Monitors Upwind and Downwind from the Eagle Ford Shale (2014) [49]

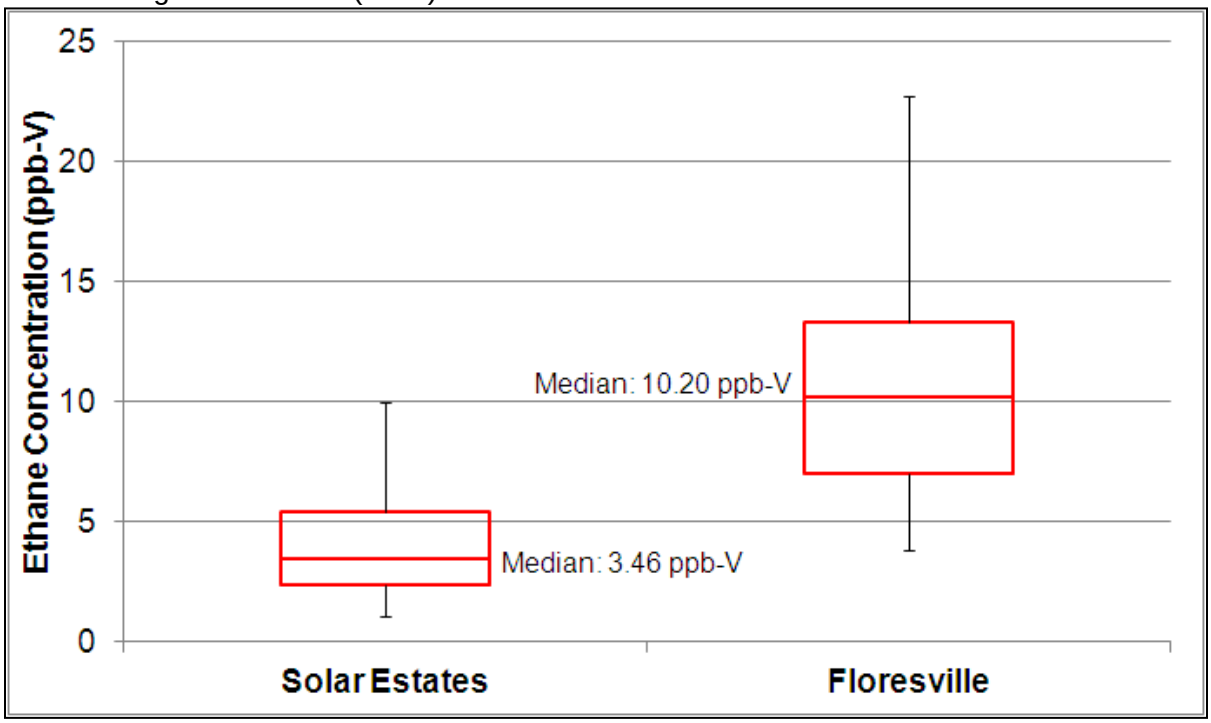

[49] *Ibid.*

Figure 4-16: Difference in Ethylene Concentration Between Monitors Upwind and Downwind from the Eagle Ford Shale (2014)

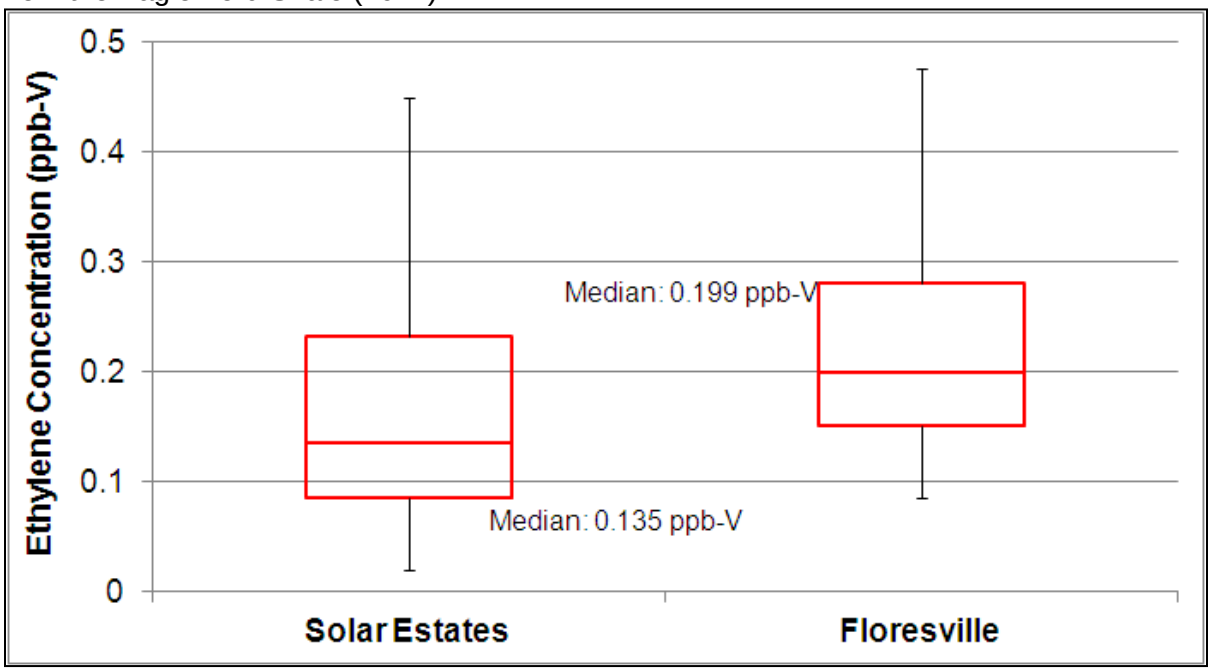

4.5 UT Mobile Monitoring Study

Between May 10 and June 12, 2014, The University of Texas conducted a mobile monitoring study of VOC and NO_X emissions in and adjacent to the Eagle Ford Shale.[50] A total of 12 trips and 22 canister samples of VOCs were taken, along with continuous sampling of Total Non-Methane Hydrocarbons (TNMHC) and NO_X on upwind and downwind legs of the route. Each day except the first had at least one upwind and at least one downwind canister sample. One outcome of this study was to determine if the observations at the Floresville Auto-GC monitor were representative of the mean of downwind samples collected by UT and thus, a reliable indicator of VOC transport.[51] Figure 4-17 compares speciated observations at the Auto-GC monitor with mean downwind speciated canister measurements collected in the study. Given their strong relationship, both with and without one outlier canister sample, it was determined that the Auto-GC monitor was indeed representative of VOC concentrations downwind of the Eagle Ford Shale. There is one plotted point, isoprene, which appears to deviate from the trend line. The reasons for this are that isoprene is associated with living vegetation, including oak trees which exist in relative abundance along the downwind leg of the monitoring route compared to the Auto-GC monitor. Isoprene is also highly reactive compared to other compounds and doesn't stay concentrated as long. Therefore, mean concentrations along the route and closer to the emissions source will be higher than those farther downwind near the Auto-GC monitor.

[50]Sullivan, Dave, August 2014. "Eagle Ford Shale Mobile Monitoring Study." University of Texas at Austin Center for Energy and Environmental Resources, Austin, Texas. 582-13-30089-FY14-01. Available online: https://www.tceq.texas.gov/assets/public/implementation/air/am/contracts/reports/oth/5821330089FY1401-20140801-uta-Eagle_Ford_Shale_Mobile_Monitoring.pdf. Accessed 03/13/15.

[51] *Ibid.*

Figure 4-17: Mean Floresville Auto-GC Species Concentrations Plotted Against Mean Mobile Canister Species Concentrations and Associated R2 Values[52]

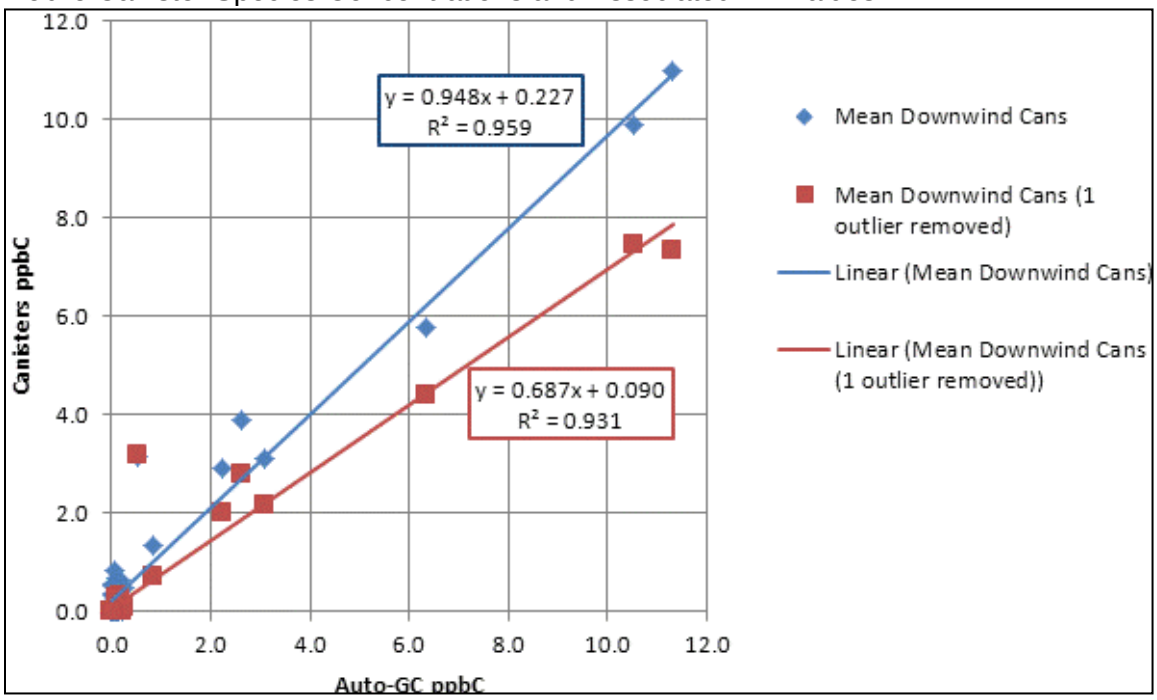

The mobile monitoring study also concluded that, on days where selected 100-meter starting altitude HYSPLIT back trajectories intersected a downwind leg of the monitoring vehicle, TNMHC concentrations increased from upwind samples to downwind samples. Table 4-9 shows the three monitoring sites used to model back trajectories and their associated mean upwind and downwind NO_X and TNMHC concentrations. This table shows that in general, concentrations were higher on average when a back-trajectory intersected a downwind leg of a monitoring route. The NO_X differences are small, but the TNMHC differences are practically significant.

Table 4-9: Mean Concentrations of NOx and TNMHC Where & When a Modeled Back-Trajectory was Near the Monitoring Vehicle

Site	Upwind				Downwind			
	NOx obs	NOx mean ppb	TNMHC obs	TNMHC mean ppbC	NOx obs	NOx mean ppb	TNMHC obs	TNMHC mean ppbC
1. Floresville	27	4.0	27	7.2	49	**6.2**	49	**48.0**
2. SA NW	8	2.4	8	0.4	23	**5.9**	23	**37.9**
3. Camp Bullis	10	**3.0**	10	31.9	20	2.8	20	**53.5**

Table 4-10 shows that mean TNMHC concentrations were higher on the downwind leg than the upwind leg for ten out of twelve trips. For NO_X concentrations, the downwind observations were higher than the upwind on only five of the twelve trips. The result is statistically significant for TNMHC (p-value = 0.019), but not for NO_X. Peak 8-hr ozone for the San Antonio MSA is included in the table and shows two days at or above the 65 ppb threshold. The average peak 8-hr ozone for only upwind monitors in the San Antonio MSA is also included, to control for other emissions factors in the urbanized area that might

[52] *Ibid.*

influence ozone concentrations downwind of the city. The highest ozone value recorded in San Antonio occurred on May 10th, although it is difficult to discern a pattern that explains the peak 8-hr ozone given the TNMHC and NO_X concentrations in the above table. It is interesting to note that the two highest ozone days, both overall and upwind only, corresponded to the only two days with decreases in both TNMHC and NO_X from upwind to downwind canisters during the sampling period.

Table 4-11 compares UT NO_X observations with NO_X readings at C59. In almost every case UT sampling had higher NO_X readings compared to NO_X recorded at the monitor, and in some cases much higher. An examination of resultant wind direction and speed at CAMS 59 might help to explain the larger differences between that monitor and the UT mobile canister samples. The largest difference occurs on 9 June. On that day at CAMS 59 there was an abrupt wind shift out of the north at the time the canister sample was taken, which might help explain why NO_X at the CAMS for that time was lower than expected.

Table 4-10: Upwind and Downwind Mean Observations by Date and Trip[53]

Date	Hourly WDR mean	Upwind				Downwind				Peak 8-hour Ozone San Antonio MSA	Average Peak 8-hr Upwind Ozone
		Start /stop	Number of obs.	NO_X: mean ppb	TNMHC: mean ppbC	Start /stop	Number of obs.	NO_X: mean ppb	TNMHC: mean ppbC		
5/10	147.3	13:09-14:41	147	4.2	3.1	15:51-18:17	180	3.0	1.9	72	57.2
5/17	160.5	10:55-12:53	138	2.9	20.0	14:20-17:01	168	2.8	18.3	65	59.5
5/19	156.1	11:21-13:06	180 (178)*	3.0	33.1 (16.3)*	13:57-15:18	112	2.8	46.1	57	52.2
5/21	147.4	11:51-13:32, 17:00-17:17	158	4.8	33.5	14:19-15:51	149	4.0	45.7	41	34.6
5/22	145.3	10:55-11:18, 11:35-12:15, 15:59-16:17	153	3.4	16.0	13:02-14:55	179	3.5	24.1	34	31.4
6/2	131.9	11:32-13:26	184	1.9	15.2	14:15-16:28	131	5.5	119.6	40	34.4
6/3	113.1	11:21-13:09	181	7.8	25.5	13:58-15:13	108	4.6	136.4	41	31.2
6/5	166.3	11:39-13:36	192	3.3	18.5	14:26-16:18	186	2.0	50.7	25	23.0
6/6	153.1	10:49-12:48	190	1.3	16.3	13:36-15:25	165	4.5	30.9	25	21.8
6/9	189.5	11:02-12:47	181	3.2	5.4	13:36-15:40	181	10.2	37.4	35	30.4
6/11	158.6	11:34-13:35	191	3.9	26.5	14:23-16:42	165	3.5	37.8	53	37.4
6/12	155.8	12:04-14:08	197	2.9	17.2	15:05-16:47	170	3.1	42.5	42	28.2

* "Number of observations and TNMHC mean recalculated omitting two outlier values on 5/19/2014 are in parentheses. Omission of these two points did not change the NO_X mean".

[53] *Ibid.*

Table 4-11: Comparison Between UT's Eagle Ford Shale Mobile Monitoring Study Mean NO_X and Recorded NO_X at C59

Date	Upwind				Downwind			
	Start /stop	UT NO_X: mean ppb	C59 NO_X Readings ppb	Difference (ppb)	Start /stop	UT NO_X: mean ppb	C59 NO_X Readings ppb	Difference (ppb)
5/10	13:09-14:41	4.2	3.8	0.4	15:51-18:17	3.0	3.2	-0.2
5/17	10:55-12:53	2.9	2.1	0.8	14:20-17:01	2.8	2.0	0.8
5/19	11:21-13:06	3.0	1.8	1.2	13:57-15:18	2.8	1.7	1.1
5/21	11:51-13:32, 17:00-17:17	4.8	1.7	3.1	14:19-15:51	4.0	1.8	2.2
5/22	10:55-11:18, 11:35-12:15, 15:59-16:17	3.4	1.9	1.5	13:02-14:55	3.5	1.8	1.7
6/2	11:32-13:26	1.9	1.7	0.2	14:15-16:28	5.5	1.5	4.0
6/3	11:21-13:09	7.8	1.6	6.2	13:58-15:13	4.6	1.5	3.1
6/5	11:39-13:36	3.3	1.7	1.6	14:26-16:18	2.0	1.6	0.4
6/6	10:49-12:48	1.3	1.3	0.0	13:36-15:25	4.5	1.2	3.3
6/9	11:02-12:47	3.2		-	13:36-15:40	10.2	1.5	8.7
6/11	11:34-13:35	3.9	2.1	1.8	14:23-16:42	3.5	2.0	1.5
6/12	12:04-14:08	2.9	2.1	0.8	15:05-16:47	3.1	2.3	0.8

Table 4-12: Comparison between UT's Eagle Ford Shale Mobile Monitoring Study Mean TNMHC and Recorded TNMHC at C1038[54]

Date	Downwind			
	Start/Stop Time (CDT)	UT TNMHC: mean* ppb-C	C1038 TNMHC mean* ppb-C:	Difference (ppb)
5/10	15:51-18:17	1.9	64.7	-62.8
5/17	14:20-17:01	18.3	19.6	-1.3
5/19	13:57-15:18	46.1	20.2	25.9
5/21	14:19-15:51	45.7	17.7	28.0
5/22	13:02-14:55	24.1	17.4	6.7
6/2	14:15-16:28	119.6	61.6	58.0
6/3	13:58-15:13	136.4	118.2	18.2
6/5	14:26-16:18	50.7	25.5	25.2
6/6	13:36-15:25	30.9	14.3	16.6
6/9	13:36-15:40	37.4	47.9	-10.5
6/11	14:23-16:42	37.8	23.9	13.9
6/12	15:05-16:47	42.5	-	-

* Mean values represent the mean TNMHC of the period specified in the Start/Stop Time column.

TNMHC concentrations at CAMS 1038 were compared with the UT mobile sampler at its downwind location in Table 4-12. While there is much variation in the differences, all except three days had higher concentrations for mobile samples than the CAMS site. On June 11th, UT deployed two canister samples to measure VOCs less than 0.1 km away from the Floresville Auto-GC site for comparison purposes. Figure 4-18 shows this comparison and reveals good agreement between the two sampling methods.[55]

[54] *Ibid.*
[55] *Ibid.*

Figure 4-18: Comparison of Speciated UT Canister Samples With Speciated Floresville Auto-GC Observations

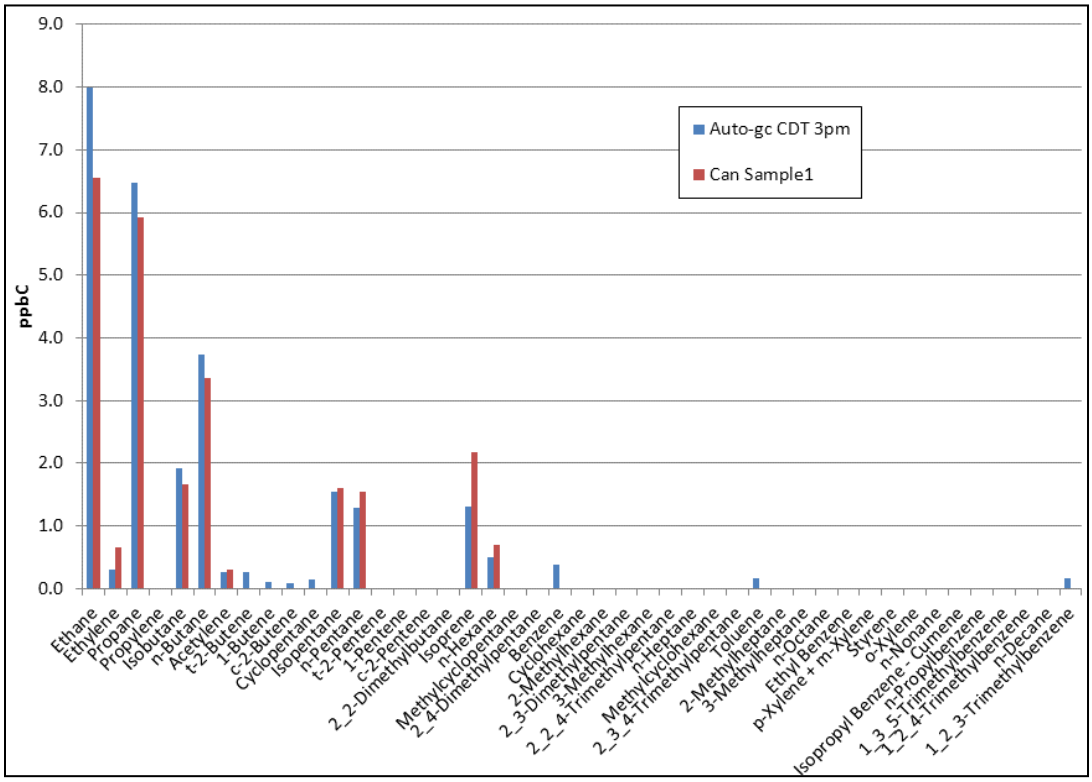

Figure 4-19 and Figure 4-20 plot the diurnal variation of ozone and NO_X at the Calaveras (C59) and Cuero (C1602) CAMS sites, respectively. Also included is the average timeframe of upwind and downwind samples taken by the UT mobile monitor. These graphs show that the times at which precursor pollutants were sampled by UT were times during which NO_X levels tend to remain steady, thereby controlling for diurnal effects when comparing upwind and downwind pollutant concentrations. Opportunities for further study might include having two monitoring vehicles running simultaneously (one each for upwind and downwind routes) during the morning hours when precursor pollutant concentrations are higher.

Figure 4-19: UT's Eagle Ford Shale Mobile Monitoring Study Sampling Time and C59 Average Hourly NO_X and 1-Hour Ozone, 2010-2014 Ozone Season Days

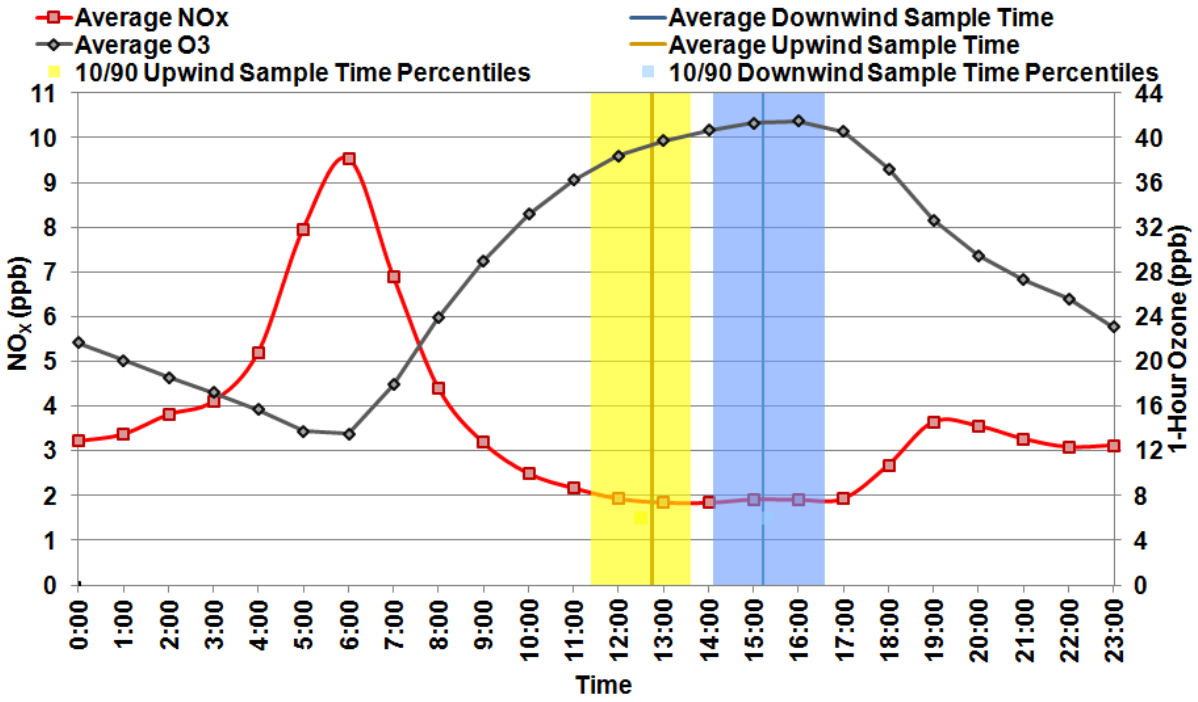

Figure 4-20: UT's Eagle Ford Shale Mobile Monitoring Study Sampling Time and C1602 Average Hourly NOX and 1-Hour Ozone, 2014 Ozone Season Days

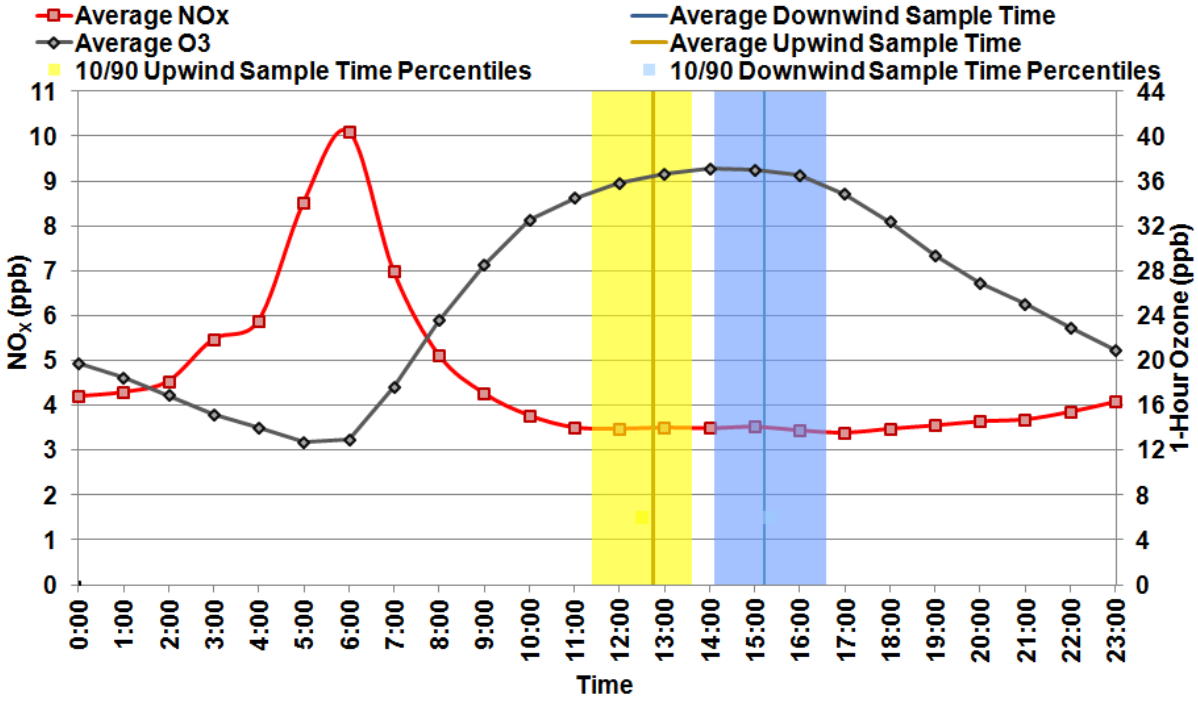

4.6 Back Trajectories

Fifty-nine percent (26 days) of the 48-hour 100-meter back trajectories ending at CAMS23 cross the Eagle Ford shale development on days exceeding the 8-hour ozone NAAQS from 2008 to 2014 (Table 4-13). Twenty one (46%) of these back trajectories cross the Eagle Ford shale development in the southern portion of the Eagle Ford, Gonzales County boundary or farther south, where most of the Eagle Ford development is occurring. For 24-hour 100-meter back trajectories, 41% (19 days) cross the Eagle Ford southern portion before arriving at CAMS23 out of a total of 44 exceedance days from 2008 to 2014.

Figure 4-21 illustrates 48-hour 100-meter back trajectories on high ozone days for CAMS23. As shown, there are a number of back trajectories that flow over the core area of Eagle Ford before arriving at the regulatory monitors in San Antonio. For C58, 43% of the back trajectories on high ozone days > 65 ppb flowed from the south and southeast from 2009 to 2014.

Table 4-13: Days of High Ozone Readings >75 ppb in San Antonio, 2008-2014

Year	Highest Regulatory Monitor	Date	Highest 8-hour Ozone Reading at a Regulatory Monitor	Does C23 48-hour 100-meter Back Trajectory Cross Eagle Ford*	Does C23 24-hour 100-meter Back Trajectory Cross Eagle Ford*
2008	C58	May 8	77	No	No
	C23	June 23	78	**Yes**	**Yes**
	C23	September 6	78	**Yes**	**Yes**
	C23	September 26	81	**Yes**[#]	**Yes**[#]
	C23	September 27	82	**Yes**[#]	**Yes**[#]
	C23	September 28	78	**Yes**[#]	**Yes**[#]
	C59	September 30	79	No	No
	C23	October 1	81	No	No
	C58	October 2	78	**Yes**	**Yes**
2009	C23	May 28	76	**Yes**[#]	**Yes**[#]
	C58	May 30	77	**Yes**	**Yes**
	C23	June 5	90	No	No
2010	C58	May 28	86	**Yes**	No
	C23	August 27	80	**Yes**[#]	No
	C23	August 28	87	**Yes**[#]	No
	C58	October 16	78	**Yes**	**Yes**
2011	C23	May 16	78	No	No
	C23	June 6	79	**Yes**	**Yes**
	C23	August 27	76	**Yes**	**Yes**
	C23	August 28	77	No	No
	C58	August 29	76	**Yes**	**Yes**
	C23	September 7	87	No	No
	C23	September 10	84	No	No
	C23	September 11	78	**Yes**	**Yes**
	C23	October 2	78	**Yes**	**Yes**
	C23	October 3	79	**Yes**	**Yes**

Year	Highest Regulatory Monitor	Date	Highest 8-hour Ozone Reading at a Regulatory Monitor	Does C23 48-hour 100-meter Back Trajectory Cross Eagle Ford*	Does C23 24-hour 100-meter Back Trajectory Cross Eagle Ford*
2012	C23	May 17	76	No	No
	C23, C58	June 26	89	**Yes**	**Yes**
	C58	June 27	90	**Yes**	**Yes**
	C23	August 20	77	No	No
	C58	August 21	87	No	No
	C58	August 22	76	No	No
	C58	September 10	90	No	No
	C23	September 19	81	No	No
2013	C58	May 13	77	**Yes**	**Yes**
	C58	June 3	79	No	No
	C58	June 4	87	**Yes**	**Yes**
	C58	July 4	83	**Yes**	**Yes**
	C58	July 5	84	**Yes**	**Yes**
	C58	August 18	79	No	No
	C58	August 29	78	**Yes**	**Yes**
	C58	August 30	80	**Yes**	**Yes**
	C23	September 23	85	No	No
	C58	September 25	87	No	No
2014	C59	May 30	81	No	No
	C23	October 23	76	**Yes**	No

* 48-hour 100-meter back trajectory ending at each monitor during the highest peak 1-hour ozone reading

[#] the back trajectory crosses only the northern portion (north of Gonzales County) of the Eagle Ford Shale Development that is not heavily developed

Figure 4-21: CAMS58 48-hour Back Trajectories on Days with 8-Hour Ozone > 75 ppb and the Location of Eagle Ford, 2009-2014

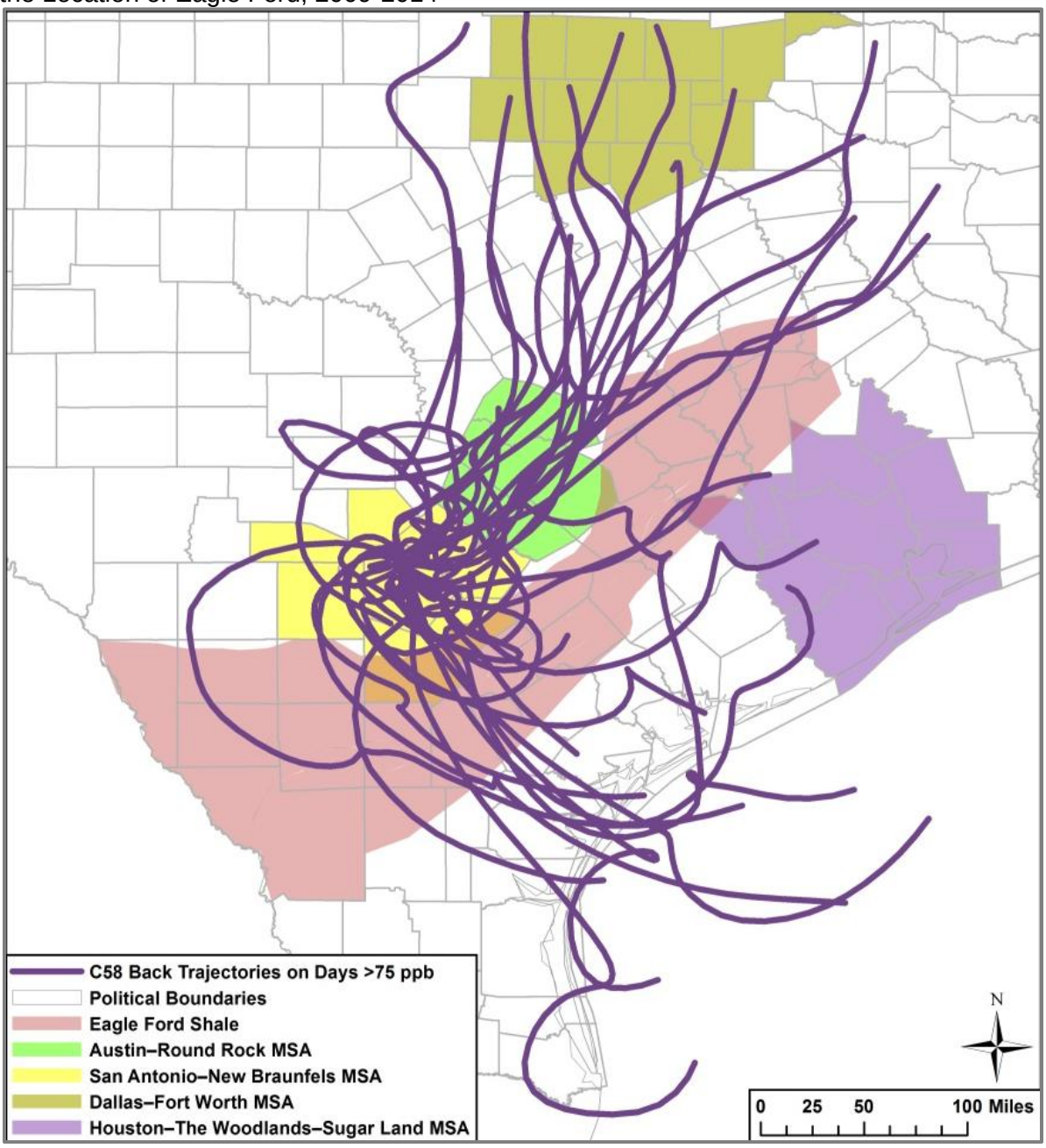

100-meter 24 hour back trajectories

Only three high ozone days listed in Table 4-13 are able to be analyzed using the Floresville Auto-GC monitor. Table 4-14 gives the daily average concentrations of ethane and ethylene at the Solar Estates monitor west of Corpus Christi and the Floresville monitor on and leading up to these high ozone days. Ethane enhancement across the shale ranged from 5 ppb-V to 13 ppb-V during the 2013 episode and from 9 ppb-V to 16 ppb-V during the 2014 event. The first two high ozone days (August 29-30) show enhancement of ethylene between 0.022 ppb-V and 0.256 ppb-V across the Eagle Ford. There does not appear to be an enhancement of ethylene across the shale for the 2014 high ozone event event.

Table 4-14: Enhancement of Ethane and Ethylene Across the Eagle Ford on High Ozone Days (2013 – 2014)

	Solar Estates Auto-GC (Upwind)		**Floresville Auto-GC (Downwind)**	
	Ethane (ppb-V)	Ethylene (ppb-V)	Ethane (ppb-V)	Ethylene (ppb-V)
August 27, 2013	3.248	0.206	16.504	0.462
August 28, 2013	6.073	0.303	17.582	0.348
August 29, 2013	4.649	0.246	9.934	0.350
August 30, 2013	4.168	0.304	13.632	0.326
October 21, 2014	10.621	0.884	26.845	0.581
October 22, 2014	11.948	0.924	25.246	0.575
October 23, 2014	13.430	0.767	22.611	0.663

However, in mapping the back trajectories in relation to the Auto-GC sites, it is evident that the locations of the upwind and downwind Auto-GC monitors do not reflect transport conditions during the October 2014 event. The 48-hr back trajectory for that day misses the most intensive shale activity and is well away from the upwind monitor location. Figure 4-22 shows the path of the back trajectories for the three high ozone events captured by the Floresville monitor. The October 2014 event could have been more a factor of transport of ozone and its precursors from the Houston area than from the Eagle Ford Shale. It should be stressed that back trajectory models have uncertainties associated with the accuracy and resolution of the meteorological monitoring network, and should not be interpreted as precise tracks of air parcels.

Figure 4-22: 48-Hr Back Trajectories on Select High Ozone Days and Locations of Auto-GC Monitors

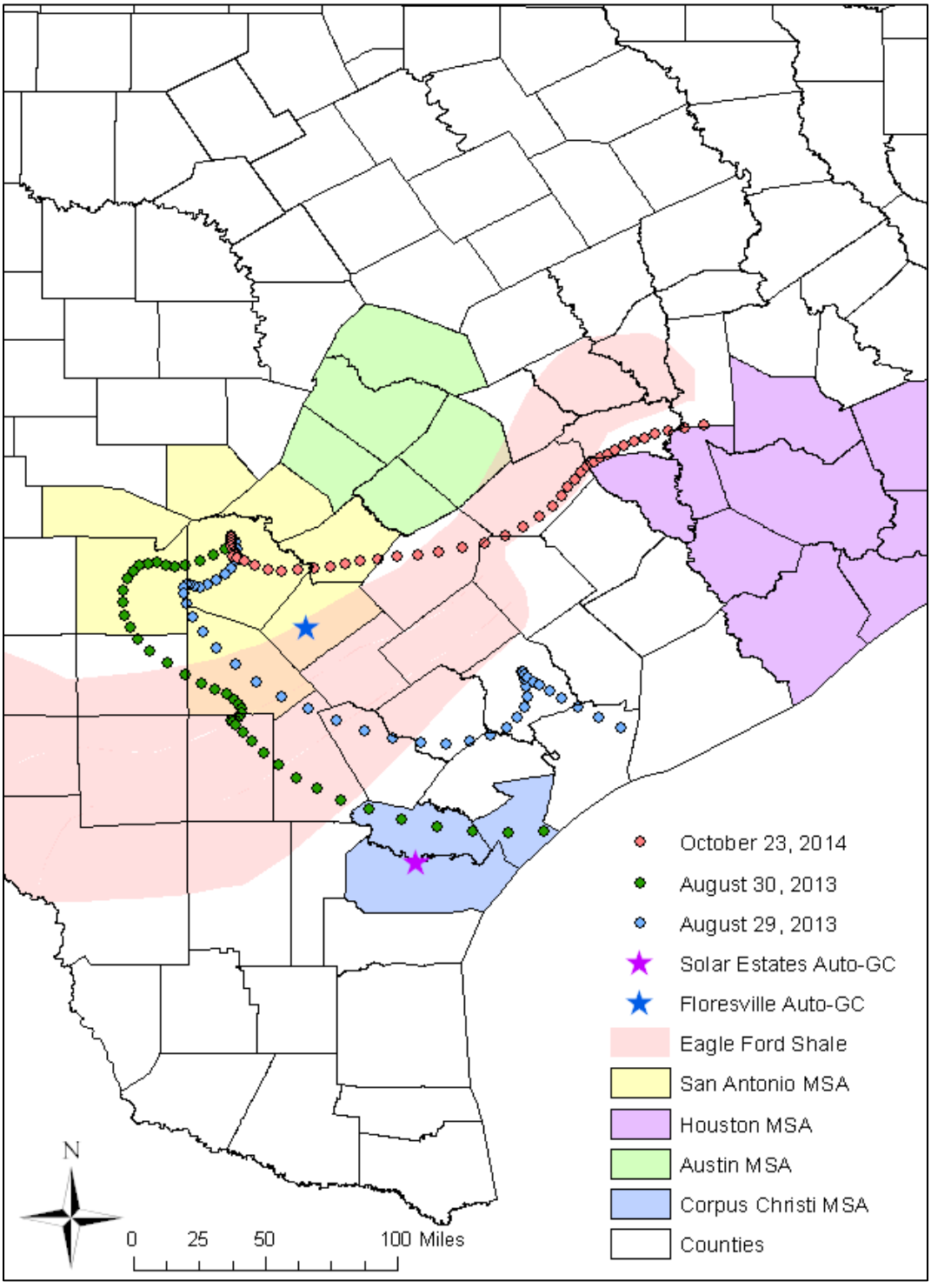

4.7 Eagle Ford Photochemical Modeling Runs

A 2012 base case run was performed with and without the 2012 Eagle Ford emission inventory. Tile plots of the difference in predicted maximum ozone levels for these runs are provided in Figure 4-23. A total of 2 future year scenarios were developed from the June 2006 modeling episode with TCEQ approved Eagle Ford emission inventory.

2018 Without Eagle Ford Emission Inventory

- WRF v3.2
- CAMx 5.40
- Local 2018 San Antonio-New Braunfels MSA emission data including construction equipment, landfill equipment, quarry equipment, agricultural tractors, combines, commercial airports, point sources, and heavy duty truck idling

2018 Moderate Eagle Ford Emission Inventory

- WRF v3.2
- CAMx 5.40
- Local San Antonio-New Braunfels MSA emission data including construction equipment, landfill equipment, quarry equipment, agricultural tractors, combines, commercial airports, point sources, and heavy duty truck idling
- Eagle Ford 2018 Emission Inventory Moderate Scenario

Figure 4-23: Predicted Daily Maximum Difference in 8-hour Ozone Concentrations in the 4-km Subdomain, 2018 Eagle Ford - Base Case[56]

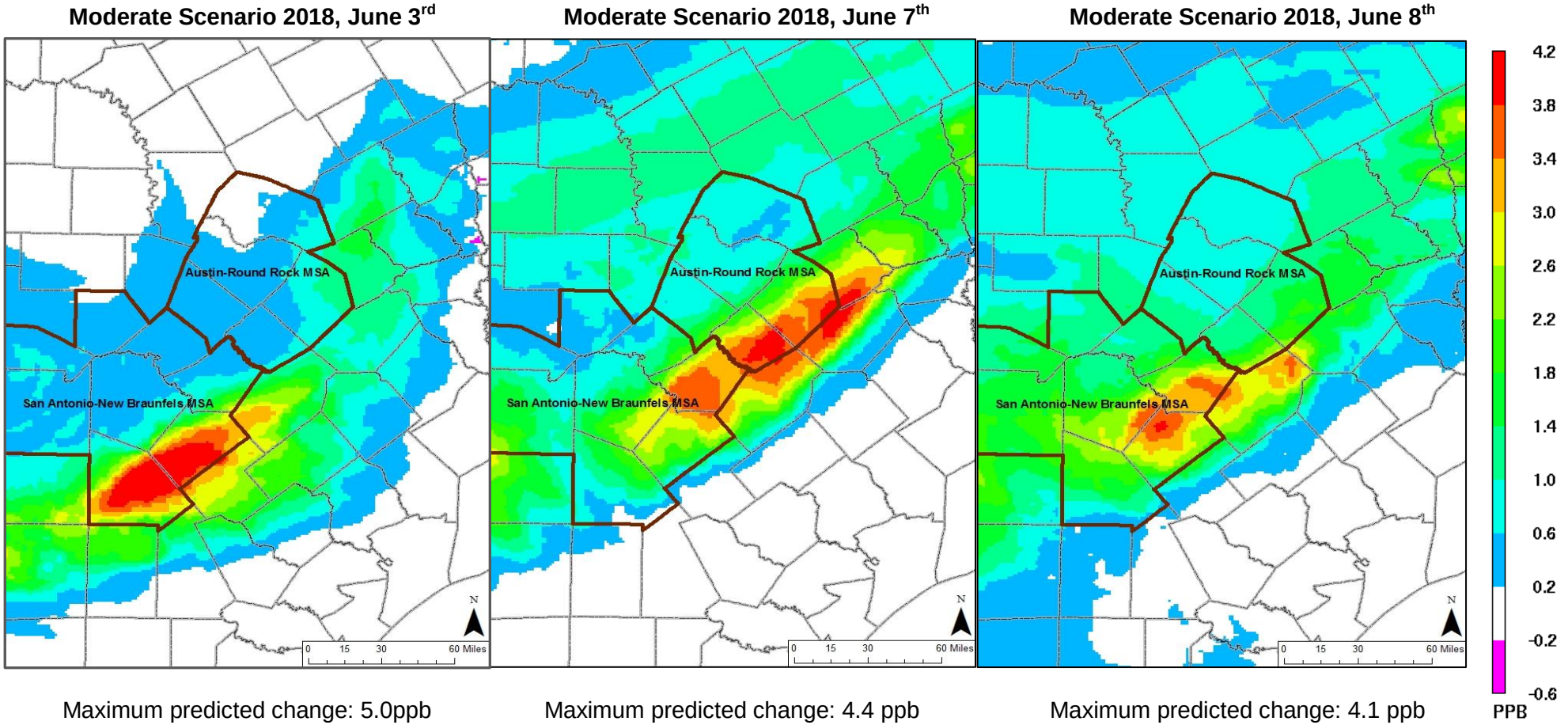

Maximum predicted change: 5.0ppb

Maximum predicted change: 4.4 ppb

Maximum predicted change: 4.1 ppb

[56] Alamo Area Council of Governments. "Development of the Extended June 2006 Photochemical Modeling Episode." October 2013. Available online: https://www.aacog.com/DocumentCenter/View/19262. Accessed 04/13/2015.

Moderate Scenario 2018, June 9th

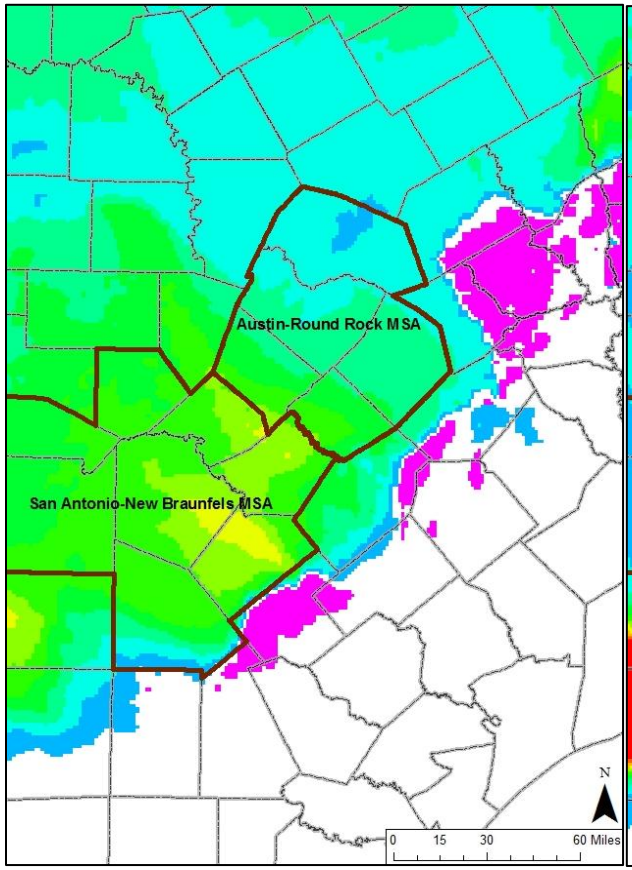

Maximum predicted change: 3.8 ppb

Moderate Scenario 2018, June 13th

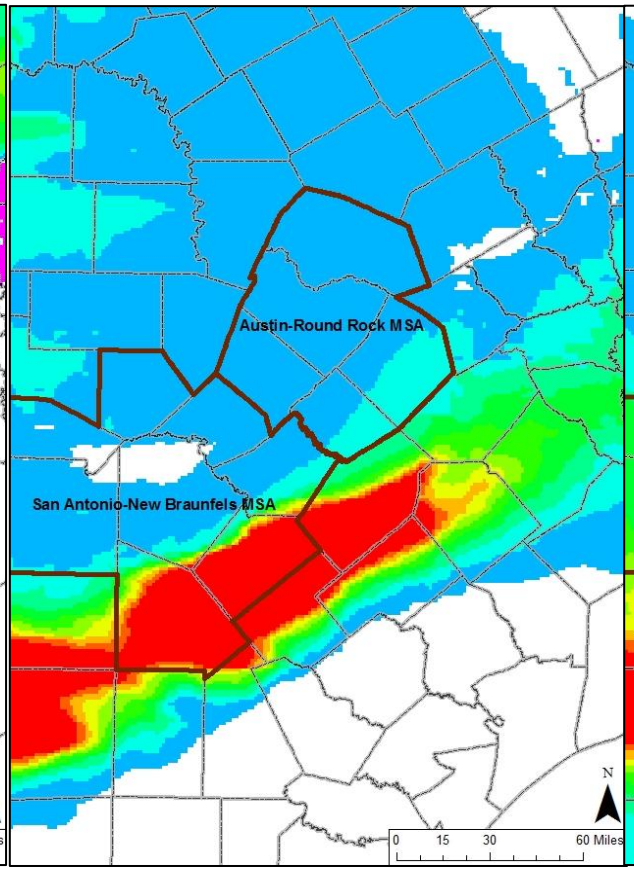

Maximum predicted change: 11.3 ppb

Moderate Scenario 2018, June 14th

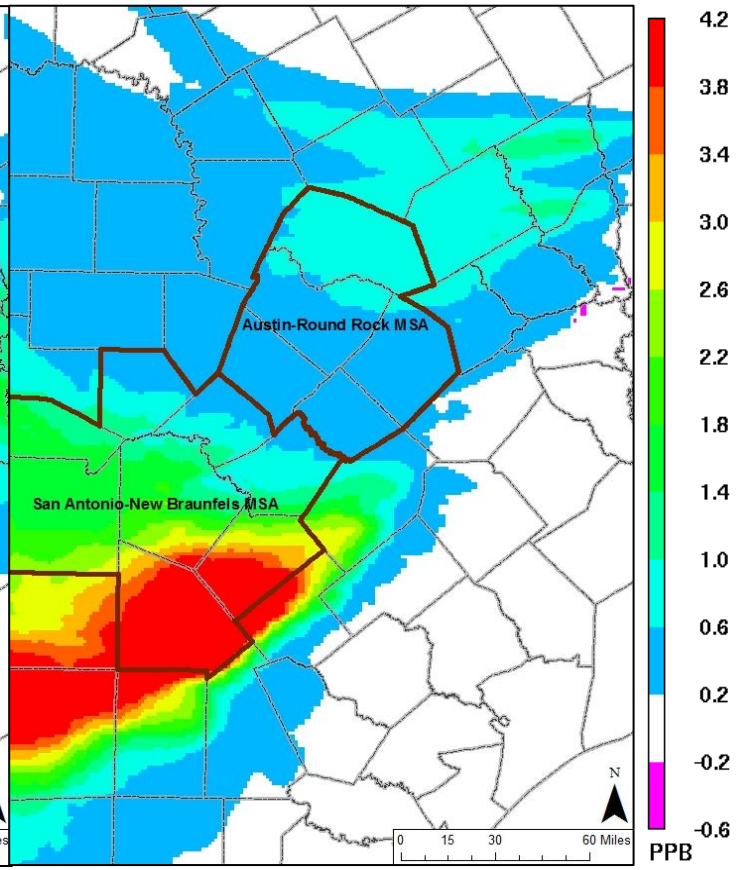

Maximum predicted change: 9.4 ppb

Moderate Scenario 2018, June 26th **Moderate Scenario 2018, June 27th** **Moderate Scenario 2018, June 28th**

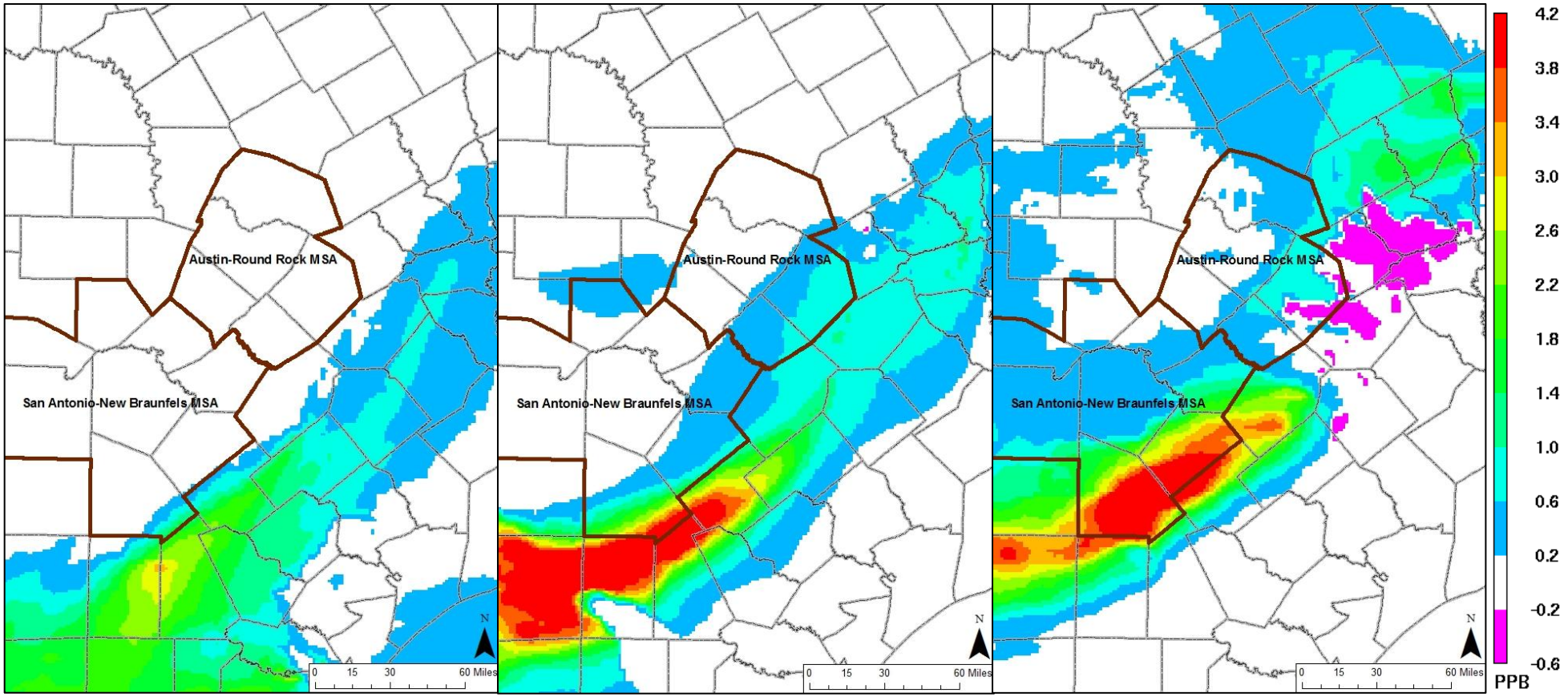

Maximum predicted change: 4.3 ppb

Maximum predicted change: 6.1 ppb

Maximum predicted change: 5.7 ppb

Moderate Scenario 2018, June 29th

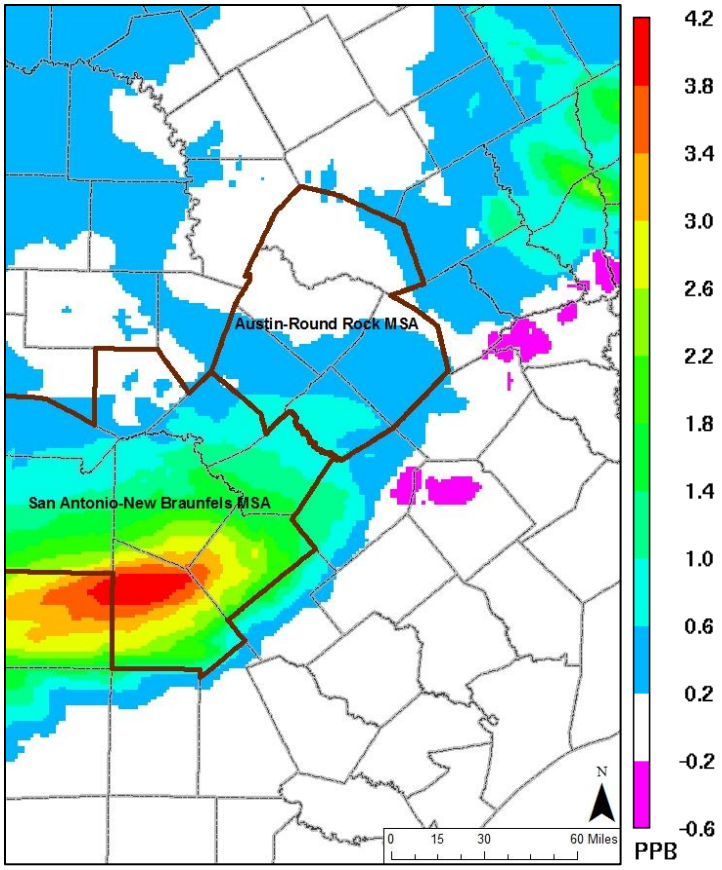

Maximum predicted change: 4.2 ppb

Table 4-15: Maximum Change in 8-Hour Ozone at each Monitor, Eagle Ford Emission Inventory, Moderate Scenario, 2018, ppb.

Monitor	6/3	6/7	6/8	6/9	6/13	6/14	6/26	6/27	6/28	6/29	Maximum Change	Percentage of Total Ozone
C23	0.58	1.69	1.96	2.38	0.31	2.24	0.00	0.08	0.40	1.53	2.38	2.6%
C58	0.61	1.32	1.55	2.38	0.24	1.77	0.00	0.08	0.36	1.18	2.38	2.6%
C59	3.34	3.02	3.77	2.90	5.99	3.90	0.00	0.22	2.84	3.23	5.99	7.7%
C622	2.46	3.06	3.77	2.90	2.20	3.08	0.00	0.20	2.42	2.83	3.77	4.5%
C678	0.99	3.02	3.66	2.87	0.62	2.72	0.00	0.16	0.90	2.39	3.66	4.1%

4.8 Summary of the Effect of the Eagle Ford Shale on the San Antonio Region

- The Eagle Ford Shale formation contains oil and gas reserves that require intensive extraction techniques to release them. Only recently has hydraulic fracturing become economically and technologically feasible. The numbers of gas wells and oil leases increased exponentially between 2009 and 2013.
- Eagle Ford Shale emissions of NO_X were estimated to be 121 tons per ozone season day. Emissions of VOCs were estimated to be 223 tons per ozone season day. By 2018, using the moderate development scenario, emissions are projected to increase to 302 tons per day of NO_X and 929 tons per day of VOCs.
- By 2018, storage tanks, mid-stream sources, and loading loss will account for over 75% of VOC emissions. Mid-stream sources will account for over half of all NO_X by 2018.
- In 2012, over 50% of all Eagle Ford NO_X and VOC emissions originated in just four of the 26 counties that comprise the formation: LaSalle, Karnes, Dimmit, and Webb. This proportion is expected to remain about the same under the 2018 moderate development scenario.
- An Automated Gas Chromatograph was installed in Floresville in July 2013. This monitor records hourly concentrations of 46 different VOC species. Yet another Auto-GC was installed farther southeast, deeper into the shale play at the Karnes County Courthouse in December 2014. Trends are difficult to determine given such a limited dataset, but insights into transport of VOCs can still be obtained through analysis.
- A factor analysis of VOCs in Floresville concluded that there are two factors that influence VOC levels: oil and gas exploration and vehicle combustion. Most compounds are associated with a combination of the two factors, but one usually dominates over the other. Those compounds that are a factor of oil and gas exploration tend to be more concentrated downwind of the Eagle Ford Shale. The ones that are a factor of vehicle combustion are more concentrated downwind of those sources.
- Of the 46 species reported at the Auto-GC, six have been identified by TCEQ as HRVOCs, which react quicker than other compounds to produce ozone. The six HRVOCs account for only 1.4% of the daily average VOC concentration by volume for 2014 at the Floresville monitor. HRVOCs tend to be more associated with vehicle combustion rather than oil and gas exploration.
- VOC concentrations exhibit a diurnal pattern where concentrations are greatest just before sunrise when mixing heights are lower. A seasonal pattern also appears to exist, with greater concentrations of VOCs occurring in the colder winter months. The ozone season coincides with the seasonal minimum for VOC concentrations.
- There is no weekday/weekend effect for VOCs or HRVOCs except for random variation.
- Morning resultant wind directions appear to play a role in determining ethane concentrations. Winds out of the east and southeast more typically bring higher ethane levels. This relationship is not as well defined for ethylene, other HRVOCs, or for NO_X, and high concentrations are more likely to occur from any direction. This is consistent with the latter two compounds being factors of vehicle combustion, which is not limited to the Eagle Ford Shale.
- The Eagle Ford Shale provides an enhancement of VOC concentrations on days where back trajectories cross the formation. Average enhancement for ethane is over 6 ppb-V, but can be as much as 40 ppb-V, as observed by UT. Enhancement of HRVOCs like ethylene are not as substantial, but still present.
- Since 2008, 46% of all 48-hour back trajectories ending at CAMS 23 crossed the most heavily developed area of the Eagle Ford Shale on days that recorded a violation of the 2008 NAAQS.

- Photochemical modeling estimates that the Eagle Ford Shale could have an impact on in San Antonio, given moderate projected emissions levels in 2018.

5 Background Ozone and Ozone Transport into San Antonio Area

This section explores meteorological factors contributing to transport of background ozone into the San Antonio area. In urbanized areas, not all ozone formation is necessarily caused by emissions produced locally, because anthropogenic precursors and ozone can be naturally transported over long distances. Analysis of regional ozone transport can provide better understanding of the dynamics of ozone formation on high ozone days in the San Antonio region.

Transported ozone periodically arrives in San Antonio at concentrations above the proposed ozone standard (60 ppb to 70 ppb) ranges. Figure 5-1 shows the 48-hour back trajectory of such an episode, when transported pollutants from industrialized regions caused a high ozone reading (87 ppb) at CAMS23 located northwest of San Antonio. Local emission contributions can further exacerbate the problem on high ozone days. The following chapter examines analysis of upwind monitors, ozone and precursors transport, ozone levels in adjacent regions, aircraft sampling, and photochemical modeling.

Figure 5-1: Transported Ozone and Ozone Precursors to San Antonio on a High Ozone Day

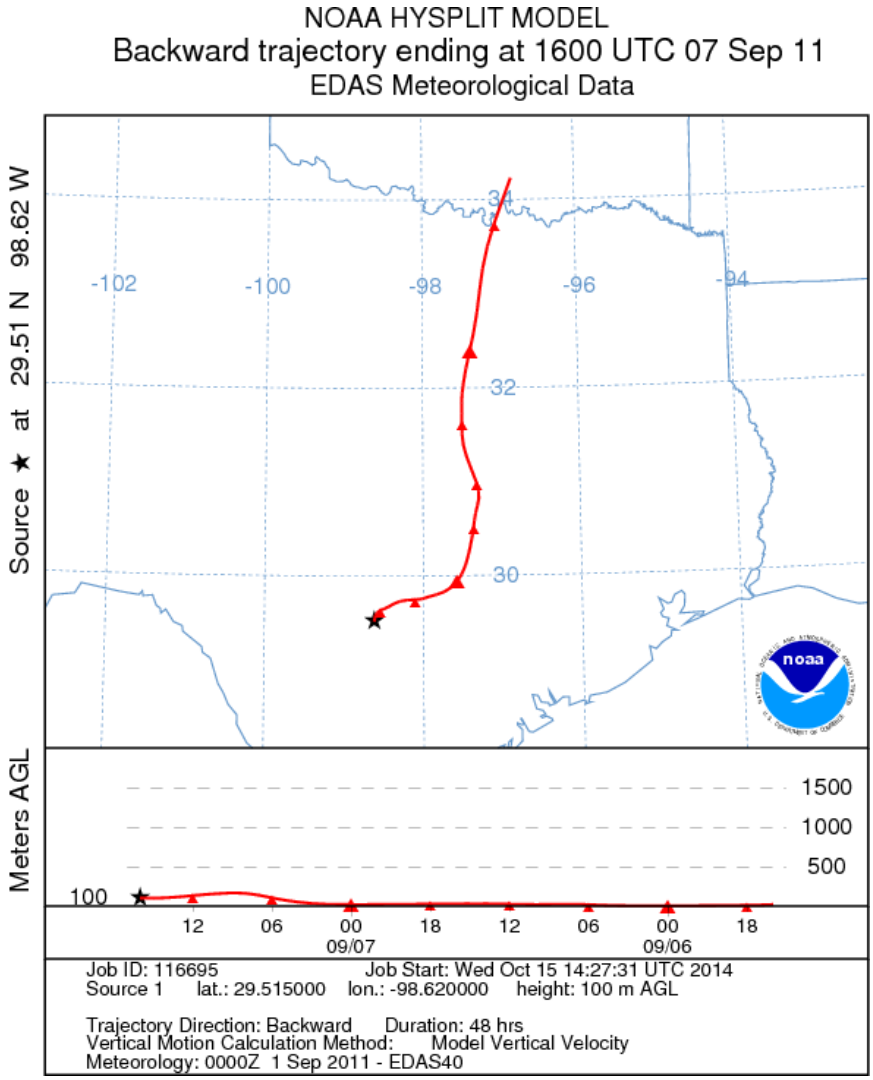

5.1 Upwind Monitors

"It is easy to confuse the words upwind (upstream) and downwind (downstream). In meteorology, a wind direction is the direction the wind is coming from. For example, a Northwest wind is a wind flowing from Northwest toward Southeast. Upwind is the direction the wind is coming from. If the wind is blowing from the Northwest (blowing toward the Southeast) then the upwind direction is toward the Northwest and the downwind direction is toward the Southeast."[57] Winds from various directions may bring different emissions to the area. Ozone levels recorded at upwind monitors on high ozone days can be used to evaluate transported ozone to the region.

In Figure 5-2, the C59, C622, C504, C505, and C506 monitors, represented by yellow bars, are located up-wind on high ozone days: The downwind monitors: C23 and C58, located in urbanized areas, have 2014 ozone design values at or above the current national standard, while the upwind monitors have design values within the current national standard, but still below the proposed standard. This indicates that ozone precursors generated in urbanized areas mixed with transported ozone and ozone precursors can cause elevated ozone readings at downwind monitors and can play an important role in local ozone formation.

Figure 5-2: Ozone Design Values for Each Monitor within the San Antonio Region, 2014

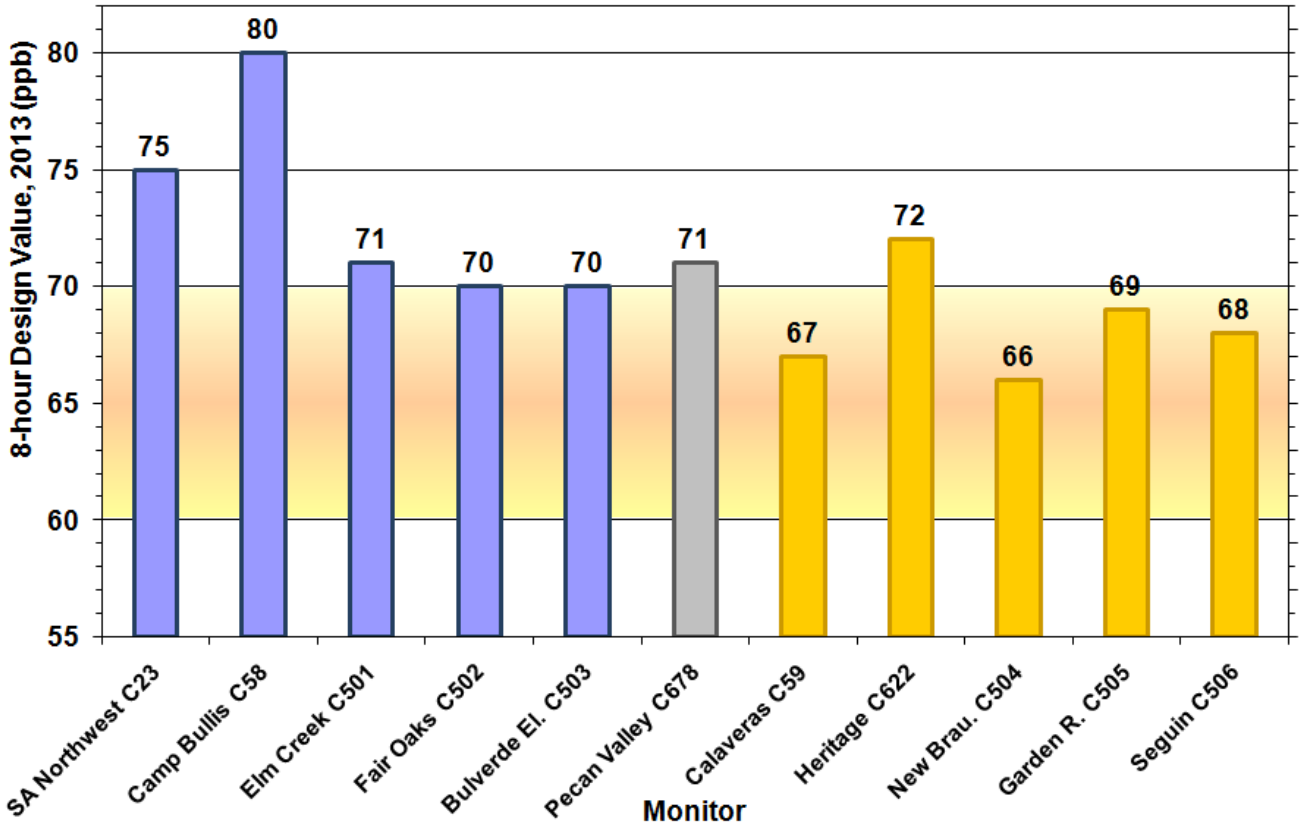

Although still significant amounts of transported ozone arrive in the San Antonio region, these amonuts have decreased over the last five years. In contrast, the difference between the highest downwind local ozone readings and lowest upwind ozone local readings has slightly increased as shown in figure 5-4. From 2006 to 2014, the 4th highest 8-hour average ozone readings at upwind

[57] Haby's Weather School, Oct. 2014, Available online: http://www.theweatherprediction.com/habyhints/32/. Accessed 05/08/15

monitors decreased approximately 9.0 ppb (Figure 5-3).[58] The 4th highest eight-hour average ozone level for one upwind monitor, C505, was below the minimum proposed standard of 60 ppb. All other monitors were within the proposed standard range.

Figure 5-3: Trend in San Antonio Region Upwind Monitors Annual 4th Highest 8-hour Average Ozone Levels

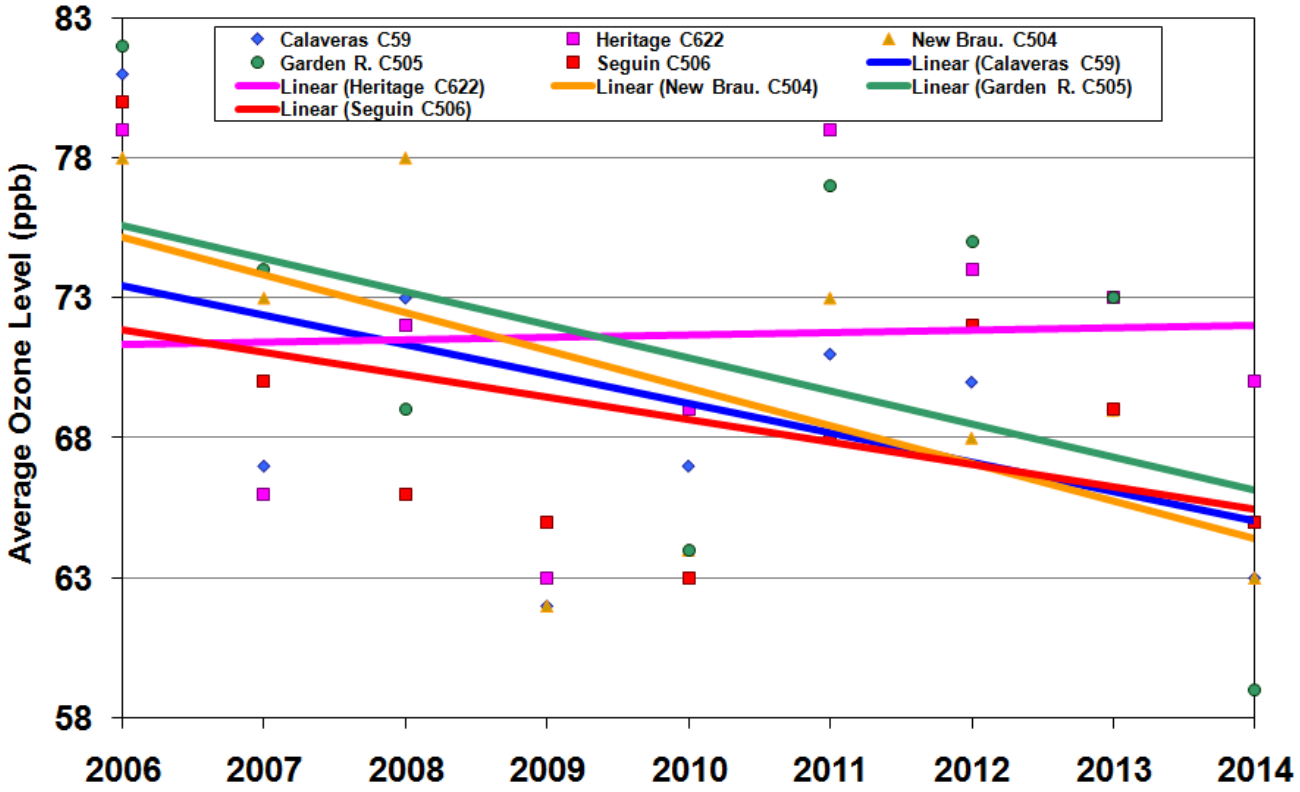

The average amount of background ozone for all ozone season days has decreased over the last 12 years: from 41.3 ppb in 2003 to 33.6 in 2014, or almost 8 ppb. This trend is statistically significant at $\alpha = 0.05$. Local contributions to ozone levels appear to have increased by 2 ppb over the same time period (Figure 5-4). This trend is also statistically significant and has a p-value of 0.016. When considering average locally produced ozone as a percentage of average total ozone, a strong trend of increasing shares of local contribution to total ozone is apparent, starting in 2006 (p-value = 0.0007). In 2003, using the comparison between the lowest and highest ozone recorded in the region, the average local contribution to ozone could account for almost 22% of the average total ozone for all ozone season days. Over time, that number has increased to almost 29% in 2014. The percent shares of transport and background ozone from 2003 to 2014 can be seen in Table 5-1: Percentage of Estimated Local and Background Ozone from 2003-2014.

[58] The results are statistically significant. C59: $\sigma = 7.3$, C622: $\sigma = 6.1$, C504: $\sigma = 7.6$, C505: $\sigma = 7.4$, C506: $\sigma = 6.8$.

Figure 5-4: San Antonio Local and Background Yearly Average Ozone Levels on all Ozone Season Days

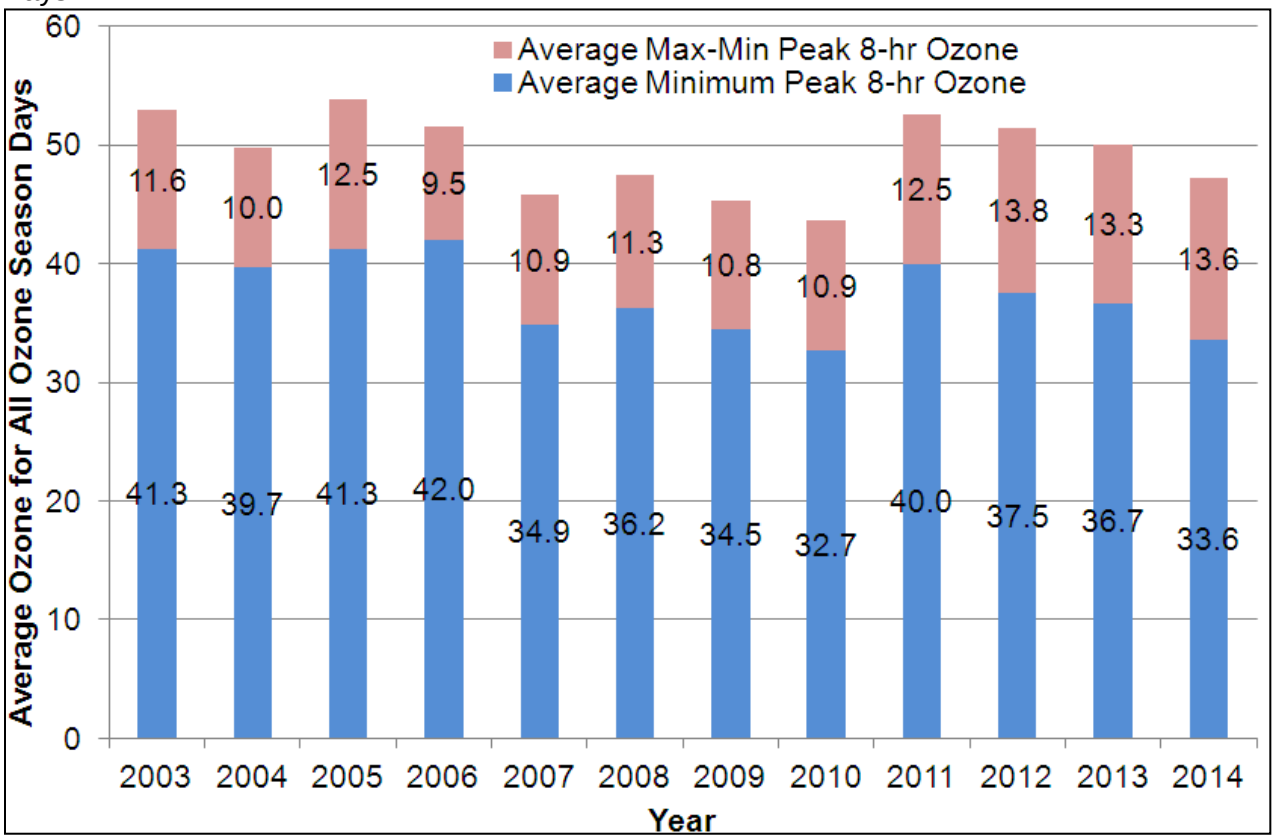

Figure 5-5: San Antonio Local and Background Yearly Average Ozone Levels during Days When Ozone > 65 ppb

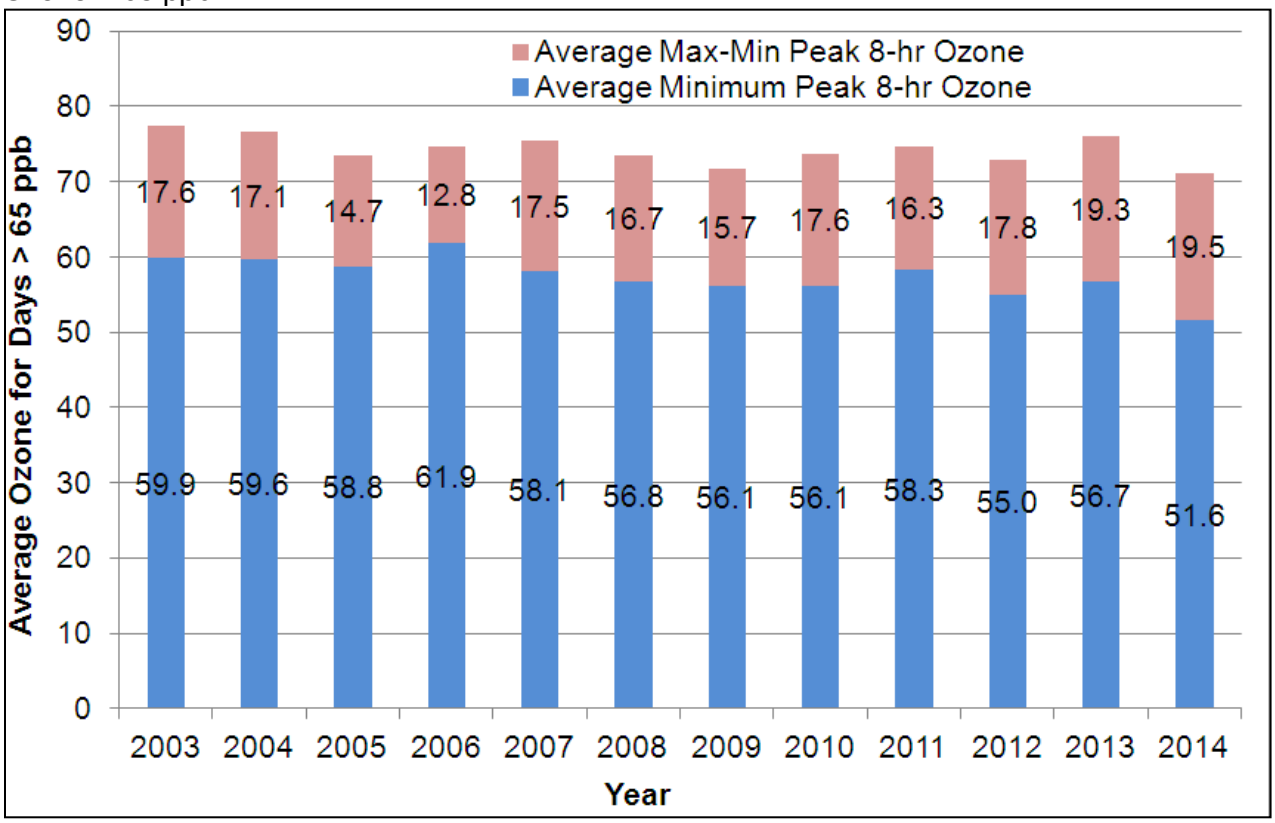

Figure 5-5 shows average upwind and downwind ozone concentrations on days that exceeded 65 ppb ozone. In 2010, the difference was 23.9% on days where ozone > 65 ppb, while in 2014, the difference was increase 27.4%. From 2003-2014, this trend is statistically significant with an R^2 of 0.598 and a p-value of 0.0032. The difference on high ozone days decreased significantly from 57.42 in 2003 to 49.95 in 2014 (p-value = 0.0006) and locally produced ozone increased significantly (p-value = 0.0017). This result increased for ozone days over 65 ppb, from 22% in 2003 to 27% in 2014. Since 2005, background ozone has accounted for a greater share of total ozone concentrations on days with high ozone compared to all ozone season days. For example, in 2014 the share of background ozone on all ozone season days was 71.2%. On high ozone season days, this percentage was 72.6%.

Table 5-1: Percentage of Estimated Local and Background Ozone from 2003-2014

Year	All Ozone Season Days		All Days With Ozone > 65 ppb	
	Estimated Local	Estimated Background	Estimated Local	Estimated Background
2003	21.9%	78.1%	22.7%	77.3%
2004	20.1%	79.9%	22.3%	77.7%
2005	23.2%	76.8%	20.0%	80.0%
2006	18.4%	81.6%	17.1%	82.9%
2007	23.8%	76.2%	23.1%	76.9%
2008	23.8%	76.2%	22.7%	77.3%
2009	24.4%	75.6%	21.9%	78.1%
2010	25.0%	75.0%	23.9%	76.1%
2011	23.8%	76.2%	21.8%	78.2%
2012	26.9%	73.1%	24.5%	75.5%
2013	26.6%	73.4%	25.4%	74.6%
2014	28.8%	71.2%	27.4%	72.6%

Figure 5-7 shows daily peak 8-hour average ozone levels in the San Antonio area and the background ozone transported into the region from 2005-2014. Background ozone concentrations were determined by averaging the lowest 8-hour peak ozone readings from upwind monitors in the San Antonio area. In Figure 5-6, San Antonio's contribution to ozone is derived from the difference between the measured peak ozone reading on a particular day and the average background ozone reading on the same day. Since the R^2 value for the relationship between peak ozone concentrations and San Antonio's contribution is only 0.13, there is a high degree of variability, which indicates local contributions are not good indicators of peak values. On the other hand, the R^2 value for the relationship between peak ozone and background ozone is 0.81, which indicates a very strong relationship. Background ozone levels are much better indicators of peak 8-hr ozone values in the San Antonio area.

Analysis of historical data shown in
Figure 5-8 reveals that the average total number of high ozone days > 60 ppb at upwind monitors has decreased by 79% from 2005 to 2014. However, this trend has not been steady with 2011 showing a large (~200%) increase in the average number of high ozone days at each level of the proposed ozone standard. This increase in the average number of high ozone days coincides with a decrease in the estimated share of ozone that was locally formed. This suggests that 2011 was characterized by an increase in transported ozone into the San Antonio region. Since 2011, the average number of high ozone days has been decreasing and was near 2009-2010 levels by 2014.

Figure 5-7: Measured Peak 8-Hour Ozone in the San Antonio Area and the Background Contribution to that Peak, 2005 – 2014

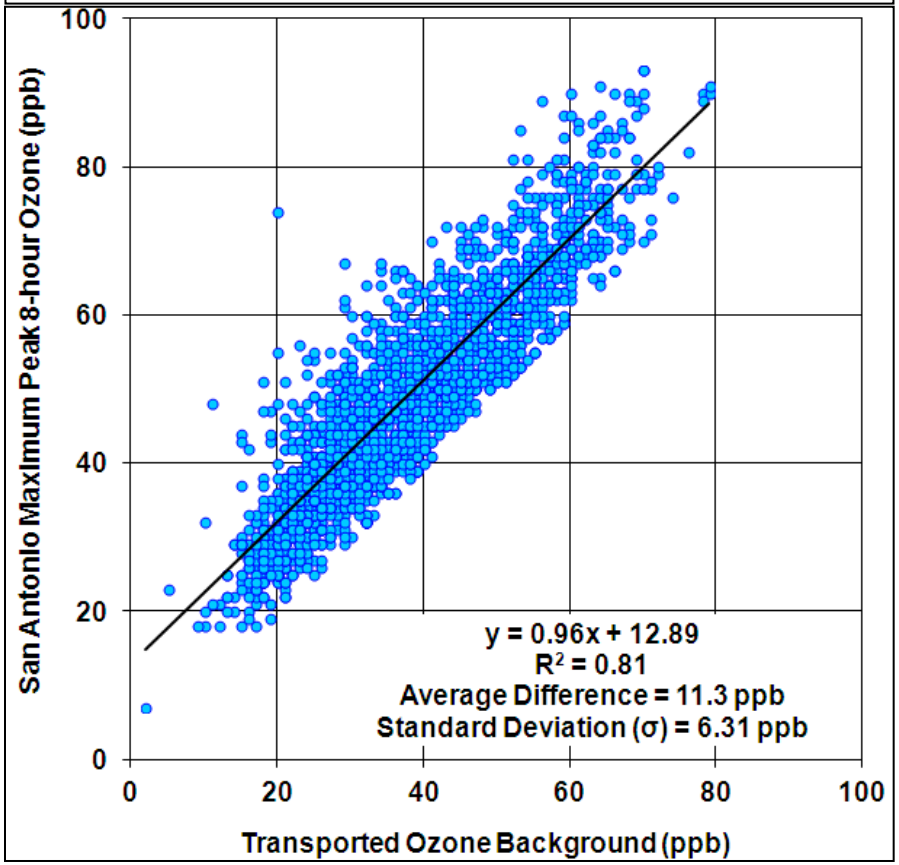

Figure 5-6: Measured Peak 8-Hour Ozone in the San Antonio Area and the Local San Antonio Contribution to that Peak, 2005 – 2014

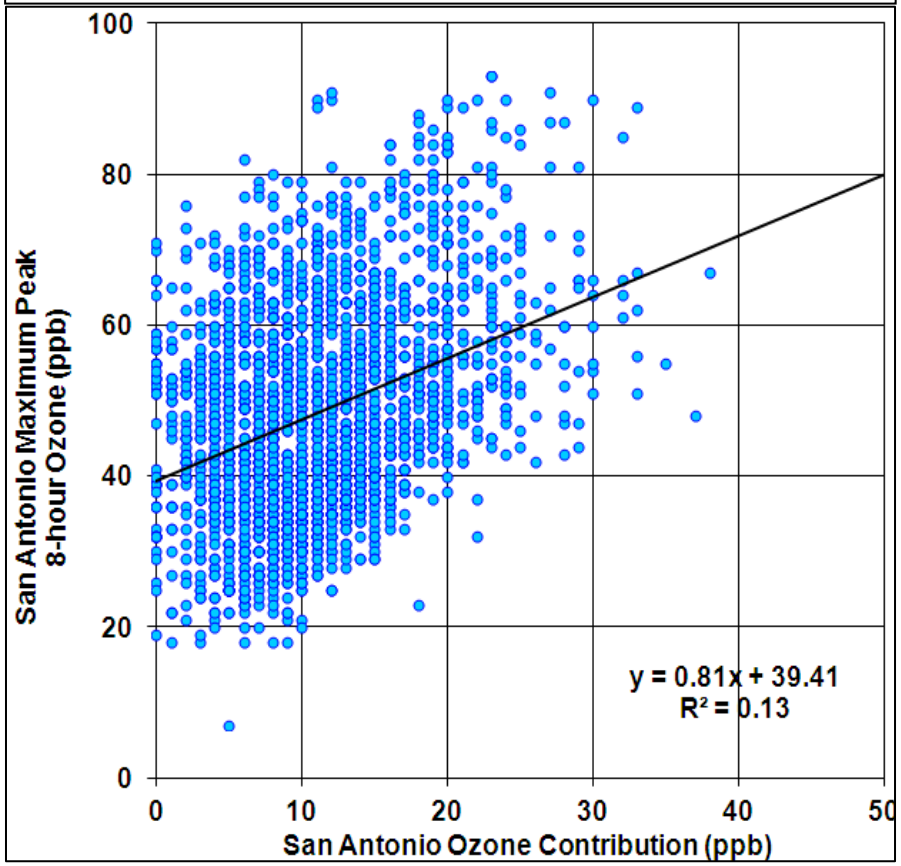

Figure 5-8: Average Number of High Ozone Days at Upwind Monitors by Proposed Standards

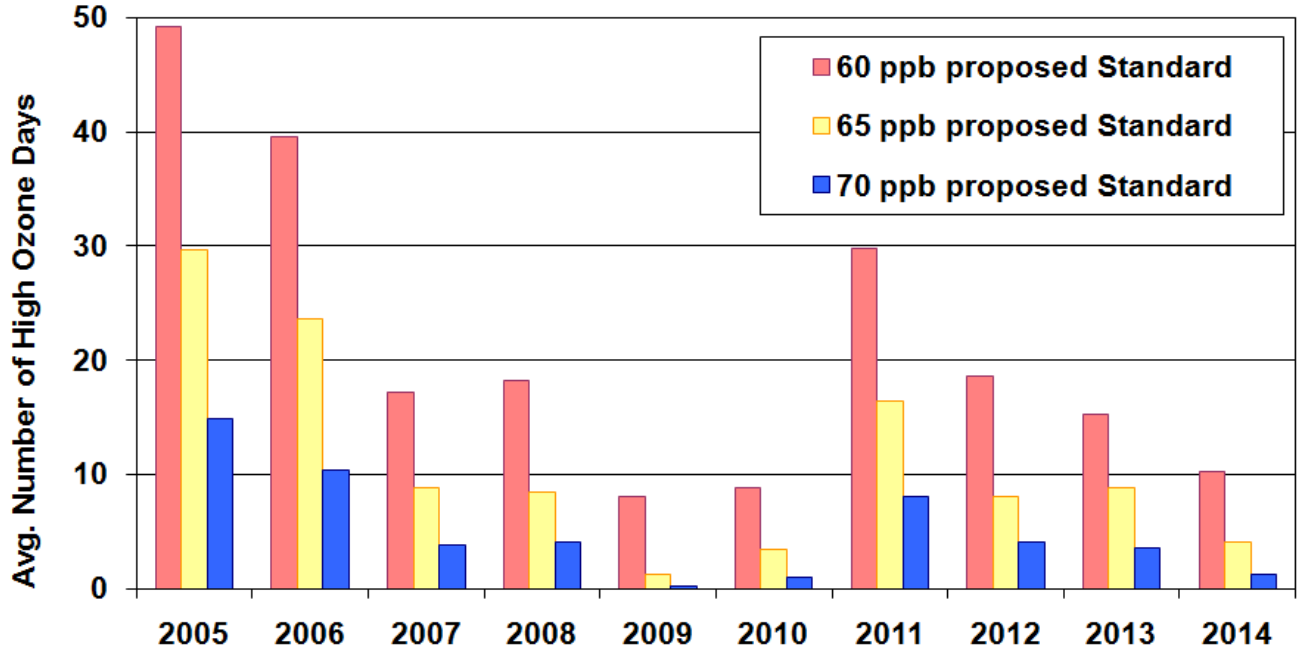

5.2 Back Trajectories

Within an urban area, not all ozone formation is caused by emissions produced locally because anthropogenic precursors, along with ozone formed by them, are often transported over long distances. Therefore, tracking wind parcels coming to the region plays important role in identifying the source of transported ozone. The Air Resources Laboratory of NOAA maintains the Hybrid Single Particle Lagrangian Integrated Trajectory (HYSPLIT) model and allows public use via the Internet at their Realtime Environmental Applications and Display System (READY) webpage.[59] This versatile model can be run as a trajectory (parcel displacement) or air dispersion model, using either forecast or archived meteorological data. The model and database are applicable across the United States, which provides a national reference for air trajectory and dispersion modeling needs. The back trajectories needed for the analyses of transport were created using this model.

The approximate pathways of air entering San Antonio on days of interest were determined using HYSPLIT model. Figure 5-9 contains air mass back trajectories over 48 hours (2 day path) for air parcels terminating at C58 on two high ozone days during the June 2006 photochemical modeling episode. By creating back trajectories, air parcels were analyzed to determine emission sources and causes of elevated ozone concentrations. According to TCEQ, "The meteorological dynamics that cause air to rise or fall, and that determine its path can affect air quality by carrying air pollutants many kilometers from their sources."[60] Given a final geographic destination for an air parcel, back trajectories show the path followed by the air parcel before reaching the destination. Back trajectories track air displacement over time, distance, and emission source regions.

[59]NOAA, Feb. 26, 2019. "Realtime Environmental Applications and Display sYstem (READY)". Available online: http://www.arl.noaa.gov/ready.html. Accessed 05/13/15.

[60] TCEQ, Air Monitoring, Sept. 24, 2009. "Air Trajectories: Where did the Air Come from and Where is It Going?". Available online: http://www.tceq.state.tx.us/compliance/monitoring/air/monops/airtraj.html. Accessed 05/13/15.

Figure 5-9: High Ozone Back Trajectories Beginning at CAMS 58, June 8 and 9, 2006

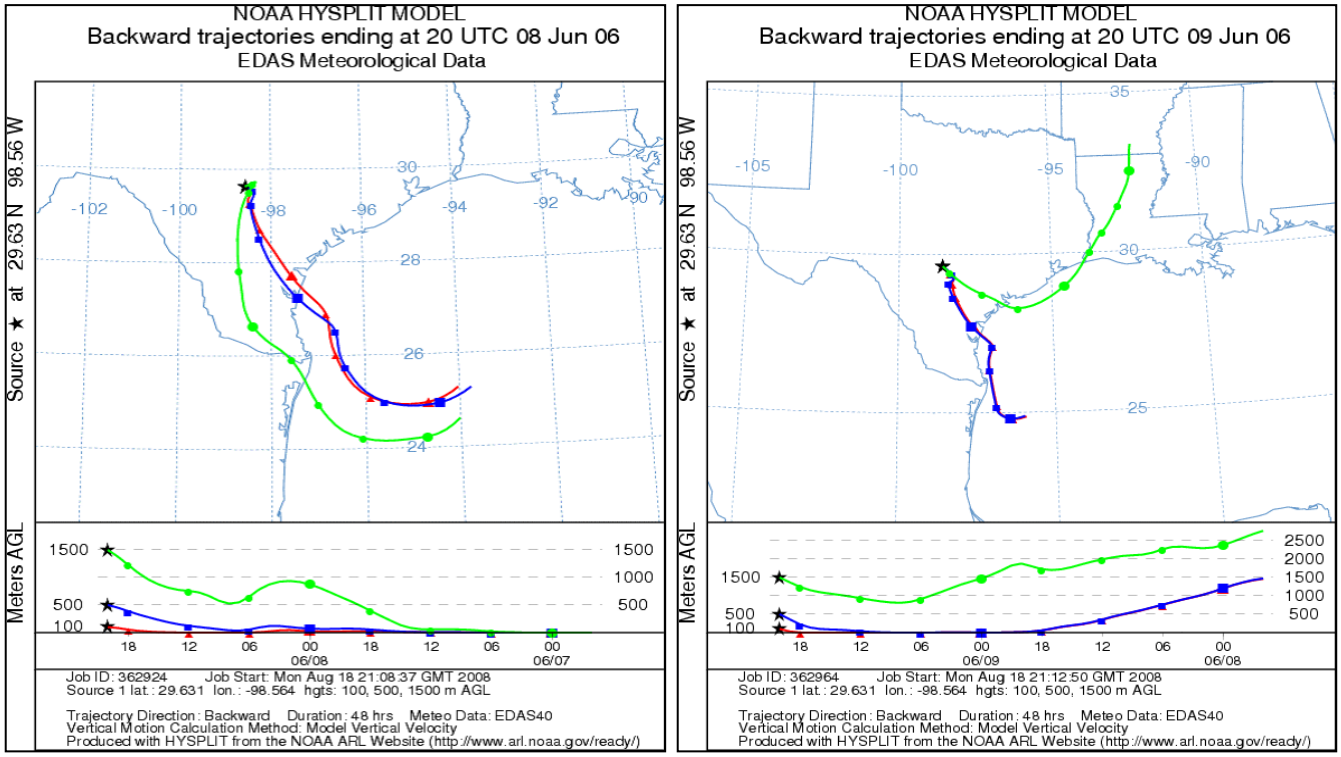

As displayed in the above figures, back trajectories are split into 100 (red), 500 (blue), and 1,500-meter (green) elevations. The plots show that winds came from the southeast on these high ozone days at both the 100-meter and 500-meter elevations. By using the data represented in these figures, wind directions and emission source regions can be estimated.

When using the HYSPLIT model, limitations of trajectory analysis should be noted. TCEQ states that "it is important to point out that transport layer back trajectories for ozone episodes are based upon archived upper air data from meteorological models, and interpolated from a coarse grid which smoothes out the local perturbations and geographical details. Trajectories developed from transport layer winds do not necessarily represent the wind fields at the surface, especially on a day-to-day basis. Individual trajectories have error bars, which increase with time and distance, and so must be interpreted with caution. However, when a large number of trajectories for ozone episodes are analyzed statistically, they provide a reliable picture of the most likely flow patterns and source regions affecting an area."[61]

"Surface winds and surface trajectories have the opposite limitations. Winds measured at surface sites reflect only the surface conditions and the geographic features near the measurement site. Surface winds measured at CAMS and other surface stations may be affected by local obstructions and may not represent areas outside the immediate vicinity of the measurement site. Surface winds also do not necessarily represent the wind speed and direction in the transport layer. Therefore individual trajectories based on winds at surface monitors must be interpreted carefully. However, conclusions drawn from time and space averages of surface winds are reliable if used in a general

[61] Technical Support Section, Technical Analysis Division TCEQ, December 13, 2002. "Conceptual Model for Ozone Formation in the Houston-Galveston Area Appendix A to Phase I of the Mid Course Review Modeling Protocol and Technical Support Document". Austin, Texas. p. 21. Available online: http://www.tceq.state.tx.us/assets/public/implementation/air/am/docs/hgb/protocol/HGMCR_Protocol_Appendix_A.pdf. Accessed 05/11/15.

rather than site or day specific sense."[62] Both back trajectories and surface wind measurements should be used to analyze patterns on high ozone days along with other meteorological factors.

By running 100-meter and 1,000-meter 48-hour back trajectories for the 131-high ozone days > 65 ppb in the San Antonio area as recorded at C58 from 2009 to 2014, spatial patterns were identified on high ozone days. Figure 5-10 shows C58 back trajectories on high ozone days greater than 65 ppb. The HYSPLIT model produces air parcel positions for every hour by latitude, longitude, and height. Back trajectories demonstrate that, on high ozone days, it is rare for air arriving at C58 to come from the west, northwest, or southwest. A quantitative refinement of this data is presented in Figure 5-11. For this analysis, the region of central Texas within a 400-km radius of C58 was partitioned into octants: northern, northeastern, eastern, southeastern, etc. The region was further subdivided by distance boundaries: area within 80 km of C58, 80 to 160 km of C58, etc., out to 400 km from C58. Figure 5-11 contains the percentage of hourly air parcel positions within each sub-division and the total for each octant is located just outside the 400-km circle. The total for each distance sub-division of these octants will be referred to as "bin counts".

For days exceeding 65 ppb, 3.0% of the bin counts were located in the northern octant and within 80 km of C58; 1.6% were in the same octant, but between 80 and 160 km of C58. Due north of C58, outside the 400-km boundary, the percentage in bold, 9.8%, indicates the percentage of all hourly coordinates that passed through the northern octant within 400 km of the monitor. About 65% of 100-meter 48-hour back trajectories came from the northeast, east, and southeast on days of high ozone > 65 ppb. Most of the rest of the back trajectories on high ozone days > 65 ppb were from the south (16.7%) and north (9.8%). Winds from the west, northwest, and southwest were less common on high ozone days > 65 ppb (8.1%). The development of the Eagle Ford Shale may increase the number of high ozone days with winds originating from the south and southeast. The percentage of bin counts in the west, southwest, and south octants on high ozone days > 65 ppb increased since the last Conceptual Model in 2011. The other octants experienced a decrease in percentage of bin counts for high ozone days.

Back trajectories on low ozone days were predominately from the Gulf of Mexico where there are very few anthropogenic emission sources (

[62] *Ibid*.

Figure 5-12: Density of Hourly Back Trajectory Bin Counts on Low Ozone Days < 40 ppb, 2009 – 2014

Figure 5-13: Density of Hourly Back Trajectory Bin Counts on High Ozone Days > 65 ppb, 2009 – 2014

). These 48-hour back trajectories often traveled hundreds of kilometers over the Gulf of Mexico before arriving in the San Antonio region. Far fewer back trajectories on low ozone days were from the north and northeast regions. The few back trajectories that were from the north on low ozone days tended to travel west of large anthropogenic emissions sources in Dallas and Austin before arriving in the San Antonio area. On high ozone days > 65 ppb, there was a different pattern of back trajectories. Figure 5-13 shows there were a higher percentage of back trajectories that passed over Dallas and Austin on high ozone days. Such air parcels can accumulate significant amounts of ozone and ozone pre-cursor emissions before arriving at San Antonio monitors.

Distribution of back trajectory endpoints showed a similar pattern on low and high ozone days (Figure 5-14 and Figure 5-15). Most back trajectory endpoints on low ozone days were far out in the Gulf of Mexico, while back trajectory endpoints on days of high ozone tended to originate over East Texas or near the Texas coast. The locations of back trajectory endpoints on high ozone days indicate transport may have a significant impact on local ozone. The trajectories originated in areas that contain large emissions sources. Background sources of transport can accumulate for several days over Texas before arriving at San Antonio monitors. Also, the endpoints on high ozone days > 65 ppb tended to be closer to San Antonio, signifying lower wind speeds on high ozone days.

Figure 5-10: Pattern of High Ozone Days > 65 ppb Air Parcel Paths Arriving in San Antonio, 2009 – 2014

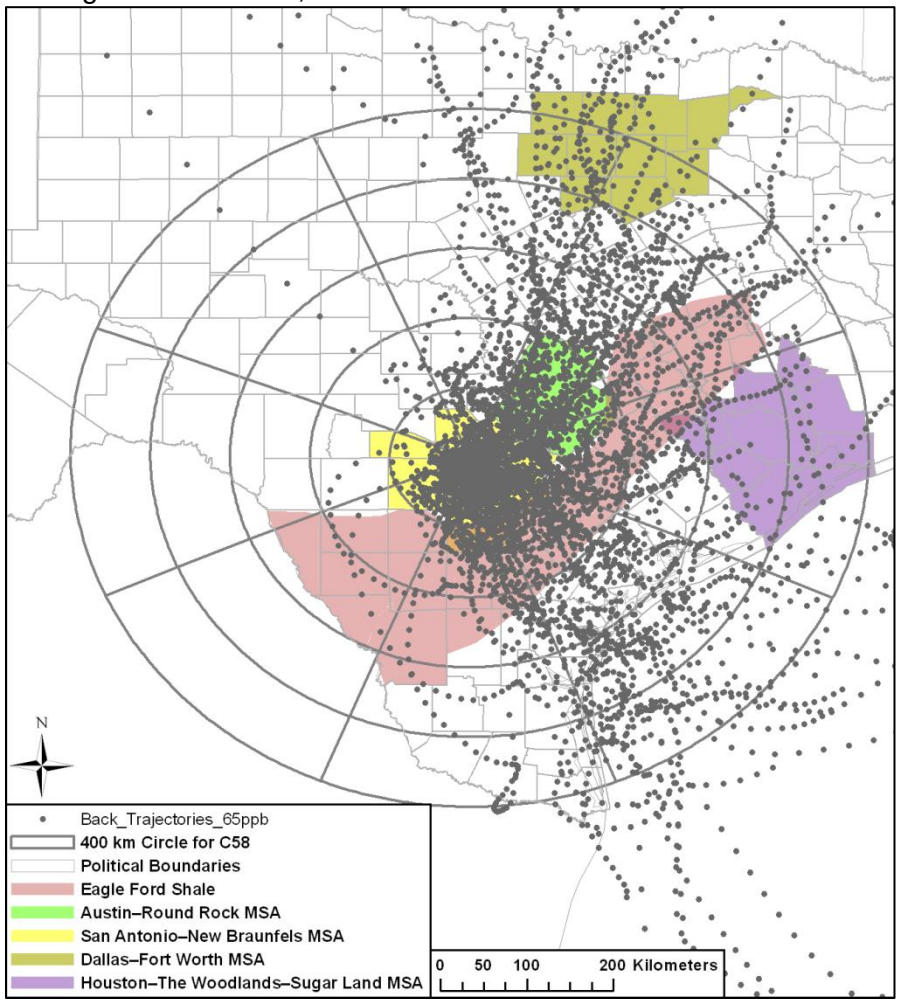

Figure 5-11: Back Trajectory Percentages by Directional Octant on High Ozone Days > 65 ppb, 2009-2014

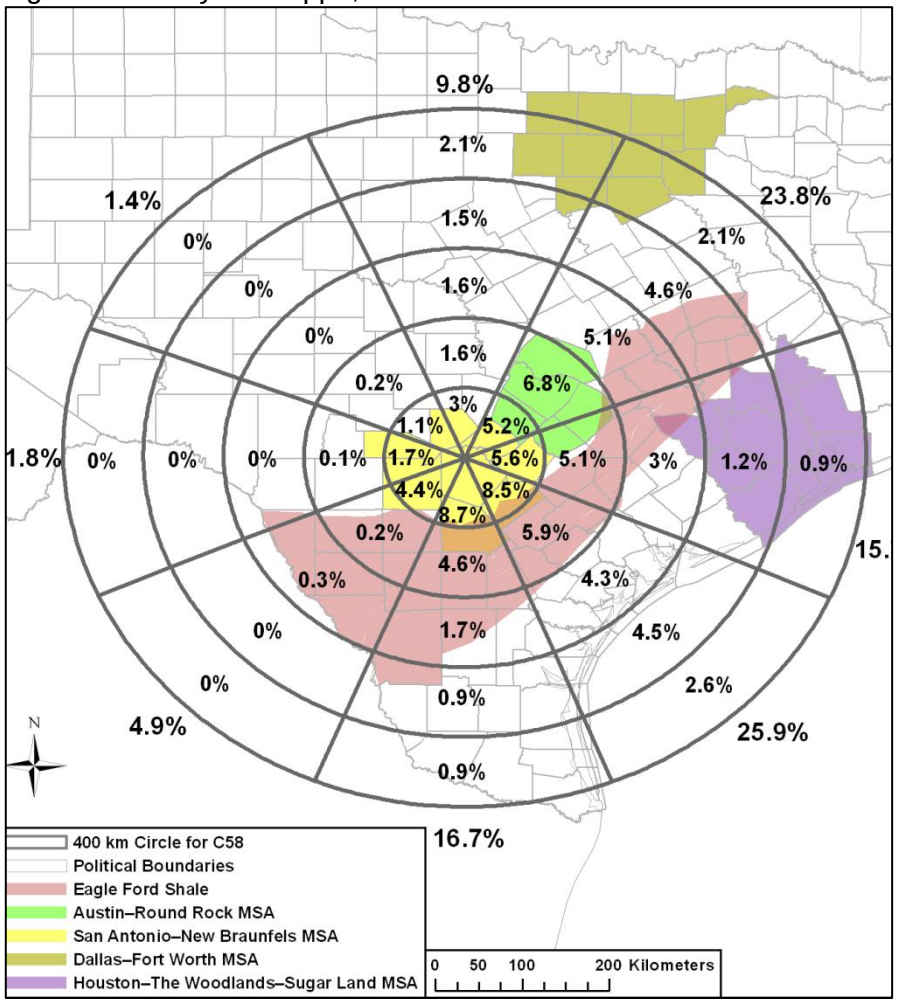

100 meter 48 hour back trajectories ending at C58

Figure 5-12: Density of Hourly Back Trajectory Bin Counts on Low Ozone Days < 40 ppb, 2009 – 2014

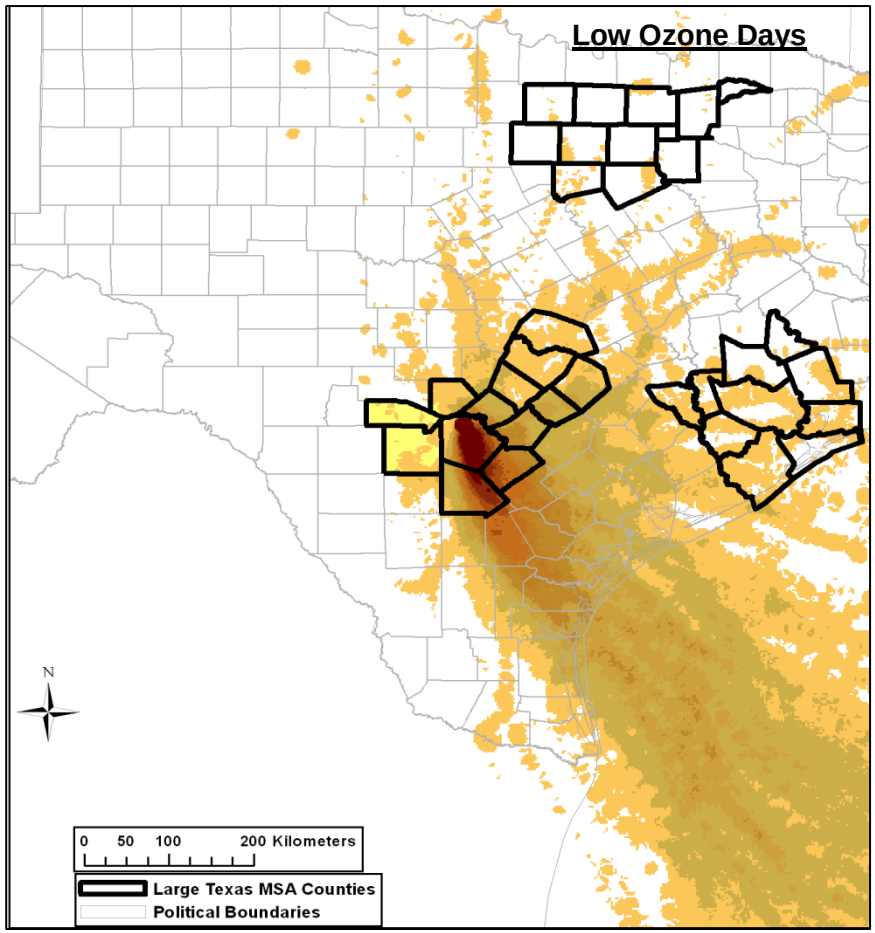

Figure 5-13: Density of Hourly Back Trajectory Bin Counts on High Ozone Days > 65 ppb, 2009 – 2014

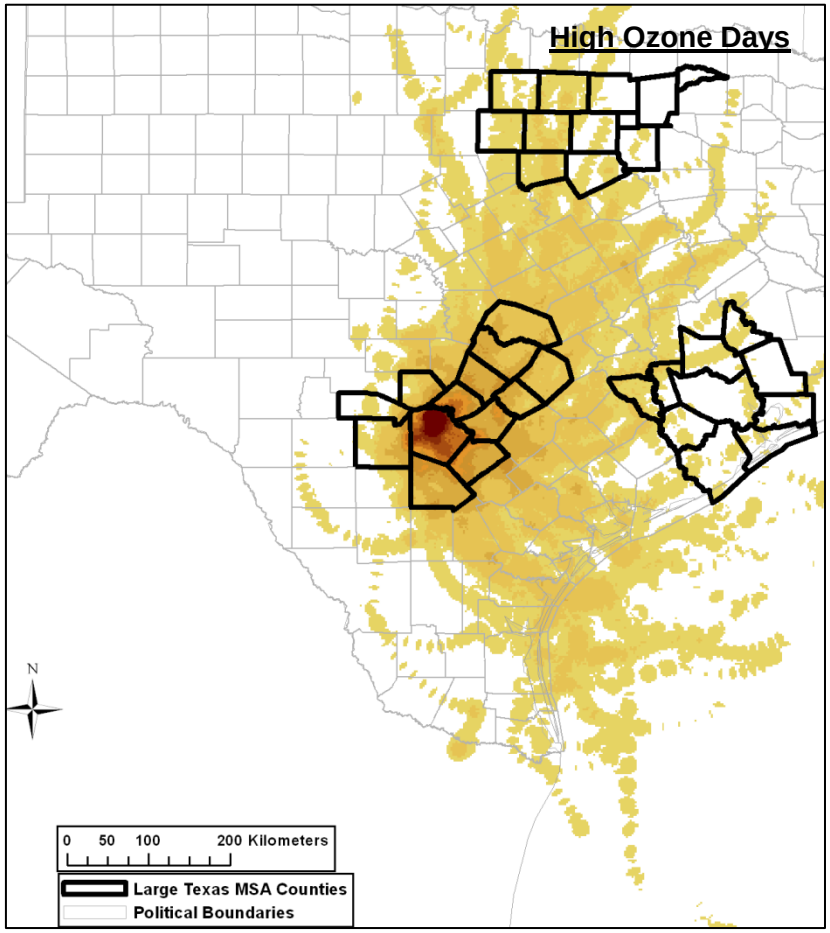

Figure 5-14: Density of 48-hour End Point Back Trajectory Counts on Low Ozone Days < 40 ppb, 2009 – 2014

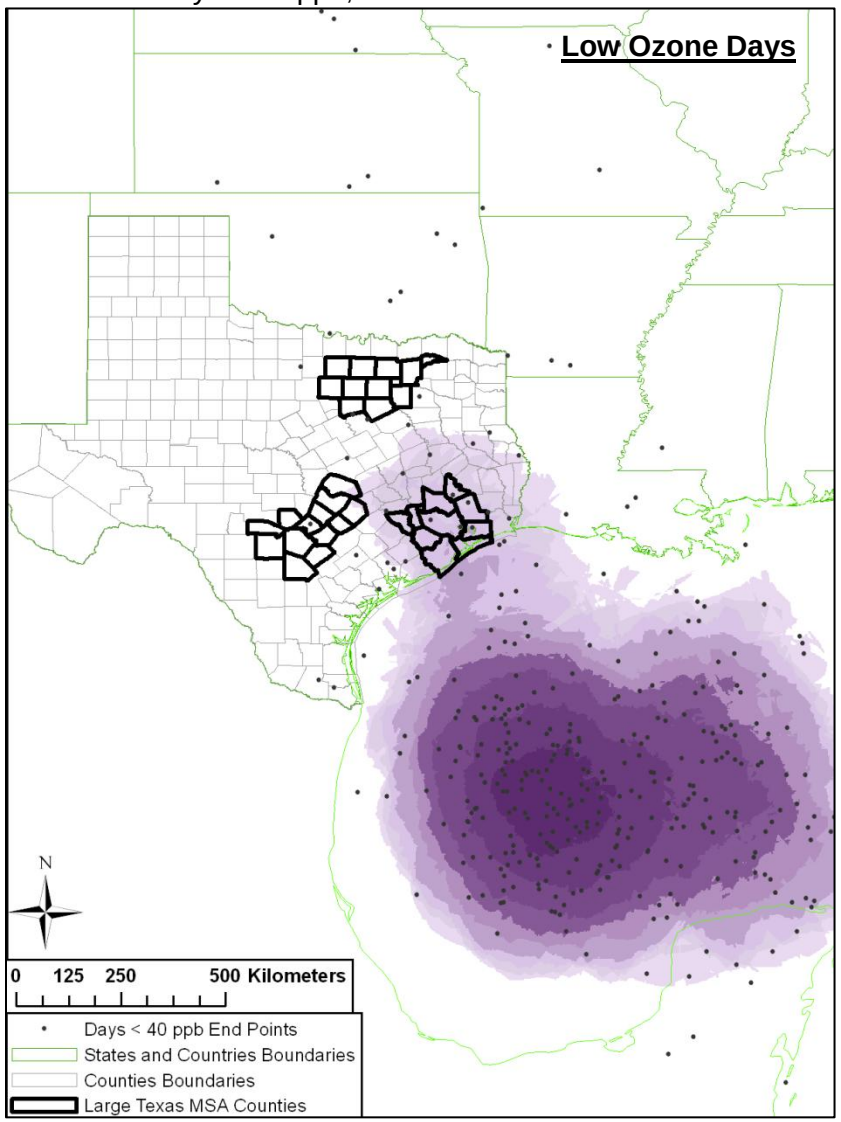

Figure 5-15: Density of 48-hour End Point Back Trajectory Counts on High Ozone Days > 65 ppb, 2009 – 2014

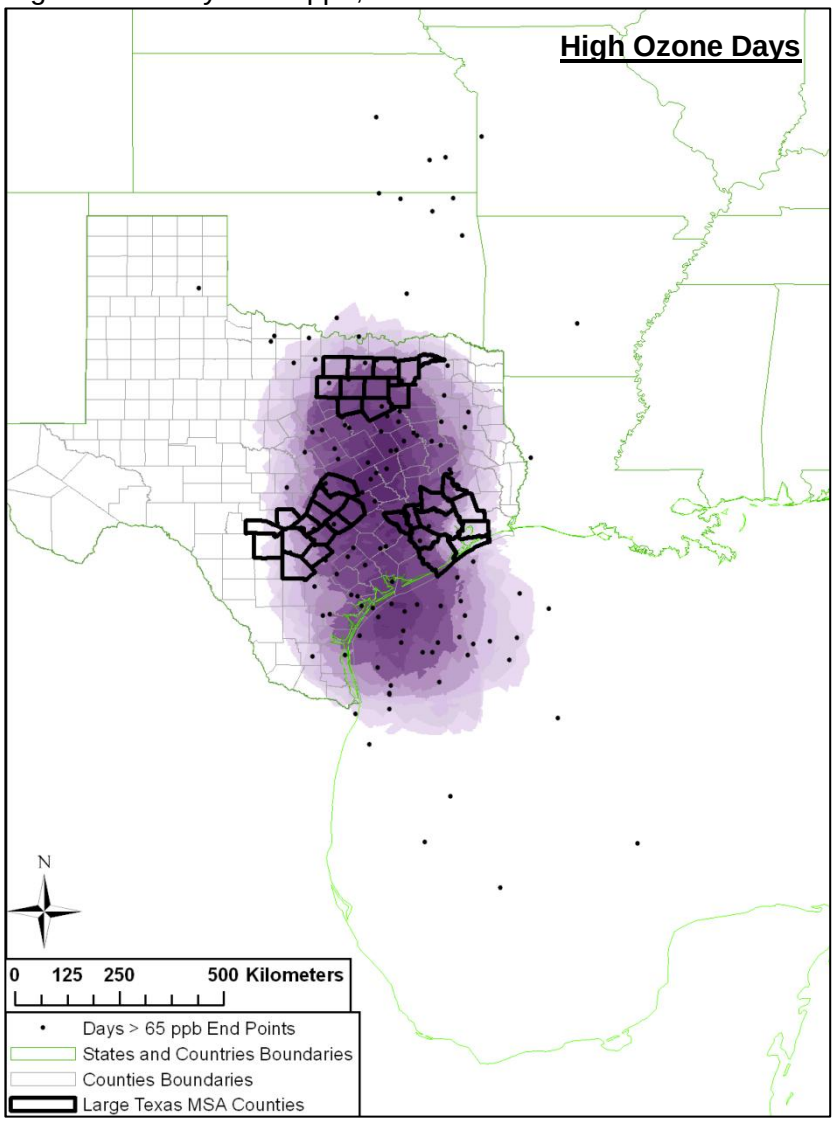

Analysis of back trajectories on high and low ozone days revealed that the largest share of the 100-meter back trajectories on low ozone days came from the southeast (48.0%). These 48-hour back trajectories on low ozone days often originated over the Gulf of Mexico. There are few anthropogenic emission sources over the Gulf of Mexico compared to areas east and northeast of San Antonio. Figure 5-16: Statistical Analysis of San Antonio's 400-km Back Trajectory Wind Directions: <40 ppb and >65 ppb Ozone Season Days 2009-2014 shows that this pattern was significantly different on high ozone days when northeast 100-meter back trajectories occurred with similar frequency as southeast back trajectories. On low ozone days, only 9.9% of back trajectories were from the north and northeast compared to 33.6% on high ozone days > 65 ppb. There were also a significant number of back trajectories from the Southeast and south on high ozone days (Table 5-2).

Figure 5-16: Statistical Analysis of San Antonio's 400-km Back Trajectory Wind Directions: <40 ppb and >65 ppb Ozone Season Days 2009-2014

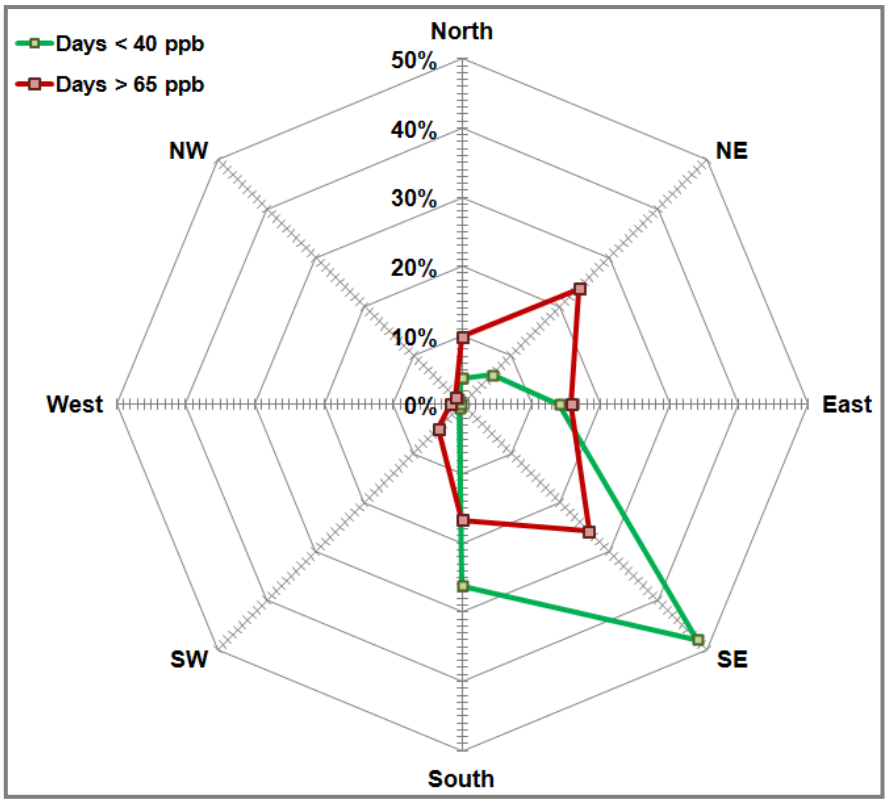

Table 5-2: Density of Hourly Back Trajectory Bin Counts by Direction, 2009 – 2014

Monitor	Direction	Days < 40 ppb		Days > 65 ppb	
		n	%	n	%
C58	North	352	3.8%	537	9.8%
	Northeast	571	6.1%	1,297	23.8%
	East	1,300	13.9%	858	15.7%
	Southeast	4,489	48.0%	1,411	25.9%
	South	2,447	26.2%	912	16.7%
	Southwest	69	0.7%	265	4.9%
	West	20	0.2%	98	1.8%
	Northwest	96	1.0%	78	1.4%

100 meter 48 hour back trajectories ending at C58

Back trajectories were analyzed to determine the origin distance from C58 on high ozone days > 65 ppb and low ozone days < 40 ppb. The statistical analysis included 100-meter back trajectories on 109 high ozone days and 410 days of low ozone from 2009 to 2014. As shown in Table 5-3, 88.6% of the 48-hour back trajectories on high ozone days > 65 ppb originated within 402 km of C58, whereas on low ozone days only 50.4% originated within the same distance. Back trajectories on high ozone days originated closer to San Antonio and traveled shorter distances. These findings indicate winds are often lighter on high ozone days.

Table 5-3: Density of Hourly Back Trajectory Bin Counts by Distance, 2009 – 2014

Monitor	Distance	Days < 40 ppb		Days > 65 ppb	
		n	%	n	%
C58	0-80 km	2,141	11.6%	2,083	33.8%
	81-161 km	2,380	12.8%	1,340	21.8%
	162-241 km	1,865	10.1%	870	14.1%
	242-322 km	1,450	7.8%	693	11.3%
	323-402 km	1,508	8.1%	470	7.6%
	403-805 km	6,108	33.0%	541	8.8%
	> 805 km	3,076	16.6%	160	2.6%

100 meter 48 hour back trajectories ending at C58

Back trajectories and daily weather maps were reviewed to classify days as “stagnated”, “weak transport”, or “transport” on high ozone days and low ozone days (<40 ppb). Days when the 48-hour 100-meter back trajectories stayed within about 402 km of San Antonio were called “stagnated” days (less than 2.2 m/s over the 48 hour period), especially if the back trajectory changed direction several times. If the 48-hour back trajectory originated farther than 805 km from San Antonio, the back trajectory was labeled as “transport” (winds >4.5 m/s over the period). All other back trajectories were labeled as “weak transport”. The data provided in Table 5-4 shows that 62 percent of high ozone days > 65 ppb had stagnated back trajectories compared to only 7 percent of low ozone days. Low ozone days had a higher percentage of “transport” days (62%) compared to high ozone days (7%).

Figure 5-17: Cumulative Back Trajectory Distance, 2009-2014.

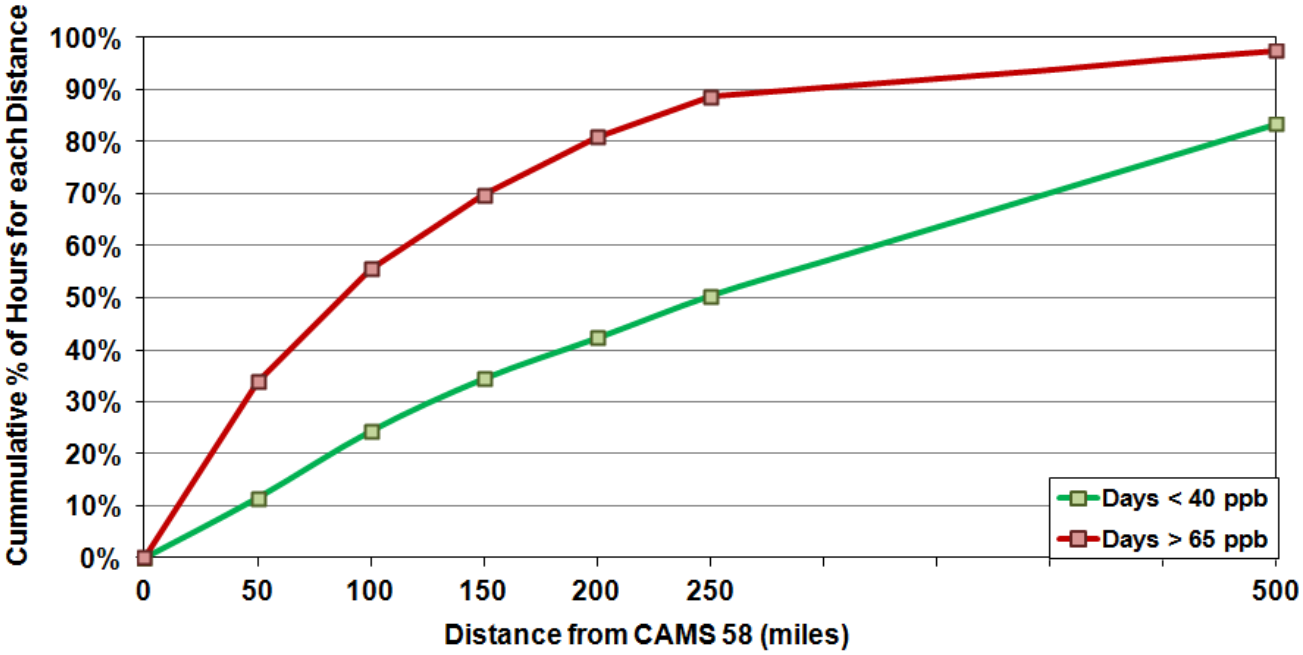

100 meter 48 hour back trajectories ending at C58

Table 5-4: Back Trajectories Classification on High Ozone Days and Low Ozone Days, 2009 - 2014

Back Trajectory Classification (2009-2014)	Stagnated		Weak Transport		Transport		Total	
	Number of Days	Percent	Number of Days	Percent	Number of Days	Percent	Number of Days	Percent
High Ozone Days > 65 ppb	68	62.4%	33	30.3%	8	7.3%	114	100%
Low Ozone Days < 40 ppb	29	7.1%	128	31.2%	253	61.7%	410	100%

Back trajectories were then analyzed on a monthly basis, as shown in Table 5-5. For each month of ozone season, the number of stagnated, weak transport, and transport days were determined. The month that had the most high ozone days with stagnant conditions present was August at 20.6%. The month that had the most high ozone days with either transport or weak transport was May, with almost 27%. The spring ozone peak is defined as the months of May and June while the fall ozone peak is defined as August and September. High ozone days during the fall ozone season peak are characterized by stagnant weather conditions and the spring ozone season peak has more high ozone days with transport conditions present. A Chi-Square test using the phi coefficient confirms that this pattern is statistically significant at $\alpha = 0.05$[63].

Table 5-5: Back trajectory classification on high ozone days by month and seasonal peak, 2009-2014

Time Period	Stagnated		Weak Transport		Transport	
	Number of Days	Percent	Number of Days	Percent	Number of Days	Percent
April	5	7.4%	3	9.1%	1	12.5%
May	11	16.2%	9	27.3%	2	25.0%
June	11	16.2%	6	18.2%	1	12.5%
July	1	1.5%	3	9.1%	1	12.5%
August	14	20.6%	7	21.2%	1	12.5%
September	13	19.1%	5	15.2%	1	12.5%
October	13	19.1%	0	0%	1	12.5%
Total	**68**	**100%**	**33**	**100%**	**8**	**100%**
Spring Season	27	39.7%	18	54.5%	4	50.0%
Fall Season	40	58.8%	12	36.4%	3	37.5%

San Antonio's peak ozone readings were plotted against peak ozone readings in other Texas cities to determine the correlation between urban areas (Figure 5-18 to Figure 5-24). Austin had the highest correlation with San Antonio ozone readings ($R^2 = 0.83$ for all days): the cities are close geographically and have similar mobile source emission profiles. Also, back trajectories and photochemical modeling analysis indicate San Antonio monitors can be impacted by transport from Austin. When dividing the ozone season into its spring peak (May and June) and fall peak (late August to early October) components, the correlation between monitor pairs is higher in the spring. As discussed earlier, the spring ozone peak is characterized by more transported ozone than the fall peak, which tends to have more stagnated conditions. Stagnant conditions imply greater variability of atmospheric conditions over a given area, hence, fall monitor correlations on high ozone days are lower than associated spring correlations for every monitor pair. During the spring ozone peak, stagnant conditions led to high ozone 40% of the time. Winds during the fall ozone season peak were more from the east/southeast and stagnated, with 59% of 48-hour back trajectories originating within 402 km of San Antonio.

Table 5-6 shows the R^2 value between San Antonio and Austin was the highest of any Texas urban area for the entire range of the proposed ozone standard.

[63] $\varphi = -0.46$ with 81 cases

Both Victoria and Waco ozone readings had a strong correlation with peak ozone in San Antonio on all days. Houston had the second highest R^2 value on days that exceeded 65 ppb, indicating that San Antonio is commonly impacted by transport from Houston during high ozone events. The three cities that are the farthest away from San Antonio - Dallas, Tyler/Longview, and Waco – generally had the lowest correlation with ozone readings in San Antonio.

Figure 5-18: Daily Maximum 8-hour Ozone in San Antonio and Austin, 2005-2014

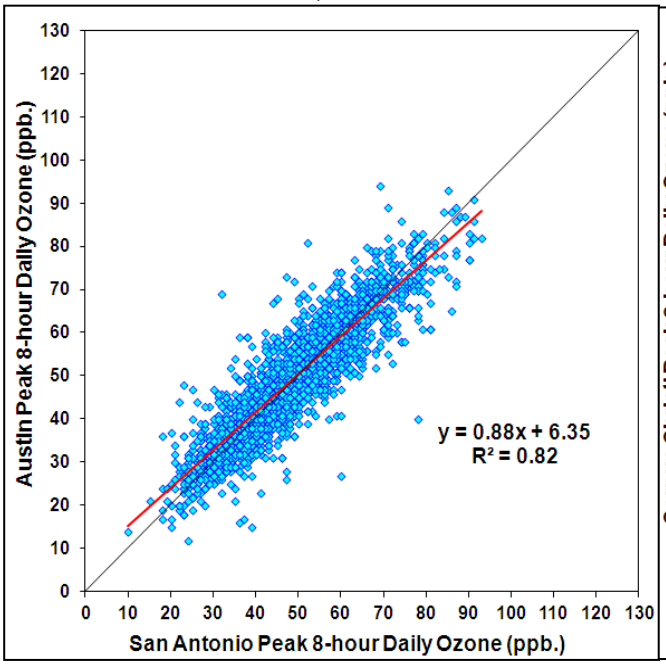

Figure 5-19: Daily Maximum 8-hour Ozone in San Antonio and Corpus Christi, 2005-2014

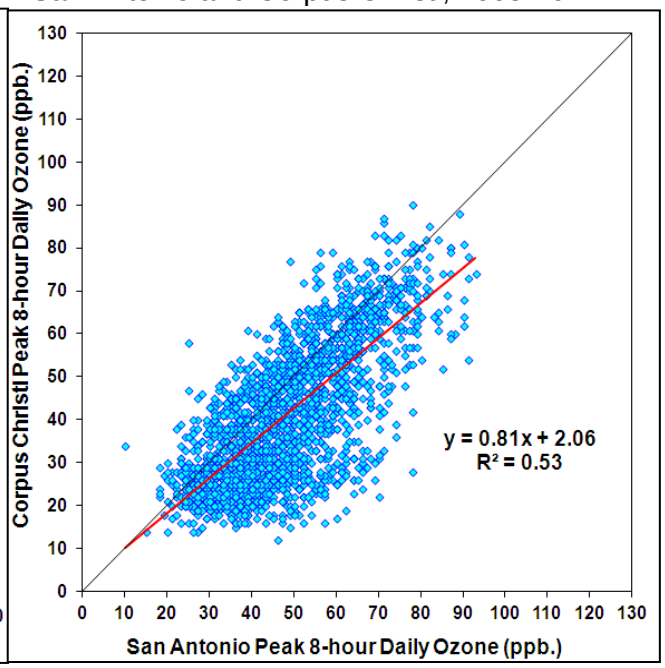

Figure 5-20: Daily Maximum 8-hour Ozone in San Antonio and Houston, 2005-2014

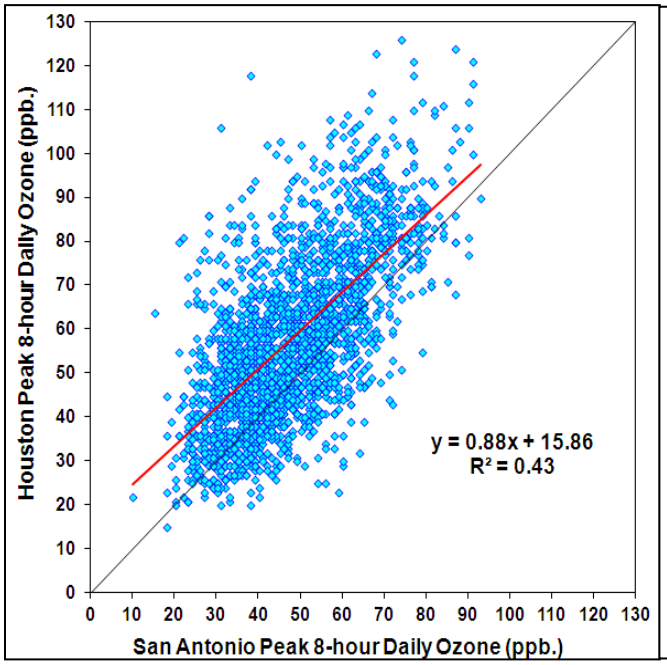

Figure 5-21: Daily Maximum 8-hour Ozone in San Antonio and Dallas, 2005-2014

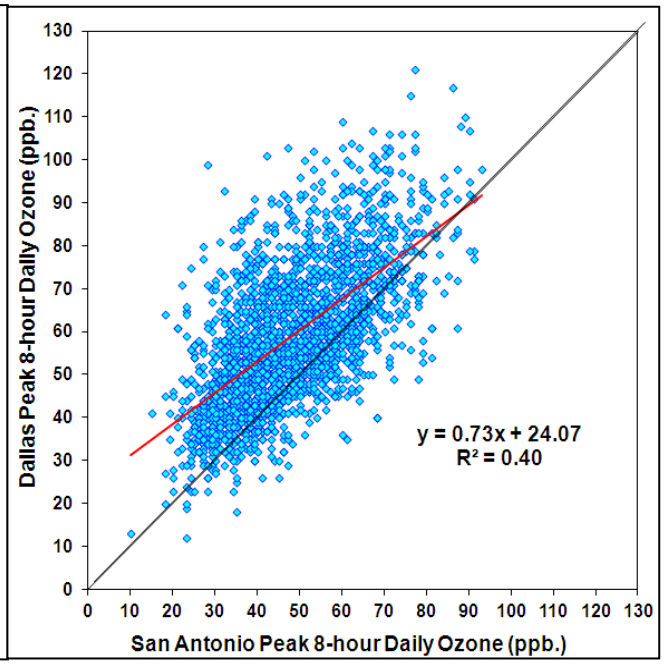

Figure 5-22: Daily Maximum 8-hour Ozone in San Antonio and Waco, 2006-2014

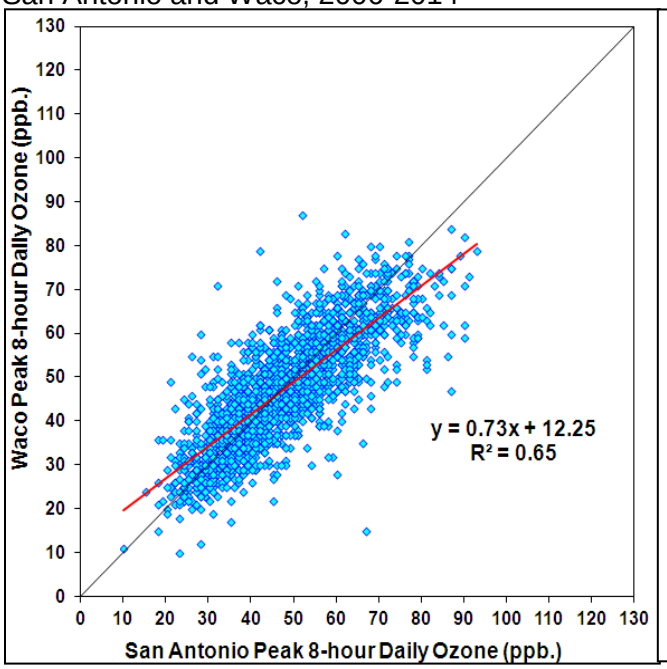

Figure 5-23: Daily Maximum 8-hour Ozone in San Antonio and Tyler/Longview, 2005-2014

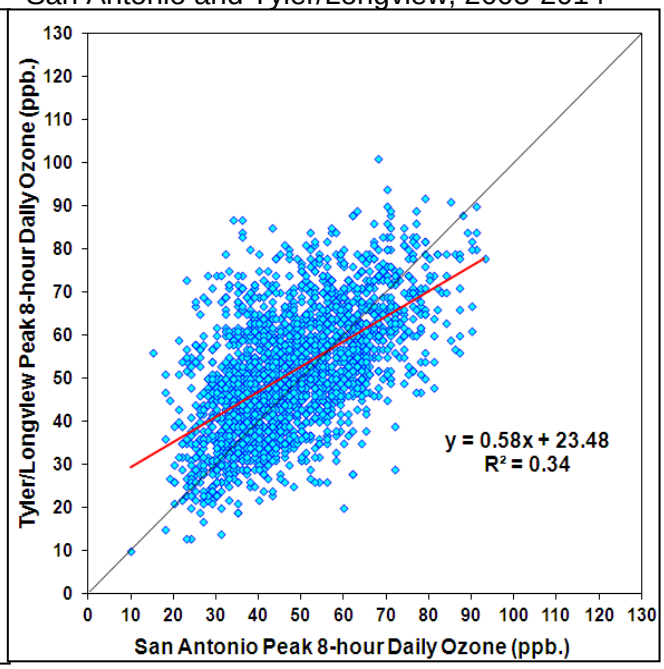

Figure 5-24: Daily Maximum 8-hour Ozone in San Antonio and Victoria, 2005-2014

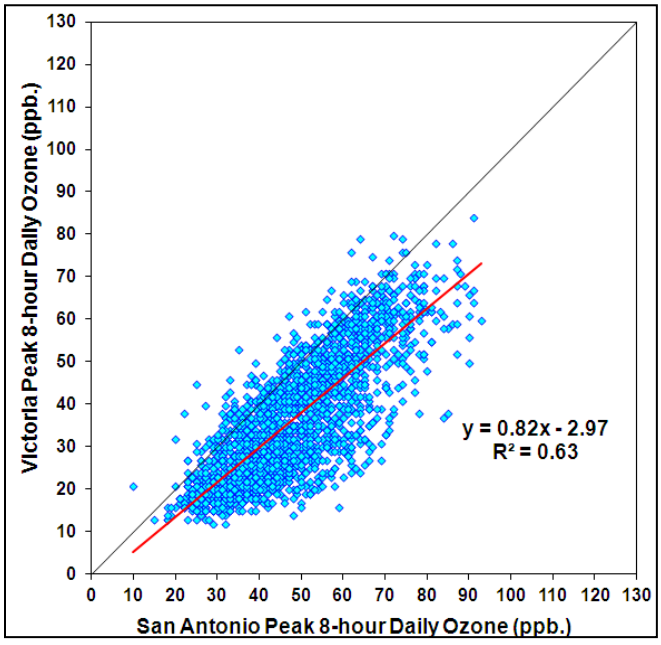

When dividing the ozone season into its spring peak (May and June) and fall peak (late August to early October) components, the correlation between monitor pairs is higher in the spring. As discussed earlier, the spring ozone peak is characterized by more transported ozone than the fall peak, which tends to have more stagnated conditions. Stagnant conditions imply greater variability of atmospheric conditions over a given area, hence, fall monitor correlations on high ozone days are lower than associated spring correlations for every monitor pair. During the spring ozone peak, stagnant conditions led to high ozone 40% of the time. Winds during the fall ozone season peak were more from the east/southeast and stagnated, with 59% of 48-hour back trajectories originating within 402 km of San Antonio.

Table 5-6: Correlation of San Antonio Peak 8-Hour Ozone Readings with Other Urban Areas, 2005 – 2014

Proposed Standard	Parameter	Austin	Corpus Christi	Dallas	Houston	Tyler/ Longview	Waco	Victoria
All Days	R^2	0.83	0.53	0.39	0.43	0.34	0.66	0.49
	Standard Dev. (σ)	6.0	11.3	13.4	14.7	13.1	8.3	12.0
	Average Difference	0.8	-7.0	11.0	10.0	3.7	-0.4	-13.3
> 65 ppb	R^2	0.26	0.10	0.06	0.10	0.04	0.06	0.05
	Standard Dev. (σ)	7.1	12.8	14.0	14.4	11.6	9.2	15.4
	Average Difference	-2.6	-10.6	4.7	10.0	-5.8	-8.5	-17.9

Additional analysis of back trajectory end points was conducted to determine if a more causal relationship of peak 8-hr ozone daily values between different cities exists. Only the back trajectory end points that originated around the three major urban areas were analyzed: Houston, Dallas, Corpus Christi, and Austin. For any given day, if the back trajectory originated in one of these areas, the 8-hr ozone for that city on the origin day was compared to the 8-hr ozone for San Antonio two days later. Figure 5-22 shows the relationship between peak 8-hr daily ozone in each urban area compared to San Antonio on days that back trajectories originated in any of the urban areas.

Figure 5-25: Peak 8-Hr Daily Ozone for San Antonio and Selected Urban Areas 2009-2014

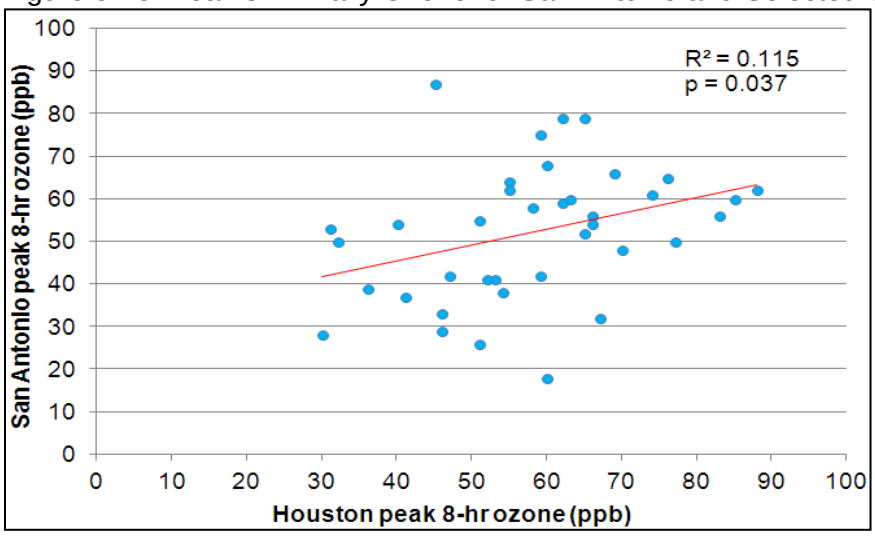

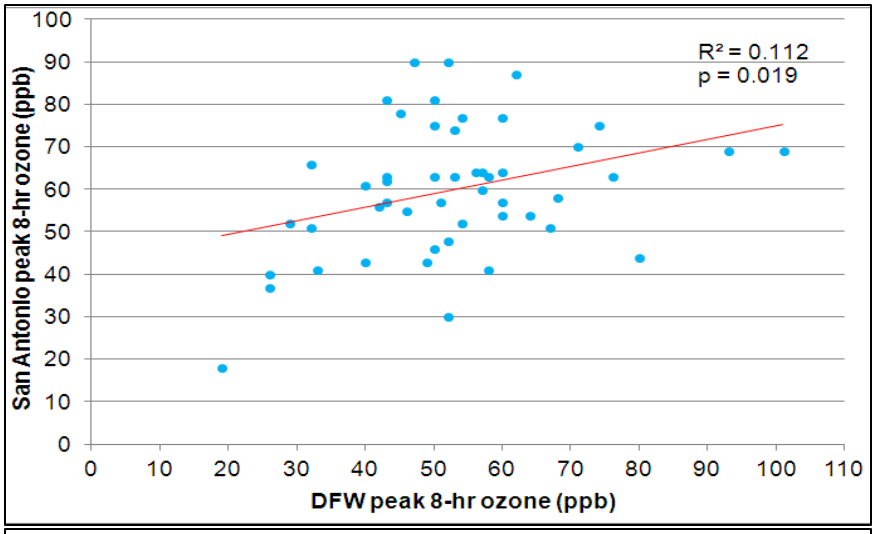

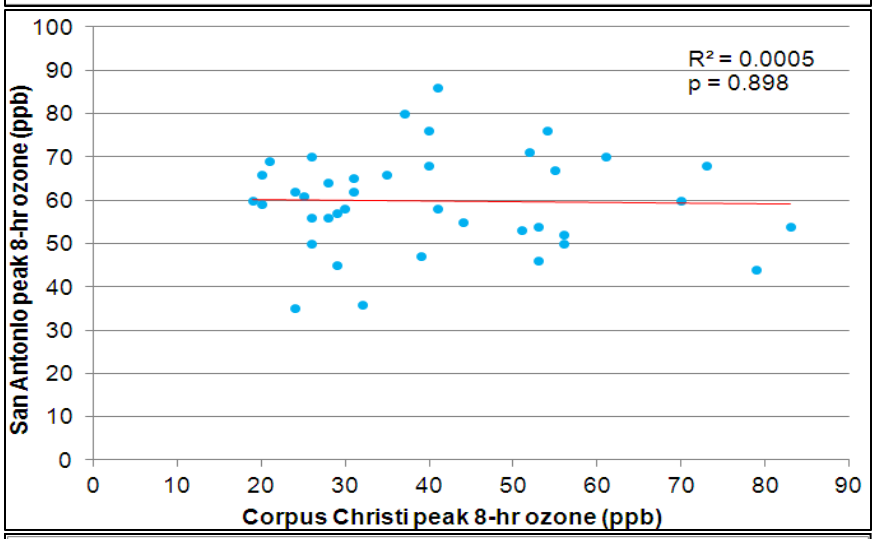

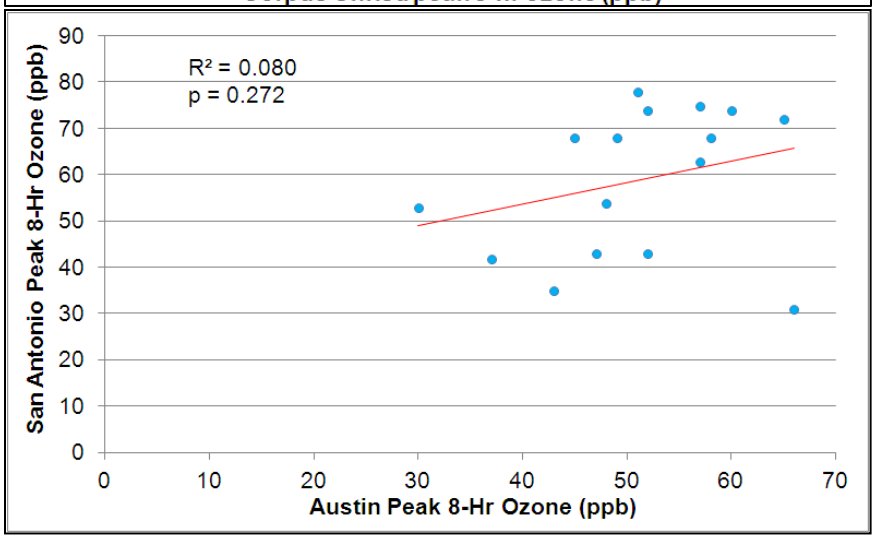

The scatterplots and associated R^2 values show that there is a significant relationship ($\alpha = 0.05$) between peak 8-hr daily ozone in Houston and Dallas and peak 8-hr daily ozone in San Antonio two days later on days when 48-hr back trajectories originated in either Houston or Dallas. The scatterplots for Corpus Christi and Austin show no significant relationship. There were far fewer 48-hour back trajectory endpoints near Austin due to its proximity to San Antonio. For a 48-hour back trajectory to originate near Austin implies more stagnated conditions, less mixing of ozone and its

precursors, and greater variation of pollutant concentrations across the region. In addition, back trajectories originating from Dallas-Fort Worth usually pass through the Austin area before reaching San Antonio. These factors might explain why the correlation between Austin and San Antonio is weaker than that of Dallas or Houston.

5.3 Sampling of Industrial and Urban Plumes by Aircraft

Baylor Institute of Air Science (BIAS) collected continuous O_3, NO_X, SO_2, and CO measurements from urban and industrial plumes using a Cessna 172 aircraft in the Austin region. The aircraft also collected meteorological data (temperature, pressure, wind speed, wind direction) and volatile organic compound (VOC) canister samples.[64] Examining the data collected by aircraft on September 17, 2007 reveals the extent of the Houston urban ozone plume and its impact downwind of the source region (Figure 5-26).[65] Portions of the Houston ozone plume were above 85 ppb as the aircraft tracked ozone concentrations towards Waco. These transported pollutants can mix down to the surface and impact monitors in other urban areas including San Antonio.

Other cities and industrial facilities upwind of local monitors can impact ozone and emission precursor transport into the San Antonio region. The BIAS Cessna also collected air samples in the Austin region during September 2006.[66] Austin urban and Alcoa-Sandow facility ozone plumes are shown in Figure 5-27 traveling southwest of the Austin urban core towards San Antonio.[67] Multiple regions and industrial plumes can impact San Antonio on high ozone days. These plumes will make it very difficult for San Antonio to attain a stricter ozone standard.

[64] Maxwell Shauck, *et. al.* Baylor Institute for Air Science, Baylor University and Martin Buhr, Air Quality Design, Inc., March 2007. "Airborne Air Quality Sample Collection in Central Texas during the 2006 Ozone Season". Waco, Texas p. 1.
[65] CAPCOG, July 11, 2008. "Preliminary Discussion Draft of CACAC Comments for TCEQ Public Meeting on Ozone NNA Designation". Austin, Texas.
[66] Maxwell Shauck, Grazia Zanin, Sergio Alvarez, Levi Kauffman, Timothy Compton,
Baylor Institute for Air Science Airborne, and Martin Buhr, Air Quality Design, Inc., March 2007. "Air Quality Sample Collection in Central Texas during the 2006 Ozone Season: Final Report". Baylor University, Waco, Texas. Sponsored by Capital Area Council Of Governments (CAPCOG), Austin, Texas, p. 1.
[67] *Ibid*., p. 20.

Figure 5-26: Baylor University Airborne Ozone (ppbv) Sampling: Houston Urban Ozone Plume – September 17, 2007

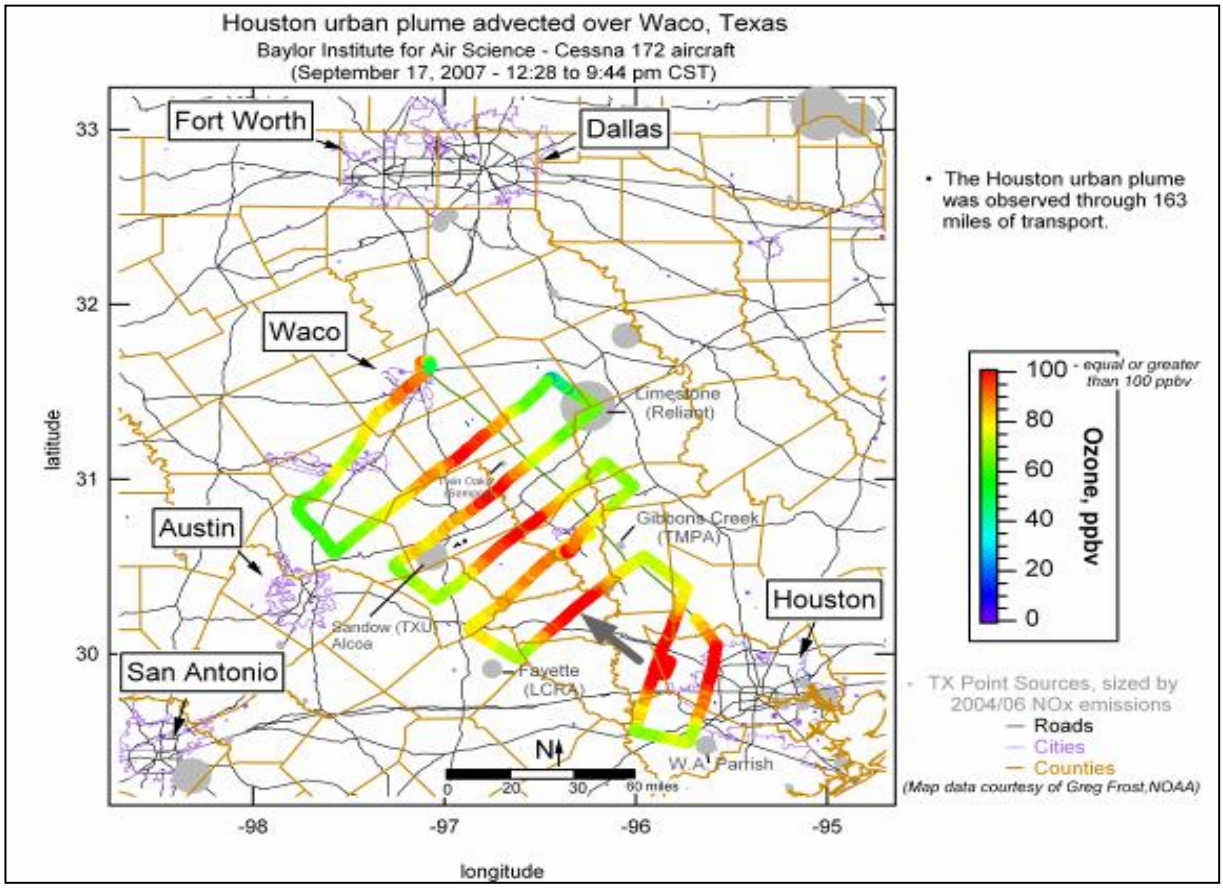

Figure 5-27: Baylor University Airborne Ozone (ppbv) Sampling: Austin and Alcoa-Sandow Facility Ozone Plume – September 19, 2006

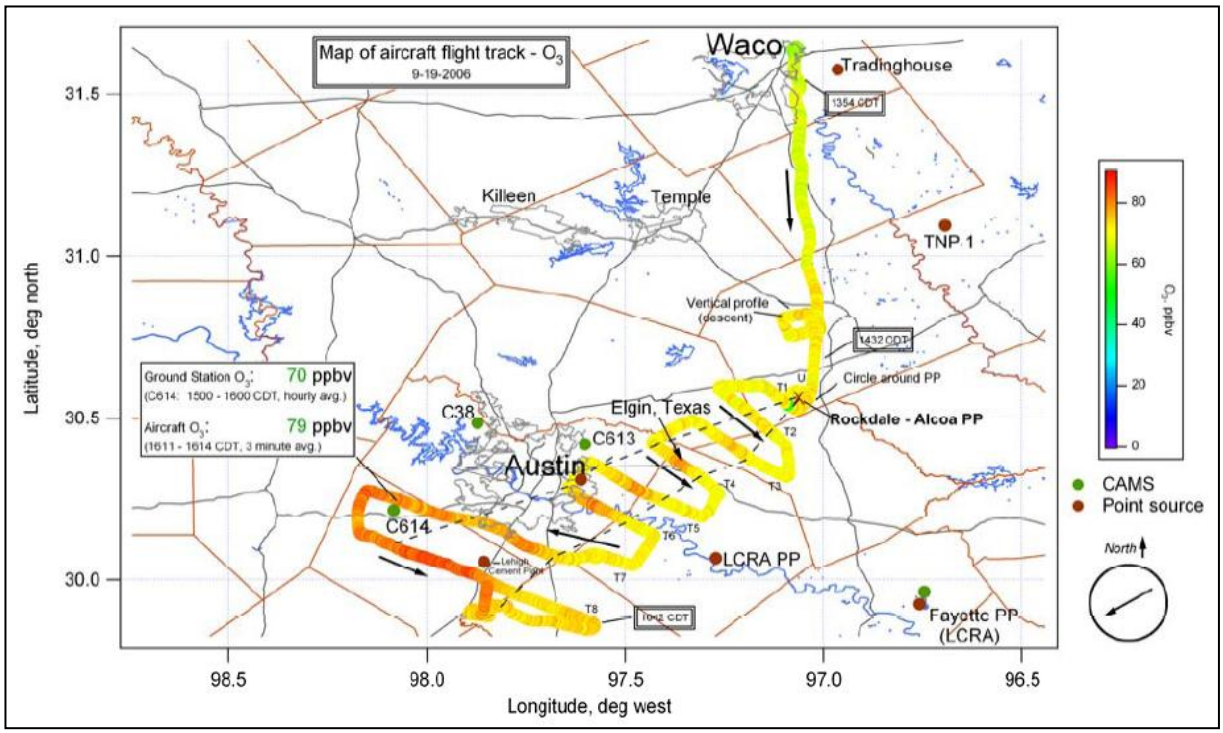

5.4 Transport Analysis in the Photochemical Model

Past modeling efforts included the development of a May 29th to June 16th, 2006 photochemical modeling episode for the San Antonio, Austin, and Dallas areas. The modeled episode included several periods of high ozone in these cities.[68] Once complete, the June 2006 model was projected to the year 2018 using forecasted changes in such variables as population, land use, and emissions. Since photochemical models simulate the atmospheric and meteorological conditions that impact high ozone during a particular episode, an important advantage the models provide is the ability to test various scenarios, such as changes in emission rates, under the same set of meteorological conditions that favor high ozone concentrations.

Photochemical model sensitivity runs are used throughout model development as diagnostic tools. The process used to conduct the analysis involves perturbing model inputs, re-running the model, and analyzing model outputs. Results are analyzed in terms of whether the model responded to changes in input and, further, whether the model responded in a manner considered appropriate for the input modifications. In the zero-out runs, for example, all anthropogenic emissions from a discrete geographical areas are removed from the CAMx model to determine their impact on ozone concentrations in the target area, which was San Antonio for this analysis. Furthermore, the analyses are run for future time periods to provide an indication of ozone sensitivity given expected changes in population and other factors. Figure 5-28 shows these photochemical model predictions of ozone concentrations across central Texas. These predictions are based on projected emissions data derived from the 2018 moderate production scenario in the Eagle Ford.

[68] TCEQ. "Daily Maximum 8-hour Ozone Averages." Austin, Texas. Available online: http://www.tceq.state.tx.us/cgi-bin/compliance/monops/8hr_monthly.pl. Accessed 05/13/15.

Figure 5-28: Predicted Daily Maximum 8-hour Ozone Concentrations in the 4-km Subdomain, 2018 Eagle Ford Moderate Scenario

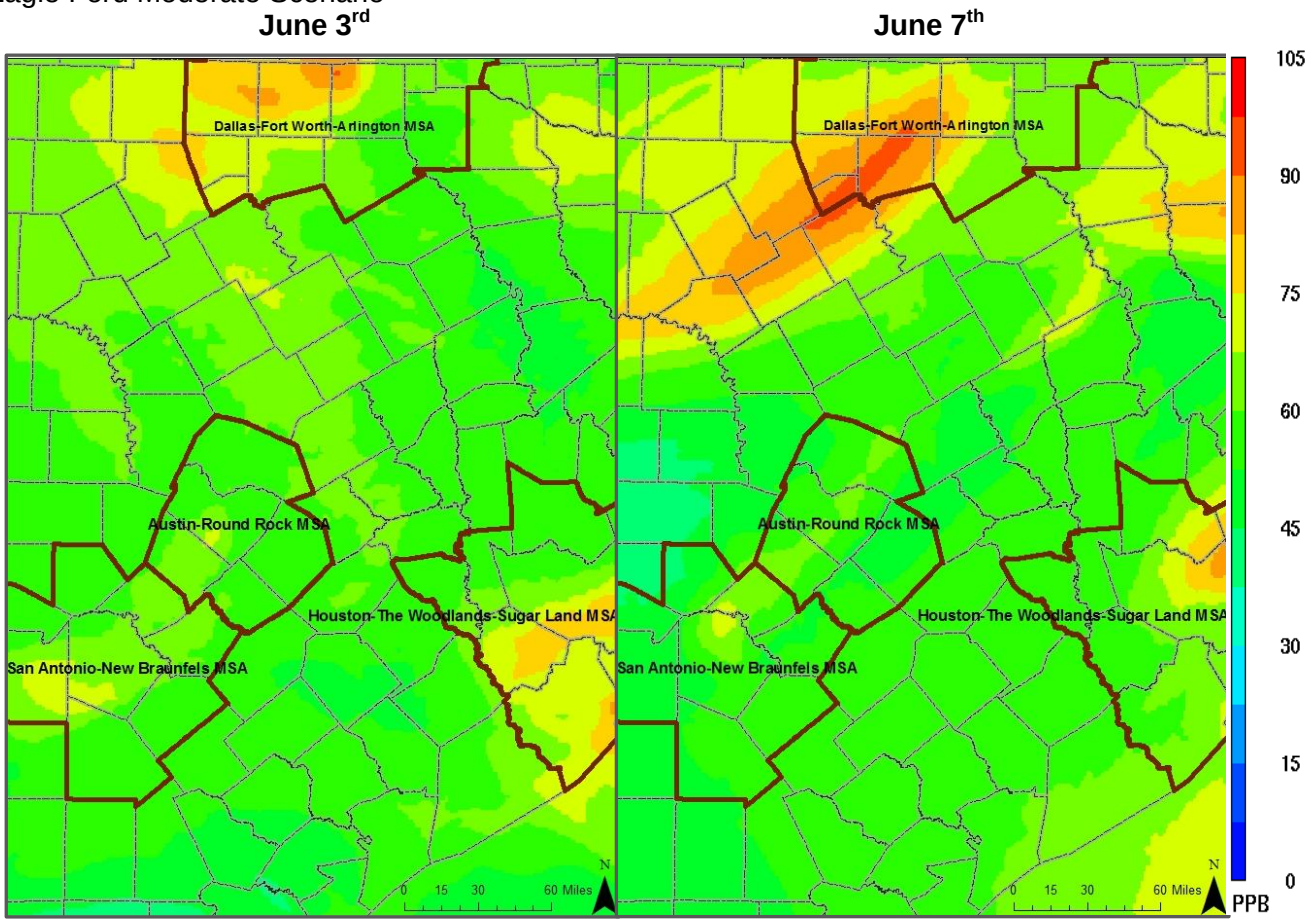

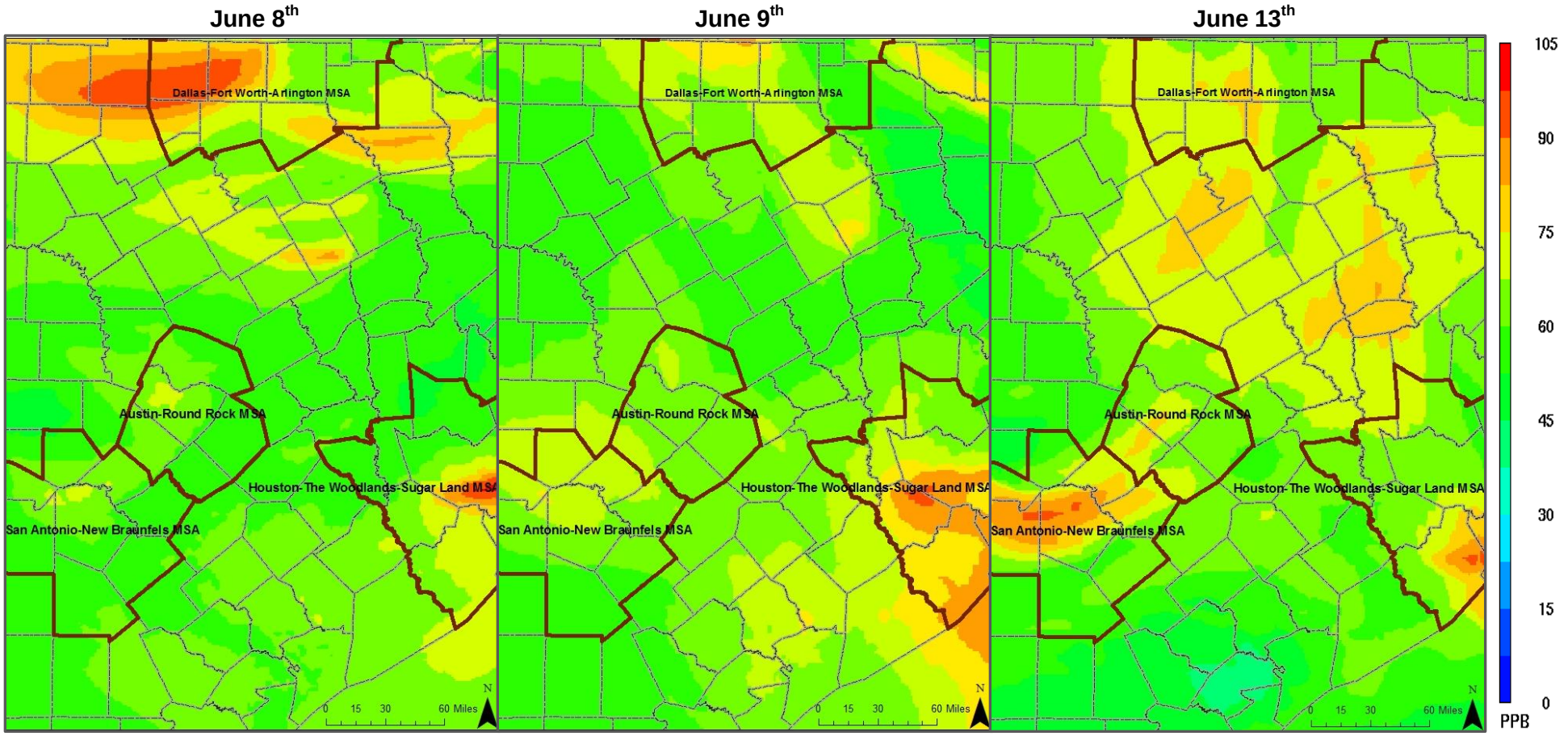
June 8th
June 9th
June 13th
Dallas-Fort Worth-Arlington MSA
Austin-Round Rock MSA
Houston-The Woodlands-Sugar Land MSA
San Antonio-New Braunfels MSA
0 15 30 60 Miles
N
105
90
75
60
45
30
15
0
PPB

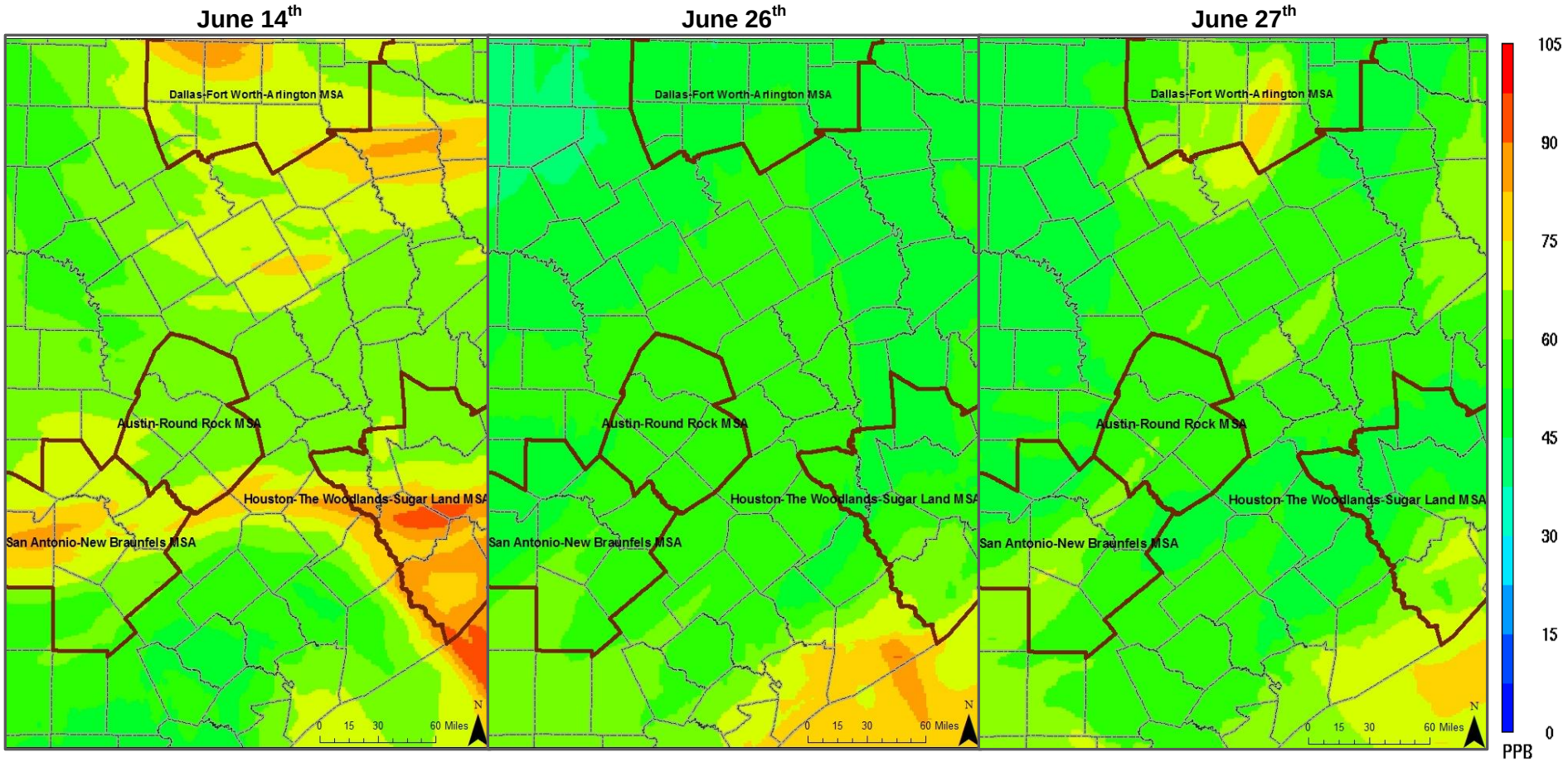
June 14th
June 26th
June 27th
Dallas-Fort Worth-Arlington MSA
Austin-Round Rock MSA
Houston-The Woodlands-Sugar Land MSA
San Antonio-New Braunfels MSA
0 15 30 60 Miles
N
105
90
75
60
45
30
15
0
PPB

June 28th

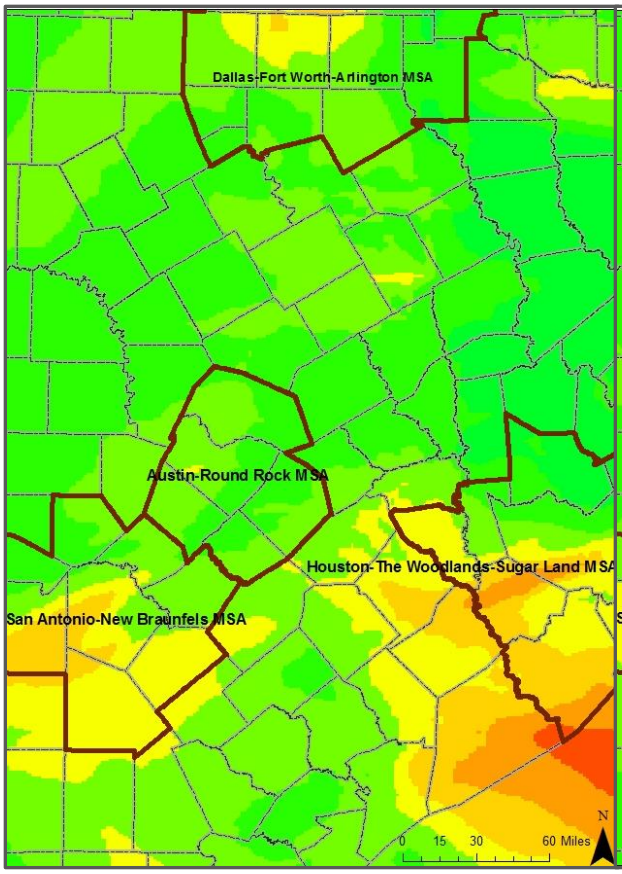

June 29th

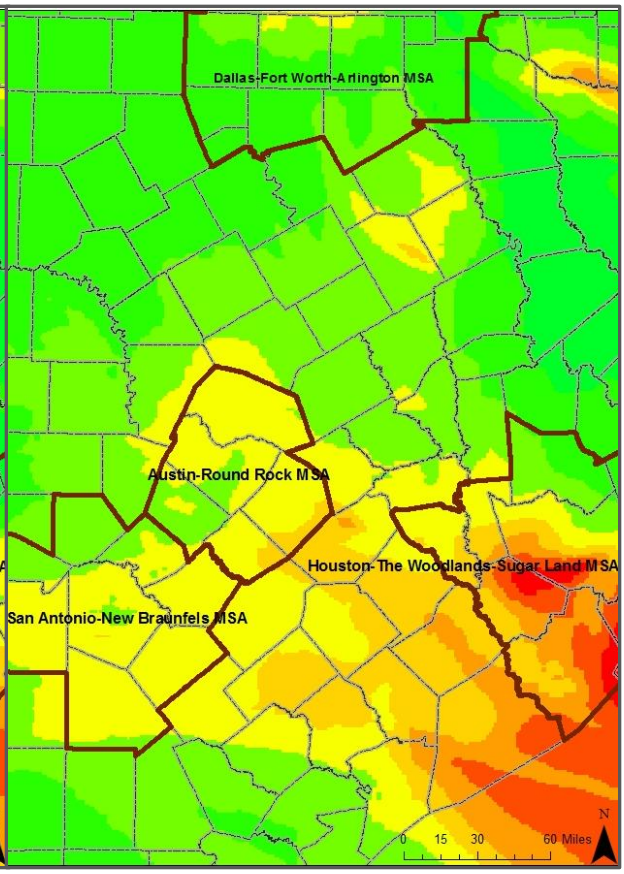

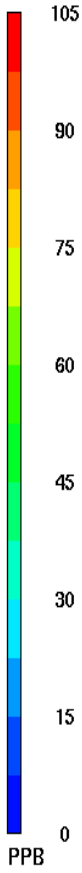

5.5 Regional Point Source Contributions

Figure 5-29 and Figure 5-30 identify total NO_X and VOC emissions, by county, from large industrial point sources in 2013[69]. Many counties in south, east, and northeast Texas contain large NO_X and VOC point sources. These point sources are located in regions that are typically upwind of San Antonio on days when the region experiences high ozone levels. NO_X and VOC point sources can play a significant role in creating elevated ozone concentrations, especially during days when large air masses from the northeast move into the San Antonio region.

New power plants, cement kilns, and other point sources must be taken into consideration when conducting air analyses, because they can have significant impacts on San Antonio's future air quality. As shown in Figure 5-31, permits have been issued for new electric generation units located northeast and southeast of San Antonio. These regions are typically upwind of San Antonio on high ozone days. Potential point sources can generate significant additional NO_X and VOC emissions, making it more difficult for San Antonio to comply with stricter ozone standards. Development of the Eagle Ford Shale oil and gas deposits southeast of San Antonio could increase ozone pre-cursor emissions upwind of San Antonio on high ozone days.

Figure 5-29: Point Source Emissions of NO_X and VOCs by County, 2013

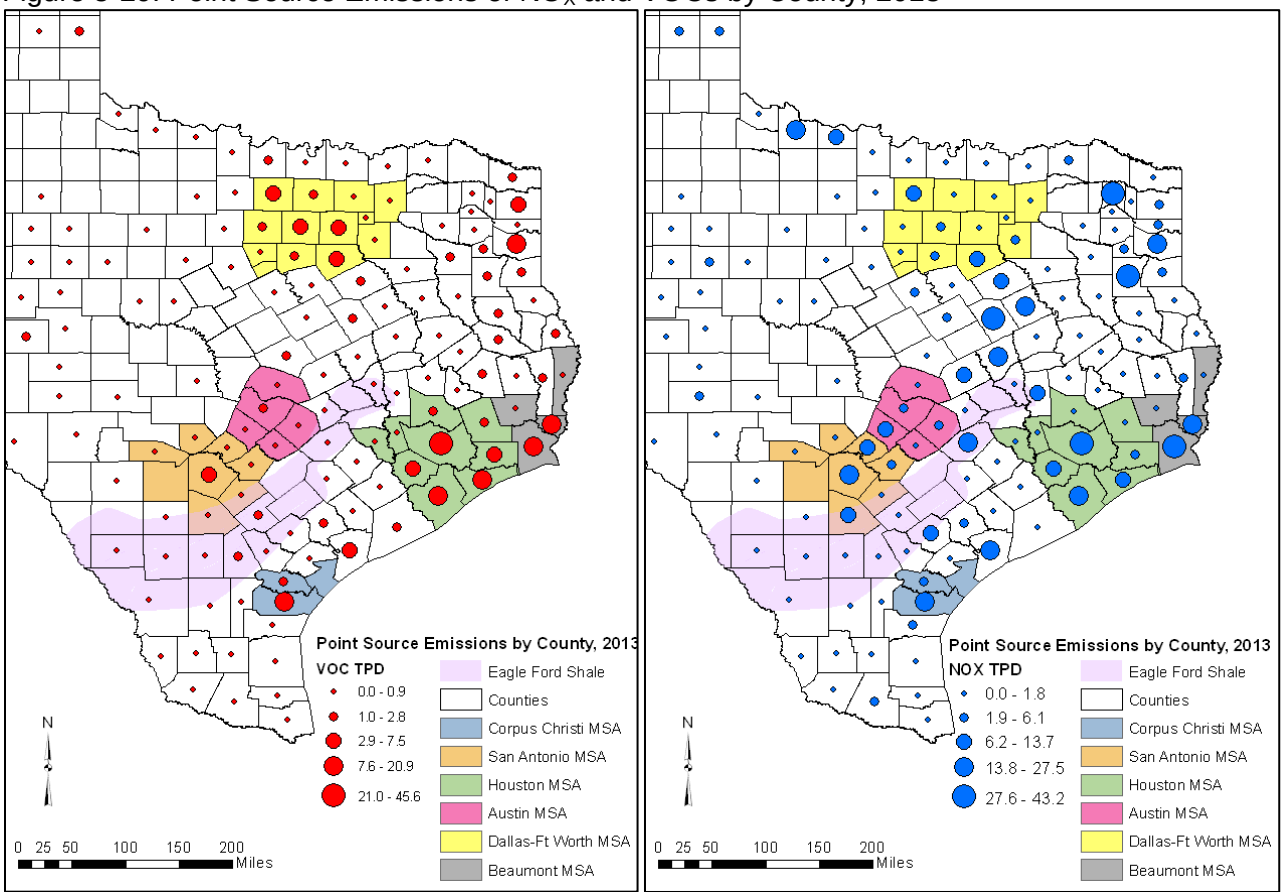

[69] TCEQ. June 16, 2010. "Detailed Data from the Point Source Emissions Inventory". Austin, Texas. Available online: http://www.tceq.texas.gov/implementation/air/industei/psei/psei.html. Accessed 05/13/15 and Alamo Area Council of Governments, October 2013. "Emissions Trend Analysis for the San Antonio-New Braunfels MSA: 1999, 2002, 2006, 2012, 2018, & 2023". San Antonio – Bexar County Metropolitan Planning Organization

Figure 5-30: Total Emissions of NOx and VOC by County, 2013

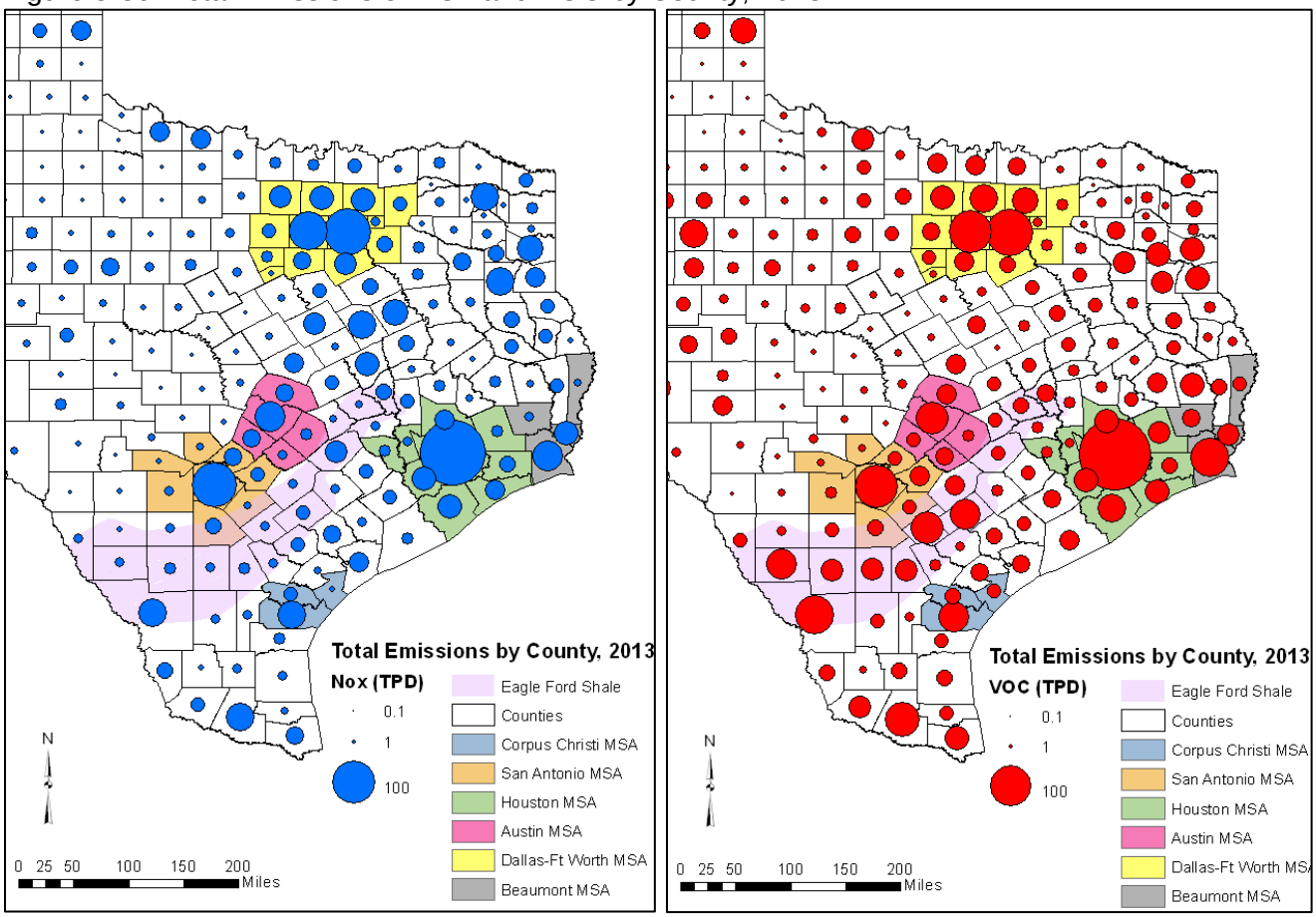

Figure 5-31: County Totals for Newly-Permitted Electric Generation Units in Eastern Texas, post-2007

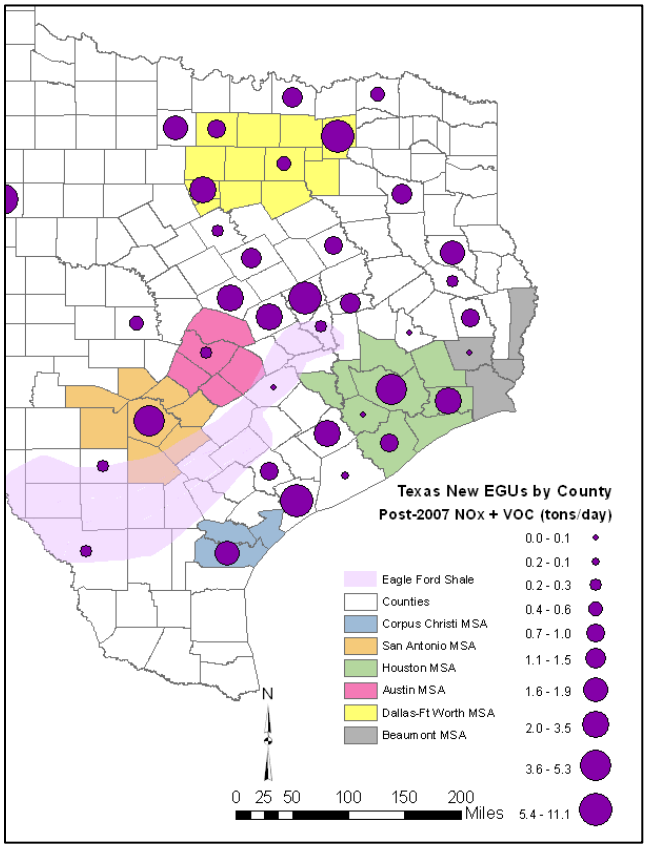

5.6 Background Ozone and Ozone Transport Summary

Analysis of background ozone and ozone transport indicates a number of regional factors that contribute to elevated local ozone concentrations. Typical background conditions associated with high ozone events are identified through the study of regional meteorology and emissions. Findings on background ozone and ozone transport that typify high ozone events include:

- The timing, location, and intensity of ozone events are influenced by the interaction between local and regional wind patterns.
- Surface back trajectories on days with low ozone were predominately from the southeast, while winds on high ozone days were from the northeast, east, and southeast. A similar pattern occurred with 1,000-meter back trajectories where days of high ozone values are associated with winds that originate from the northeast, east, and southeast.
- 48-hour back trajectories on low ozone days tended to originate far out in the Gulf of Mexico, while the back trajectories on high ozone days tended to originate closer to San Antonio and over Eastern Texas.
- Back trajectories on high ozone days originated closer to San Antonio and travelled a shorter distance to arrive at local ozone monitoring stations indicating winds are often lighter on high ozone days.
- The San Antonio local contribution (the difference between the maximum peak ozone reading and the minimal peak ozone readings at ozone monitors on high ozone days > 65 ppb) was 19.5 ppb or 27.4% in 2014.
- The annual 4th highest eight-hour average ozone reading and the number of high ozone days at upwind monitors decreased from 2006 to 2010. In 2011, these values increased and then resumed a decreasing trend through 2014.

- The amount of transported ozone has decreased over the last 5 years: from 56.1 ppb in 2010 to 51.6 ppb in 2014 on average for all days over 65 ppb. The difference between upwind and downwind ozone readings within the San Antonio region has increased in the last 5 years, from 17.6 ppb in 2010 to 19.5 ppb in 2014. The decrease in transported ozone is significant, but the increase in locally formed ozone is not. Taken as a percentage of total ozone, the increase in locally formed ozone is statistically significant.
- Austin ozone readings had a high correlation with San Antonio readings because the cities are close to each other. Also, back trajectories and photochemical modeling analyses showed San Antonio monitors can be impacted by transport from Austin.
- Houston had a strong correlation with San Antonio on high ozone days suggesting that San Antonio is impacted by transport from Houston. The cities that are the farthest away from San Antonio, Dallas and Tyler/Longview, had the lowest correlation with ozone readings in San Antonio.
- On days when back trajectories originated around Houston or Dallas, there was a moderate and statistically significant correlation between 8-hr peak ozone for each city on all days.
- Aircraft sampling indicated large ozone plumes from Houston and industrial facilities can impact areas hundreds of kilometers downwind including San Antonio. Depending on wind direction, this may increase ozone in the San Antonio region and make it more difficult to comply with a stricter 8-hour ozone standard.
- There was a reduction of 17.1 ppb in the 2013 ozone design value when all local anthropogenic emissions from the eight-county San Antonio MSA were removed from the photochemical model (24.7% reduction).
- New point sources being built in Texas may make it more difficult for San Antonio to attain proposed stricter 8-hour ozone standard.

6 SEASONAL OZONE DIFFERENCES

Ozone readings fluctuate by season depending on several factors including variations in transport, meteorology, chemical loss of ozone, and upper stratospheric ozone levels. Since transport is a significant factor in local ozone concentrations, seasonal variations in wind direction, speed and direction of back trajectories, and chemical loss are important considerations during the conceptual model process.

6.1 Annual Ozone Variation

Represented in Figure 6-1 are the semi-monthly frequencies for days exceeding the 65 ppb proposed ozone standard from 2005 – 2014. More exceedances of the proposed 65 ppb standard occur during the second seasonal peak (42% of all days > 65 ppb) than the first seasonal peak (36% of all days > 65 ppb). The two ozone season peaks have very different metrological and transport factors that impact local monitored ozone. Since the two ozone seasonal peaks vary greatly by emission sources, transport, and intensity, different control measures might be needed to reduce ozone based on time of year.

Figure 6-1: Number of Days with 8-hr Ozone Averages > 65 ppb by Semi-monthly Periods for San Antonio, 2005 – 2014

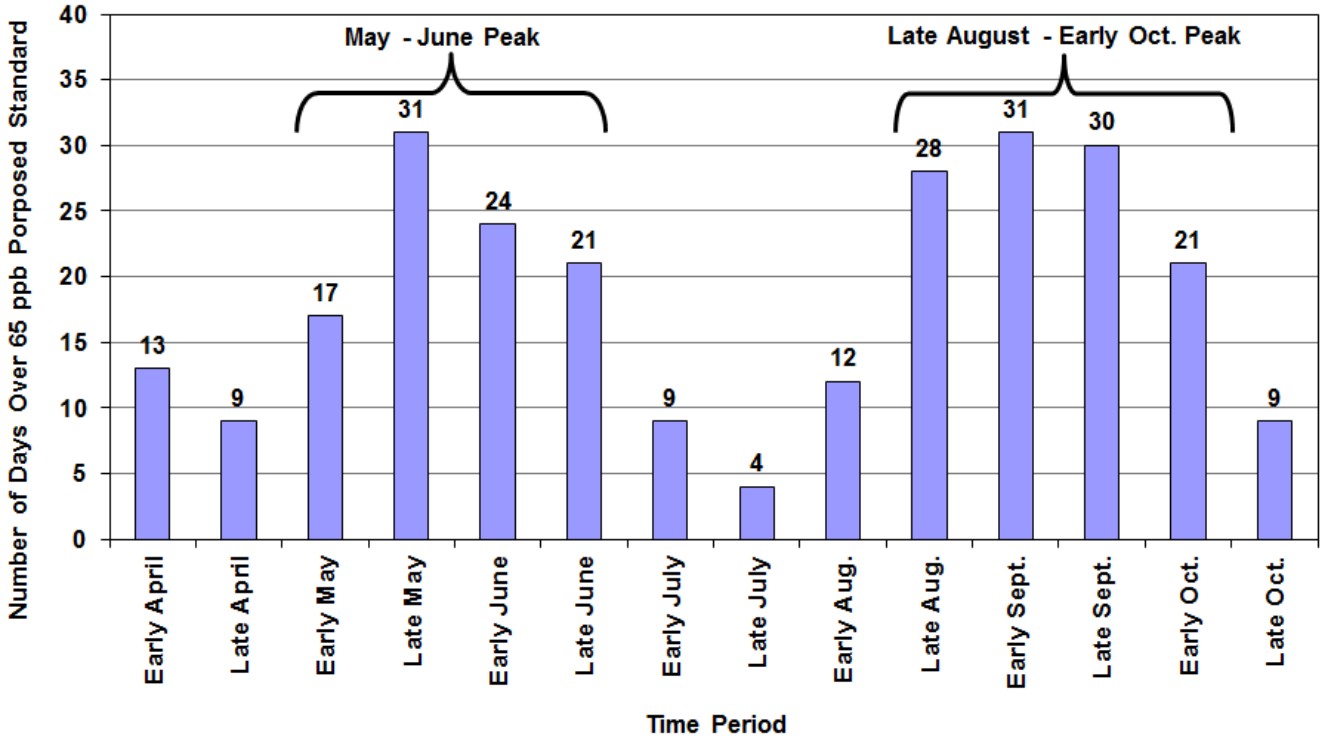

The chi-square (X^2) goodness-of-fit test[70] and Phi (φ) test were performed on the semi-monthly distribution of high ozone proposed 65 ppb ozone standard to determine whether the distributions are random or significant in the San Antonio region. The chi-square value was compared to a probability chart to determine if the results are significant.[71] The results are significant at 99.5% (61.27 chi

[70] Jones, James, Professor of Mathematics, Richland Community College. "Math 170: Intro to Statistics Chapter 12 Lecture Notes". Available online: http://www.richland.edu/james/lecture/m170/ch12-fit.html. Accessed 01/06/15.

[71] Jones, James, Professor of Mathematics, Richland Community College. "Table: Chi-Square Probabilities". Available online: http://www.richland.edu/james/lecture/m170/tblchi.html. Accessed 01/06/15.

square result > 29.82 from the probability chart for 13 degrees of freedom and 0.005 probability values).

The results of the Phi (φ) test for the 65 ppb proposed standard (0.48) was greater than 0.2 and therefore the results indicate a significant variability in the frequency of high ozone days over the period. The chi-square test confirms high ozone days do not occur with equal frequency in the San Antonio region. It is not just as likely for a high ozone day to occur during one given semi-monthly period as during another given time period. Both tests indicate that high ozone days appear to follow a seasonal (non-random) pattern with peaks and valleys during the ozone season.

6.2 Meteorological Seasonal Variations

According to multivariate correlation analysis, individual metrological factors that had the highest correlation with days exceeding eight-hour average ozone concentrations of 65 ppb were humidity at 2 p.m., diurnal temperature change, morning wind direction, and back trajectory direction. Due to the influence of these factors in the formation of ground level ozone, each factor was analyzed to determine the extent to which monthly variations of these factors impact ozone levels. The frequencies of days with meteorological conditions deemed conducive to ozone formation were plotted with frequencies of high ozone days on a monthly basis. The results of these comparisons are provided in Table 6-1.

6.2.1 Seasonal Wind Direction Variation

C23 and C58 average hourly wind vector plots for all days during the months of June through September are presented in Figure 6-3 and Figure 6-4. Wind speeds and directions are similar during the months of June, July, and August at both monitors, but show a different pattern for September. Plots for June, July, and August show the characteristic dominance of south-easterly winds during these months. During September winds at both monitors reverse during the day, which results in an easterly average daily resultant wind vector. C58 experiences particularly calm winds during the middle of the day and a shorter, more northeasterly average daily resultant wind vector. During September, however, the wind vector plot for C58 indicates there is a flow reversal of winds arriving at the monitor from the northwest in the morning before 7 am, which does not occur during the other three months. Table 6-2 summarizes the average daily wind vector for each month at C23 and C58. It shows the tendency for early high ozone days to be characterized by stronger winds and late season high ozone days to be more stagnant, as discussed in section 5.2.

Table 6-1

6.2.2 Humidity

As demonstrated in section 3.3.2., humidity has one of the strongest correlations with ozone among meteorological factors, with an R^2 value of 0.27 for all days. Lower relative humidity is related to high rates of ozone formation. The relationship between relative humidity and ozone was further investigated by comparing the frequency of low humidity days versus the frequency of high ozone days by each month of the ozone season. Figure 6-2 displays the percentage of days in each month from 2005-2014 that had relative humidity below 38.3% versus the percentage of days when 8-hour ozone averages were above 65 ppb. There is significant variation by month, with little predictability between average monthly humidity and ozone readings.

6.2.3 Diurnal Temperature Change

A moderate correlation exists between the magnitude of temperature changes within a single day (from the overnight low to the afternoon high) and ozone values from 2005-2014. Comparing the percentage of high ozone days (greater than 65 ppb ozone) versus the percentage of days with a large diurnal temperature change (greater than 12.7°C) by month, as displayed in Figure 6-2, indicates no significant correlation between the two factors.

6.2.4 Solar Radiation

The correlation between peak daily solar radiation and peak 8-hour ozone has an R^2 value of 0.15. Because ozone formation requires sunlight, a positive correlation between daily peak solar radiation and peak 8-hour ozone is expected. The monthly frequencies of days that have peak solar radiation of >1.16 langleys/minute were graphed with the monthly frequencies of days with peak 8-hour ozone >65 ppb. Although sunlight is necessary for ozone formation, there was no correlation between how many days each month had high solar radiation and how many had high ozone.

Figure 6-2: Selected Meteorological Observations at C58 and High Ozone Occurrence by Month, 2005-2014

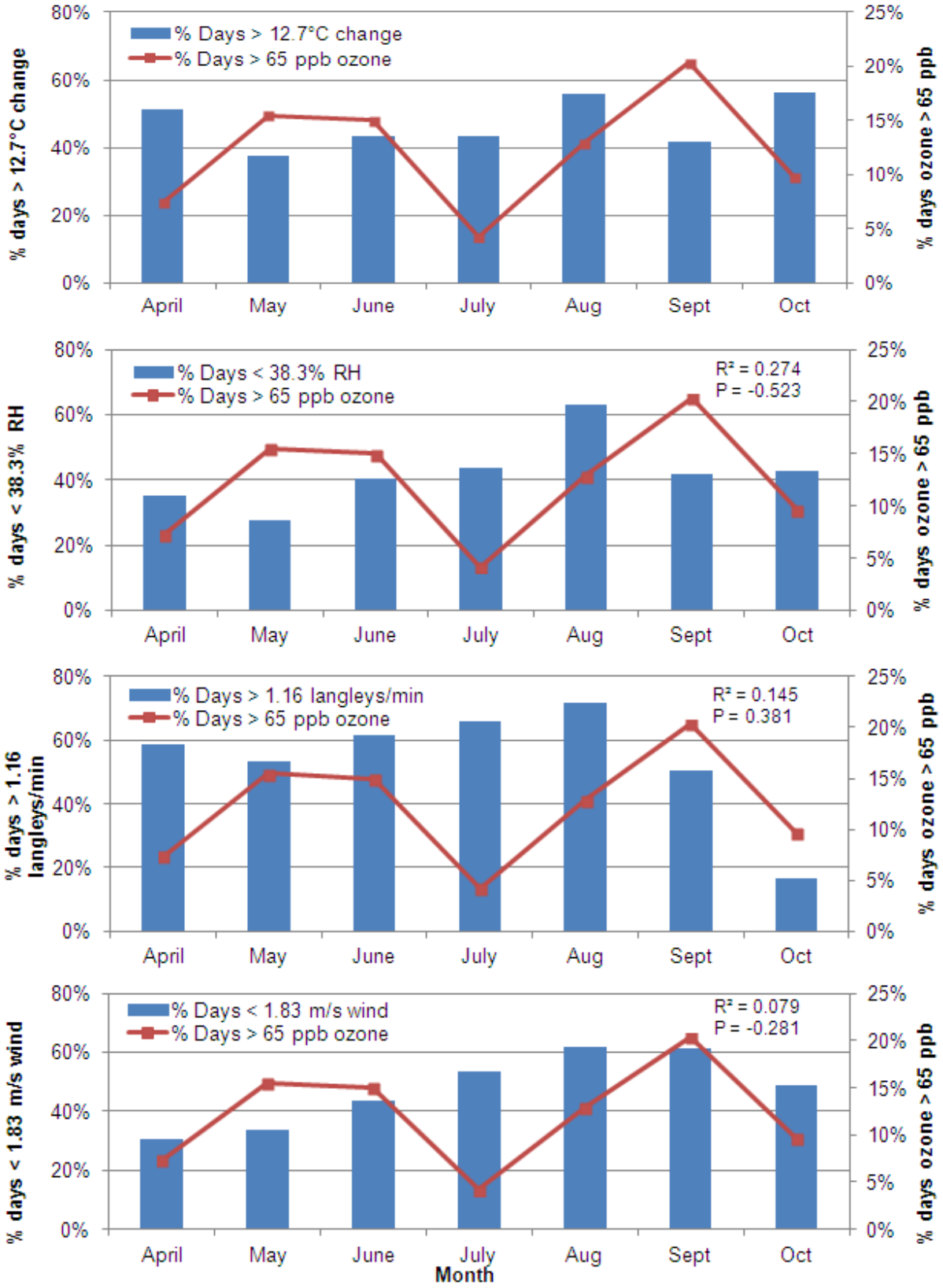

6.2.5 Seasonal Wind Direction Variation

C23 and C58 average hourly wind vector plots for all days during the months of June through September are presented in Figure 6-3 and Figure 6-4. Wind speeds and directions are similar during the months of June, July, and August at both monitors, but show a different pattern for September. Plots for June, July, and August show the characteristic dominance of south-easterly winds during these months. During September winds at both monitors reverse during the day, which results in an easterly average daily resultant wind vector. C58 experiences particularly calm winds during the middle of the day and a shorter, more northeasterly average daily resultant wind vector. During September, however, the wind vector plot for C58 indicates there is a flow reversal of winds arriving at the monitor from the northwest in the morning before 7 am, which does not occur during the other three months. Table 6-2 summarizes the average daily wind vector for each month at C23 and C58. It shows the tendency for early high ozone days to be characterized by stronger winds and late season high ozone days to be more stagnant, as discussed in section 5.2.

Table 6-1: R^2 and P-Values of Selected Meteorological Parameters Correlated with Monthly Ozone Days Over 65 ppb

Parameter	R^2	p-value
Diurnal temperature change > 22.8°F	0.319	0.186
Relative humidity < 38.3%	0.274	0.228
Solar radiation > 1.16 langleys/min	0.145	0.399
Wind speed < 1.83 m/s	0.079	0.542

Opportunities for future analysis include considering the frequencies of days each month where all of the above meteorological parameters were met and comparing with the monthly frequencies of peak 8-hour ozone over 65 ppb.

Table 6-2: Resulting Wind Direction and Wind Speed > 65 ppb, 2005 - 2014

Monitor	Month	All Day		Morning		Afternoon		Ozone	
		Wind Direction (degrees)	Wind Speed (m/s)	Wind Direction (degrees)	Wind Speed (m/s)	Wind Direction (degrees)	Wind Speed (m/s)	Average Peak 8-hr (ppb)	Number of days > 65 ppb
C23	May	128	1.87	133	1.26	137	2.05	49.3	33
	June	141	2.25	160	1.62	143	2.45	42.1	28
	July	139	1.87	157	1.27	138	2.16	37.9	7
	Aug.	140	1.67	169	0.92	137	1.91	44.0	27
	Sept.	102	0.94	62	0.54	110	1.21	46.8	43
	Oct.	112	0.85	63	0.51	137	1.05	43.8	21
C58	May	136	1.57	142	0.99	140	2.02	50.6	37
	June	147	2.06	164	1.46	147	2.51	45.5	40
	July	145	1.71	161	1.13	143	2.24	41.1	8
	Aug.	146	1.40	186	0.68	141	1.99	47.7	34
	Sept.	87	0.43	337	0.57	106	1.15	48.2	46
	Oct.	105	0.28	340	0.54	135	0.92	44.5	27

Figure 6-3: Hourly Average Resultant Wind Vectors at C23 by Month, 2005-2014

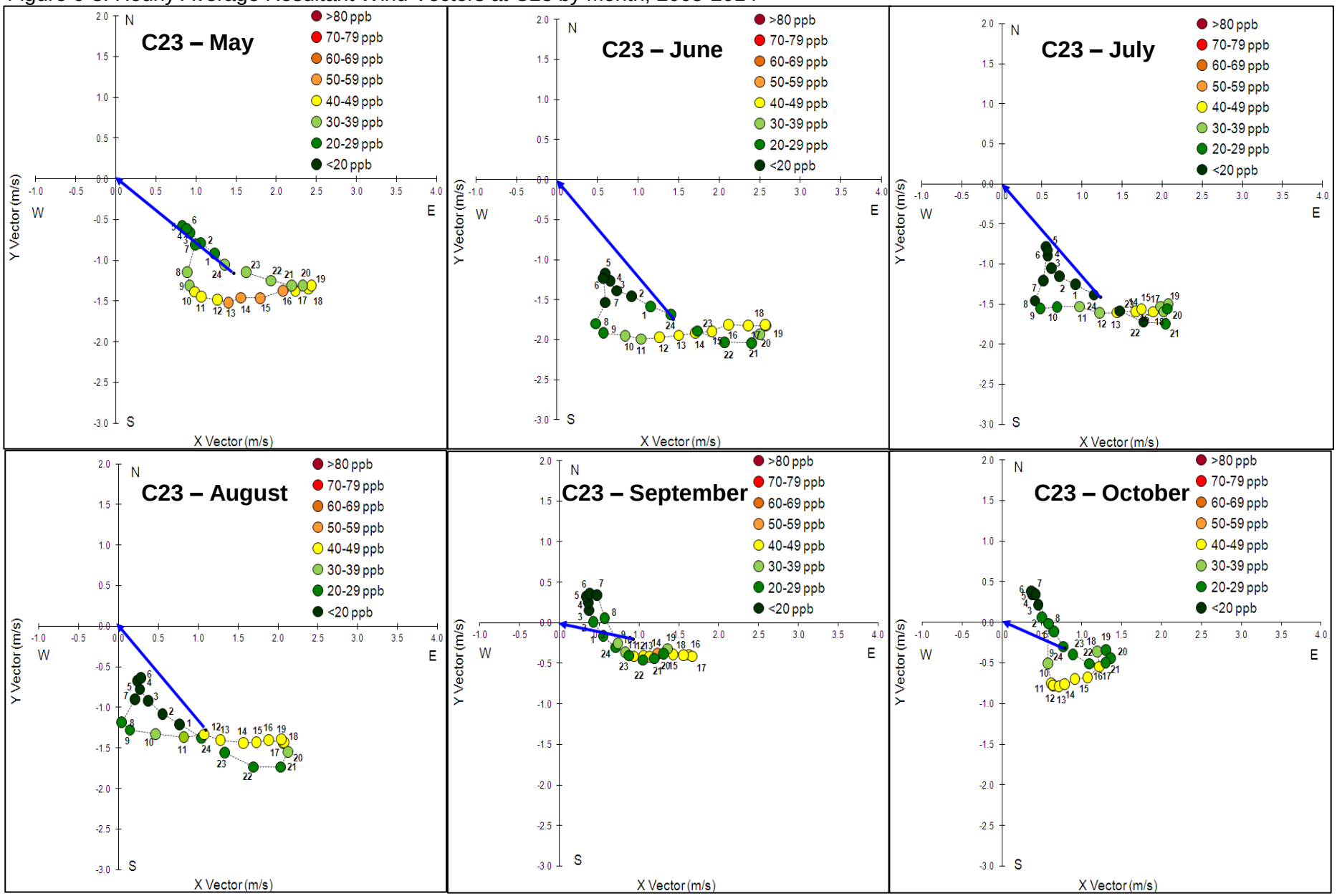

Figure 6-4: Hourly Average Resultant Wind Vectors at C58 by Month, 2005-2014

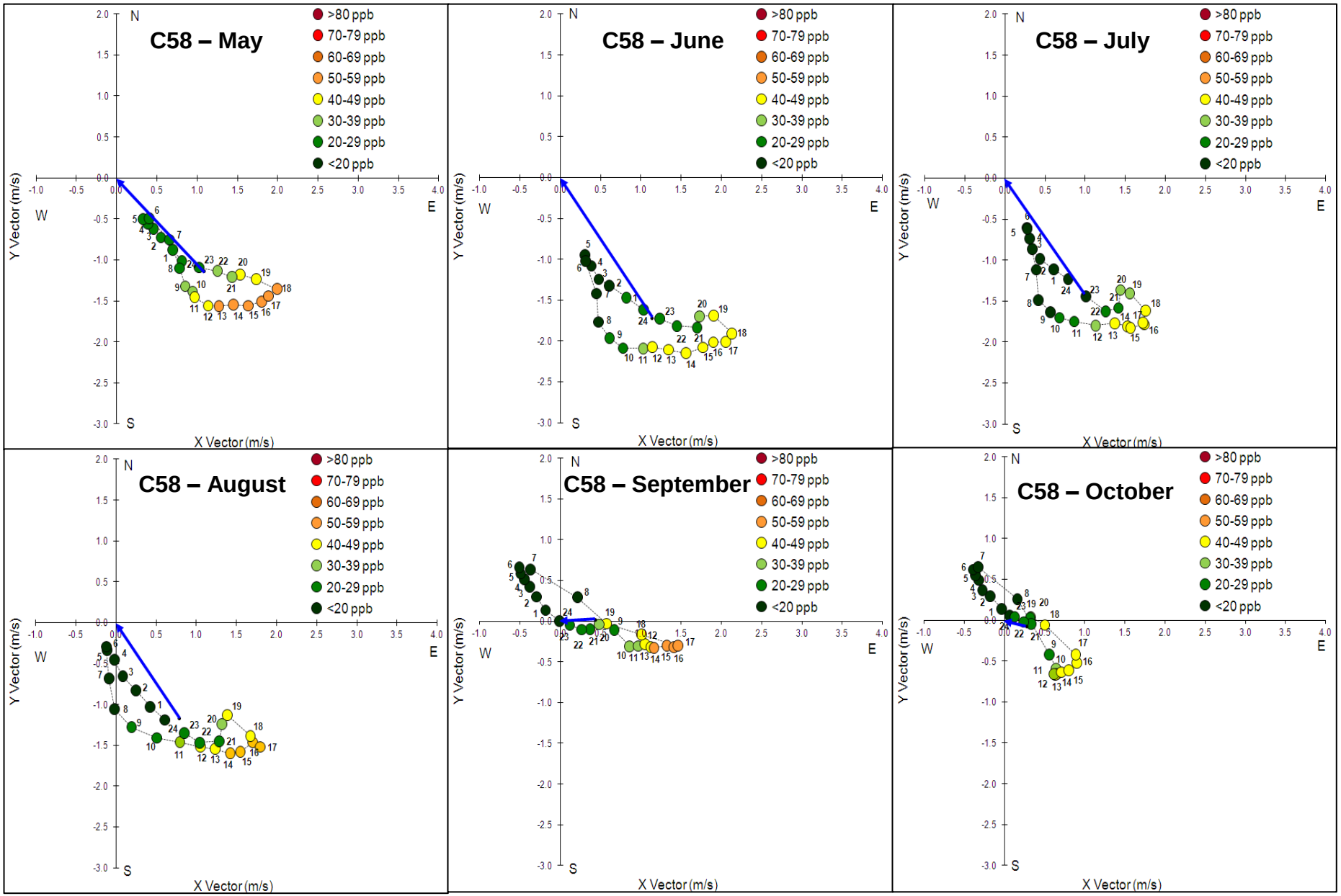

6.2.6 Back Trajectory Direction

Back trajectories were analyzed by month to determine if there were seasonal variations on high ozone days. As
Figure 6-5 shows, there were pronounced differences in seasonal wind flow on days of high ozone. The largest percentage of 48-hour 100-meter back trajectories, 59%, on high ozone days > 65 ppb, originated from the southeast or south during the month of June, while only 17% originated from the north or northeast. A similar pattern occurred on high ozone days in May and July. High ozone days in September had different patterns of back trajectories. High ozone day wind trajectories during September were from the north or northeast (58%), while few back trajectories were from the south or southeast (20%). August back trajectories were from both the north/northeast and south/southeast (Table 6-3).

Figure 6-5: Statistical Analysis of San Antonio's 400-km Back Trajectory Wind Directions By Month, High Ozone Days > 65 ppb, 2009-2014

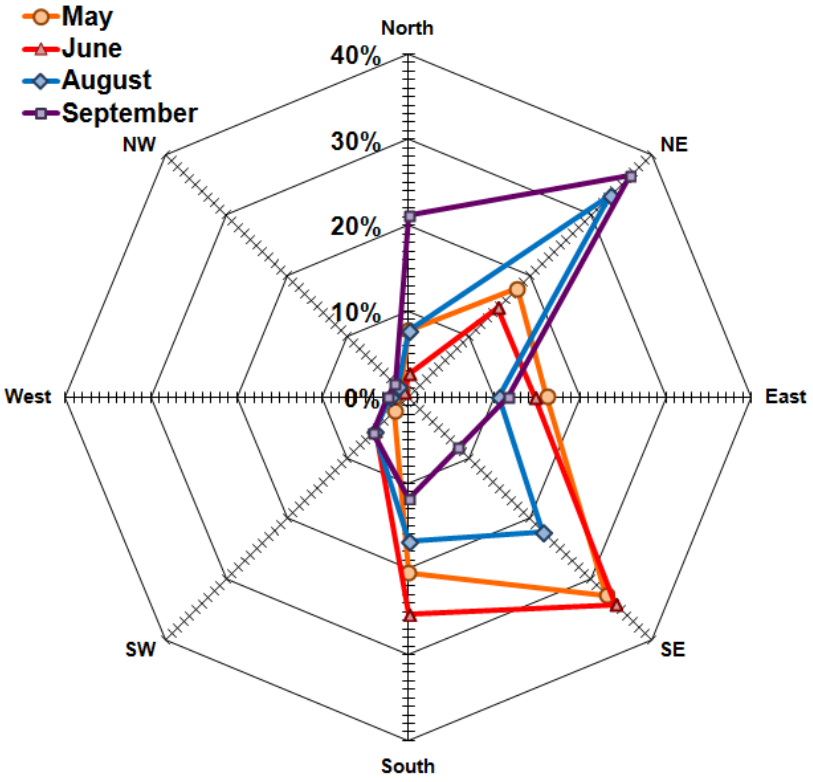

Table 6-3: Back Trajectories Direction by Month for Days > 65 ppb, 2009 - 2014

Month	North	NE	East	SE	South	SW	West	NW	Total
April	12.2%	22.7%	22.0%	32.5%	7.7%	1.0%	0.0%	1.9%	100.0%
May	7.7%	17.9%	16.1%	32.6%	20.4%	2.4%	1.7%	1.2%	100.0%
June	2.7%	14.7%	14.7%	34.1%	25.3%	5.5%	2.3%	0.7%	100.0%
July	5.8%	14.4%	14.8%	56.0%	8.9%	0.0%	0.0%	0.0%	100.0%
August	7.7%	33.2%	10.6%	22.2%	16.8%	5.6%	2.2%	1.7%	100.0%
September	21.1%	36.5%	11.7%	8.2%	11.9%	5.9%	2.4%	2.2%	100.0%
October	5.9%	11.6%	28.8%	23.9%	17.4%	9.8%	1.6%	1.1%	100.0%

Back trajectories on days > 65 ppb were analyzed to determine the distance of the origin from C58 during each month. From Table 6-4 there does appear to be significant variation in the number of days with stagnated back trajectories by month. A chi-square statistical test confirms this with a p-value of 0.035. However, because this variation among stagnated back trajectories reflects the overall lack of high ozone days in July and to a lesser extent, April, the percentage of stagnated back

trajectories by month was also used to test for significance. With a p-value of 0.11, there was no significant difference in the percentage of stagnated back trajectories by month. During May, June, August, and September, 53% to 63% of the back trajectories originated within 400 km of CAMS58. On days greater than 65 ppb in October, 71% of the 48-hour back trajectories originated within 400 km of CAMS 58 (Table 6-4). There were far fewer cases of transport back trajectories leading to high ozone; however, there is significant variation in the percentage of transport back trajectories by month (p-value < 0.001). April has the highest share of transport back trajectories at 27% and June has the lowest at 5%

Table 6-4: 48-Hour Back Trajectories Classification by Month for Days > 65 ppb, 2009 – 2014

Month	Stagnated (within 400 km)		Weak Transport (400-800 km)		Transport (more than 800 km)		Total	
	n	Percent	n	Percent	n	Percent	n	Percent
April	5	45%	3	27%	3	27%	11	100%
May	14	56%	9	36%	2	8%	25	100%
June	10	53%	8	42%	1	5%	19	100%
July	3	43%	3	43%	1	14%	7	100%
August	15	63%	7	29%	2	8%	24	100%
September	15	54%	8	29%	5	18%	28	100%
October	10	71%	3	21%	1	7%	14	100%

6.3 Seasonal Variation at Upwind Monitors

There is a significant amount of ozone transport during the spring and fall ozone season peaks. The values in Figure 6-6 represent the average highest ozone readings at upwind monitors compared to the lowest average readings at downwind monitors, by month. This data indicates April is distinguished as the month with the highest average ozone transport at 43.4 ppb, but the smallest difference between upwind and downwind monitors at 7.8 ppb. Transport in July decreases because there is reduced transport of upper stratospheric ozone mixing with ground level emissions due to chemical loss of upper stratospheric ozone. The amount of transported ozone increases during the fall seasonal peak in late August to early October.

Figure 6-6: Average San Antonio Background Ozone by Month, All Days, 2005-2014

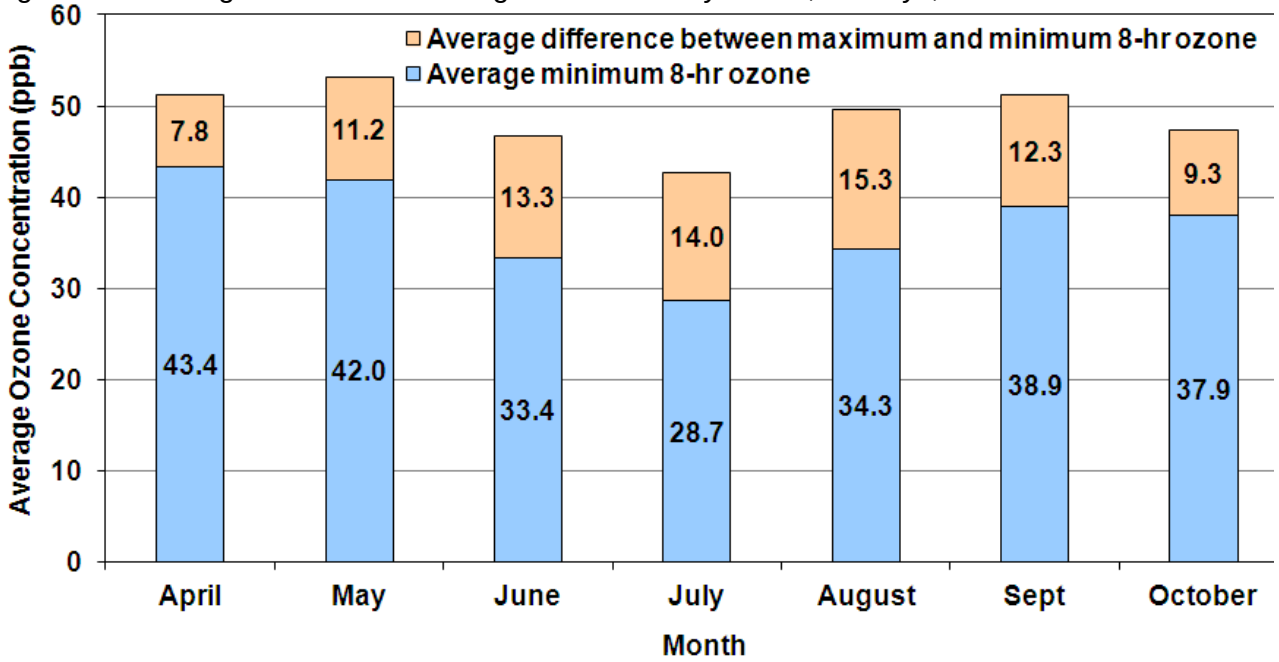

6.4 Tropospheric and Stratospheric Seasonal Ozone Variation

Several studies have found that stratospheric and tropospheric ozone exchange decreases from the spring to the fall seasons. Figure 6-7 shows the "time series of northern midlatitude total ozone between 30ºN and 60ºN averaged from 1987 to 1997. The thick line represents the time mean, while shading represents the range of values obtained from 1979 to 1996."[72] According to Cordero and Kawa, there is weak downward motion in the circulation of the lower midlatitude stratosphere between 15 and 20 km in altitude (the lower portion of the stratosphere) during the early summer (May-June).[73] The authors note that this motion occurs as an exception to the general upward motion in the Northern Hemisphere (NH) stratosphere during the early summer.

Figure 6-7: Total Ozone Mapping Spectrometer (TOMS) Total Ozone 30ºN – 60ºN Average

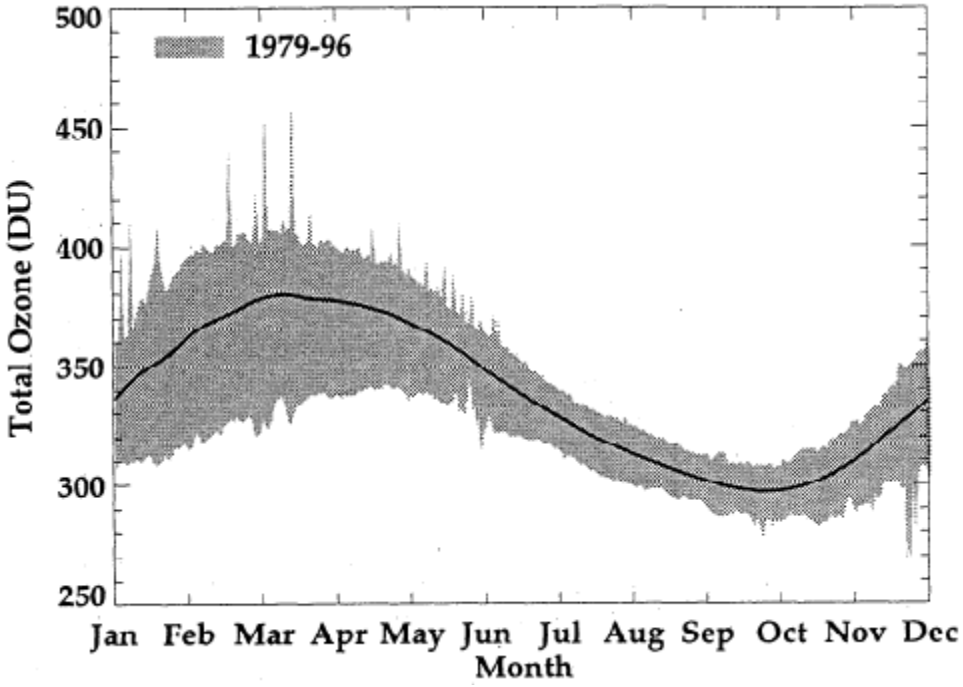

Since stratospheric ozone is much higher in concentration than tropospheric ozone, as shown in Figure 6-8,[73] this motion can introduce elevated ozone levels into the troposphere of the midlatitudes (i.e. Texas) that counteracts the ozone-moderating effects of the transport of relatively unpolluted air from the Gulf of Mexico during June. This is a potential explanation as to why elevated ozone concentrations are more likely to occur in May and June than July in much of Texas. In mid to late summer (July-August), the circulation shifts to a downward motion north of 40ºN, and the vertical transport becomes increasingly stronger through September and October.[73] This phenomenon might likewise add to the elevated tropospheric ozone present in the northeast U.S. which is sometimes transported into Texas during the fall ozone season peak in late August to early October.

A springtime ozone maximum occurring at midlatitudes in the northern hemisphere has also been referred to and modeled in a study by Mauzerall et al.[74] According to the authors, the discrepancy

[72] Cordero E.C. and Kawa S.R. "Ozone and Tracer Transport Variation in the Summer Northern Hemisphere Stratosphere", Journal of Geophysical Research. 106.D11 (June 16, 2001): 228. Available online: http://www.met.sjsu.edu/~cordero/research/Papers/jgr2001.pdf. Accessed 04/01/15.
[73] Schoeberl M.R. "Chapter 7: Ozone and Stratospheric Chemistry", 1999 EOS Science Plan. Ed. Greenstone R. and King, M.D. National Aeronautics and Space Administration, 1999. p.305. Available online: http://eospso.gsfc.nasa.gov/sites/default/files/publications/SciencePlan.pdf. Accessed 05/13/15.
[74] Mauzerall, D.L., Narita, D., Akimoto, H., Horowitz, L., Walters, S., Hauglustaine, D.A., and Brasseur, G. "Seasonal Characteristics of Tropospheric Ozone Production and Mixing Ratios Over East Asia: A Global Three

between the observed and modeled ozone concentrations in winter and spring was most likely due to an under-representation in the model of the influx of stratospheric ozone, which has a broad maximum from winter to spring. They also stated the combination of such stratospheric influx with a sharp increase in photochemical buildup from February to May could explain the observed spring maximum from April to May observed at mid-latitude sites.

Figure 6-8: Distribution of Atmospheric Ozone by Altitude in Partial Pressure

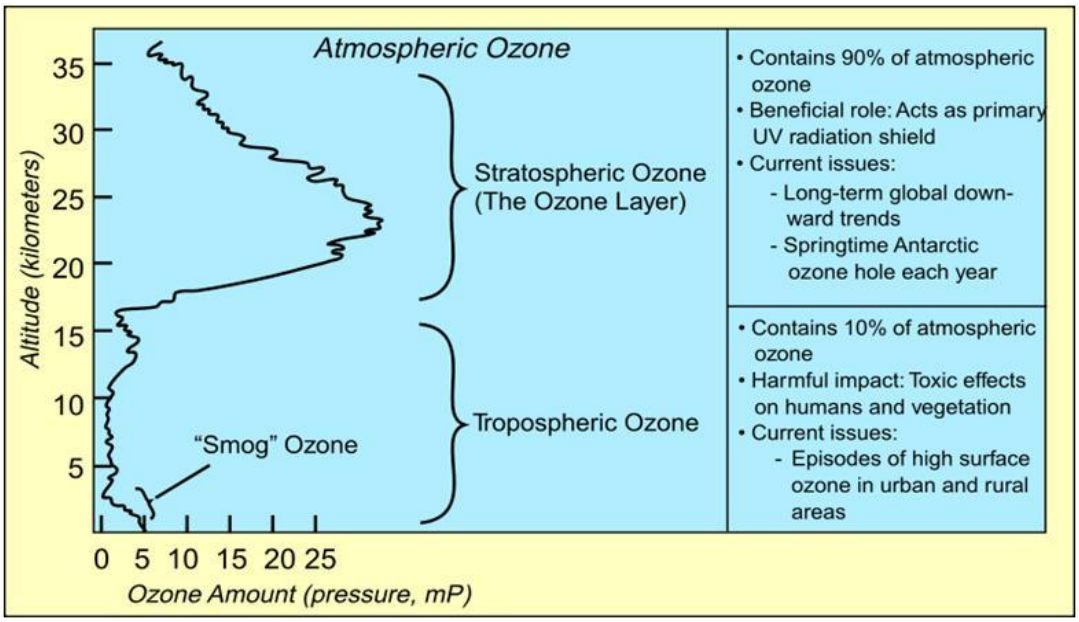

The observed decline in tropospheric and stratospheric ozone in the Northern Hemisphere from the spring to the fall seasons can be explained by increased chemical destruction of ozone. Chemical loss of tropospheric and stratospheric ozone can occur through the catalysis by NO_X in the summer time. Crutzen and Brühl addressed "the cause of the largely natural total ozone decline in the stratosphere from its spring maximum to fall minimum in the northern hemisphere and show that this is mainly due to NO_X-catalyzed ozone destruction".[75] "For all years, net ozone production takes place between the "subtropical barrier", at about 30° N, and 50° N. Nevertheless, also in this latitude region the ozone content declines due to transport to higher latitudes where very strong chemical ozone loss takes place due to summer time NO_X activation."[76]

As evidence of elevated background ozone caused by transport and/or introduction from the upper atmosphere, there is a strong correlation between tropospheric ozone at 1 to 2.5 km above the surface and ground level ozone on the west coast of North America.[77] Further research is needed to determine the correlation between stratospheric and upper tropospheric ozone levels and ground level ozone in the San Antonio region. The decrease in tropospheric ozone from spring to summer

---

Dimensional Transport Model Analysis." American Geophysical Union, 2000. p. 2-21. Available online: http://www.princeton.edu/~mauzeral/syllabi/jointpaper.pdf. Accessed 04/09/15.

[75] Crutzen, Paul J. and Brühl, Christoph, Atmospheric Chemistry Division, Max Planck Institute for Chemistry, Mainz, Germany, "Catalysis by NOx as the Main Cause of the Spring to Fall Stratospheric Ozone Decline in the Northern Hemisphere", The Journal of Physical Chemistry. A, 2001, 105(9), (December 21, 2000): pp 1579–1582.

[76] *Ibid*.

[77] Huang, M., et al, July 30, 2010. "Impacts of Transported Background Ozone on California Air Quality During the ARCTAS-CARB Period – A Multi-Scale Modeling Study." Available online: http://www.atmos-chem-phys.net/10/6947/2010/acp-10-6947-2010.pdf. Accessed 06/09/15.

may result in less vertical ozone transport between atmospheric layers and a decrease in the number of ozone exceedances observed in July.

Although concentrations are typically low in July, ozone levels again increase in the fall in San Antonio. Local wind directions change in the fall and local and regional meteorological patterns become more conducive to high ozone days. There is an increase in the frequency of stagnated winds with local or short-range transport emissions from the northeast which can cause elevated ozone during August, September, and October.

6.5 Ozone Seasonal Difference Summary

Seasonal variations in ozone levels are impacted by transport of ozone and ozone precursors into the San Antonio region.

- From April through June, a seasonal increase in the number of high ozone days develops in most Texas cities. This period represents the first and longest high ozone seasonal peak that San Antonio typically experiences. However, by early July the number of high ozone days declines. The next seasonal increase covers a period beginning in August and ending in late October, during which the frequency of high ozone days is slightly lower than the spring period.
- There is much variation in measures of humidity versus ozone by month, with little predictability for ozone based on humidity alone.
- Although the magnitude of temperature change within a single day has a relatively high correlation with ozone values, diurnal temperature change during any given month is a poor predictor for high ozone occurrence.
- Resultant wind vectors are shorter in July than in June, indicating more stagnated winds for July compared to June, yet July actually experiences fewer high ozone days. Hourly wind vectors plotted for each week in June indicate that wind speed is fairly well correlated with ozone levels. In the month of July, weekly plots generally have resultant wind vectors of smaller magnitude than in June, but weekly 8-hour ozone values are significantly lower. This analysis gives further evidence that factors other than prevailing wind/horizontal air movement may have greater influence on local ozone levels during the month of July.
- Back trajectories tended to travel increasingly shorter distances each month from June through September indicating stagnant air conditions. Back trajectories in June, July, and August originated predominantly from the southeast and south, but back trajectories in September originated equally as often from the northeast, east, and southeast, with smaller fractions originating from the north and south.
- There is a significant amount of ozone transport during the spring and fall ozone season peaks. During the ozone season, the month most affected by transport (highest ozone average measured at upwind monitors) is April, but the month is also characterized by the smallest difference between upwind and downwind monitors, indicating less locally-produced ozone. Transport is lowest in July before increasing again into the late summer and fall because there is reduced transport of upper stratospheric ozone mixing with ground level emissions due to chemical loss of upper stratospheric ozone. The mid summer months of June through August account for the largest fractions of local contributions to ozone.
- It is possible that a combination of greater tropospheric-stratospheric air exchange combined with higher North American stratospheric ozone levels during the early months of the ozone season is partially responsible for the higher ground level ozone observed in San Antonio during these months. Likewise, the secession of this phenomenon could explain the decrease in ground level ozone from late June through July which occurs before air mass stagnation and northeasterly transport contributes to a rebound in ground level ozone measurements.

7 METEOROLOGICAL PATTERNS DURING SAN ANTONIO OZONE EVENTS

Computer simulations that replicate high ozone events are valuable tools on which to base control strategy analyses and predict the impacts of socioeconomic factors, such as changes in population and land use, on ozone formation. Simulations must account for the complex chemical and atmospheric processes that influence ozone formation, dispersion, and deposition. Because simulations are based on atmospheric and meteorological conditions coinciding with local elevated ozone episodes, they allow analysts to predict the impact of emission controls and other emission rate perturbations under "worse case" circumstances.

According to EPA guidance, preferred modeling episodes should exhibit a variety of local and regional meteorological conditions conducive to the formation of high ozone, contain days in which observed concentrations are close to the baseline design value, be supported by extensive air quality and meteorological data bases, and include a sufficient number of high ozone days. Other factors that increase the suitability of modeling a particular high ozone event over another episode include prior modeling of the event by other regions, concurrence with a time period included in the calculation of the current baseline design value, and the inclusion of several weekend high ozone days.

7.1 June 2006 Photochemical Modeling Episode

A photochemical modeling episode is being updated for the May 24th to July 2nd, 2006 high ozone event. TCEQ, Austin, San Antonio, and other potential non-attainment areas are modeling this high ozone event in support of SIP development. The June 2006 episode occurred during the TexAQS II study in Texas and is therefore supported by a wealth of data and technical analysis. Furthermore, the episode falls within the 2006-2010 modeling design value period. During the June 2006 episode, meteorology was typical of conditions on high ozone days, which is ideal for modeling purposes (Table 7-1). Temperatures ranged from 30.3^{o} C on June 2nd to a peak of 36.7^{o} C on June 13th. The ozone event was characterized by high solar radiation on all high ozone days besides June 2nd and low afternoon relative humidity from 20% to 38%.

Back trajectories at 100 meters were primarily from the southeast (38.8%) and south (22.7%) during the episode on high ozone days greater than 60 ppb (Figure 7-1). There were also some winds from the east (15.8%) and northeast (13.7%) on several episode days. The June 26th, 2006 high ozone day had unusually high wind speed (9.5 mph) and the back trajectory indicated the winds traveled a significant distance before arriving at C58. There were 3.3 cm of precipitation on the June 18th high ozone day. Although it is uncommon to experience precipitation on a high ozone day, the rainfall occurred between 2 a.m. and 5 a.m. in the morning, before sunrise.

Table 7-1: June 2006 Episode Meteorological Conditions Compared to Typical Meteorological Conditions in the San Antonio Region on Days > 65 ppb.

Episode	Date	Peak 1-hour ppb Ozone at regulatory monitors	Peak 8-hour ppb Ozone at regulatory monitors	Diurnal Temperature Change C58 > 12.7°C[1]	Relative Humidity at C5004 2p.m. < 38.3%[2]	Max. Solar Radiation at C58 > 1.16 langleys /min.[1]	Morning Wind Direction at C58 (6-9 am)	Afternoon Wind Speed at C58 < 2.75 (m/s)[2]	Precipitation (cm) at C678	Back Trajectory Distance < 1065 (km)[2]	Back Trajectory Direction
June 2006	2	78	66	**10.7**	35.5%	**0.94**	NW	2.73	0	579	NE
	3	86	80	14.2	27.5%	**1.15**	NW	1.21	0	418	E
	4	81	73	14.4	30.9%	1.28	**SW**	1.68	0	576	SE
	6	76	66	**12.3**	26.9%	1.27	**S**	2.15	0	983	SE
	7	87	76	13.3	31.8%	1.31	**SW**	1.70	0	1,065	SE
	8	96	84	14.5	29.6%	1.29	**SW**	1.93	0	1,062	SE
	9	86	77	16.2	29.6%	1.37	NW	2.68	0	953	SE
	10	74	69	16.6	24.8%	1.36	**SW**	2.56	0	737	SE
	12	78	70	**12.4**	30.0%	1.30	**S**	2.13	0	893	SE
	13	106	93	20.1	20.2%	1.30	NW	2.09	0	781	SE
	14	94	90	14.8	29.4%	1.31	NE	2.71	0	484	SE
	15	71	67	**10.7**	32.1%	1.26	**SE**	**4.30**	0	758	SE
	18	79	71	12.7	**38.8%**	1.35	E	1.11	**3.3**	**2,372**	SE
	26	86	78	12.9	26.1%	1.32	N	**4.57**	0	**1,650**	N
	27	98	82	15.4	23.1%	1.24	N	0.78	0	**1,225**	N
	28	101	87	18.0	22.3%	1.34	NW	2.42	0	950	NE
	29	94	91	13.7	27.8%	1.17	W	1.95	0	497	E
	30	87	71	**11.4**	30.3%	1.28	**SE**	1.60	0	837	E

[1]Based on the 20 percentile for all Ozone Days > 65 ppb from 2005-2014
[2]Based on the 80 percentile for all Ozone Days > 65 ppb from 2005-2014

Figure 7-1: May 29th to July 2nd, 2006 Photochemical Modeling Episode Days > 65 ppb
100 meter, 48-hour back trajectories ending at CAMS58

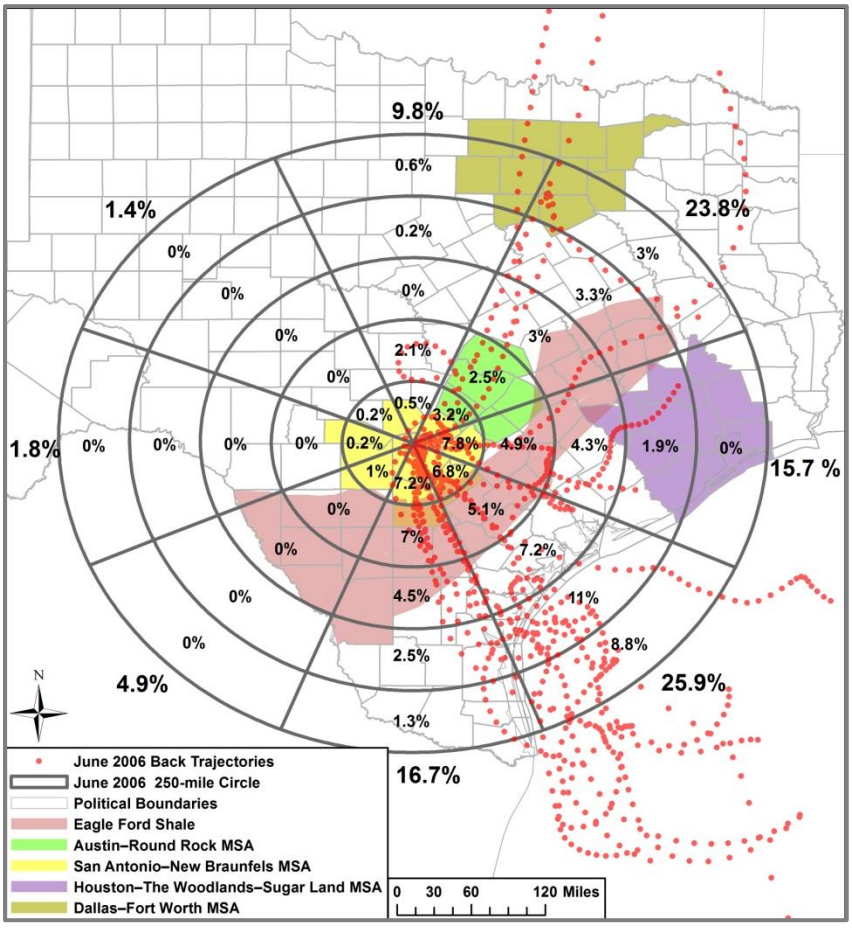

7.2 High Ozone Events in the San Antonio Area

Analysis of high ozone events from recent years can be used to isolate possible modeling episodes. TCEQ archived air quality data indicates that the number of high ozone days > 75 pbb, > 70 ppb, > 65 ppb, and > 60 ppb varies from year to year. After compiling a list of high ozone days occurring in 2010 to 2014, possible ozone episodes were identified for photochemical modeling.

When developing a list of candidate episodes for modeling, only the most recent four years (2010-2014) of high ozone events were considered because earlier years are neither feasible nor cost effective for emission inventory and photochemical modeling development. Also, preference is placed on recent high ozone events, since TCEQ and AACOG has developed the June 2006 episode. Earlier high ozone events would not reflect current emissions and air quality measurements needed for testing control strategies. A list of six high ozone events was defined:

- August 23 - 29, 2010
- September 28 - October 17, 2010
- August 27 – September 24, 2011
- June 6 – 28, 2012 (Potential TCEQ episode)
- August 20 – September 21, 2012
- August 15 – 31, 2013

All high ozone events listed above represent episodic cycles of ozone formation in the San Antonio region. According to the EPA, “preference should be given to modeling” ozone cycles rather than individual high ozone days.[78] TCEQ has started work on a June 2012 episode that may be beneficial to the San Antonio-New Braunfels MSA. Table 7-2 shows the days above 65 ppb, day of the week, peak 1-hour ozone, peak 8-hour ozone, and potential candidate episodes from 2010-2104.

[78] U.S. Environmental Protection Agency Office of Air Quality Planning and Standards Air Quality Analysis Division Air Quality Modeling Group, April 2007. “Guidance on the Use of Models and Other Analyses for Demonstrating Attainment of Air Quality Goals for Ozone, PM2.5, and Regional Haze”. Research Triangle Park, North Carolina. EPA -454/B-07-002. p. 142. Available online: http://www.epa.gov/scram001/guidance/guide/final-03-pm-rh-guidance.pdf. Accessed 04/13/15.

Table 7-2: 2010-2014 Days > 70 ppb and Possible Modeling Episodes

Date	Day of Week	Peak 1 Hour	Peak 8 Hour	Notes
05/28/10	Friday	96	86	
05/29/10	Saturday	74	71	
08/25/10	Wednesday	77	72	Candidate Episode
08/26/10	Thursday	79	72	
08/27/10	Friday	85	80	
08/28/10	Saturday	98	87	
09/30/10	Thursday	85	73	Candidate Episode
10/06/10	Wednesday	84	75	
10/07/10	Thursday	85	75	
10/08/10	Friday	80	72	
10/16/10	Saturday	91	78	
04/13/11	Wednesday	79	72	
05/16/11	Monday	88	78	
05/17/11	Tuesday	75	72	
05/26/11	Thursday	83	75	
06/06/11	Monday	90	79	
08/27/11	Saturday	82	76	Candidate Episode
08/28/11	Sunday	87	77	
08/29/11	Monday	83	76	
09/06/11	Tuesday	77	71	
09/07/11	Wednesday	96	87	
09/08/11	Thursday	83	72	
09/09/11	Friday	77	71	
09/10/11	Saturday	90	84	
09/11/11	Sunday	80	78	
09/12/11	Monday	78	72	
09/20/11	Tuesday	83	71	
09/22/11	Thursday	84	71	
10/02/11	Sunday	86	78	
10/03/11	Monday	87	79	
10/15/11	Saturday	81	74	
04/18/12	Wednesday	76	71	
04/22/12	Sunday	79	74	
05/17/12	Thursday	84	76	
06/09/12	Saturday	83	75	Candidate Episode (TCEQ Episode)
06/22/12	Friday	77	72	
06/23/12	Saturday	85	74	
06/26/12	Tuesday	100	89	
06/27/12	Wednesday	96	90	

Date	Day of Week	Peak 1 Hour	Peak 8 Hour	Notes
08/20/12	Monday	86	77	Candidate Episode (Potential TCEQ Ozone Season Episode)
08/21/12	Tuesday	93	87	
08/22/12	Wednesday	83	76	
08/23/12	Thursday	81	71	
09/10/12	Monday	108	90	
09/11/12	Tuesday	78	72	
09/19/12	Wednesday	94	81	
09/21/12	Friday	94	75	
04/12/13	Friday	77	71	
05/13/13	Monday	86	77	
06/03/13	Monday	90	79	
06/04/13	Tuesday	92	87	
07/03/13	Wednesday	80	71	
07/04/13	Thursday	87	83	
07/05/13	Friday	93	84	
08/17/13	Saturday	79	74	Candidate Episode
08/18/13	Sunday	86	79	
08/19/13	Monday	76	74	
08/29/13	Thursday	87	78	
08/30/13	Friday	93	80	
08/31/13	Saturday	86	74	
09/23/13	Monday	104	85	
09/24/13	Tuesday	82	74	
09/25/13	Wednesday	94	87	
05/10/14	Saturday	85	72	
05/30/14	Friday	91	81	
09/30/14	Tuesday	83	72	

7.2.1 Description of 2010-2014 High Ozone Events

August 23 - 29, 2010

High eight-hour average ozone values between 62 and 87 ppb were recorded from August 25th to 29th, 2010. During this period, moderate winds were recorded from the north/northwest in the early morning while shifting to the northeast and southeast during the afternoon. C58 recorded high temperatures between 30.4^{o} C and 34.0^{o} C with no precipitation. On most days wind speeds were between 1.9 and 3.1 mph, but wind speeds picked up on August 25th, reaching 4.1 mph. On August 24th a front went through the San Antonio area causing clear skies and stagnated air conditions that supported elevated ozone levels. During most of the episode, a constant high-pressure system existed over the mid and southwest U.S. including San Antonio with few frontal movements.

September 28 - October 17, 2010

A period of high ozone occurred during late September and early October 2010. Recorded peak 8-hour ozone averages were between 63 ppb and 78 ppb on several days during the high ozone event. During this time period, light winds were recorded from the northwest in the early morning. In the afternoon, several different wind directions were recorded on high ozone days: south, southeast, and north. On most high ozone days, back trajectories indicated stagnated air conditions in the San Antonio area. Recorded maximum and minimum peak temperatures were only moderate, between 24.2 and 30.2^{o} C, however recorded maximum solar radiation was high.

There was a high upper air pressure system and stagnant air over the south central U.S. from September 28th to October 1st, 2010. By October 2nd the high pressure system moved away from the region and peak ozone levels decreased. Another high-pressure system was over south Texas between October 5th and 8th,which also coincided with a period of elevated ozone. A front moved through Texas on October 13th resulting in a high pressure system arriving in San Antonio by October 15th and contributing to elevated eight-hour average ozone concentrations that peaked at 78 ppb on Oct 16th.

August 27 – September 24, 2011

This period experienced a number of high ozone events, with twelve days recording 8-hr ozone values over 70 ppb at EPA regulatory monitors and an additional five days recording values over 65 ppb. Additionally, the month of August was one of the driest and hottest in central Texas history. Upper-level high pressure dominated the south central U.S., causing stagnated air and higher ozone levels through the end of the month. The pressure gradient between the high and Tropical Storm Lee in the Gulf of Mexico produced very strong winds over the region which precluded ozone formation. Ozone levels dropped during this time, but rose in the wake of T.S. Lee as northerly winds ushered in ozone precursors from the Dallas area and high pressure reestablished itself over Texas. At the same time, wildfires in Bastrop County to the northeast were ignited and spread due to the high winds. With the high pressure in place, elevated ozone levels continued for a week as a surface high pressure system became planted over Texas. Ozone levels declined once again as the surface high pressure weakened with the slow passage of a front, bringing cloudy conditions which resulted in less solar radiation and smaller diurnal temperature difference. This setup also brought a shift of winds from northerly to southeasterly. A final period of elevated ozone occurred at the end of the period after the aforementioned front finally moved through and before the arrival of the next front.

June 6 – 28, 2012

Most of this period was dominated by a southeasterly fetch from the Gulf of Mexico caused by the location of high pressure over the southeastern U.S. This produced rainy conditions over much of the eastern part of the state, limiting the transport of ozone into the San Antonio region. On the 22nd, ozone levels increased in the area as the high pressure shifted west to be over Texas. At the same time, Tropical Storm Debbie entered the eastern Gulf of Mexico. As Debbie moved away from the southeastern U.S., high pressure returned to that region and reestablished a southeasterly flow from the Gulf of Mexico, and ozone levels decreased. The highest 8-hr average ozone for the year occurred on June 27th, 90 ppb, and reached 89 ppb the day before. These two days saw substantially higher temperatures and drier air than the rest of that week, suggesting that the high pressure was at its strongest during this time.

August 20 – September 21, 2012

High pressure established itself over Texas in the wake of a stationary front that caused widespread rainy conditions leading up to this period. With high pressure in place, ozone levels increased to 87 ppb on August 21st, but by the 24th, returned to below 50 ppb as the high pressure moved east and set up southeasterly flow from the Gulf of Mexico. On August 29th, Hurricane Isaac made landfall in central Louisiana, causing a reversal of flow from southeast to north and slightly elevated ozone conditions between 60 ppb and 65 ppb. In the wake of Isaac, high pressure returned to the southeast U.S. and southeasterly winds returned over the San Antonio region. The seasonal peak 8-hr ozone of 90 ppb occurred once again on September 10th. This coincided with a rise in pressure and a shift of morning winds from southeast to north. The arrival of a cool front brought ozone levels back down to below 50 ppb through September 18th. With the passing of the front, high pressure became reestablished over the southeastern U.S., humidity levels decreased and solar radiation increased in the San Antonio region.

August 15 – 31, 2013

The beginning of this period was characterized by the passage of a frontal system that became stationary over south Texas. This caused rainy conditions over the region until the 17th and inhibited ozone formation. As conditions cleared, an area of high pressure extended over Texas, bringing drier and calmer conditions and aiding in the production of ozone. A peak 8-hr ozone of 79 ppb was recorded on the 18th at CAMS 58, which also recorded northeasterly morning winds, followed by a shift out of the southeast, causing a recirculation of emissions over the monitor. As the air mass moderated, ozone levels dropped and the dominant wind pattern became more southeasterly. As a result, the coastal areas of Texas experienced increased rainfall, which limited ozone transport into San Antonio. Another frontal passage occurred on the 26th, although rainy conditions persisted until the 29th, when high pressure once again became established over Texas. Ozone concentrations increased and peaked at 80 ppb on the 30th. The same pattern of diurnal wind shifts at CAMS 58 that existed for the first high ozone event in this period also became established for the second high ozone period.

7.2.2 Minimum Number of Days per Candidate Episode

EPA recommends selecting modeling episodes that contain a minimum of 10 days with ozone concentrates ≥ 70 ppb in order to generate "robust" relative reduction factors, used in the attainment test. However, in regions where ozone levels do not often exceed these levels for long periods of time, a minimum of 5 days is acceptable. EPA does not recommend modeling episodes with less than 5 days of ozone levels ≥ 70 ppb.[79] Due to the expense and time required to model episodes, it is not practical to model all high ozone days for a given year using a SIP quality photochemical model.

According to this criterion, an episode that does not have at least 5 days with ozone concentrations ≥ 70 ppb is not preferred. As shown in Table 7-3, the 5 high ozone events with at least 5 days of ozone ≥ 70 ppb occurring between 2010 and 2014 are:

- Sept. 28 – Oct. 17, 2010
- Aug. 27 – Sept. 24, 2011
- June 6 – 28, 2012
- Aug. 20 – Sept. 21, 2012
- Aug. 15 – 31, 2013

There was only one high ozone event with more than 10 days ≥ 70 ppb: Aug. 27 – Sept. 24, 2011, (Table 7-3). Most of the episodes have at least 10 days ≥ 60 ppb with the exception of the Sept. 28 – Oct. 17, 2010, Aug. 20 – Sept. 21, 2012 and Aug. 15 – 31, 2013 high ozone events.

Table 7-3: High Ozone Events and Number of Days Above 75 ppb, 70 ppb, 65 ppb, and 60 ppb.

High Ozone Event	Number of Days > 75 ppb	Number of Days > 70 ppb	Number of Days > 65 ppb	Number of Days > 60 ppb
Aug. 23 – 29, 2010	2	4	4	5
Sept. 28 – Oct. 17, 2010	1	5	8	10
Aug. 27 – Sept. 24, 2011	6	12	14	18
June 6 – 28, 2012	2	5	8	9
Aug. 20 – Sept. 21, 2012	5	8	9	12
Aug. 15 – 31, 2013	3	6	6	10

[79] U.S. Environmental Protection Agency Office of Air Quality Planning and Standards Air Quality Analysis Division Air Quality Modeling Group, April 2007. "Guidance on the Use of Models and Other Analyses in Attainment Demonstrations for the 8-hour Ozone NAAQS", Research Triangle Park, North Carolina. EPA -454/R-05-002. p. 63. Available online: http://www.epa.gov/scram001/guidance/guide/8-hour-o3-guidance-final-version.pdf. Accessed 05/10/15.

Only one high ozone event episode, Aug. 27 – Sept. 24, 2011, represents a time period when 8-hour ozone averages exceeded 70 ppb at C23, C59, and C58 for at least five days. There were six high ozone events that had a minimum of 4 days > 65 ppb at C23 and C58: Aug. 27 – Sept. 24, 2011, June 6 – 28, 2012, Aug. 20 – Sept. 21, 2012, and Aug. 15 – 31, 2013. All high ozone events had at least 5 days > 60 ppb at both monitors besides the Aug. 23 – 29, 2010 high ozone event (**Error! Not a valid bookmark self-reference.**)

Table 7-4: Daily Peak 8-hour Ozone Concentrations at Each Monitor during High Ozone Events , 2010-2014

Candidate Episodes	Date	C58 Ozone	C59 Ozone	C23 Ozone	# w/Min. of 5 Days > 70 ppb	# w/Min. of 5 Days > 65 ppb	# w/Min. of 5 Days > 60 ppb	# w/Min. of 10 Days > 70 ppb	# w/Min. of 10 Days > 65 ppb	# w/Min. of 10 Days > 60 ppb
Aug. 23 – 29, 2010	8/25/2010	**65**	**72**	**62**	0	0	1 (C58)	0	0	0
	8/26/2010	**72**	**62**	**69**						
	8/27/2010	**80**	**69**	**80**						
	8/28/2010	**86**	**67**	**87**						
	8/29/2010	**62**	46	57						
Total at each Monitor	# Days > 70 ppb	3	1	2						
	# Days > 65 ppb	3	3	3						
	# Days > 60 ppb	5	4	4						
Sept. 28 – Oct. 16, 2010	9/28/2010	54	**67**	52	0	1 (C58)	3 (All Monitors)	0	0	0
	9/29/2010	54	**67**	55						
	9/30/2010	53	**73**	54						
	10/1/2010	57	**63**	53						
	10/5/2010	**65**	55	**62**						
	10/6/2010	**75**	59	**69**						
	10/7/2010	**75**	**62**	**69**						
	10/8/2010	**72**	**62**	**65**						
	10/15/2010	**66**	54	60						
	10/16/2010	**78**	60	**72**						
Total at each Monitor	# Days > 70 ppb	4	1	1						
	# Days > 65 ppb	5	3	3						
	# Days > 60 ppb	6	6	5						

Candidate Episodes	Date	C58 Ozone	C59 Ozone	C23 Ozone	# w/Min. of 5 Days > 70 ppb	# w/Min. of 5 Days > 65 ppb	# w/Min. of 5 Days > 60 ppb	# w/Min. of 10 Days > 70 ppb	# w/Min. of 10 Days > 65 ppb	# w/Min. of 10 Days > 60 ppb
Aug. 27 – Sept. 24, 2011	8/27/2011	**76**	**70**	**76**	3 (All Monitors)	3 (All Monitors)	3 (All Monitors)	0	2 (C59 and C23)	3 (All Monitors)
	8/28/2011	**73**	**71**	**77**						
	8/29/2011	**76**	58							
	8/30/2011	**65**	48	**64**						
	9/4/2011	**62**	**63**	**65**						
	9/6/2011	55	**71**	**61**						
	9/7/2011	**75**	**78**	**87**						
	9/8/2011	**64**	**72**	**67**						
	9/9/2011	**66**	**69**	**71**						
	9/10/2011	**72**	**75**	**84**						
	9/11/2011	**75**	**71**	**78**						
	9/12/2011	**71**	**65**	**72**						
	9/19/2011	56	**62**	58						
	9/20/2011	**64**	59	**71**						
	9/21/2011	**61**	55	**65**						
	9/22/2011	**61**	**71**	**66**						
	9/23/2011	59	**69**	**69**						
	9/24/2011	**64**	**63**	**68**						
Total at each Monitor	# Days > 70 ppb	7	7	8						
	# Days > 65 ppb	8	10	12						
	# Days > 60 ppb	15	14	16						
June 6 – 28, 2012	6/6/2012	**66**	37	56	1 (C58)	2(C58 and C23)	2(C58 and C23)	0	0	0
	6/9/2012	**75**	53	**68**						
	6/22/2012	**71**	56	**72**						
	6/23/2012	**74**	53	**73**						
	6/24/2012	**61**	47	**61**						
	6/25/2012	**66**	**62**	**67**						
	6/26/2012	**89**	**71**	**89**						
	6/27/2012	**90**	**71**	**85**						
	6/28/2012	**70**	52	**64**						
Total at each Monitor	# Days > 70 ppb	5	2	4						
	# Days > 65 ppb	8	2	6						
	# Days > 60 ppb	9	3	8						

Candidate Episodes	Date	C58 Ozone	C59 Ozone	C23 Ozone	# w/Min. of 5 Days > 70 ppb	# w/Min. of 5 Days > 65 ppb	# w/Min. of 5 Days > 60 ppb	# w/Min. of 10 Days > 70 ppb	# w/Min. of 10 Days > 65 ppb	# w/Min. of 10 Days > 60 ppb
Aug. 20 – Sept. 21, 2012	8/20/2012	**70**	**69**	**77**	2 (C58 and C23)	2 (C58 and C23)	3 (All Monitors)	0	0	2 (C58 and C23)
	8/21/2012	**87**	**75**	**81**						
	8/22/2012	**76**	**61**	**71**						
	8/23/2012	**71**	50	**62**						
	8/28/2012		**63**	54						
	8/29/2012	60	**61**	60						
	8/31/2012	**64**	55	**63**						
	9/10/2012	**90**	**70**	**84**						
	9/11/2012	**70**	**61**	**72**						
	9/19/2012	**76**	**62**	**81**						
	9/20/2012	**68**	59	**64**						
	9/21/2012	**75**	58	**71**						
Total at each Monitor	# Days > 70 ppb	6	1	7						
	# Days > 65 ppb	9	3	7						
	# Days > 60 ppb	10	8	10						
Aug. 15 – 31, 2013	8/15/2013	**62**	41	57	1 (C58)	2 (C58 and C23)	2 (C58 and C23)	0	0	1 (C58)
	8/16/2013	**63**	55	57						
	8/17/2013	**74**	**67**	**70**						
	8/18/2013	**79**	**69**	**77**						
	8/19/2013	**74**	59	**69**						
	8/20/2013	**62**	45	55						
	8/24/2013	**62**	52	57						
	8/29/2013	**78**	60	**71**						
	8/30/2013	**80**	57	**75**						
	8/31/2013	**74**	54	**67**						
Total at each Monitor	# Days > 70 ppb	6	0	3						
	# Days > 65 ppb	6	2	6						
	# Days > 60 ppb	10	2	6						

In order to ensure there are sufficient high ozone days for attainment tests, the number of modeling days needed at each monitor was determined. The 2012 and 2018 projected emission inventories were analyzed in the existing June 2006 photochemical modeling episode. By using the 7x7 4 km grid cells around each monitor, the day-to-day variability of relative response factors (RRF) at each site was calculated (Figure 7-2). Only sites (C23, C58, C622, and C678) where the baseline 8-hour ozone averages were greater than 60 ppb on 10 or more days were used in the analysis. The CAMx photochemical model is less responsive at lower levels of the ozone standard because the background concentrations do not respond to local controls.

Figure 7-2: Daily Relative Response Factors as a Function of Daily Maximum Base Modeled Concentrations for Monitors in the San Antonio MSA, 2012 to 2018

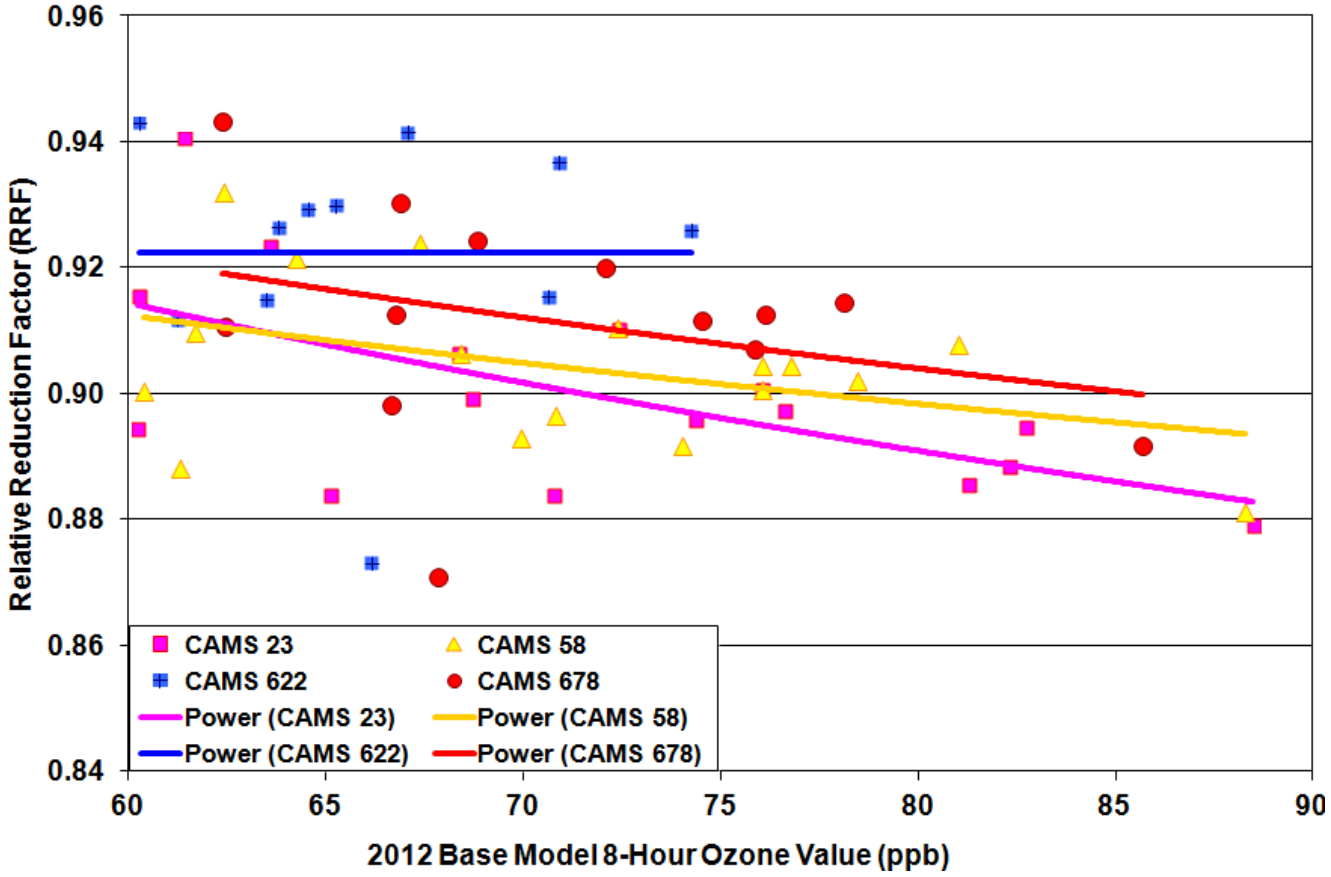

In order to choose a high ozone event with a sufficient number of days to calculate monitored attainment, the variability of the mean RRF as a function of the number of days was determined. According to the EPA, "using information on the variability of the model response on individual days, we are able to measure the variability of the mean RRF on any subset of days. The analysis used datasets of 25, 50, and 100 days. The standard deviation of the daily RRFs was used to create the datasets and measure the variability of the RRFs."[80] The mean RRF for a 50-day sample size was 0.893 at C23 and 0.900 at C58. The standard deviation of the daily RRFs was 0.0091 at C23 and 0.0085 at C58 for 70 ppb.

The number of days needed to provide the mean RRF calculation at both C23 and C58 is provided in Table 7-5. The number of days required for both a ± 1% and ± 2% accuracy at a 95% confidence interval for each proposed standard was calculated. Based on the 25-day sample, 3 to 8 days are needed to replicate the mean RRF to within ± 1% accuracy for a 95% confidence interval.

[80] *Ibid*., p. 144.

The following formula was used to calculate the number of days required to determine the mean RRF to within ± 1% and ± 2% at a 95% confidence interval:[81]

Formula (1)

$$n = \frac{N(\sigma^2)}{N(TSEM/2)^2 + \sigma^2}$$

Where:

n = Number of days (subset of mean RRF population)
N = Mean RRF population (e.g. 25, 50 or 100 days)
σ = Standard deviation of the daily RRFs
TSEM = Twice the standard error of the mean RRF (e.g. ± 1% or ± 2%)

Table 7-5: Number of Days Needed to Replicate the 25/50/100 Day Dataset Mean RRF to within ± 1% and ± 2%, with a 95% Confidence Interval

8-hour Ozone Level	CAMS	Mean RRF (50 days)	Standard Deviation (50 days)	± 1%			± 2%		
				25 days	50 days	100 days	25 days	50 days	100 days
60 ppb	C23	0.900	1.57%	8	9	9	3	3	3
	C58	0.904	1.25%	6	6	6	2	2	2
65 ppb	C23	0.894	0.93%	4	4	4	1	1	1
	C58	0.902	1.03%	4	4	5	2	2	2
70 ppb	C23	0.893	0.91%	3	4	4	1	1	1
	C58	0.900	0.84%	3	3	3	1	1	1

Table 7-6 lists the number of days when 8-hour average ozone concentrations exceeded 60 ppb, 65 ppb, and 70 ppb at CAMS 23 and CAMS 58 during each of the ozone events under analysis, and indicates whether those numbers meet the minimum days required to accurately replicate – within 1% and 2% -- the mean RRF of a 25-day dataset. In Table 7-7, each high ozone event is then combined with the existing June 2 – 30, 2006 episode to determine if the number of days is within ± 1% and ± 2% accuracy. All potential modeling episodes combined with the June 2 – 30, 2006 episode have enough high ozone days at both monitors to meet the ± 1% accuracy test for all ozone standards within the proposed range.

[81] Brian Timin, EPA. "Draft Final Ozone Guidance Comments and Proposed Changes". Presented at the 3rd PM/RH/O3 Modeling Workshop, New Orleans, LA. Available online: http://www.cleanairinfo.com/modelingworkshop/presentations/O3_Guidance_Timin.pdf. Accessed 05/03/15

Table 7-6: Minimum Numbers of Days for Each High Ozone Event, 2010-2014

Candidate Episode	CAMS	> 70 ppb			> 65 ppb			> 60 ppb		
		# of Days	Meet ± 1%	Meet ± 2%	# of Days	Meet ± 1%	Meet ± 2%	# of Days	Meet ± 1%	Meet ± 2%
Aug. 23 – 29, 2010	C23	2	**No**	Yes	3	**No**	Yes	4	**No**	Yes
	C58	3	Yes	Yes	3	**No**	Yes	5	**No**	Yes
Sept. 28 – Oct. 17, 2010	C23	1	**No**	Yes	3	**No**	Yes	5	**No**	Yes
	C58	4	Yes	Yes	5	Yes	Yes	6	Yes	Yes
Aug. 27 – Sept. 24, 2011	C23	8	Yes	Yes	12	Yes	Yes	16	Yes	Yes
	C58	7	Yes	Yes	8	Yes	Yes	15	Yes	Yes
June 6 – 28, 2012	C23	4	Yes	Yes	6	Yes	Yes	8	**No**	Yes
	C58	5	Yes	Yes	8	Yes	Yes	9	Yes	Yes
Aug. 20 – Sept. 21, 2012	C23	7	Yes	Yes	7	Yes	Yes	10	Yes	Yes
	C58	6	Yes	Yes	9	Yes	Yes	10	Yes	Yes
Aug. 15 – 31, 2013	C23	3	**No**	Yes	6	Yes	Yes	6	**No**	Yes
	C58	6	Yes	Yes	6	Yes	Yes	10	Yes	Yes

Table 7-7: Minimum Numbers of Days for Each High Ozone Event plus the June 2006 Episode, 2010-2014

Candidate Episode	CAMS	> 70 ppb			> 65 ppb			> 60 ppb		
		# of Days	Meet ± 1%	Meet ± 2%	# of Days	Meet ± 1%	Meet ± 2%	# of Days	Meet ± 1%	Meet ± 2%
Aug. 23 – 29, 2010 + June 2 – 30, 2006	C23	10	Yes	Yes	15	Yes	Yes	20	Yes	Yes
	C58	7	Yes	Yes	8	Yes	Yes	15	Yes	Yes
Sept. 28 – Oct. 17, 2010 + June 2 – 30, 2006	C23	9	Yes	Yes	15	Yes	Yes	21	Yes	Yes
	C58	8	Yes	Yes	10	Yes	Yes	16	Yes	Yes
Aug. 27 – Sept. 24, 2011 + June 2 – 30, 2006	C23	16	Yes	Yes	24	Yes	Yes	32	Yes	Yes
	C58	11	Yes	Yes	13	Yes	Yes	25	Yes	Yes
June 6 – 28, 2012 + June 2 – 30, 2006	C23	12	Yes	Yes	18	Yes	Yes	24	Yes	Yes
	C58	9	Yes	Yes	13	Yes	Yes	19	Yes	Yes
Aug. 20 – Sept. 21, 2012 + June 2 – 30, 2006	C23	15	Yes	Yes	19	Yes	Yes	26	Yes	Yes
	C58	10	Yes	Yes	14	Yes	Yes	20	Yes	Yes
Aug. 15 – 31, 2013 + June 2 – 30, 2006	C23	11	Yes	Yes	18	Yes	Yes	22	Yes	Yes
	C58	10	Yes	Yes	11	Yes	Yes	20	Yes	Yes

Without including the June 2006 photochemical modeling episode, the Aug. 23 – 29, 2010, Sept. 28 – Oct. 17, 2010 and Aug. 15 – 31, 2013 events did not have enough high ozone days to meet the RRF test with ± 1% accuracy at C23 for the 70 ppb and 60 ppb threshold. Therefore, these episodes are not considered suitable modeling episodes. Below is a list of high ozone events and their ranking in accordance with EPA's modeling guidance on the minimum number of days per high ozone event, as calculated for a 70 ppb threshold[82].

- Aug. 27 – Sept. 24, 2011
- Aug. 20 – Sept. 21, 2012
- June 6 – 28, 2012
- Aug. 15 – 31, 2013 - not preferred
- Aug. 23 – 29, 2010 - not preferred
- Sept. 28 – Oct. 17, 2010 - not preferred

The episodes that are not preferred will be left in the list of high ozone events, so they can be analyzed against other EPA criteria.

7.3 Air Quality Characteristics of High Ozone Events

The initial candidate episode selection, as stated, is based on the number of high ozone days and if the high ozone event occurred in 2010 or later. The list was further reduced by the first desirability factor: episodes that meet EPA guidance on the minimum number of high ozone days. The analysis of these events will focus on the local and regional criteria listed in chapters 2, 3, and 5. From this analysis, candidates can become more or less desirable as a possible choice for future modeling. Rankings based on this desirability are presented in Chapter 8.

The ozone characteristics analyzed for modeling desirability include:

- Local ozone seasonal peaks
- Day of the week correlation
- One-hour and 8-hour peak correlation
- Site specific design value v. high ozone concentrations comparison (± 10 ppb of design value at each CAMS)

Local Ozone Seasonal Peaks

The San Antonio region typically experiences two *seasonal peaks* during the ozone season: May - June and August – October. All of the high ozone events in the San Antonio region from 2010 to 2014 were within the two ozone seasonal peaks.

[82] U.S. Environmental Protection Agency Office of Air Quality Planning and Standards Air Quality Analysis Division Air Quality Modeling Group, April 2007. "Guidance on the Use of Models and Other Analyses in Attainment Demonstrations for the 8-hour Ozone NAAQS", Research Triangle Park, North Carolina. EPA - 454/R-05-002. p. 63. Available online: http://www.epa.gov/scram001/guidance/guide/8-hour-o3-guidance-final-version.pdf. Accessed 05/10/15.

Day of the week correlation

Since it is common for high ozone concentrations to occur on weekend days in the San Antonio region, a Saturday or Sunday high ozone day should be included in a modeling episode. The June high ozone event on which the 2006 modeled episode was based included four weekend days when 8-hour ozone concentrations exceeded 65 ppb. This episode already provides sufficient days on weekends to meet the requirement of having a weekend day.

The September 2012 high ozone event did not have any days > 65 ppb on the weekend, while the June 2012 and August 2010 high ozone event only had one day > 65 ppb on the weekend. The other 3 high ozone events had a sufficient number of high ozone days on the weekends: October 2010 had 2 days, August 2013 had 3 days, and September 2011 had 5 days > 65 ppb on the weekend.

One-hour to Eight-hour Correlation

There is a strong correlation between peak one-hour and eight-hour ozone on high ozone days in the San Antonio area. The average difference between one-hour and eight-hour ozone on high ozone days when eight-hour averages exceeded 65 ppb is 8.81 ppb with a standard deviation of 4.10 ppb at regulatory monitors (Table 7-8). Anomalies, such as elevated one-hour high values, are not typical on high ozone days in San Antonio and these events should be avoided in a modeling episode.

Table 7-8: Comparison between 1-hour and 8-hour Ozone on Days > 65 ppb, 2005-2014

Number of High Ozone Days	Average Peak 1 hour Ozone	Average Peak 8 hour Ozone	Difference	Standard Deviation
259	82.19	73.37	8.81	4.10

Table 7-9 lists the observed and predicted one-hour ozone for high ozone events from 2010 to 2014. The predicted one-hour values are based on the recorded eight-hour values for the day. The September 2012 high ozone event had two days that were not within two standard deviation: September 10th, 2012 and September 21st, 2012. Likewise, the June 2012 had one day, June 25th, 2012, that was not within two standard deviations. The days that were not within two standard deviation had spikes in peak one hour ozone between 18 to 25 ppb higher than the 8 –hour average. The other four high ozone events had every day within two standard deviation.

Table 7-9: Observed and Predicted Correlation with Trend Line for 2010 - 2014 High Ozone Events, Days > 65 ppb

High Ozone Event	Day	Observed Peak 8-hour Ozone, ppb	Observed Peak 1-hour Ozone, ppb	Predicted Peak 1-Hour Ozone, ppb	Observed 1 Hour minus Predicted 1 Hour, ppb	Within 1 Standard Deviation	Within 2 Standard Deviation
Aug. 23 – 29, 2010	8/25/2010	72	77	81	4	Yes	Yes
	8/26/2010	72	79	81	2	Yes	Yes
	8/27/2010	80	85	89	4	Yes	Yes
	8/28/2010	87	98	96	-2	Yes	Yes
Sept. 28 – Oct. 16, 2010	9/28/2010	67	83	76	-7	**No**	Yes
	9/29/2010	67	83	76	-7	**No**	Yes
	9/30/2010	73	85	82	-3	Yes	Yes
	10/6/2010	75	84	84	0	Yes	Yes
	10/7/2010	75	85	84	-1	Yes	Yes
	10/8/2010	72	80	81	1	Yes	Yes
	10/15/2010	66	81	75	-6	**No**	Yes
	10/16/2010	78	91	87	-4	**No**	Yes
Aug. 27 – Sept. 24, 2011	8/27/2011	76	82	85	3	Yes	Yes
	8/28/2011	77	87	86	-1	Yes	Yes
	8/29/2011	76	83	85	2	Yes	Yes
	9/6/2011	71	77	80	3	Yes	Yes
	9/7/2011	87	96	96	0	Yes	Yes
	9/8/2011	72	83	81	-2	Yes	Yes
	9/9/2011	71	77	80	3	Yes	Yes
	9/10/2011	84	90	93	3	Yes	Yes
	9/11/2011	78	80	87	7	**No**	Yes
	9/12/2011	72	78	81	3	Yes	Yes
	9/20/2011	71	83	80	-3	Yes	Yes
	9/22/2011	71	84	80	-4	**No**	Yes
	9/23/2011	69	78	78	0	Yes	Yes
	9/24/2011	68	70	77	7	**No**	Yes
June 6 – 28, 2012	6/6/2012	66	78	75	-3	Yes	Yes
	9/6/2012	75	83	84	1	Yes	Yes
	6/22/2012	72	77	81	4	Yes	Yes
	6/23/2012	74	85	83	-2	Yes	Yes
	6/25/2012	67	92	76	-16	**No**	**No**
	6/26/2012	89	100	98	-2	Yes	Yes
	6/27/2012	90	96	99	3	Yes	Yes
	6/28/2012	70	74	79	5	**No**	Yes
Aug. 20 – Sept. 21, 2012	8/20/2012	77	86	86	0	Yes	Yes
	8/21/2012	87	93	96	3	Yes	Yes
	8/22/2012	76	83	85	2	Yes	Yes
	8/23/2012	71	81	80	-1	Yes	Yes
	9/10/2012	90	108	99	-9	**No**	**No**
	9/11/2012	72	78	81	3	Yes	Yes
	9/19/2012	81	94	90	-4	**No**	Yes
	9/20/2012	68	82	77	-5	**No**	Yes
	9/21/2012	75	94	84	-10	**No**	**No**

High Ozone Event	Day	Observed Peak 8-hour Ozone, ppb	Observed Peak 1-hour Ozone, ppb	Predicted Peak 1-Hour Ozone, ppb	Observed 1 Hour minus Predicted 1 Hour, ppb	Within 1 Standard Deviation	Within 2 Standard Deviation
Aug. 15 – 31, 2013	8/17/2013	74	79	83	4	Yes	Yes
	8/18/2013	79	86	88	2	Yes	Yes
	8/19/2013	74	76	83	7	**No**	Yes
	8/29/2013	78	87	87	0	Yes	Yes
	8/30/2013	80	93	89	-4	**No**	Yes
	8/31/2013	74	86	83	-3	Yes	Yes

Site Specific Design Value v. High Ozone Concentrations Comparison

According to the EPA selection criteria, episodes with high ozone values close to site-specific design values (ozone concentrations within ±10 ppb of design values for each CAMS) are more desirable for modeling. For this measure, a weighted modeling design value covering a five-year period that straddles the high ozone event, is calculated for each regulatory-sited CAMS monitor. A weighted modeling design value was used in the calculations because it "takes into account the emissions and meteorological variability that occurs over the full five year period".[83] Also, the weighted modeling design value "is thought to be more representative of the baseline emissions and meteorology period".[84] There are three regulatory monitors with a current modeling design value greater than 65 ppb: C23, C58, and C59 (Table 7-10).

Table 7-10: Weighted Modeling Design Values, San Antonio CAMS, 2010-2014

CAMS Station	Weighted Modeling Design Value	**± 10 ppb of design value**
C23	77	**67 – 87**
C58	80	**70 - 90**
C59	68	**58 - 78**

In Table 7-11, observed ozone concentrations are compared to the ± 10 ppb range of the weighted modeling design value. The right-hand column lists the percentage of those days > 65 ppb that were within ± 10 ppb of design value. Using this percentage, the desirability of the episodes can be estimated for this criterion. "Ambient (and modeled) concentrations that are more than 10 ppb above the design value are preferable to episodes with ambient concentrations that are more than 10 ppb below the design value."[85]

Most of the days for the August 2013, September 2012, and September 2010 days are within 10 ppb of the weighted modeling design value at all regulatory monitors on days > 65 ppb. The September 2011 also had between 78 percent of the days within 10 ppb of the design value. The correlation was weaker for the October 2010, 58%, and June 2012, 50%, candidate episodes.

[83] U.S. Environmental Protection Agency Office of Air Quality Planning and Standards Air Quality Analysis Division Air Quality Modeling Group, October 2005. "Guidance on the Use of Models and Other Analyses for Demonstrating Attainment of Air Quality Goals for Ozone, PM2.5, and Regional Haze", Research Triangle Park, North Carolina. EPA -454/R-05-002. p. 14. Available online: http://www.epa.gov/scram001/guidance/guide/8-hour-o3-guidance-final-version.pdf. Accessed 05/10/15.
[84] *Ibid*., p. 14.
[85] *Ibid*., p. 60.

Table 7-11: High Ozone Event Peak 8-Hour Ozone on Days > 65 ppb Compared to the Site-Specific Weighted Modeling Design Values and the % of Daily Ozone Readings within ±10 ppb, 2010-2014.

Candidate Episode	Day	C23	C58	C59	% within 10 ppb of the proposed 65 ppb Standard
Aug. 23– 29, 2010	8/25/2010	62	65	72	83%
	8/26/2010	69	72	62	
	8/27/2010	80	80	69	
	8/28/2010	87	86	67	
Sept. 28 – Oct. 16, 2010	9/28/2010	52	54	67	58%
	9/29/2010	55	54	67	
	9/30/2010	54	53	73	
	10/6/2010	69	75	59	
	10/7/2010	69	75	62	
	10/8/2010	65	72	62	
	10/15/2010	60	66	54	
	10/16/2010	72	78	60	
Aug. 27 – Sept. 24, 2011	8/27/2011	76	76	70	78%
	8/28/2011	77	73	71	
	8/29/2011		76	58	
	9/6/2011	61	55	71	
	9/7/2011	87	75	78	
	9/8/2011	67	64	72	
	9/9/2011	71	66	69	
	9/10/2011	84	72	75	
	9/11/2011	78	75	71	
	9/12/2011	72	71	65	
	9/20/2011	71	64	59	
	9/22/2011	66	61	71	
	9/23/2011	69	59	69	
	9/24/2011	68	64	63	
June 6 – 28, 2012	6/6/2012	56	66	37	50%
	9/6/2012	43	47	30	
	6/22/2012	72	71	56	
	6/23/2012	73	74	53	
	6/25/2012	67	66	62	
	6/26/2012	89	89	71	
	6/27/2012	85	90	71	
	6/28/2012	64	70	52	
Aug. 20 – Sept. 21, 2012	8/20/2012	77	70	69	85%
	8/21/2012	81	87	75	
	8/22/2012	71	76	61	
	8/23/2012	62	71	50	
	9/10/2012	84	90	70	
	9/11/2012	72	70	61	
	9/19/2012	81	76	62	
	9/20/2012	64	68	59	
	9/21/2012	71	75	58	

Candidate Episode	Day	C23	C58	C59	% within 10 ppb of the proposed 65 ppb Standard
Aug. 15 – 31, 2013	8/17/2013	70	74	67	89%
	8/18/2013	77	79	69	
	8/19/2013	69	74	59	
	8/29/2013	71	78	60	
	8/30/2013	75	80	57	
	8/31/2013	67	74	54	

7.4 Meteorological Conditions during High Ozone Events

Local Meteorology

Meteorological conditions for each ozone event were compared to meteorological conditions that occur on typical high ozone days. In chapter 3, ozone season days over several years were compared with various conditions to determine the variety of meteorological conditions associated with high ozone days. Table 7-12 lists diurnal temperature change, relative humidity, solar radiation, morning wind direction, afternoon wind speeds, precipitation, back trajectory distance and back trajectory direction for each high ozone event from 2010 to 2014.

Meteorological conditions during the Aug. 23 – 29, 2010 high ozone event were typical, based on historical data. However, humidity was a little higher (43%+) and solar radiation (1.0 langleys/min) was a little lower than typical on August 26th and 29th. Daily peak temperatures were lower than typical during the Sept. 28 – Oct. 16, 2010 high ozone event. Conversely, the high solar radiation, low humidity, and stagnated winds experienced during this timeframe were typical for high ozone days. Back trajectory distance was longer than expected on the September 28th and 30th, and October 15th high ozone days. The Aug. 27 – Sept. 24, 2011 high ozone event was characterized by much lower relative humidity than expected for the high ozone days in the period. Morning wind direction was out of the southwest on August 29th and September 12th, but either northwest or north on the other high ozone days. Back trajectories indicated transport conditions on September 6th, 9th, and 23rd. The June 6 – 28, 2012 episode had one high ozone day, June 9th, with higher than expected relative humidity and one high ozone day, the 28th, with southerly winds. All other high ozone days had typical meteorological conditions. For the Aug. 20 – Sept. 21, 2012 episode, there were a handful of high ozone days with atypical conditions. Relative humidity was higher than expected on August 22nd and 23rd, and September 20th, with the latter two days also reporting southerly morning wind directions. One day during this period, September 19th, recorded 0.06" of precipitation at CAMS 678. For the Aug.15 – 31, 2013 high ozone event, three high ozone days had atypical meteorological conditions. Afternoon wind speeds were stronger than expected on August 17th, solar radiation was less on the 19th, and morning wind direction was out of the southwest on the 31st.

Wind Direction

Statistical analyses of C23 and C58 afternoon wind direction plots are located in Table 7-13 and Table 7-14, respectively. The morning wind directions at C23 and C58 during the Aug. 20 – Sept. 21, 2012 high ozone event most closely matched historical data for typical wind directions during periods of elevated ozone. Afternoon wind direction at C23 for the June 6 – 28, 2012 high ozone event most closely matched historical data, and at C58, the Aug. 15 – 31, 2013 event was the better match. However, in both afternoon cases, the Aug. 20 – Sept. 21, 2012 event had an absolute difference that was within 2% of the best match for each CAMS.

Table 7-12: Comparison of 2010 - 2014 High Ozone Event Meteorological Conditions to Typical Meteorological Conditions in the San Antonio Region on High Ozone Days > 65 ppb.

Candidate Episode	Date	Peak 8-hour ppb Ozone at regulatory monitors	Diurnal Temperature Change C58 > 12.7°C[1]	Relative Humidity at C5004 2p.m. < 38.3%[2]	Max. Solar Radiation at C58 > 1.16 langleys /min.[1]	Morning Wind Direction at C58 (6-9 am)	Afternoon Wind Speed at C58 < 2.75 (m/s)[2]	Precipitation (inches) at C678 - None	Back Trajectory Distance < 1065 km[2]	Back Trajectory Direction
Aug. 23 – 29, 2010	8/25/2010	72	**8.6**	37.8%	1.18	N	**3.62**	0	**1,646**	N
	8/26/2010	72	**6.7**	**45.3%**	**0.98**	N	2.73	0	**1,530**	N
	8/27/2010	80	14.7	24.3%	1.19	N	**3.39**	0	822	NE
	8/28/2010	87	18.4	27.8%	1.35	NW	2.12	0	700	NE
Sept. 28 – Oct. 16, 2010	9/28/2010	67	20.6	30.4%	1.27	NW	0.88	0	**1,394**	N
	9/29/2010	67	17.8	32.1%	1.26	NW	1.69	0	314	N
	9/30/2010	73	15.5	36.5%	1.26	NW	**3.74**	0	**1,321**	N
	10/06/2010	75	18.5	23.3%	1.23	NW	1.38	0	566	E
	10/07/2010	75	20.4	22.7%	1.22	NW	1.01	0	315	E
	10/08/2010	72	20.7	26.5%	1.21	NW	1.74	0	217	SE
	10/15/2010	66	18.5*	19.8%	1.17	NW	1.31	0	**1,341**	N
	10/16/2010	78	14.6*	29.0%	1.16	NW	1.74	0	219	NE
Aug. 27 – Sept. 24, 2011	8/27/2011	76	16.2	19.8%	1.32	NW	1.85	0	484	SE
	8/28/2011	77	16.7	13.8%	1.24	NW	2.46	0	77	**S**
	8/29/2011	76	16.1	13.5%	1.30	**SW**	2.61	0	707	SE
	9/06/2011	71	19.4	13.2%	1.38	N	1.89	0	**2,163**	N
	9/07/2011	87	21.9	11.4%	1.35	NW	**2.79**	0	698	N
	9/08/2011	72	17.7	12.3%	1.33	NW	**2.93**	0	996	N
	9/09/2011	71	20.4	14.9%	1.33	NW	2.36	0	**1,336**	N
	9/10/2011	84	19.1	14.3%	1.23	NW	1.02	0	446	NE
	9/11/2011	78	20.2	17.9%	1.28	NW	2.34	0	407	N
	9/12/2011	72	19.6	18.3%	1.28	**SW**	2.37	0	885	SE
	9/20/2011	71	17.6	27.2%	1.24	NW	1.00	0	753	N
	9/22/2011	71	15.9	32.1%	1.21	NW	1.30	0	748	SE
	9/23/2011	69	**12.3**	32.1%	1.27	N	1.24	0	**1,627**	N
	9/24/2011	68	19.2	24.1%	1.21	NW	2.10	0	843	N

Candidate Episode	Date	Peak 8-hour ppb Ozone at regulatory monitors	Diurnal Temperature Change C58 > 12.7°C[1]	Relative Humidity at C5004 2p.m. < 38.3%[2]	Max. Solar Radiation at C58 > 1.16 langleys /min.[1]	Morning Wind Direction at C58 (6-9 am)	Afternoon Wind Speed at C58 < 2.75 (m/s)[2]	Precipitation (inches) at C678 - None	Back Trajectory Distance < 1065 km[2]	Back Trajectory Direction
June 6 – 28, 2012	6/06/2012	66	14.4	38.1%	1.41	NW	2.41	0	639	SE
	6/09/2012	75	16.2	**45.3%**	1.38	W	2.60	0	549	N
	6/22/2012	72	14.3	33.8%	1.33	NW	2.00	0	914	E
	6/23/2012	74	15.5	32.3%	1.42	NW	2.55	0	299	E
	6/25/2012	67	17.5	26.7%	1.41	NW	1.95	0	328	SE
	6/26/2012	89	18.7	26.5%	1.32	NW	2.00	0	457	SE
	6/27/2012	90	14.2	32.4%	1.33	NW	2.38	0	206	SE
	6/28/2012	70	12.9	32.6%	1.34	**S**	2.62	0	858	**S**
Aug. 20 – Sept. 21, 2012	8/20/2012	77	19.3	36.4%	1.39	NW	1.03	0	398	NE
	8/21/2012	87	13.2	35.6%	1.32	NE	2.29	0	620	N
	8/22/2012	76	**11.3**	**42.2%**	1.22	NE	2.72	0	745	NE
	8/23/2012	71	12.8	**42.5%**	1.36	**SW**	1.77	0	575	NE
	9/10/2012	90	20.8	16.4%	1.34	NW	1.26	0	591	N
	9/11/2012	72	19.2	26.8%	1.34	NW	2.61	0	330	NE
	9/19/2012	81	14.7	36.8%	1.29	NW	0.56	**0.06**	673	N
	9/20/2012	68	15.1	**44.6%**	1.29	**S**	1.47	0	322	NE
	9/21/2012	75	21.3	31.0%	1.31	NW	1.21	0	153	SE
Aug. 15 – 31, 2013	8/17/2013	74	15.1	28.8%	1.31	N	**3.93**	0	557	NE
	8/18/2013	79	15.6	27.6%	1.22	NW	1.41	0	727	NE
	8/19/2013	74	14.6	31.5%	**1.13**	NW	2.24	0	468	NE
	8/29/2013	78	16.4	33.0%	1.30	W	1.77	0	385	SE
	8/30/2013	80	14.8	29.4%	1.32	W	0.99	0	398	SE
	8/31/2013	74	14.6	33.9%	1.27	**SW**	1.84	0	679	SE

*Diurnal Temperature Changes at C23 (Data was not available at C58)
[1]Based on the 20 percentile for all Ozone Days > 65 ppb from 2005-2014
[2]Based on the 80 percentile for all Ozone Days > 65 ppb from 2005-2014

Table 7-13: Comparison of High Ozone Events Wind Direction to Typical Wind Direction on High Ozone Days > 65 ppb at C23, 2005-2014 (Absolute Percentage Difference)

Monitor	Episode	N	NE	E	SE	S	SW	W	NW	Absolute Difference
Morning Wind Direction (6 - 9 a.m.) at C23 on Days > 65 ppb	All Days (2005-2014) > 65ppb	31.8%	20.2%	10.4%	6.4%	5.2%	5.8%	8.7%	11.6%	-
	June 2 – 30, 2006	12.5%	25.0%	0.0%	12.5%	0.0%	12.5%	12.5%	25.0%	69.8%
	Aug. 23 - 29, 2010	33.3%	66.7%	0.0%	0.0%	0.0%	0.0%	0.0%	0.0%	96.0%
	Sept. 28 - Oct. 17, 2010	66.7%	0.0%	0.0%	0.0%	0.0%	0.0%	0.0%	33.3%	113.3%
	Aug. 27 - Sept. 24, 2011	58.3%	0.0%	0.0%	0.0%	0.0%	8.3%	25.0%	8.3%	90.8%
	June 6 - 28, 2012	16.7%	0.0%	0.0%	16.7%	16.7%	0.0%	16.7%	33.3%	103.1%
	Aug. 20 - Sept. 21, 2012	14.3%	42.9%	14.3%	0.0%	0.0%	0.0%	0.0%	28.6%	**87.0%**
	Aug. 15 - 31, 2013	0.0%	16.7%	33.3%	0.0%	0.0%	16.7%	33.3%	0.0%	117.0%
Afternoon Wind Direction (noon - 3p.m.) at C23 on Days > 65 ppb	All Days (2005-2014) > 65ppb	1.2%	6.9%	35.3%	37.0%	16.8%	2.3%	0.0%	0.6%	-
	June 2 – 30, 2006	0.0%	0.0%	75.0%	25.0%	0.0%	0.0%	0.0%	0.0%	79.5%
	Aug. 23 - 29, 2010	0.0%	33.3%	66.7%	0.0%	0.0%	0.0%	0.0%	0.0%	115.6%
	Sept. 28 - Oct. 17, 2010	0.0%	0.0%	33.3%	0.0%	66.7%	0.0%	0.0%	0.0%	99.8%
	Aug. 27 - Sept. 24, 2011	8.3%	0.0%	41.7%	0.0%	25.0%	16.7%	0.0%	8.3%	87.9%
	June 6 - 28, 2012	0.0%	16.7%	50.0%	33.3%	0.0%	0.0%	0.0%	0.0%	**48.9%**
	Aug. 20 - Sept. 21, 2012	14.3%	0.0%	28.6%	28.6%	14.3%	14.3%	0.0%	0.0%	50.2%
	Aug. 15 - 31, 2013	0.0%	16.7%	0.0%	83.3%	0.0%	0.0%	0.0%	0.0%	112.1%

Table 7-14: Comparison of High Ozone Events Wind Direction to Typical Wind Direction on High Ozone Days > 65 ppb at C58, 2005-2014 (Absolute Percentage Difference)

Monitor	Episode	N	NE	E	SE	S	SW	W	NW	Absolute Difference
Morning Wind Direction (6 - 9 a.m.) at C58 on Days > 65 ppb	All Days (2005-2014) > 65ppb	9.6%	3.8%	4.8%	6.7%	7.2%	7.7%	5.3%	55.0%	-
	June 2 – 30, 2006	11.8%	5.9%	5.9%	11.8%	11.8%	23.5%	5.9%	23.5%	117.9%
	Aug. 23 - 29, 2010	66.7%	0.0%	0.0%	0.0%	0.0%	0.0%	0.0%	33.3%	66.7%
	Sept. 28 - Oct. 17, 2010	0.0%	0.0%	0.0%	0.0%	0.0%	0.0%	0.0%	100.0%	90.0%
	Aug. 27 - Sept. 24, 2011	0.0%	0.0%	0.0%	0.0%	0.0%	25.0%	0.0%	75.0%	74.6%
	June 6 - 28, 2012	0.0%	0.0%	0.0%	0.0%	12.5%	0.0%	12.5%	75.0%	65.1%
	Aug. 20 - Sept. 21, 2012	0.0%	22.2%	0.0%	0.0%	11.1%	11.1%	0.0%	55.6%	**50.2%**
	Aug. 15 - 31, 2013	16.7%	0.0%	0.0%	0.0%	0.0%	16.7%	33.3%	33.3%	87.5%
Afternoon Wind (noon - 3p.m.) at C58 on Days > 65 ppb	All Days (2005-2014) > 65ppb	3.3%	6.7%	12.9%	52.2%	23.4%	1.0%	0.5%	0.0%	-
	June 2 – 30, 2006	0.0%	5.9%	23.5%	47.1%	23.5%	0.0%	0.0%	0.0%	21.4%
	Aug. 23 - 29, 2010	0.0%	66.7%	0.0%	33.3%	0.0%	0.0%	0.0%	0.0%	119.9%
	Sept. 28 - Oct. 17, 2010	0.0%	0.0%	0.0%	40.0%	60.0%	0.0%	0.0%	0.0%	73.1%
	Aug. 27 - Sept. 24, 2011	0.0%	25.0%	12.5%	25.0%	37.5%	0.0%	0.0%	0.0%	64.7%
	June 6 - 28, 2012	12.5%	0.0%	12.5%	75.0%	0.0%	0.0%	0.0%	0.0%	64.0%
	Aug. 20 - Sept. 21, 2012	0.0%	11.1%	11.1%	33.3%	44.4%	0.0%	0.0%	0.0%	50.8%
	Aug. 15 - 31, 2013	0.0%	16.7%	0.0%	66.7%	16.7%	0.0%	0.0%	0.0%	**49.0%**

7.4.1 Extreme Weather during High Ozone Events

Meteorology during extreme weather can be difficult to model and could make an ozone event less desirable for modeling. Hurricanes and other tropical depressions can impact the weather in the San Antonio region. These types of systems often come inland from the Gulf of Mexico. Historical weather reports[86] and NOAA daily weather maps[87] were checked every day during high ozone events. Table 7-15 lists extreme weather events associated with each candidate episode between 2010 and 2014. There was no extreme weather during the Aug. 25 – 29, 2010, Sept. 28 – Oct. 16, 2010, and Aug. 15 – 31, 2013 high ozone events.

Table 7-15: Extreme weather events during each potential modeling episode

Event	Rain (cm)	Events	Extreme Weather
June 2 – 30, 2006	3.86	1	T.S. Alberto (June 13-14)
Aug. 23 – 29, 2010	0.28	0	None
Sept. 28 – Oct. 17, 2010	0	0	None
Aug. 27 – Sept. 24, 2011	1.40	2	T.S. Lee (September 2-6, 2011) Bastrop County Complex Fire (September 4-October, 2011)
June 6 – 28, 2012	0.10	1	T.S. Debby (June 25-27, 2012)
Aug. 20 – Sept. 21, 2012	10.29	1	Hurricane Isaac (August 26-September 1)
Aug. 15 – 31, 2013	0.15	0	None

7.5 Background Ozone and Ozone Transport during High Ozone Events

The combined numbers of air parcels by back trajectory octant and distance from C58 are used to typify air parcel distribution on high ozone days. About 65% of 100-meter 48-hour back trajectories ending at C58 came from the northeast, east, and southeast on high ozone days greater than 65 ppb. Most of the other back trajectories were from the south (17%) and north (10%). Back trajectories from the west, northwest, and southwest were rare on high ozone days (8%). Figure 7-3 through Figure 7-8 indicate the percentage of air parcels within each direction for each high ozone event in 2010. The maps include non-attainment and potential non-attainment areas within a 400-km diameter centered around C58.

In Table 7-16 the directional ratios of the air parcel hourly points from the HYSPLIT model for the combination of all 2009 - 2014 high ozone days greater than 65 ppb are compared to the directional ratios for each individual high ozone event including the modeled June 2006 episode. To be a strong candidate for modeling, the episode's back trajectory patterns should exhibit a high correlation with typical air parcel movement on high ozone days in San Antonio. For each high ozone event, the absolute difference was calculated using the following formula:

Formula (2)

$$AD = \Sigma [\ |(TRAJ_{episodeA} - TRAJ_{2000\text{-}2010A})|\ ]$$

Where:

[86] National Weather Service Austin/San Antonio. "September 2011 Weather In Review". http://www.srh.noaa.gov/images/ewx/wxevent/sep2011.pdf. Accessed 04/13/15.

[87] NOAA National Centers for Environmental Prediction, Hydrometeorological Prediction Center. Daily Weather Maps. Available online: http://www.hpc.ncep.noaa.gov/dailywxmap/index.html. Accessed 04/13/15.

AD = Absolute Difference
$TRAJ_{episodeA}$ = Episode Back Trajectories Percentage for Direction A (North, NW, West, SW, South, SE, East, NE)
$TRAJ_{2000\text{-}2010A}$ = 2009-2014 Back Trajectories Percentage for Direction A

A lower absolute difference indicates a better fit with all back trajectories on days with peak ozone greater than 65 ppb.

During the June 2006 episode, a greater percentage of back trajectories originated from the southeast (39%) and south (23%) than is typical of high ozone days. Whereas the episode had fewer back trajectories from the east (16%) and northeast (14%) than typical for elevated ozone days. As noted in Chapter 3, back trajectories exhibit different patterns in the spring seasonal ozone peak and the fall seasonal ozone peak. By combining a spring season episode, the existing June 2006, and a fall season episode listed above, the models can replicate a variety of back trajectory directions on typical high ozone days. The June 2006 episode was combined with the other high ozone events between 2010 and 2014 to provide a variety of back trajectories to compare with typical back trajectories on high ozone days. The absolute total bias calculated for these episode combinations are below 30% with the exception of the June 2012 episode. All of the fall high ozone episodes between 2009 and 2014 improved the variety of back trajectories, with the Aug. 20 – Sept. 21, 2012 episode resulting in the biggest improvement with a total bias of 10%. Table 7-16 shows each episode pairing and the absolute differences between each pairing and the 2009-2014 average for high ozone days.

When combining trajectory data for the June 2012 and June 2006 episodes, there was poor correlation with typical back trajectory directions on high ozone days. Adding this episode with the existing June 2006 episode did not significantly increase the variety of back trajectory directions available for modeling on high ozone days. By adding this high ozone event, the absolute bias improved by less than one percent when compared to the June 2006 episode alone. This high ozone event would not be recommended for modeling based on the back trajectory analysis.

Hourly back trajectory distance was calculated for each high ozone event. For all high ozone days from 2009 to 2014, 88.6% of hourly counts were within 400 km of C58, while 8.8% of the counts were between 400 and 800 km of C58. Hourly back trajectory counts beyond 800 km on high ozone days were 2.6%. The hourly back trajectory distances during the September 2011 and June 2012 high ozone events provided the best match with back trajectories for all high ozone days > 65 ppb.

The high ozone event with the weakest relationship with typical back trajectory distance was the August 2010 high ozone period (Table 7-17). Back trajectories during this high ozone event traveled significantly farther in 48 hours compared to average high ozone days. The results indicate there was above-normal transport into the San Antonio region during this episode. The September 2012 and August 2013 high ozone events experienced much less ozone transport than would normally be expected. When pairing these two events with the June 2006 episode, the absolute bias was the smallest of all episode pairings.

Figure 7-3: August 25th to 29th, 2010 Candidate Photochemical Modeling Episode High Ozone Days > 65 ppb.

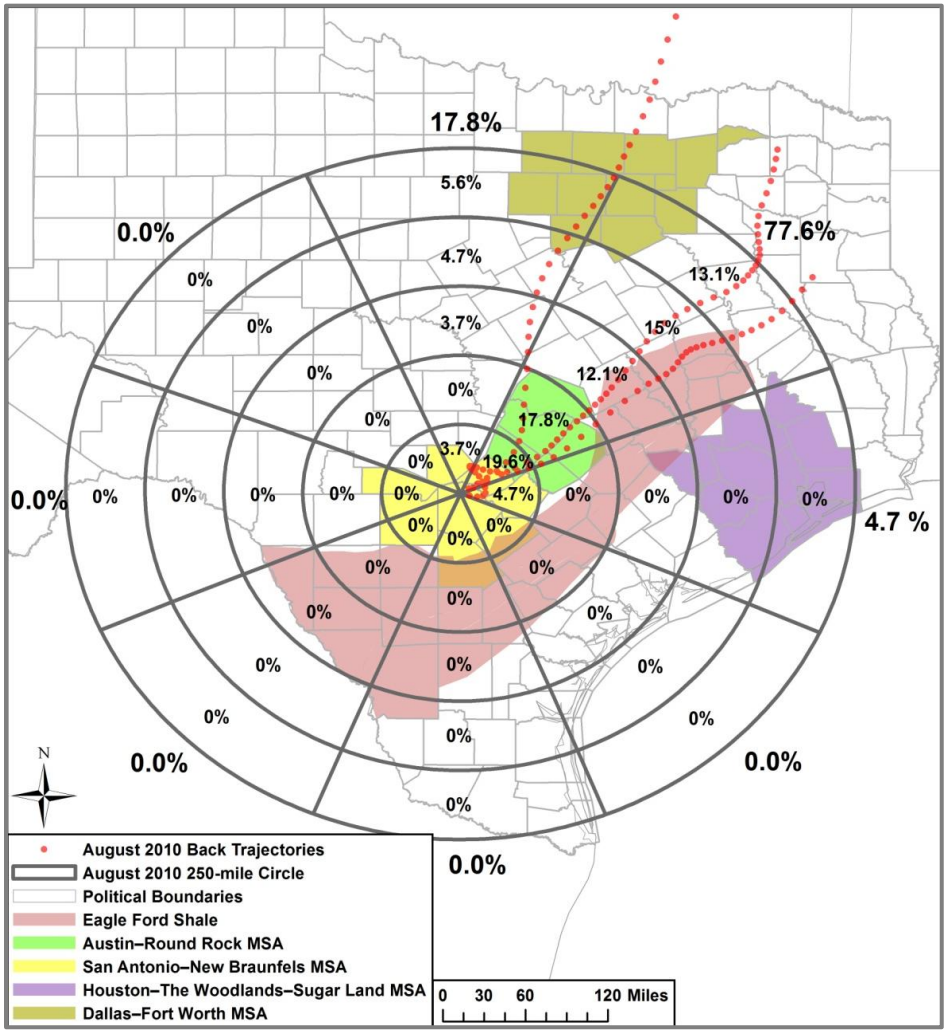

Figure 7-4: September 28th to October 16th, 2010 Candidate Photochemical Modeling Episode High Ozone Days > 65 ppb

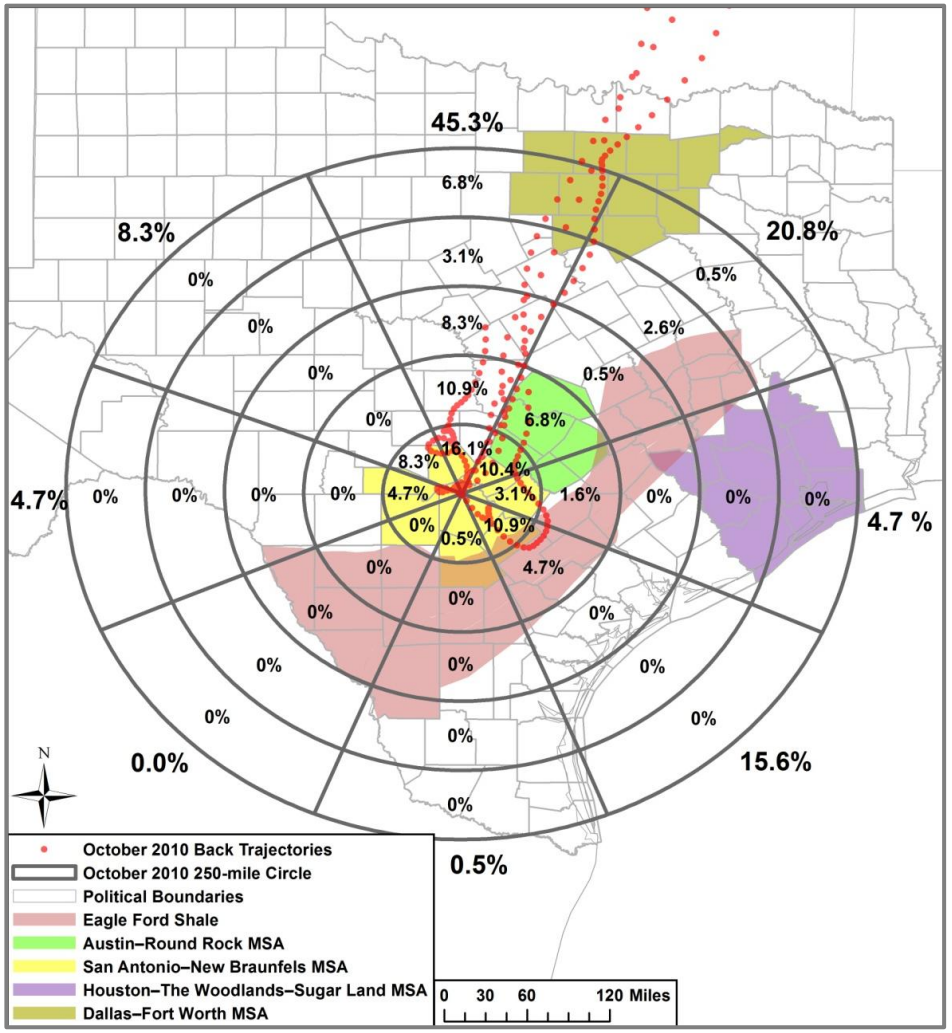

Figure 7-5: August 27 - September 24, 2011Candidate Photochemical Modeling Episode High Ozone Days > 65 ppb.

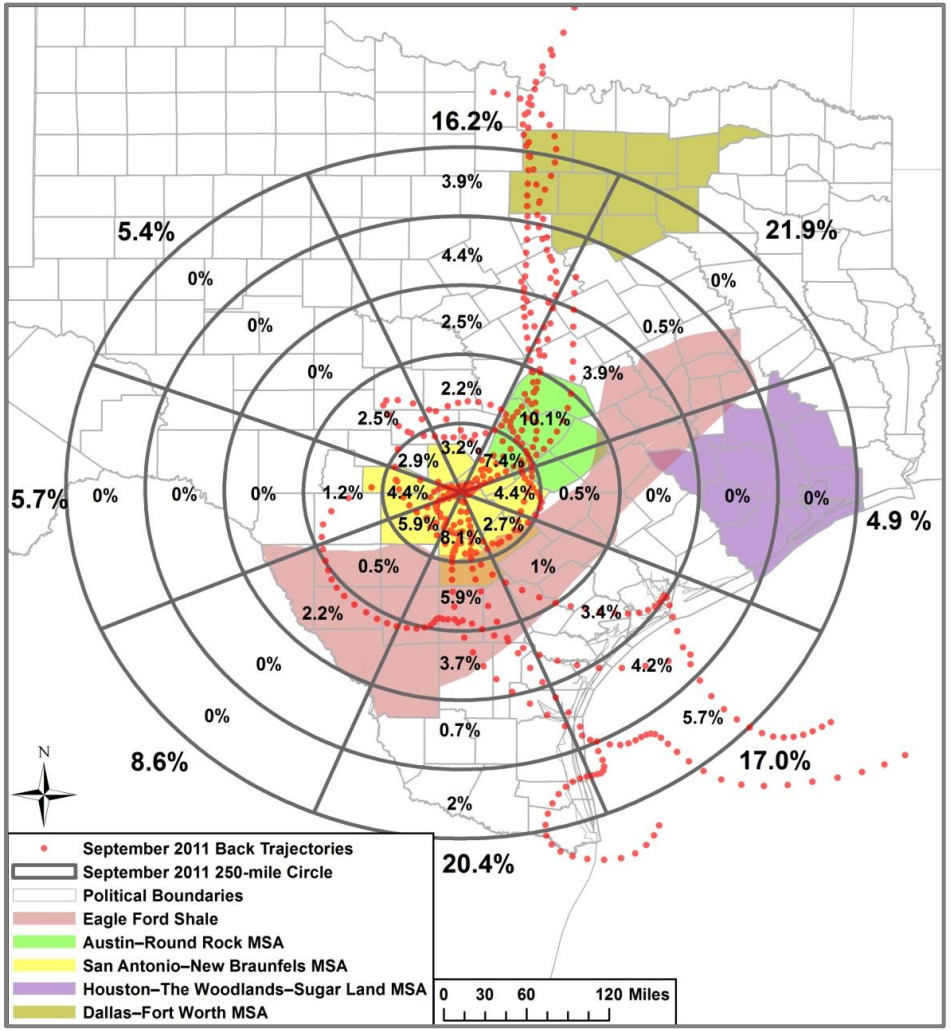

Figure 7-6: June 6 - 28, 2012 Candidate Photochemical Modeling Episode High Ozone Days > 65 ppb.

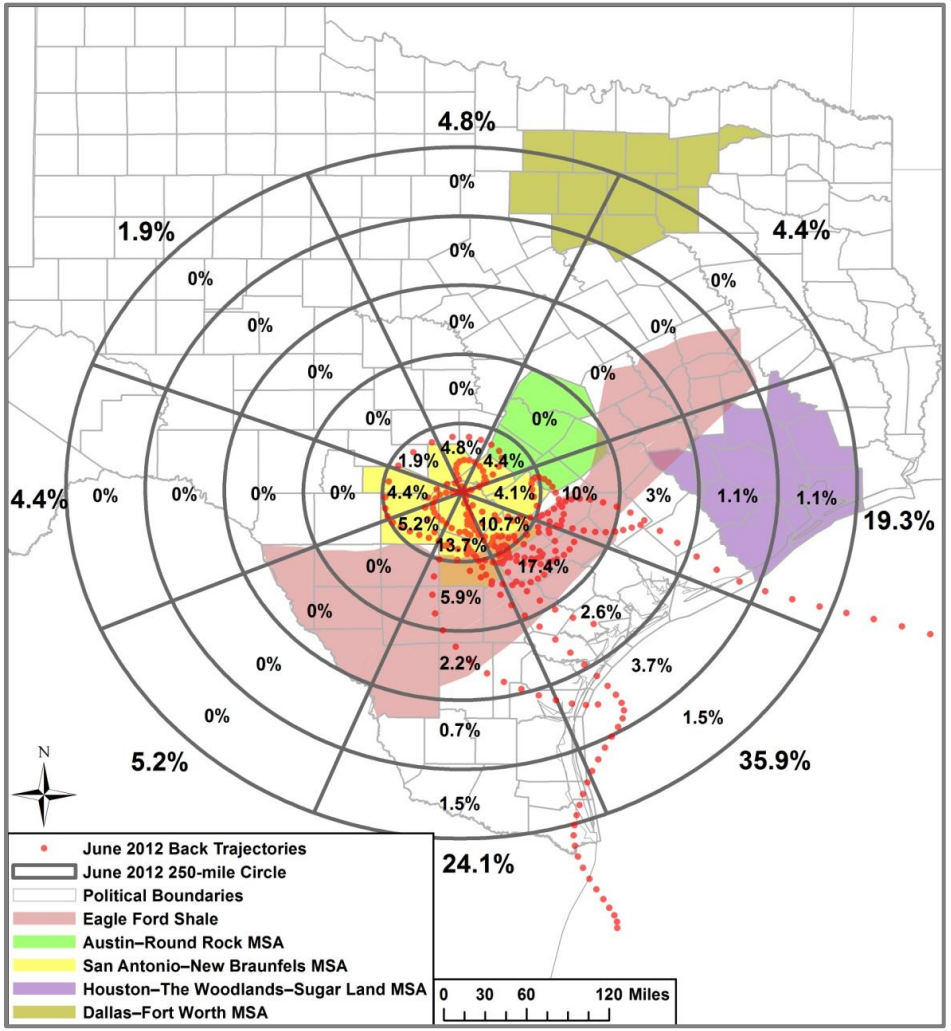

Figure 7-7: August 20 - September 21, 2012 Candidate Photochemical Modeling Episode High Ozone Days > 65 ppb.

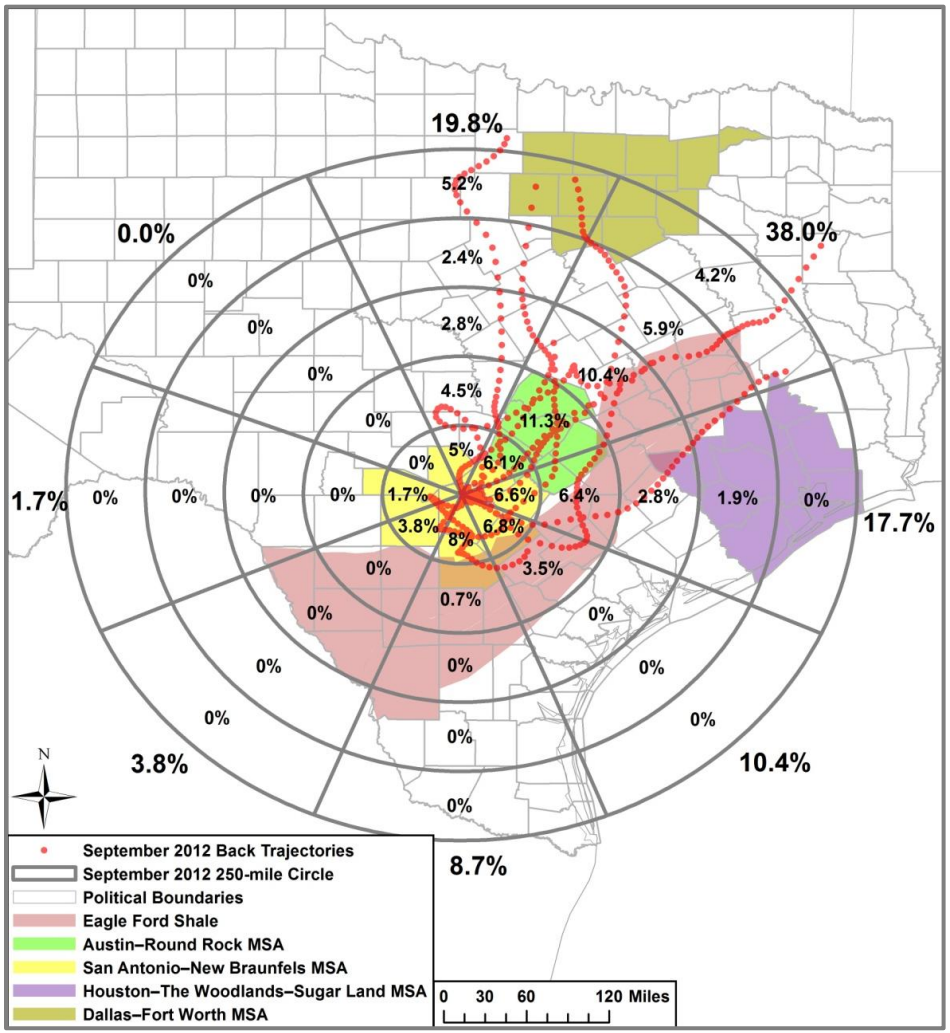

Figure 7-8: August 15 - 31, 2013, 2010 Candidate Photochemical Modeling Episode High Ozone Days > 65 ppb.

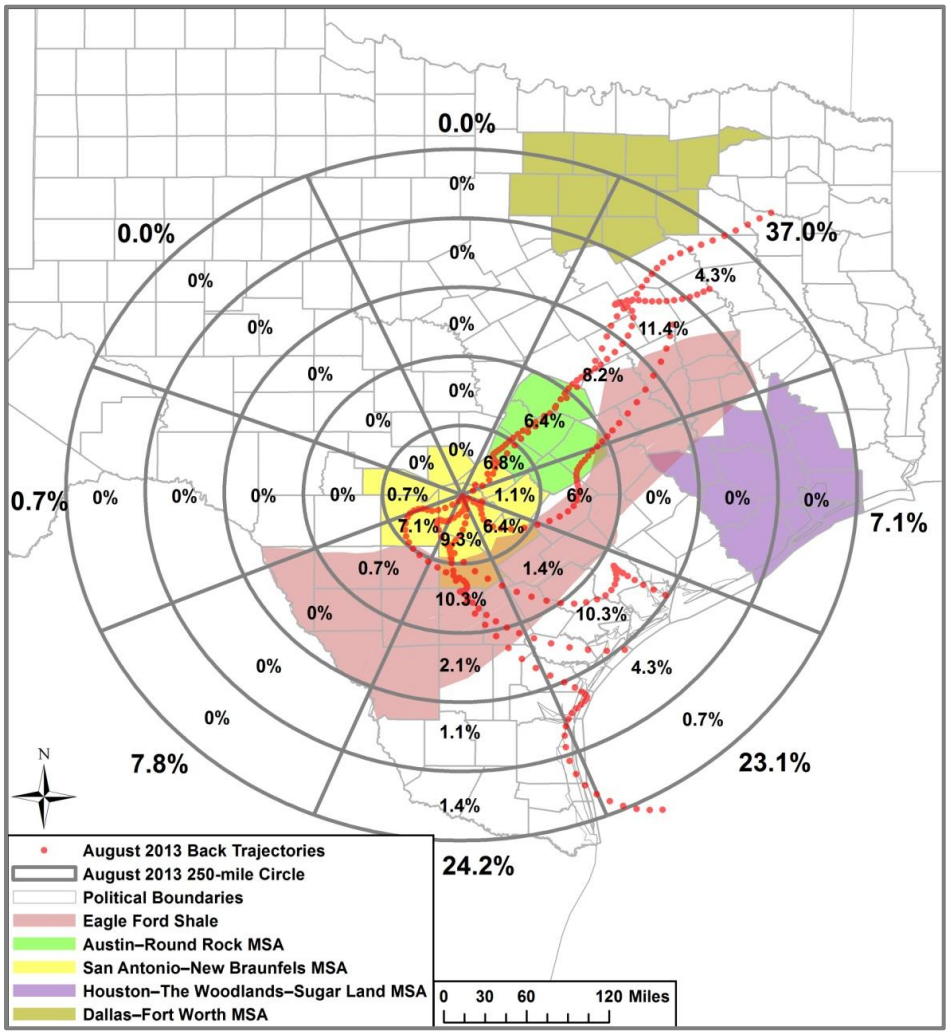

Table 7-16: Octant Percentages and Comparative Ratios for Each High Ozone Event Combined with the Existing June 2006 Episode's Back Trajectories on Days > 65 ppb

Potential Episodes	Southwest	West	Northwest	North	Northeast	East	Southeast	South	Absolute Total Bias
2009-2014 all exceedance days	4.9%	1.8%	1.4%	9.8%	23.8%	15.7%	25.9%	16.7%	-
June 2006 episode	1.0%	0.2%	0.2%	3.3%	15.1%	18.9%	38.9%	22.5%	43.9%
August 2010 and June 2006	0.8%	0.1%	0.1%	5.4%	24.2%	16.9%	33.2%	19.2%	22.8%
October 2010 and June 2006	0.7%	1.2%	2.1%	13.2%	16.5%	15.6%	33.4%	17.3%	24.3%
September 2011 and June 2006	4.0%	2.3%	2.2%	8.4%	17.8%	13.4%	30.2%	21.6%	21.2%
June 2012 and June 2006	2.2%	1.4%	0.7%	3.8%	11.9%	19.0%	38.0%	22.9%	43.3%
September 2012 and June 2006	2.1%	0.8%	0.1%	10.0%	24.3%	18.4%	27.4%	16.9%	10.3%
August 2013 and June 2006	3.1%	0.3%	0.1%	2.3%	21.9%	15.3%	34.0%	23.0%	28.8%

Table 7-17: Distance from C58 Back Trajectory Counts and Percentages for Each High Ozone Event on Days > 65 ppb

Potential Episodes	< 400 km		400 - 800 km		> 800 km		Absolute Difference
	Count	Percentage	Count	Percentage	Count	Percentage	
2009-2014 all exceedance days	5,456	88.6%	541	8.8%	160	2.6%	-
June 2006 episode	628	72.7%	203	23.5%	33	3.8%	31.9%
August 2010 and June 2006	735	72.9%	235	23.3%	38	3.8%	31.4%
October 2010 and June 2006	820	74.3%	246	22.3%	38	3.4%	28.7%
September 2011 and June 2006	1,035	77.0%	266	19.8%	43	3.2%	23.2%
June 2012 and June 2006	898	78.0%	221	19.2%	33	2.9%	21.3%
September 2012 and June 2006	1,052	81.2%	211	16.3%	33	2.5%	15.0%
August 2013 and June 2006	909	78.9%	210	18.2%	33	2.9%	19.4%

7.6 Consideration for Regional Joint Modeling

Beyond the EPA recommended criteria listed above, a major factor involved in the selection of a new photochemical modeling episode is the cost of photochemical model development. If episode modeling can be combined with existing modeling efforts in other cities or several regions can share the cost of modeling, a high ozone event can become more desirable. The proposed lowering of the NAAQS ozone concentration standard jeopardizes the attainment status of several Texas regions; therefore it would be efficient to develop any new modeling episode with these regions. Table 7-18 shows there were high ozone readings in other Texas cities during every high ozone event that occurred in the San Antonio region.

Table 7-18: Maximum 8-Hour Averages for Selected Cities within Texas during High Ozone Events in San Antonio, 2010-2014.

Candidate Episode	Date	San Antonio	Austin	Corpus Christi	Victoria	Houston	Dallas	Tyler/ Longview	Waco	Temple*	Beaumont
Aug. 23 – 29, 2010	8/25/2010	**72**	**72**	**76**		**81**	**67**	**67**			**68**
	8/26/2010	**72**	**72**	**82**	**70**	**76**	**82**				**67**
	8/27/2010	**80**	**80**	**80**	**73**	**88**	**92**	**74**	**75**		**68**
	8/28/2010	**87**	**78**	**80**	**68**	**68**	**91**	**71**	**75**		
	8/29/2010						**67**				
Sept. 28 – Oct. 16, 2010	9/28/2010	**69**				**85**					**76**
	9/29/2010	**67**		**74**		**88**					**81**
	9/30/2010	**73**	**71**	**72**	**67**	**88**		**66**	**66**		**76**
	10/1/2010			**75**		**86**					**70**
	10/2/2010			**74**		**74**					
	10/3/2010			**72**							
	10/4/2010					**66**					
	10/5/2010										
	10/6/2010	**75**	**69**	**71**		**78**	**67**	**78**			
	10/7/2010	**75**	**70**	**83**		**92**	**66**	**80**			**80**
	10/8/2010	**72**	**76**	**79**		**94**	**72**	**74**	**75**		**85**
	10/9/2010					**88**		**77**			**74**
	10/10/2010							**78**			
	10/13/2010					**67**					
	10/14/2010										
	10/15/2010	**66**		**70**		**87**					**72**
	10/16/2010	**78**	**73**	**70**		**95**	**68**	**71**	**72**		**78**
Aug. 27 – Sept. 24, 2011	8/27/2011	**76**	**66**			**88**	**96**	**78**	**78**		**78**
	8/28/2011	**78**	**74**	**72**		**101**	**103**	**81**	**81**		**84**
	8/29/2011	**76**	**82**			**102**	**90**	**67**	**75**		**96**
	8/30/2011		**74**			**100**	**83**	**77**	**72**		**79**
	8/31/2011					**83**	**77**	**71**			
	9/1/2011						**80**				
	9/2/2011						**69**				
	9/3/2011						**71**				

Candidate Episode	Date	San Antonio	Austin	Corpus Christi	Victoria	Houston	Dallas	Tyler/ Longview	Waco	Temple*	Beaumont
Aug. 27 – Sept. 24, 2011	9/4/2011	**66**	**70**						**69**		**66**
	9/5/2011			**77**							**71**
	9/6/2011	**79**	**73**	**83**	**70**	**89**	**74**				
	9/7/2011	**90**	**86**	**79**	**74**	**80**	**83**	**78**	**84**		
	9/8/2011	**75**	**75**	**76**	**80**	**108**	**72**	**72**	**75**		**67**
	9/9/2011	**74**	**78**	**81**	**74**	**91**	**72**	**76**	**72**		**87**
	9/10/2011	**84**	**75**	**82**	**70**	**84**	**69**	**63**	**73**		**76**
	9/11/2011	**84**	**82**	**72**	**67**	**83**	**72**	**68**	**71**		**73**
	9/12/2011	**78**	**80**			**82**	**91**	**74**	**70**		**72**
	9/13/2011		**72**			**70**	**82**	**79**	**68**		
	9/14/2011		**68**			**80**	**69**	**66**	**72**		
	9/15/2011					**85**			**68**		**72**
	9/16/2011					**78**		**70**			**67**
	9/17/2011							**68**			
	9/18/2011										
	9/19/2011	**68**	**67**			**77**					
	9/20/2011	**71**	**75**			**82**	**82**	**72**	**75**		**84**
	9/21/2011		**69**			**84**	**95**	**79**	**75**		**72**
	9/22/2011	**79**	**73**			**85**	**72**	**66**			**72**
	9/23/2011	**75**		**83**	**67**	**93**					
	9/24/2011	**74**	**79**		**66**	**92**	**72**	**74**	**70**		**75**
June 6 – 28, 2012	6/6/2012	**66**				**75**	**63**				
	6/7/2012					**85**					**75**
	6/8/2012					**67**	**81**				
	6/9/2012	**75**				**76**	**75**				
	6/10/2012										
	6/11/2012										
	6/12/2012										
	6/13/2012										
	6/14/2012										
	6/15/2012										
	6/16/2012										
	6/17/2012					**74**					
	6/18/2012										
	6/19/2012										

Candidate Episode	Date	San Antonio	Austin	Corpus Christi	Victoria	Houston	Dallas	Tyler/ Longview	Waco	Temple*	Beaumont
June 6 – 28, 2012	6/20/2012										
	6/21/2012					**66**	**73**				
	6/22/2012	**72**				**68**	**83**		**66**		
	6/23/2012	**74**	**68**			**67**	**74**		**66**		**71**
	6/24/2012					**71**	**87**				
	6/25/2012	**70**	**75**	**69**		**94**	**107**	**67**	**74**		**75**
	6/26/2012	**89**	**87**	**88**	**68**	**136**	**110**	**84**	**78**		**112**
	6/27/2012	**90**	**81**		**66**	**106**	**95**	**80**	**82**		**84**
	6/28/2012	**70**	**61**			**75**	**78**	**74**			
Aug. 20 – Sept. 21, 2012	8/20/2012	**81**	**81**		**68**	**97**	**83**	**66**	**76**		**67**
	8/21/2012	**87**	**72**			**80**					
	8/22/2012	**76**	**66**			**68**	**79**	**70**			
	8/23/2012	**71**					**71**	**69**			
	8/24/2012										
	8/25/2012										
	8/26/2012										
	8/27/2012					**74**					
	8/28/2012		**66**			**71**					
	8/29/2012		**66**	**68**			**69**		**69**		
	8/30/2012		**69**	**66**							
	8/31/2012	**66**					**81**		**67**		
	9/1/2012										
	9/2/2012										
	9/3/2012										
	9/4/2012										
	9/5/2012						**66**				
	9/6/2012						**89**				
	9/7/2012						**72**				
	9/8/2012										
	9/9/2012					**67**	**67**				
	9/10/2012	**90**	**77**			**77**	**79**	**67**			**68**
	9/11/2012	**72**				**80**	**74**		**66**		
	9/12/2012						**72**				
	9/13/2012										
	9/14/2012										

Candidate Episode	Date	San Antonio	Austin	Corpus Christi	Victoria	Houston	Dallas	Tyler/ Longview	Waco	Temple*	Beaumont
Aug. 20 – Sept. 21, 2012	9/15/2012										
	9/16/2012										
	9/17/2012										
	9/18/2012										
	9/19/2012	**81**		**69**		**71**					
	9/20/2012	**72**	**68**			**87**	**79**				**69**
	9/21/2012	**75**				**81**	**82**	**74**			
Aug. 15 – 31, 2013	8/15/2013						**67**				
	8/16/2013					**94**	**81**				
	8/17/2013	**75**	**70**	**68**		**80**	**72**				
	8/18/2013	**79**	**70**	**69**		**69**	**69**				
	8/19/2013	**74**	**66**			**78**	**78**	**66**	**69**		
	8/20/2013						**85**				
	8/21/2013						**66**				
	8/22/2013										
	8/23/2013						**66**				
	8/24/2013						**69**				
	8/25/2013										
	8/26/2013										
	8/27/2013										
	8/28/2013					**83**					
	8/29/2013	**78**				**78**	**83**				
	8/30/2013	**80**	**69**			**78**	**89**	**73**			**69**
	8/31/2013	**74**	**69**			**84**	**85**	**70**			

*Temple ozone monitors did not start operating until 2014

8 CONCLUSION AND SUMMARY OF HIGH OZONE EVENTS

Forecasting future air quality and modeling air quality control strategies are among the basic elements of a SIP. Since control strategy modeling requires extensive technical analyses of control strategy impacts under the variety of meteorological conditions that are conducive to high ozone, it is important that each photochemical modeling episode be built upon a time period characterized by such meteorological conditions. The conceptual model examines air quality trends, meteorology patterns, precursor emissions, and ozone transport on high ozone days in San Antonio and serves as a basis for ranking candidate episodes. Continued research on ozone formation in San Antonio is necessary to ensure the region meets attainment standards.

Since 2004, San Antonio's 8-hour ozone design value has decreased from 91 ppb to 80 ppb. The 2012-2014 design value (truncated average) was 75 ppb at C23 and 80 ppb at C58, indicating that the San Antonio region ended 2014 with two regulatory monitors exceeding 70 ppb, the high end of the range under consideration for the revised ozone standard. One monitor, C59, was above the mid-point of the range under consideration for the revised standard. While the design values have generally decreased since 2004, they increased in 2012 and are still higher than the period from 2009-2011. Significant reductions in the number of exceedances over 65 ppb have occurred from 2006 through 2010, but in 2011 they nearly doubled over the previous year. A cluster of regulatory and non-regulatory monitors located north and northwest of the San Antonio urban core (CAMS 23, 58, 502, 503, and 505) often records ozone values exceeding the proposed revision to the standard. Local and transported emissions often impact these monitors on high ozone days.

There is no significant variability in the frequency of high ozone days by the day of the week. Based on data for ozone concentrations that exceeded the range of values under consideration for the revised standard, high ozone days occurred on both weekdays and on weekends. Between 2005 and 2014, 31.6% percent of high ozone days > 60 ppb occurred on the weekends. A different mixture of emission sources could be impacting ozone formation on the weekend than weekdays and different control strategies may be needed to reduce peak ozone concentrations.

Local conditions that typify high ozone events include light winds over Texas, limited frontal movement, no precipitation, and clear skies. Typical local meteorological conditions that are conducive to ozone formation include days with no precipitation, low atmospheric moisture content present in the afternoon, and clear skies. There was no significant correlation between peak temperature and ozone readings. Mixing heights are typically lower in the early morning hours and experience a rapid rise in the late morning through early afternoon on high ozone days.

The timing, location, and intensity of ozone events are influenced by the interaction between local and regional wind patterns. The wind vectors on high ozone days were more stagnated and frequently originated from the east and northeast. Often on high ozone days, the wind at C23 slowly changed direction at the monitor from the north to the east in a clockwise fashion during the day. The directions of the wind vectors indicate emissions transport occurs from the north and northeast on high ozone days and combines with local and transported emissions from the urban area east of the monitor later in the day to form ozone. C58 wind vectors show there is a flow reversal of winds arriving at the monitors from the northwest in the morning before 7:00 to out of the southeast later in the day. Such shifts in winds with a rotational wind pattern is similar to observed winds in Houston when heating of the atmosphere in the morning mixes winds aloft down to the surface. These wind patterns can facilitate recirculation of

pollutants, allowing local ozone precursor emissions and ozone to combine with transported and local emissions from the previous day and form greater concentrations of ozone.

The strongest multivariate correlation at the 60 ppb threshold was back trajectory direction - diurnal temperature change and humidity - back trajectory distance. The strongest multivariate correlation for days over the 65 ppb and 70 ppb standard was humidity – back trajectory distance. Wind Speed – humidity and humidity – back trajectory direction were also strongly correlated with high ozone days. The lowest correlation with high ozone days was wind speed - afternoon wind direction, temperature - wind speed, and temperature - afternoon wind direction.

Of the five NO_X monitors in the San Antonio area, only one, C678, records moderate amounts of NO_X emissions, likely due to its proximity to major highways. Although C678 records the highest NO_X in the region, NO_X emissions at the monitor significantly decreased from 2000 to 2014. The decrease in NO_X can be attributed to controls put on major NO_X sources including power plants and cement kilns, and most importantly, significant reductions of NO_X emissions from on-road and off-road vehicles. Local NO_X emissions should continue a downward trend, in large part due to improvements in vehicle emission standards, while local VOC emissions will likely remain steady. C59 is an upwind monitor site on most high ozone days and NO_X readings are low at the monitor, indicating that there was not a significant amount of NO_X being transported into San Antonio from the southeast from 2000 to 2014.

Surface back trajectories on days with low ozone were predominately from the southeast, while winds on high ozone days were from the northeast, east, and southeast. A similar pattern occurred with 1,000-meter back trajectories in which days of high ozone values are associated with winds that originate from the northeast, east, and southeast. Back trajectories on high ozone days originated closer to San Antonio and were shorter, indicating transport level winds are often weaker on high ozone days. End points of 48-hour back trajectories on low ozone days tended to originate far out in the Gulf of Mexico.

The difference between the maximum peak ozone readings and the minimal peak ozone readings at ozone monitors on high ozone days > 65 ppb from 2005-2014 was 18.5 ppb or 24.7%, suggesting that San Antonio adds an estimated 19 ppb or 25% to the ambient ozone concentrations. Ozone readings at upwind monitors have decreased by an average of 0.8 ppb per year since 2005 on all days, and by 5.8 ppb on days when 8-hour averages exceeded 60 ppb. Likewise, the number of high ozone days > 60 ppb at upwind monitors decreased 66 percent between 2005 and 2014. There was a similar decrease in the number of high ozone days at the upwind monitors for the 65 ppb (72%) and 70 ppb (84%) thresholds. Although the amount of transported ozone has decreased over the last five years, local contribution to ozone has actually been increasing in the last three to five years.

Aircraft sampling indicated large ozone plumes from upwind urban areas and industrial facilities could impact areas hundreds of kilometers downwind including the San Antonio area. This may increase the ozone at downwind monitor sites and cause the region to have difficulty attaining a stricter 8-hour ozone standard. Additionally, new point sources being built in Texas may increase ozone-forming emissions in the San Antonio area in the future and possibly weaken the region’s ability to meet federal ozone standards for years to come.

From April through June, there is a seasonal increase in the number of high ozone days in most Texas cities. This period represents the first and longest high ozone seasonal peak that San Antonio typically experiences. However, by early July the number of high ozone days decline. The next seasonal increase covers a period beginning in August and ending in late October, during which the frequency of high ozone days is slightly lower than the spring period.

Analysis of seasonal trends showed that back trajectories arrive from progressively shorter distances from June through September, indicating progressively stagnated air parcels. The directions of back trajectory origin have strong southeast and south components, with a minor east component during the months of June, July, and August. In September, however, back trajectories originate with almost equal frequency from the northeast, east, and southeast, with small percentages originating from the north and south.

There is a significant amount of ozone transport during the spring and fall ozone season peaks. Transported ozone is highest in April, but average local contribution is lower in April. Transport is lowest in July before increasing again in the late summer and fall. The summer months of June through August account for the largest fractions of local contributions to ozone. A combination of greater tropospheric-stratospheric air exchange combined with higher North American stratospheric ozone levels during the early months of the ozone season may be partially responsible for the higher ground level ozone observed in San Antonio during these months. Likewise, the cessation of this phenomenon could explain the decrease in ground level ozone from late June through July, which occurs before air mass stagnation and northeasterly transport contribute to an increase in ground level ozone measurements during the fall ozone seasonal peak.

The meteorology and transport patterns during high ozone events from 2005 to 2014 were analyzed to determine whether the episodes were suitable for photochemical modeling. To be suitable for modeling, high ozone events should include days with observed concentrations that are close to site-specific design values and reflect meteorological conditions that are commonly observed. In ranking the high ozone events for desirability, the selection criteria were reviewed and all events were weighted against typical meteorological conditions on high ozone days. The first step was to compare each episode with desirable criteria. The recommended criteria used for episode selection are listed below. Ozone and meteorological conditions evaluated for each high ozone event included:

- ✓ **Number of High Ozone Days**
  - *Number of Days at C23 Ozone > 65 ppb*
  - *Number of Days at C58 Ozone > 65 ppb*
- ✓ **Typical Seasonal and Daily Variation of High Ozone Days**
  - *Within Ozone Seasonal Peaks*
  - *Weekend High Ozone Day*
- ✓ **Monitored Ozone Values**
  - *One-Hour/8-hour Correlation*
  - *Percent of High Ozone Days ± 10 ppb of Design Value*
  - *Occurs during the three-year period used to calculate the design value*
- ✓ **Typical Local Meteorological Characteristics of High Ozone Days**
  - *Diurnal Temperature Change at C58* - Large Change (>12.7^{o} C)
  - *Relative Humidity at C5004* - low afternoon humidity (<38.3% relative humidity)
  - *Solar Radiation at C58* - Clear skies (>1.16 langleys/min.)
  - *Morning Wind Direction at C58* - Northwest, North, Northeast, and East
  - *Afternoon Wind Speed at C58* - low speed (<2.75 m/s)
  - *Precipitation at C678* - no precipitation
- ✓ **Typical Regional Meteorological Characteristics on High Ozone Days**
  - *Extreme Weather Events* - unusual meteorological events
  - *Back Trajectory Distance* - less than 1065 km
  - *Back Trajectory Direction* - North, Northeast, East, and Southeast

✓ **Joint Modeling (Cost Reduction)**

Table 8-1 list the degrees of desirability from 0 to 4 for each high ozone event based on the above criteria for days greater with recorded ozone at regulatory monitors greater than 65 ppb. The following degrees of desirability are provided on the table:

- White = 0 / excellent
- Yellow = 1 / good
- Light Orange = 2 / fair
- Orange = 3 / weak
- Red = 4 / poor

The methodologies used to determine the degrees of desirability are listed in Appendix A. These degrees (0-4) are only relevant within each category and do not have the same value from one category to another. It is important for a high ozone event to have high readings at both C58 and C23 because they are the regulatory monitors currently in excess of 70 ppb, the high end of the range under consideration for the proposed revision to the ozone standard. In order to test control strategies for possible ozone reduction, the episode should demonstrate characteristics typical of periods of high ozone at the regulatory monitors that record the highest ozone in the region and at as many additional monitors as possible.

Table 8-2 provides a summary of the ranking for each high ozone event that occurred between 2010 and 2014 with respect to the mid range of the proposed revision to the ozone standard: 65 ppb. The Aug. 20– Sept. 21, 2012 high ozone event had the highest ranking. This event extended a sufficient number of days at C58 to model and data collected during the event indicated ozone readings representative of the design value, typical wind directions at C23 and C58 on high ozone days, and typical back trajectory distances on high ozone days. The Aug. 27 – Sept. 24, 2011 and June 6 – 28, 2012 high ozone events also had high rankings. The former episode had enough exceedances at C23 while the June 2012 event did not. However, the June 2012 event is under consideration for modeling by another city, which makes it more desirable than the September 2011 episode. For each of these three events, there are extensive meteorological and ozone data sets available that would benefit modeling efforts.

The other high ozone events are not under consideration for modeling by other cities. The events in 2010 are particularly poor modeling candidates as the meteorological conditions were not representative of typical conditions during these events. For the 2013 event, the meteorological conditions were more representative, but the number of exceedances at each CAMS were not, and 1-hr and 8-hr peak ozone did not correlate well with each other. Additionally, this event is not being considered for modeling anywhere else, making the 2013 event more expensive to model.

Table 8-1: Ratings for High Ozone Events Selection Criteria for the San Antonio Region, 2010-2014 Based on Days in which 8-hour Ozone Averages > 65 ppb

High Ozone Event	# Days at **C23** Ozone > 65 ppb	# Days at **C58** Ozone > 65 ppb	Within Ozone Seasonal Peak	Weekend High Ozone Day	One-Hour/Eight-Hour Correlation	% of High Ozone Days ± 10 ppb of Design Value	Within the Latest Design Value	Typical Local Meteorological Conditions	Wind Direction at C23 and C58	Extreme Weather Events	Back Trajectories Distance	Back Trajectories Direction	Joint Modeling (Cost Reduction)	Sum of Scores
June 2 – 30, 2006	**2**	**0**	**0**	**0**	**1**	**3**	**3**	**1**	**1**	**3**	**2**	**0**	**0**	16
Aug. 23 – 29, 2010	**4**	**4**	**0**	**1**	**0**	**0**	**2**	**3**	**4**	**0**	**3**	**4**	**4**	29
Sept. 28 – Oct. 17, 2010	**4**	**3**	**0**	**0**	**4**	**3**	**2**	**0**	**3**	**0**	**2**	**3**	**4**	28
Aug. 27 – Sept. 24, 2011	**0**	**2**	**0**	**0**	**1**	**1**	**1**	**0**	**2**	**3**	**0**	**0**	**4**	14
June 6 – 28, 2012	**3**	**2**	**0**	**1**	**1**	**3**	**0**	**0**	**1**	**1**	**2**	**0**	**0**	14
Aug. 20 – Sept. 21, 2012	**2**	**1**	**0**	**2**	**3**	**0**	**0**	**1**	**0**	**3**	**0**	**1**	**0**	13
Aug. 15 – 31, 2013	**3**	**3**	**0**	**0**	**2**	**0**	**0**	**0**	**3**	**0**	**1**	**0**	**4**	16

*Note: The smaller the number, the better the rating. However, ***all aspects are not equal in value***, so the final rating is for comparison, only. Before episode selection, all aspects must be weighed based on the contribution to the episode as a whole.

Table 8-2: Summary of Scores for each High Ozone Event, 2010-2014

High Ozone Event	Total Score
June 2 – 30, 2006	16
Aug. 23 – 29, 2010	29
Sept. 28 – Oct. 17, 2010	28
Aug. 27 – Sept. 24, 2011	14
June 6 – 28, 2012	14
Aug. 20 – Sept. 21, 2012	13
Aug. 15 – 31, 2013	16

In Table 8-3, the candidates are divided into three groups: suitable candidate episodes, other potential desirable candidate episodes, and undesirable candidate episodes. The table lists a summary of the high ozone event choices and significant characteristics. This ordering is not steadfast and is based on the desired selection criteria of each episode. No value was placed on the importance of the criteria; thus, judgment should not lie solely on the ratings in this conclusion, but should be based on the analysis of the data with respect to the importance it bears on modeling. These candidates represent the choices available for a new photochemical model. In making a final selection for potential future photochemical modeling episodes, these aspects as well as any new data, should be considered.

Table 8-3: Summary of high ozone event choices and associated characteristics

High Ozone Event	Desirable Characteristics	Undesirable Characteristic
Suitable Candidate Episodes		
Aug. 20 – Sept. 21, 2012	**Within Ozone Seasonal Peak** **TexAQS II Meteorological and Ozone Data Available** **Model is already under development by other areas in Texas** **Typical back trajectory distance on high ozone days**	**Contains only 7 days above 65 ppb at C23** **Back Trajectory directions are not typical on high ozone days** **Poor correlation between 1-hr and 8-hr ozone values** **No high ozone days on weekends**
Other Desirable Candidate Episodes		
Aug. 15 – 31, 2013	**Within Ozone Seasonal Peaks** **TexAQS II Meteorological and Ozone Data Available** **Typical local meteorological conditions on high ozone days** **Typical Back Trajectory direction on high ozone days**	**Contains only 6 days above 65 ppb at C23 and C58** **Not under consideration for joint modeling** **Wind direction at C23 & C58 not typical on high ozone days**
June 6 – 28, 2012	**Typical Back Trajectory direction on high ozone days** **TexAQS II Meteorological and Ozone Data Available** **Model is already under development by other areas in Texas** **Within Ozone Seasonal Peaks** **Typical local meteorological conditions on high ozone days**	**Contains only 6 days above 65 ppb at C23** **Tropical Storm Debbie occurred during this Episode** **Only 50% of high ozone days are ± 10 ppb of the weighted design value at C23 & C58 (70 ppb standard)**
Aug. 27 – Sept. 24, 2011	**Within Ozone Seasonal Peaks** **Typical local meteorological conditions on high ozone days** **Typical Back Trajectories on high ozone days** **TexAQS II Meteorological and Ozone Data Available** **Contains 12 days above 65 ppb at C23**	**Wind Direction is not typical of high ozone days** **Bastrop County fire occurred during this Episode** **Tropical Storm Lee occurred during this Episode** **Not under consideration for joint modeling**
Candidates Episodes Not Recommended		
Sept. 28 – Oct. 17, 2010	**Within Ozone Seasonal Peaks** **TexAQS II Meteorological and Ozone Data Available** **Typical meteorological conditions on high ozone days**	**Contains only 3 days above 65 ppb at C23** **Only 53% of high ozone days are ± 10 ppb of the weighted design value at C23 and C58 (70 ppb standard)** **Only one weekend exceedance** **Back Trajectories are not typical on high ozone days** **Poor correlation between 1-hr and 8-hr ozone values** **Not under consideration for joint modeling**
Aug. 23 – 29, 2010	**Good Correlation between one-hour and eight hour ozone values** **Within Ozone Seasonal Peaks**	**Contains only 3 days above 65 ppb at C23 and C58** **Not under consideration for joint modeling** **Only one weekend exceedance of proposed standard** **Does not have typical local meteorological conditions** **Back Trajectories are not typical on high ozone days** **Wind direction is not typical of high ozone days**

APPENDIX A: RATINGS CRITERIA FOR EPISODE SELECTION

1. # Days at C23 Ozone > Proposed 65 ppb Standard
   - ranking of 4 = C23 had less than 5 days
   - ranking of 3 = C23 had 5-6 days
   - ranking of 2 = C23 had 7-8 days
   - ranking of 1 = C23 had 9-10 days
   - ranking of 0 = C23 had more than 10 days

2. # Days at C58 Ozone > Proposed 65 ppb Standard
   - ranking of 4 = C58 had less than 5 days
   - ranking of 3 = C58 had 5-6 days
   - ranking of 2 = C58 had 7-8 days
   - ranking of 1 = C58 had 9-10 days
   - ranking of 0 = C58 had more than 10 days

3. Within Ozone Seasonal Peak
   - ranking of 4 = If episode is not within the ozone seasonal peaks
   - ranking of 2 = If episode had only 1 - 5 days > 65 ppb within the ozone seasonal peaks
   - ranking of 0 = If the full episode is within the ozone seasonal peaks

4. Weekend High Ozone Days
   - ranking of 2 = no weekend high ozone days
   - ranking of 1 = one weekend high ozone days
   - ranking of 0 = two or more weekend high ozone days

   note: no ranking of 3 or 4 were allocated because this criteria was not considered as significant because the existing June 2006 already has several weekend high ozone days

5. One-Hour/8-hour Correlation
   - ranking of 4 = if less than 51% of the days are within one standard deviation
   - ranking of 3 = if 51-60% of the days are within one standard deviation
   - ranking of 2 = if 61-70% of the days are within one standard deviation
   - ranking of 1 = if 71-80% of the days are within one standard deviation
   - ranking of 0 = if more than 80% of the days are within one standard deviation

6. % of High Ozone Days ± 10 ppb of Design Value
   - ranking of 4 = <50% of the days at regulatory monitors within ± 10 ppb of the Design Value
   - ranking of 3 = 50% - 59.9% of the days at regulatory monitors within ± 10 ppb of the Design Value
   - ranking of 2 = 60% - 69.9% of the days at regulatory monitors within ± 10 ppb of the Design Value
   - ranking of 1 = 70% - 80% of the days at regulatory monitors within ± 10 ppb of the Design Value
   - ranking of 0 = >80% of the days at regulatory monitors within ± 10 ppb of the Design Value

7. Within the Latest Design Value
   - ranking of 3 = Episode Occurred before 2010
   - ranking of 2 = Episode Occurred in 2010
   - ranking of 1 = Episode Occurred in 2011
   - ranking of 0 = Episode Occurred between 2012 and 2014

8. Typical Local Meteorological Conditions - based on the percentage of unusual meteorological conditions on high ozone days (For example, high ozone days when diurnal temperature <

12.7°C, Relative Humidity at 2p.m. > 38.3%, Max. Solar Radiation < 1.16 langleys /min , Afternoon Wind Speed < 1.83 m/s, Precipitation > 0 cm)

- ranking of 4 = >20% unusual meteorological conditions
- ranking of 3 = 15% - 19.9% unusual meteorological conditions
- ranking of 2 = 10% - 15.9% unusual meteorological conditions
- ranking of 1 = 5% - 9.9% unusual meteorological conditions
- ranking of 0 = <5% unusual meteorological conditions

9. Wind Direction at C23 and C58
   - ranking of 4 = If the average absolute difference of Wind Direction is >95% at C23 and C58
   - ranking of 3 = If the average absolute difference of Wind Direction is 85% - 95% at C23 and C58
   - ranking of 2 = If the average absolute difference of Wind Direction is 75% - 84.4% at C23 and C58
   - ranking of 1 = If the average absolute difference of Wind Direction is 65% - 74.9% at C23 and C58
   - ranking of 0 = If the average absolute difference of Wind Direction is <65% at C23 and C58

10. Extreme Weather Events
    - One point for each extreme weather event, and
    - One point if total rainfall is between 0.2 and 1.0 inches
    - Two points if total rainfall > 1.0 inches

11. Back Trajectories Distance
    - ranking of 4 = if the absolute difference in back trajectories is > 55%
    - ranking of 3 = if the absolute difference in back trajectories is 45% - 55%
    - ranking of 2 = if the absolute difference in back trajectories is 35% - 44.9%
    - ranking of 1 = if the absolute difference in back trajectories is 25% - 34.9%
    - ranking of 0 = if the absolute difference in back trajectories is < 25%

12. Back Trajectories Direction
    - ranking of 4 = if the absolute difference in back trajectories is > 110%
    - ranking of 3 = if the absolute difference in back trajectories is 90% - 109.9%
    - ranking of 2 = if the absolute difference in back trajectories is 70% - 89.9%
    - ranking of 1 = if the absolute difference in back trajectories is 50% - 69.9%
    - ranking of 0 = if the absolute difference in back trajectories is < 50%

13. Joint Modeling (Cost Reduction)
    - ranking of 4 = If the episode is not already under development by another entity in Texas
    - ranking of 0 = If the high ozone event is already under development by another entity in Texas